Bone Mineral Density
and Vascular Calcification
in Children and Young Adults
with Chronic Kidney Disease

Presented for the degree of Doctor of Philosophy

to University College London

Alexander D. Lalayiannis

UCL Great Ormond Street Hospital for Children Institute of Child Health,
London, UK

Declaration

I, *Alexander D. Lalayiannis* confirm that the work presented in this thesis is my own. Where information has been derived from other sources, I confirm that this has been indicated in the thesis.

Signed…………………………………………………………………..

Acknowledgements

There are many people I would like to thank for helping me through the last five years. I'd firstly like to thank the children, young adults and their families for taking part in the study. They selflessly participated and donated their time, and for this I am grateful.

My journey from the very beginning would not have been possible without help and guidance from my supervisor Prof Rukshana Shroff. Her passion for science and the pursuit of knowledge is inspiring; her dedication and work ethic are unparalleled. She has been a supervisor for 5 years, but will be a mentor for life.

I am grateful for all of Charlie's sage advice, Nicola's help and Mary's guidance. The study would not have been possible without all my collaborators: Varvara, David, Duncan, Manish, Amrit, Kristian and Simon.

I would like to express my deepest appreciation to Kidney Research UK and Kids Kidney Research for entrusting me with the grants to make this PhD possible, and for their support during my studies.

A special thank you not only for the hand-holding when I was finding my feet around GOSH, but more importantly the banter, chats and friendship to Selmy Silva and Nadine Goodman.

Thank you to David Milford for believing in me and urging me to follow my dream. His impetus was the priming force I needed and his mentorship is always invaluable.

Thank you to my sister Leonie and family for being so supportive and encouraging. Thank you to my brother Raphael who put me up in his London flats *and* put up with me and my early morning starts for years!

To my parents, Sharon and Nick, thank you for always believing in me, being my champions and working so hard to provide me with the best opportunities in life. I would not have achieved all I have without you.

Finally, I would like to thank my children Aris, Leda, and Hector for being patient with me and for their understanding during all those times I had to be away.

To my wife Gemma, this thesis is only because of you and for you.

Abstract

Introduction

Older adults with chronic kidney disease (CKD) can have low bone mineral density (BMD) with concurrent vascular calcification. It is not known if mineral accrual by the growing skeleton protects young people with CKD from extraosseous calcification. My hypothesis was that children and young adults with increasing BMD do not develop vascular calcification.

Methods

Multicentre longitudinal study in children and young people (5-30 years) with CKD stages 4-5 or on dialysis. Cortical (Cort) and trabecular (Trab) BMD were assessed by peripheral quantitative Computed Tomography and lumbar spine BMD by DXA (Dual Energy X-ray Absorptiometry). Vascular calcification was assessed by cardiac CT for coronary artery calcification (CAC) and ultrasound for carotid intima-media thickness (cIMT). Arterial stiffness was measured by pulse wave velocity (PWV) and carotid distensibility.

Results

One hundred participants (median age 13.82 years) were assessed at baseline and 57 followed-up after a median of 1.45 years. The cohort had a significant bone and cardiovascular disease burden. 10% suffered at least one previous atraumatic fracture, and 58% reported bone pain affecting activities of daily living. The majority had evidence of vascular calcification and arterial stiffness with increased cIMT and PWV z-scores. 10%

had CAC at baseline. Baseline TrabBMD was independently associated with cIMT (R^2=0.10, β=0.34, p=0.001). An annualised increase in TrabBMD was an independent predictor of cIMT increase (R^2=0.48, β=0.40, p=0.03), with 6-fold greater odds of an increase in ΔcIMT in those with an increase in ΔTrabBMD [(95%CI 1.88 to 18.35), p=0.003]. Young people that demonstrated statural growth (n=33) had attenuated vascular changes compared to those with static growth.

Conclusion

These hypothesis generating studies suggest that children and young adults with CKD or on dialysis may develop vascular calcification even as BMD increases. A presumed buffering capacity of the growing skeleton may offer some protection against extraskeletal calcification.

Impact Statement

This is the first longitudinal study to examine bone and vascular health simultaneously in a cohort of children and young people with chronic kidney disease. Children as young as five years old to young adults aged 30 years old were included as the skeleton continues to mineralise until the third or fourth decade of life. This study has shown that young people with chronic kidney disease suffer from poor bone health with atraumatic fractures and bone pain affecting activities of daily living. They also had significant subclinical cardiovascular disease; structural vessel changes associated with calcification were evident and probably lead to functional changes manifesting as arterial stiffening.

This thesis suggests that the processes of bone demineralisation and vascular calcification happen simultaneously. In fact, vascular calcification seemed to progress even in the context of increasing bone mineral density. Young people with CKD who demonstrated ongoing linear growth had an attenuation of vascular changes whereas those who had stopped growing demonstrated a deterioration in structural and functional measures of vascular health.

The work undertaken for this thesis and the corresponding published manuscripts will raise awareness not only of the high burden of cardiovascular disease in young patients with CKD, but also the need for attention to the concurrent mineral bone disorder. One of the most challenging aspects of CKD-MBD management in young people is to reconcile the need for minerals such as calcium and phosphate for optimal

skeletal mineralisation whilst avoiding an excess calcium intake that can predispose to vascular calcification.

This thesis also highlights the need for more accurate biomarkers that reflect bone turnover and mineralisation as well as potentially vascular calcification. This would enable a clinician to tailor and adapt treatments to each individual patient. This in turn would address patient level outcomes such as bone pain and fractures, as well as cardiovascular morbidity and mortality.

List of Abbreviations

25(OH)D	25-hydroxyvitamin D
ACEi	angiotensin converting enzyme inhibitor
Aix	augmentation index
ALP	alkaline phosphatase
ARB	angiotensin receptor blocker
BMAD	bone mineral apparent density
BMC	bone mineral content
BMD	bone mineral density
BMI	body mass index
BP	blood pressure
CAC	coronary artery calcification
CAKUT	congenital abnormalities of the kidneys and urinary tract
CCA	common carotid artery
cIMT	carotid intima media thickness
CKD	chronic kidney disease
CSMI	cross sectional moment of inertia
CT	computed tomography
CVD	cardiovascular disease
DBP	diastolic blood pressure
DC	distensibility coefficient
DXA	dual energy X-ray absorptiometry
FGF23	fibroblast growth factor 23
GFR	glomerular filtration rate
GH	growth hormone
HD	haemodialysis
HDF	haemodiafiltration
HHD	home haemodialysis
HTN	hypertension
LCSA	lumen cross-sectional area
LVH	left ventricular hypertrophy
LVMI	left ventricular mass index
MBD	mineral bone disorder
PD	peritoneal dialysis
iPTH	intact parathyroid hormone
PWA	pulse wave analysis
PWV	pulse wave velocity
qCT	quantitative computed tomography
ULN	upper limit of normal
WCSA	wall cross sectional area

List of Figures

List of Tables

Table of Contents

Chapter 1-Introduction

Introduction

Young people with CKD suffer from significant morbidity and mortality related to their disease. Despite advances in paediatric nephrology and the overall gradual improvement in all-cause mortality in the last two decades, cardiovascular disease remains the leading cause of death in children and young people with CKD. They also suffer from a disproportionate bone disease burden which manifests as bone pain, bone deformities, poor height attainment and fractures.

In chronic kidney disease, as the glomerular filtration rate decreases, there is a steady, gradual and progressive mineral dysregulation that occurs. It is now known that this process is linked to bone demineralisation, and extra-skeletal calcification. The calcification happens in soft tissues, but most notably in blood vessels, causing arterial stiffening. The combination of bone demineralisation and vascular calcification cause the significant morbidity and mortality associated with CKD.

Recent clinical studies have shown that the two processes of bone demineralisation and vascular calcification occur simultaneously in older adults. These results cannot be extrapolated to children on account of the skeleton of children being in a different physiological and metabolic state (with ongoing mineralisation and growth). There have been no longitudinal studies in children examining bone demineralisation and vascular calcification and their potential association.

In this introductory chapter, I have set out the definitions of the conditions and disorders discussed, and elaborated on the epidemiology and clinical studies pertaining to chronic kidney disease-mineral and bone disorder in children and young people.

Section I- Definitions

1.1.1 Definitions: chronic kidney disease- mineral bone disorder (CKD-MBD)

The term chronic kidney disease-mineral bone disorder was coined to encompass the key processes that drive and cause the clinical manifestations of bone disease, cardiovascular disease and biochemical abnormalities, and to reflect their associations (Moe et al., 2006). The Kidney Diseases - Improving Global Outcomes body at the 2003 National Kidney Foundation Controversies Conference on Mineral Metabolism and Bone Disease in CKD (Moe et al., 2006) defined CKD-MBD as "A systemic disorder of mineral and bone metabolism due to CKD manifested by either one or a combination of the following":

1   Abnormalities of serum calcium, phosphorus, PTH, and vitamin D metabolism.

2   Abnormalities in bone turnover, mineralization, volume, linear growth, or strength.

3   Vascular or other soft-tissue calcification.

Table 1.1 Definition of CKD-MBD, its constituent processes and the clinical effects. Adapted from the 2009 KDIGO CKD-MBD Clinical Practice Guideline ('KDIGO clinical practice guideline for the diagnosis, evaluation, prevention, and treatment of

Chronic Kidney Disease-Mineral and Bone Disorder (CKD-MBD),' 2009).

CKD-MBD	
A systemic disorder of mineral and bone metabolism due to CKD manifested by either one or a combination of the following:	
Laboratory Abnormalities	Calcium, Phosphate, Parathyroid hormone, Vitamin D
Bone Abnormalities	Bone turnover, mineralisation, volume, growth or strength
Vascular Calcification	Extra-skeletal calcification
Resulting in: **Cardiovascular Disease** **Fractures** **Mortality**	

1.1.2 Pathogenesis of chronic kidney disease- mineral bone disorder

CKD-MBD arises through a complex interplay of the kidneys, bone and parathyroid glands. As the glomerular filtration rate reduces, through loss of nephron number,

irrespective of cause, the kidneys become increasingly unable to excrete phosphate sufficiently, leading to hyperphosphataemia (Borzych et al., 2010). In addition, the reduced hydroxylation of Vitamin D to 1,25-dihydroxyvitamin D from the kidneys leads in turn to reduced intestinal absorption of calcium resulting in hypocalcaemia. The combination of these two biochemical changes of hyperphosphataemia and hypocalcaemia, stimulates PTH production by the parathyroid glands and FGF23 secretion by osteocytes, in an attempt to maintain phosphate and calcium in the normal range (Wan et al., 2013, Portale et al., 2014, Levin et al., 2007). PTH acts on the phosphate sodium co-transporter inducing phosphaturia. FGF23 and its co-receptor, Klotho, activates FGF receptor 1 and induces renal phosphate excretion and suppresses 1a-hydroxylase activity (Bacchetta et al., 2012). In fact, a rise in FGF23 has been shown in early CKD stages, prior to clinically detectable PTH and phosphate serum rises (Portale et al., 2014, Isakova et al., 2011, Wesseling-Perry et al., 2012). A study by Isakova et al (Isakova et al., 2011) for the Chronic Renal Insufficiency Cohort Study Group, showed that FGF23 levels were markedly raised in an adult CKD cohort (n=3879), compared to healthy controls, even with normal phosphate and PTH levels. The serum levels of FGF23 increased significantly as the eGFR decreased. Similar findings were published by Portale et al (Portale et al., 2014), showing that FGF23 was raised in earlier CKD stages, compared to phosphate and PTH in 464 children.

There is a wide prevalence of vitamin D deficiency in children and adults with CKD (Shroff et al., 2017), and the absence of replete Vitamin D levels contributes to the lower 1,25-dihydroxyvitamin D levels and the development of the secondary

hyperparathyroidism.

The main aim of these compensatory pathways is the attempt to normalize the hypocalcaemia, by mobilizing calcium out of its primary reservoir, the bone, and reduce the hyperphosphataemia by increasing phosphaturia.

Section II- Bone Health in CKD
1.2.1 Normal Bone Formation and Growth

The major role of bone is often considered to be the mechanical function of providing an anchoring point for muscles and tendons, allowing mobility and maintaining structure and body posture. In fact, the skeleton is a metabolically active organ and is fundamental in the homeostasis of key minerals such as phosphate and calcium. It is comprised of organic and non-organic components, that are intricately linked in a continuous cycle of formation, resorption and re-formation called remodelling (Figure 1.2.1).

Figure 1.2.1. Cycle of bone remodelling by osteoblasts and resorption by osteoclasts.

(Adapted from Lalayiannis et al, 2019 (Lalayiannis et al., 2019))
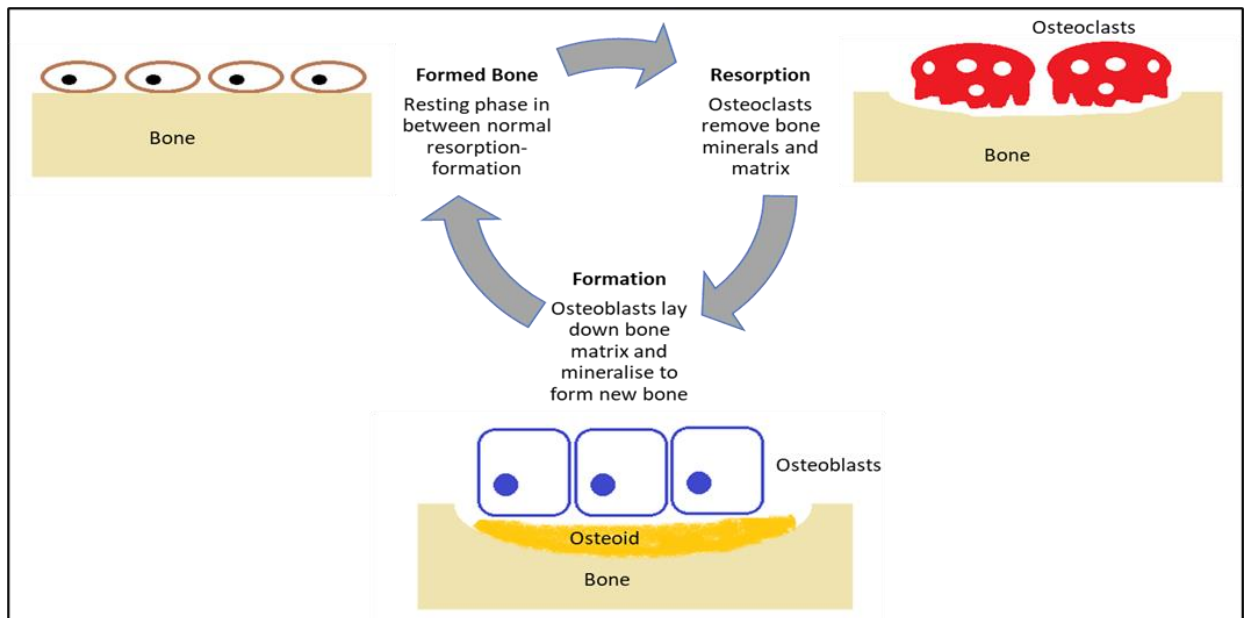
Initially, bone formation is driven by osteoblasts with an organic matrix deposition, that is then mineralised to form bone. Mineral deposition is a lengthy process and lags behind bone formation by around 30 days (Katsimbri, 2017). In trabecular bone- the innermost bone compartment- it completes in around 90 days, but cortical bone requires 120 days (Katsimbri, 2017). During periods of rapid growth such as in childhood and adolesence, mineralization lags behind bone formation by 6-12 months (Stagi et al., 2013b).

Once bone is formed, it undergoes a continuous process of remodelling through resorption and reformation. It is a perpetual process, with old bone being replaced by new bone (Kini and Nandeesh, 2012, Manolagas, 2000).

There are two main cell types that control remodelling; osteoblasts and

osteoclasts.

Osteoblasts produce an organic proteinaceous material by secreting procollagen. The end peptides are cleaved off during matrix formation resulting in type 1 collagen fibres. These fibres act as the scaffold around which mineralisation occurs (Vasikaran et al., 2011). Matrix vesicles in the osteoid release phosphates that combine with calcium to form hydroxyapatite [$Ca_5(PO_4)_3$ or $Ca_{10}(PO_4)_6(OH)_2$] (Katsimbri, 2017). Whilst hydroxyapatite is formed of calcium and phosphate primarily, the crystals also contain small amounts of sodium, magnesium and carbonate (Stagi et al., 2013b). These crystals are not water-soluble, so end up deposited in the spaces between the collagen fibres. This process of mineralisation continues, so long as there is sufficient phosphate and calcium (Orimo, 2010).

In a child's life, bone formation is paramount, but growth and height attainment on the path to adulthood require bone elongation. This longitudinal growth happens by modelling and bone formation between the epiphyses and metaphyses of the long bones. The so-called growth plates move gradually away from the bone centre producing the required elongation (Kuizon and Salusky, 1999, Bacchetta et al., 2012). There are several key influencers of this physiological process such as sex hormones, and nutrition. A fundamental driver is growth hormone, as it enables differentiation of chondrocytes to osteogenic cells, thereby increasing proliferation, increasing IGF1 production that stimulates expansion of the chondrocytes. This in turn increases type 1 collagen deposition and promotes further bone growth (Kuizon and Salusky, 1999). The largest

23

impact on bone formation and mineralisation is the availability of minerals, as the building blocks of the skeleton. The key mineral involved in bone mineralisation is calcium.

1.2.2 Calcium accrual from childhood through young adulthood

Bone modelling and formation are the processes by which bone is created and grows. This is the predominant driver in early life. The skeleton also relies on mechanical forces to adapt and change in shape (Frost, 2002). Remodelling is responsible for mineral homeostasis and repair of micro-damaged bone. It resorbs old bone and forms new bone. Whilst this is the predominant state in later life after maximum height is attained, it does occur during childhood. In the growing skeleton, the balance of modelling and remodelling is positive, tipped towards more bone mineral being laid down than resorbed. This allows for mineral accumulation and skeletal growth (Clarke, 2008, Seeman, 2003).

Bone mass -the amount of mineral deposited- on the other hand, depends on the balance between bone resorption and formation. Both phases of bone metabolism-modelling and remodelling - are crucial in order to maintain good bone strength and prevent fractures. The availability of minerals such as calcium is important to this process.

The bone is the natural reservoir of calcium in the body. More than 99% of the

calcium is stored in the skeleton. This calcium accrual begins in infancy, at which point the skeleton contains little calcium (25g) and continues until more than 1000g in elemental calcium is accrued by adulthood. This is an additional reason the childhood skeleton is in a positive balance and has a higher daily demand for elemental calcium (Matkovic and Heaney, 1992). It is vital, therefore that there is adequate dietary calcium available from childhood through puberty and young adulthood.

A way to study calcium uptake by the skeleton is by calcium balance studies. These are complex arrangements only practically done in research settings, where the study subject is given a precise amount of elemental calcium in the diet that has been measured. All excretions including urine and stool are measured for calcium. The subject is effectively placed in a metaphorical 'metabolic cage'. An aggregated report of 519 calcium balance studies performed on participants from birth to 30 years old, by Matkovic et al showed that calcium balance correlated positively with dietary or supplemental oral calcium intake. The highest calcium requirement was in the first year of life (503±91mg/day) and during pubertal growth (396±164mg/day), dropping thereafter to normal adult requirements (114±133mg/day) (Matkovic and Heaney, 1992). This suggests that the growing skeleton has a requirement for higher intestinal calcium absorption and uptake to keep up with the mineralisation process (Matkovic and Heaney, 1992).

Clinical studies that have examined bone mineral density by imaging have also associated oral calcium intake with mineral accrual in childhood (Chan et al., 1995,

Johnston et al., 1992). Bonjour and colleagues showed with a randomised double-blinded, placebo controlled study that in pre-pubescent girls, a higher dietary calcium intake is associated with a larger increase in radial and femoral BMD compared to placebo (Bonjour et al., 1997). A study of 82 twelve year old girls over 18 months showed that an increased dietary calcium intake (through increased dairy consumption) resulted in a significant increase of BMD (9.6% v 8.5%, p=0.02) and bone mineral content (27.0% v 24.1%, p=0.009) by DXA (Cadogan et al., 1997). A further randomised clinical trial of 354 girls, in pubertal stage 2 at entry into the study, over 4 years showed that oral calcium supplementation significantly influenced bone mineral density, with higher radial and total body BMD by DXA in the supplementation group (Matkovic et al., 2005).

Calcium isotope techniques have demonstrated that increased dietary calcium absorption is the main driver of net calcium accrual to bone in infants and adolescents (Abrams et al., 1991, Abrams, 1999). The higher calcium requirements in children are also reflected in the higher normal values for serum total calcium in children, particularly during periods of active growth in infancy. These reach adult levels by 5 years of age.

The 2016 US National Osteoporosis Foundation's review found that 90% of randomised control trials using calcium supplement pills showed a statistically significant effect on BMD and/or BMC accrual. This was especially seen in children with a lower calcium intake at baseline (Weaver et al., 2016).

In summary, dietary calcium intake is fundamental to bone mineral density and mineral content deposition.

1.2.3 Peak bone mass

The positive balance of mineral acquisition by the skeleton starts in infancy and continues into adulthood. A cross sectional study of over 300 infants and toddlers showed that between ages 1 and 36 months, lumbar spine BMC increased about 5-fold and aBMD by DXA increased 2-fold (p<0.0001). There comes a point at which the maximum genetic and environmentally determined amount of mineral is deposited, after which there is a gradual decline and the modelling/resorption cycle tips towards a negative state. The point at which the mineralisation reaches its zenith is termed 'peak bone mass'. PBM is defined as 'the amount of bone gained by the time a stable skeletal steady state has been attained during adulthood' (Weaver et al., 2016) (Figure 1.2.2).

Figure 1.2.2 Bone mass trajectory through life and peak bone mass (Adapted from Weaver et al, 2016 (Weaver et al., 2016))
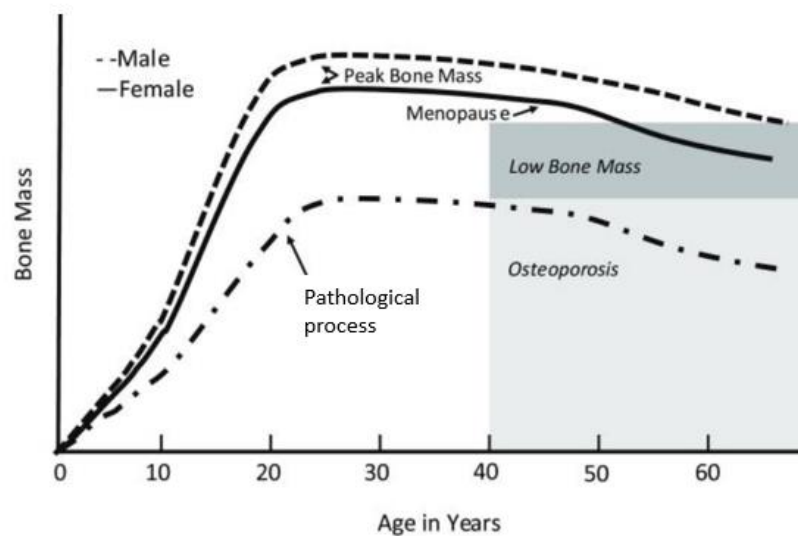
Peak bone mass is reached in the third or fourth decade of life, after which there is a natural decline.

PBM is an important concept and milestone in the lifecycle of the skeleton, as depending on the mass reached, the individual may enter a low bone mass state or an osteoporotic state later in life. There is a natural decline after the age of 40 years, known to be exacerbated with the menopause in healthy women. Any pathological condition or disorder which disrupts the mechanism of calcium intake, metabolism and deposition in the bones may lead to poor mineralisation (Weaver et al., 2016).

The attainment of PBM is not achieved at the same age uniformly. Clinical studies have shown the timing differs by sex and by skeletal site. A large regional cohort follow up study in Canada called the Saskatchewan Pediatric Bone Mineral Accrual Study followed 164 children, aged 8-14 years, into their early 30s with dietary information and whole body DXA scans (Whiting et al., 2004, Baxter-Jones et al., 2011). They examined the relationship between sex, age, height velocity, height attainment and PBM through DXA imaging. They showed that physical growth and height gain precedes mineralisation. Peak height velocity was reached at 11.8 years for females and 13.5 years for males. PBM (defined as highest bone mineral content by total body DXA) was reached an average of 7 years after peak height velocity. Maximum bone length was reached 5 years after peak height velocity, and bone mineralisation 2 years after that (18.8 and 20.5 years for females and males respectively). At important frequently imaged sites, such as the hips and lumbar spine, PBM was achieved 5 years after PHV (Baxter-Jones et al., 2011). This would suggest that PBM occurs by the end of the second or early in the third decade of life.

A study of 156 healthy adult women, showed that the mineral accrual stopped by 28.3 to 29.5 years of age (Recker et al., 1992). Lin et al, studying 300 healthy girls and women aged 6 to 32 years, found that bone mineral content was highest in the early twenties (23.0 ±1.4 years); but increases in bone mineral content were seen into the early thirties (Lin et al., 2003). These cross-sectional studies suggest that PBM is achieved in the third or early fourth decade of life.

In summary, approximately 25% of PBM is formed around the two year interval of PHV which happens in adolescence (Baxter-Jones et al., 2011), but PBM is likely achieved by the end of the third decade of life. As bone mineral accrual in infancy, childhood and adolescence is closely linked with calcium intake and particularly oral calcium absorption (Chan et al., 1995, Johnston et al., 1992), any condition which disrupts this mechanism may lead to poor mineralisation (Weaver et al., 2016), and PBM may not be achieved.

1.2.4 Bone mineralisation and fractures

PBM is considered to be a foundation of good quality bone, and a key determinant of bone strength, alongside density, microarchitecture and geometry. As the mineral components of bone account for two thirds its dry weight (Stagi et al., 2013b), it is important to recognise that normal bone mass accrual during growth is key in preventing fractures in later life (Weaver et al., 2016). In a prospective study of 125

healthy girls over 8 years, girls who sustained at least one fracture (n=42, cumulative incidence 46.6%) were more likely to have lower bone mass by DXA (Ferrari et al., 2006). Conversely, a study of children who had sustained a forearm fracture (n=224) and non-injured controls (n=200) showed that both BMD by radial pQCT (-0.9%, p<0.05) and by radial, spine, and hip DXAs (-2.7 to -3.3%, p<0.01) was lower in children with fractures than controls (Kalkwarf et al., 2011).

This is significant for two reasons. Firstly, any fracture in childhood has been shown to increase further fractures. In a retrospective cohort follow up study of 601 individuals between birth and 18 years of age showed that any previous fracture in childhood increased the HR for a subsequent fracture by 1.90 (95% CI 1.51 to 2.39) after one fracture. This HR for a subsequent fracture increased to 3.04 (95% CI 2.23 to 4.15) after a second fracture (Goulding et al., 2005). Secondly, any fracture in childhood or adolescence increases the risk of a subsequent fracture in adulthood. In a mixed methods study (retrospective fracture questionnaire/prospective radiology) of over 1600 individuals, a childhood fracture increased the risk of a subsequent teenage fracture [males: RR 21.7; 95 % CI 16.0, 27.4; females: RR 8.1; 3.5, 12.8]. Adolescents with a fracture had an increased risk of an additional fracture in young adulthood [males: RR 11.5; 5.7, 17.3, females: RR 4.3; 0.7, 7.9] (Holloway et al., 2015). So bone mineralisation is key for fracture prevention in the normal healthy state. Any pathological process that affects PBM attainment may weaken the bones. This combined effect may mean that childhood CKD-MBD affects the bone in a significant manner as it affects bone turnover, volume and mineralisation, thereby contributing to an increased fracture incidence both

in childhood and in later life.

1.3 Effect of CKD-MBD on bone

With the progression of CKD, the glomerular rate reduces, leading to increasing impairment of phosphate excretion (Borzych et al., 2010). In addition, the reduction in Vitamin D activation by the kidney leads to less intestinal absorption of calcium, exacerbating hypocalcaemia. The combination of hyperphosphataemia and hypocalcaemia lead to increased FGF23 excretion by osteocytes and PTH production by the parathyroid glands (Wan et al., 2013, Portale et al., 2014, Levin et al., 2007). Both hormones target tubular receptors (such as the sodium phosphate co-transporter) to increase phosphaturia (Hruska et al., 2015). PTH increases bone resorption and turnover, thus mobilising calcium from the bone to achieve normocalcaemia (Denburg et al., 2016, Oh et al., 2002, Shroff et al., 2007). There is an additional suggested mechanism, by which FGF23 directly inhibits Wnt signaling pathways, preventing bone mineralisation, thus keeping elemental calcium more freely available (Carrillo-Lopez et al., 2016). (Figure 1.3)

Figure 1.3 Simplified schematic representation of the mineral dysregulation in CKD

(adapted from (Lalayiannis et al., 2019))
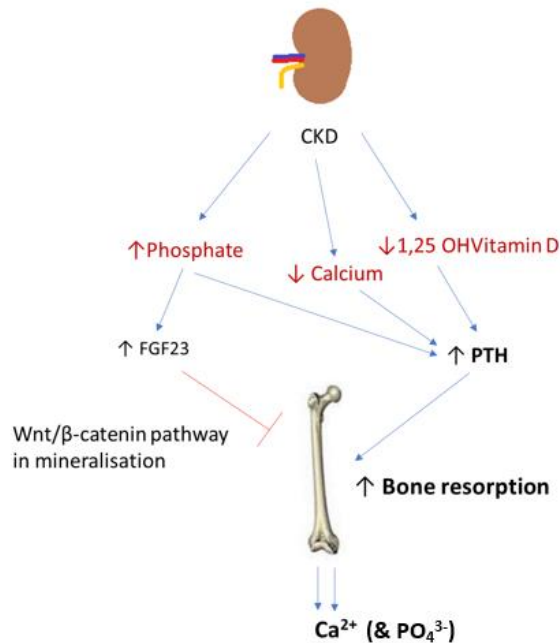
Hyperphosphataemia and hypocalcaemia lead to increased FGF23 and PTH secretion, with the aim of maintaining mineral homeostasis. These compensatory mechanisms can have a negative effect on bone mineral content.

These compensatory mechanisms, placing normocalcaemia as the key homeostatic priority, disadvantage the bone. The higher bone turnover and resorption, combined with impaired mineralisation can lead to a poorer bone quality. This includes disrupted bone architecture and decreased BMD, leading to an increased fracture risk (McNerny and Nickolas, 2017, Vasikaran et al., 2011).

1.4 CKD-MBD effects on Bone & Fractures

The effect of CKD on bone is multifaceted. CKD-MBD affects bone modelling,

remodelling and growth. This is due to increased FGF23 and PTH levels, mobilization of minerals out of bone stores and impaired mineralisation. Whilst the complete pathway and processes that lead to this defective mineralisation have not been elucidated completely (Wesseling-Perry, 2015), other effects of CKD such as poor exercise tolerance, restricted diet and poor appetite can all affect the quality of bone. It is known that the effect on bone can be seen even in early CKD stages (Denburg et al., 2013). Bone quality, and by extension strength is reliant on multiple aspects of bone structure including cortical thickness, mineralisation, bone mass and microarchitecture (Jarvinen et al., 2005, Gabel et al., 2017). CKD in a crucial period of bone development, as is the period through childhood, affecting mineral deposition can have many patient level consequences such as pain, deformities and fractures (Bacchetta et al., 2012, Wesseling-Perry and Salusky, 2013).

The important clinical effects of CKD-MBD in childhood are indeed known to include bone pain, limb deformities, and a higher fracture incidence in children with CKD compared with their healthy peers (Denburg et al., 2013, Groothoff et al., 2002b). Bone disease and growth stunting has been reported in as many as 50% of children with CKD, who do not attain their predicted height (Haffner et al., 2000).

A registry study of the International Pediatric Peritoneal Dialysis Network, showed that 15% of 890 children and adolescents had clinical symptoms and/or radiological signs of bone disease. These included radiological signs of osteodystrophy & rickets (9.4%), radiological osteopenia (4.5%), limb deformities (5%) and bone pain

(1.4%) (Borzych et al., 2010). Amongst the patients followed up over a year (n=271), 7.4% (n=20) continued to have bone disease, and 6.3% (n=17) developed de novo symptoms. The height SDS for this cohort was -2.43 ±1.64 at study entry, with 39% being below the third centile for sex and age. For the young people followed up, mean annual change in height was negative (-0.03± 1.1), indicating a continued growth impairment. In fact, children with higher PTH levels (>500ng/ml) had a more significant loss of height SDS (-0.28±0.52 SDS) per year compared to children with lower PTH levels (-0.05±0.71; p<0.05) (Borzych et al., 2010).

It is well documented that adults with CKD and on dialysis have a substantially increased risk of fractures and bone related morbidity and mortality (Alem et al., 2000, Ball et al., 2002, Mittalhenkle et al., 2004, Jadoul et al., 2006, Nickolas et al., 2006). The relative risk of hip fracture is high in young adults (<45yrs old) on haemodialysis, and hip fractures are associated with a more than 4-fold increase in mortality in dialysis patients compared to healthy peers (Alem et al., 2000, Coco and Rush, 2000, Tentori et al., 2013).

This has been shown recently in the younger CKD population. The *CKD in Children* study (CKiD) was a prospective cohort study of 537 children with CKD (22% in CKD stages 1-2, 61% in CKD stage 3) and followed up through 5 years. The median age of participants was 11 years and at enrollment, 16% reported a previous fracture. Importantly, during follow up, 67 children (43 boys and 24 girls) sustained at least one fracture. This corresponded to 395 fractures per 10,000 person-years for males and 323/10,000 person-years for females. The fracture rates were 2.4- and 3- fold higher, respectively,

than gender-specific rates of 162/10,000 person-years and 103/10,000 person-years reported in a large population-based study of fracture epidemiology in healthy children and adolescents (Cooper et al., 2004, Denburg et al., 2016). The fracture rates also exceeding those reported in a study of 12 000 adult haemodialysis patients (Jadoul et al., 2006). The CKiD study identified several independent factors associated with the increased fracture incidence. These factors were: baseline walking difficulty (HR 2.43, 95% CI 1.13-5.25, p=0.02), Tanner stages 4-5 (HR 2.38, 95% CI 1.08-5.21, p=0.04), greater height z-score (HR 1.25, 95% CI 1.01-1.55, p=0.04), higher PTH levels (HR 1.5, 95% CI 1.02, 2.22, p=0.04), and competitive sports participation (in ≥1 sport: HR 2.35, 95% CI 1.01-5.47, p=0.047; in ≥2 sports: HR 4.87, 95% CI 2.21-10.75, p<0.001). The authors also identified the only protective factor was phosphate binder use (HR 0.37, 95% CI 0.15-0.91, p=0.03). The use of a binder afforded a 63% lower fracture risk. Whilst the study was not powered to examine calcium vs non-calcium based phosphate binders, it is noteworthy that 82% of participants were on calcium containing binders, and that phosphate and FGF23 levels did not correlate with fracture risk (Denburg et al., 2016). This suggests that the calcium intake from the phosphate binder use may contribute to the beneficial effect.

Fractures and their precise association to bone mineral density have also been examined in a prospective study of 171 children and young adults (age range 5-21 years) in CKD stages 2-5 and on dialysis, with the use of tibial pQCT (Peripheral Quantitative Computed Tomography is explored and discussed in detail in subsequent chapters). The authors identified a higher fracture risk per 1 SD decrease in baseline BMD (HR 1.75,

95%CI 1.12-2.67,p=0.009) in 89 children followed up over a year. Of the follow up cohort, 6.5% suffered at least one fracture in the study's one year follow up period (incidence 556/10,000 person-years). The fractures occurred in distal long bones such as the clavicles, tibia, toes and radius. These fractures were sustained in low impact traumas, such as normal daily exercise and benign falls. Fracture risk was independently associated with any period of rapid growth in adolescence, lower calcium and 25OHD levels, and higher PTH at baseline. All were associated with lower baseline cortical BMD scores (Denburg et al., 2013). The annual change in cortical BMD was associated with baseline calcium (β -0.50, p=0.008), change in calcium (β 0.71, p=0.002), change in iPTH (β -0.28, p=0.001), and worsening renal function (β 0.10, p=0.01). This suggests perhaps that worsening renal function, hypocalcaemia and secondary hyperparathyroidism during childhood and adolescence all contribute to the increased fracture risk. There may also exist a difference depending on race background, as the CKiD study found that Black children had lower odds (OR 0.26; CI, 0.14 to 0.49; p = 0.001) of any fracture than white children at study entry (Laster et al., 2021).

The effects of childhood CKD-MBD are not limited to childhood. They have long reaching and lasting consequences into adulthood. A study of 249 young adults with onset of CKD stage 5 in childhood and followed up into adulthood showed that 36.8% had symptoms of bone disease (deformities, bone pain, aseptic bone necrosis and atraumatic fractures). 17.8% were disabled by bone disease and 61% had severe growth restriction. DXA imaging at the point of study showed very low bone mineral density z-scores at the lumbar spine (-2.12 ± 1.4) and at the femoral neck (-1.77 ± 1.4) (Groothoff

et al., 2003). In this study, 13.4% of participants had suffered at least one fracture (Groothoff et al., 2003).

Whilst the aforementioned studies document fractures and bone disease in young people in CKD stages 2-4 predominantly, it would appear that the bone disease burden from the pre-transplant period in the course of CKD may be further exacerbated post transplantation. In a prospective Finnish study of 196 children who had received a solid-organ transplant (n= 123 post kidney transplantation, 44 liver, 29 heart), followed up for 5 years, 38% of patients had at least one fracture (166 fractures in n=75 patients). This equated to a 6-fold higher fracture risk compared to the control population (All fracture incidence: 92 vs 14 fractures/1000 persons/year; $p<0.001$) and 160-fold higher vertebral fracture risk (57 vs 0.35 fractures/1000 persons/year; $p<0.001$) (Helenius et al., 2006a). Other smaller studies have shown similar findings (Valta et al., 2009, Tamminen et al., 2014, Daniels et al., 2003). This may be due to immunosuppressive regimens used as the majority of the participants in these studies were prescribed glucocorticoids, but also the persisting mineral dysregulation post transplantation. A large, European registry study of 1237 children showed that 19% had hypocalcaemia and 40% had a high PTH three years after transplantation (IQR 1.1–6.2 years) (Bonthuis et al., 2015). Even young adults, following kidney transplantation in childhood report significant bone pain and fracture burden (Bartosh et al., 2003, Helenius et al., 2006b). Forty young adults (16-27 years old) following childhood transplantation reported vertebral fractures (20%), and frequent back pain (28%) (Helenius et al., 2006b). In a survey of 57 adults post childhood renal transplantation, 19% of women and 26% of men reported at least one fracture post

transplantation (Bartosh et al., 2003).

In conclusion, MBD is prevalent in children and young people with CKD, and is associated with significant morbidity. The dysregulated mineral metabolism has a profound effect on the growing skeleton, manifesting as stunted growth, bone pain, bone deformities and fractures. These pervasive effects persist into adulthood and post transplantation.

1.5 Assessing bone health

Clinical studies have shown there is a link between bone mineral density and clinical patient level outcomes such as fractures. Assessment of bone health and bone mineral density is complex, and the methods to do so can be categorised into invasive, such as bone biopsy and non-invasive, such as radiological imaging and serum biomarkers.

1.5.1 Assessing bone- Serum Biomarkers

Although not the primary focus of this thesis, serum biomarkers of bone metabolism have been used to assess bone metabolism, or the rate of bone turnover and as surrogate measures of mineralisation. Briefly, bone biomarkers can be separated

into three broad categories. Those of bone formation, resorption and those secreted by osteocytes.

Bone formation markers generally reflect the activity of osteoblasts and correlate closely with the production of type 1 collagen (Vasikaran et al., 2011). Bone formation markers include bone specific alkaline phosphatase, osteocalcin, P1NP and P1CP. Type 1 collagen is a proteinaceous material that accounts for more than 90% of the organic component of the bone matrix (Stagi et al., 2013b). Once the collagen structure is formed, mineral deposition begins around it. Bone specific alkaline phosphatase reflects bone formation rate (Delanaye et al., 2014). BSAP varies with age and gender (Fischer et al., 2012). As would be expected with a bone formation marker, it increases at the start of puberty, is associated with height velocity and is higher in adolescent boys (Fischer et al., 2012).

Bone resorption markers include carboxyterminal cross-linking telopeptide of bone collagen (CTX) and tartrate-resistant acid phosphatase (TRAP5b). These markers arise as a result of the type 1 collagen breakdown during resorption (Vasikaran et al., 2011). Osteocytic markers such as Phosphate-regulating gene with Homologies to Endopeptidases on X chromosome (PHEX), Dentin Matrix Protein-1 (DMP1), Matrix Extracellular Phospho-glycoprotein (MEPE), sclerostin and FGF23 can regulate both osteoblastic and osteoclastic activity (Bonewald, 2011).

Whilst PTH and ALP are used in clinical practice, none of the above research biomarkers have been shown to be sensitive or specific enough to diagnose

mineralisation or bone turnover abnormalities (Sprague et al., 2016, Behets et al., 2015). There appears to be a large age, gender, pubertal stage, fasting status and circadian rhythm variation and assays are not always standardized for universal use (Glendenning, 2011, Fischer et al., 2012).

Larger pediatric studies that correlate the bone biomarkers above with the gold standard of bone histomorphometry as well as patient level outcomes such as fractures are required. PTH and ALP have been the biomarkers most commonly studied in bone biopsy studies, to ascertain their usefulness in assessing bone health in clinical practice.

1.5.2 Assessing bone- Bone biopsy

The gold standard method to assess bone is by bone biopsy. This allows for detailed assessment of the static and dynamic processes of the bone metabolic cycle. The histomorphometric categories examined are bone turnover, mineralisation and volume. This has been termed the 'TMV classification' by KDIGO ('KDIGO clinical practice guideline for the diagnosis, evaluation, prevention, and treatment of Chronic Kidney Disease-Mineral and Bone Disorder (CKD-MBD),' 2009). Low, normal or high turnover reflects the amount of resorption/formation occurring at bone level.

Bone biopsies are taken with a core needle from the iliac crest. The procedure requires a general anaesthetic in children and a prior tetracycline labeling dosing regimen (Torres et al., 2014). The tetracycline stains the bone at two time points, and

due to its UV fluorescence properties, the dynamic features of bone formation can be assessed under a microscope.

Bone biopsy studies have attempted to correlate serum biomarkers such as PTH to biopsy findings but often with mixed results (Table 1.5.2).

Table 1.5.2 Summary table of notable bone histomorphometric studies in paediatric CKD (adapted from (Lalayiannis et al.,

2019))

Authors, Year	Population (n=)	Age of population (yrs)	Key Findings on bone biopsies	Correlations with PTH	Limitations	Comments
Salusky et al, 1988 (Salusky et al., 1988)	PD (44)	6-18	Normal histology in 16% Osteitis fibrosa in 39% Aplastic lesions in 11% Osteomalacia in 9%	Bone formation rate and larger resorption areas correlated with PTH (p<0.001) PTH values were 2-3x higher in osteitis fibrosa patients	Study prior to TMV criteria. Aluminium hydroxide main phosphate binder	Focus of study primarily on aluminium staining- as aluminium hydroxide used as main type of phosphate binder.
Mathias et al, 1993 (Mathias et al., 1993)	HD (21)	16-19	High turnover disease in 38% Osteitis Fibrosa in 23% Adynamic bone in 28%	Bone formation rate corelated with PTH as well as resorption areas (p<0.001).	Study prior to TMV criteria. Aluminium hydroxide main phosphate binder	PTH also correlated inversely with serum Ca levels (p<0.001)
Goodman et al, 1994 (Goodman et al., 1994)	PD (14)	13-14	*Before calcitriol:* Osteitis Fibrosa in 79% *After calcitriol:* Normal in 43% Adynamic in 43% Osteitis fibrosa in 7% Mixed in 7%	A PTH of below 200pg/ml was strongly suggestive of adynamic bone disease	Small number of patients	Aim of study was to look at effect of intermittent calcitriol therapy over 12 months on bone biopsy indices
Salusky et al, 1994 (Salusky et al., 1994)	PD (55) [68 bone biopsies]	8-19	Osteitis fibrosa in 50% Mild hyperparathyroidism in 9% Adynamic bone lesions in 22% Normal in 19%	High PTH values strongly correlated with osteitis fibrosa lesions vs mild, adynamic or normal histology (p<0.001)		PTH >200pg/ml and Ca <10mg/dl was 85% sensitive and 100% specific for high turnover lesions PTH <200pg/ml 100% sensitive, 79% specific for adynamic bone lesions

Yalçinkaya et al, 2000 (Yalcinkaya et al., 2000)	PD (17)	7-20	High turnover disease in 47% Low turnover disease in 29% Mixed in 24%	High PTH values were significantly correlated to high turnover disease (p<0.01) vs low turnover	Small number of patients	Mean serum Ca levels higher in low turnover group vs high turnover group (p<0.001) Serum PTH >200pg/mL was 100% sensitive and 66% specific in identifying high turnover.
Ziólkowska et al, 2000 (Ziolkowska et al., 2000)	HD (21), PD(30)	7-15	Adynamic bone disease in 27% Normal bone in 37% Osteomalacia in 2% Hyperparathyroidism in 24% Mixed lesions in 10%	Higher PTH significantly correlated with high turnover disease vs adynamic or normal bone.		Serum PTH >200 pg/mL: 75% sensitive and 95% specific for identifying high-turnover disease In patients with normal bone turnover, 69% had PTH level of 50–150 pg/mL
Waller et al, 2008 (Waller et al., 2008)	Pre-Tx (11)	7-16	Low bone turnover disease in 18% Mixed lesions in 27% Hyperparathyroidism in 36%	PTH>3x ULN associated with high turnover Normal range PTH associated with low turnover	Small number of patients	
Bakkaloglu et al, 2010 (Bakkaloglu et al., 2010)	PD (161)	0-20	Low turnover in 4% Normal turnover in 39% High turnover in 57% Abnormal mineralisation in 48%	Higher PTH significantly correlated with high turnover disease vs low turnover or normal bone.		For any level of turnover, PTH was higher if mineralisation defects were present (p<0.01). PTH<400 pg/mL and ALP<400 IU/L provided the highest prediction of normal bone turnover and mineralisation
Wesseling-Perry et al, 2012 (Wesseling-Perry et al., 2012)	CKD2-5 (52)	2-21	High bone turnover in: 13% with CKD3 29% with CKD 4/5 Defective mineralisation in: 29% with CKD2 42% with CKD3 79% with CKD4/5	PTH was elevated in 36% of patients with CKD2, 71% with CKD3, and 93% with CKD4/5		PTH was directly linked to poor mineralisation (p<0.05)

Carvalho et al, 2015 (Carvalho et al., 2015)	PD (22)	2-16	High bone turnover in 54% Low bone turnover in 23% Normal turnover in 23%	PTH values higher in patients with high bone turnover (p<0.05) and mineralisation (p<0.01)	Small number of patients	Bone turnover correlated with alkaline phosphatase also (p<0.01)
Pereira et al, (Pereira et al., 2016)	HD, PD (68)	9-18	High bone turnover in 43% Normal bone turnover in 34% 'Adynamic bone' in 13% Osteomalacia 11%	Bone formation did not correlate with microCT. Bone volume measurements correlated highly with microCT	Bone biopsies from 1983 included. Likely very different treatments received	Correlations o bone histomorphometry with microCT findings discusses

Bakkaloglu et al examined bone biopsies of 161 children and young adults (up to 20 years old) on PD (Bakkaloglu et al., 2010). They showed that up to 48% of patients had mineralisation defects. Abnormal mineralisation was found in 58% of participants with high bone turnover, 38% with normal turnover and 29% with low turnover. Serum PTH and alkaline phosphatase correlated with bone turnover (r=0.61, p<0.01 and r=0.51, p<0.01 respectively) and serum calcium was inversely related to mineralisation (r=-0.35, p<0.01) but not bone turnover. The authors demonstrated that when both PTH and alkaline phosphatase levels were within 2xULN normal bone turnover and normal mineralisation were seen. Overall, higher PTH values and lower calcium values were associated with abnormal mineralisation (Bakkaloglu et al., 2010).

Salusky et al, examining biopsies of 55 children, found that serum calcium levels were higher in patients with low bone turnover (previously known as 'adynamic bone') or normal bone than in those with high PTH values. Phosphate, alkaline phosphatase and PTH levels were higher in patients with osteitis fibrosa. The combination of a high serum PTH and normal calcium value was 85% sensitive and 100% specific for identifying patients with high-turnover bone disease (Salusky et al., 1994). In general, all high turnover disease was associated with high PTH levels (>3 ULN) whereas low bone turnover and normal bone turnover were associated with lower PTH values. PTH lacked the sensitivity and specificity to distinguish between the two however.

Ziolowska et al, used biopsy findings from 51 children on PD or HD to show that high serum PTH (>200 pg/mL) was 75% sensitive and 95% specific for identifying high-turnover disease. In contrast, in patients with normal bone turnover, 69% had a PTH level

of 50–150 pg/mL (Ziolkowska et al., 2000). Overall, it is accepted that PTH may not be an effective discriminator between low and high turnover bone disease, especially in the ranges where most patients' PTH values are found (100-1000 ng/L) (Barreto et al., 2008b).

In summary, bone biopsy does offer a wealth of information and a very detailed approach to assessing the metabolic state of bone with the histomorphometric TMV classification. The 2017 KDIGO guidelines suggest that bone biopsy should be done if it is likely to affect treatment or influence management of the patient (Ketteler et al.). Despite this, due to the procedure's invasiveness and the scarce resource of expertise in histological reading of the biopsies, this is now rarely done in routine clinical practice. Bone biopsy is largely constrained to the research domain (Bakkaloglu et al., 2020).

1.5.3 Assessing bone- Available imaging techniques

In the absence of routinely available bone biopsy, imaging modalities have been employed to assess bone mineral density as a surrogate marker of bone health. There are a variety of imaging modalities available, both using ionizing radiation and no radiation, which are outlined below.

1.5.3.1 Assessing bone- Dual Energy X-ray Absorptiometry

DXA scanning is available in routine clinical practice, and is used in a variety of paediatric diseases where assessing bone mineral density is an important measure of the pathological process (Wasserman et al., 2017).

A DXA scanner produces X-rays that pass through the body of the subject and are detected on the opposite side by an electronic plate. The low level radiation (4-27microSv), at 2 different energies, enables the differentiation of soft tissue and bone (Crabtree and Ward, 2015, Adams et al., 2014). DXA allows for measurement of areal bone mineral density (g/m^2). This is calculated as bone mineral content (BMC) over projected bone area (BA). DXA scanners allow for measurements to be made at any body site. These include the spine, hips, radius or whole-body/total body (Crabtree and Ward, 2015). In paediatric practice, the commonest sites are the lumbar spine and total body less head (TBLH) (Messina et al., 2018). In adults, the hips and spine are used as this provides an assessment of sites that are particularly prone to pathological fractures.

In children, lumbar spine DXA is particularly useful because vertebrae consist of mainly trabecular bone, and this site is readily influenced by pathologic processes, due to the high metabolic rate of trabecular bone (Wasserman et al., 2017). Changes with growth and variations in development limit the use of the femoral site in pre-pubertal children, as there are yet no universally accepted way to standardize growth changes in hip DXA images. Overall, DXA scanning is objective, as it doesn't rely on the operator heavily and is fast to produce the imaging. Although the image acquisition can be

blurred by movement in very mobile children, it is not generally prone to motion artefact (Crabtree et al., 2014).

The two main pieces of information delivered by the DXA scanner software are the aforementioned bone mineral content and bone area. BMC (measured in grams) represents the amount of mineral -predominantly calcium- found in the bone. The area of bone (measured in cm^2), is the projected area of the X-rays. The ratio of the two, BMC/BA provides the areal bone mineral density of the bone imaged. The software produces the aBMD automatically, and generates the z-score of the measurements from age, sex and ethnicity matched reference databases (Gordon et al., 2014). As with any z-score, if it is below 2 standard deviation points (-2SD) this indicates an abnormally low BMD for age/sex/race (Messina et al., 2018).

It is important to note that aBMD represents a 2-dimensional image of a 3-dimensional structure. In growth restricted or short children, as the projected bone area will be smaller it may provide a misleading overestimation of BMD (Figure 1.5.3.1) (Zemel et al., 2010) or overestimate BMD in a tall child (Crabtree and Ward, 2015).

Figure 1.5.3.1. Schematic representation of DXA imaging and how size can affect areal density. (Adapted from (Fewtrell, 2003))

$2 \times 2 \times 2$ cm $3 \times 3 \times 3$ cm

Mineral weight = 16 g
Volume = 8 cm^3
Projected area = 4 cm^3
Volumetric density = 2 g/cm^3
Areal density = 4 g/cm^3

Mineral weight = 54 g
Volume = 27 cm^3
Projected area = 9 cm^3
Volumetric density = 2 g/cm^3
Areal density = 6 g/cm^3

To avoid overestimation of BMD, lumbar spine DXA aBMD results are therefore adjusted for bone size (ie growth or height of the child). The size-adjusted density measurements are known as Bone Mineral Apparent Density (BMAD). The aim of the size adjustment is to try and estimate the bone density in g/cm^3. This is consistent with the 2013 International Society of Clinical Densitometry (ISCD) Pediatric Official Positions (Crabtree et al., 2014). Reference data for lumbar spine BMAD in healthy children are available from 3598 healthy 4 to 20-year-olds from 7 UK centres (Crabtree et al., 2017). Other healthy reference datasets, adjusting for growth or height are also available (Kalkwarf et al., 2007, Ward et al., 2007, Zemel et al., 2011, Chastin et al., 2014).

An additional drawback of DXA imaging is that it superimposes the two bone compartments, cortical and trabecular bone. This means that certain sites, such as the lumbar spine are considered mainly 'trabecular sites', and others, such as the hips, mainly 'cortical sites'. Regardless, separate study of cortical or trabecular bone is not possible.

Despite this drawback, DXA imaging has been used to study CKD-MBD. In fact, in recent years, there has been emerging evidence that lower BMD by DXA is in fact predictive of an increased fracture risk in adult CKD patients. In general, the recommended imaging site in adults is the hips, as they are a major site for pathological fractures, and any possible aortic calcification can hinder the interpretation of the lumbar site imaging in the antero-posterior direction. A study of 2754 older adults showed that low BMD by femoral head and total hip DXA were associated with a higher fracture risk regardless of CKD stage (Hazard Ratio 2.69, 95% CI 1.96- 3.69) (Yenchek et al., 2012). Adult patients with lower total hip (p=0.0006) or whole body (p=0.006) BMD were more likely to have new fractures in a prospective longitudinal study (Iimori et al., 2012). Two further cross-sectional studies by Nickolas et al have shown associations between hip BMD and fracture history in adults with CKD (Nickolas et al., 2006, Nickolas et al., 2011).

DXA has been employed to study CKD-MBD in children as well, and a summary of important studies is provided in Table 1.5.3.1.

Table 1.5.3.1. Summary of key studies employing DXA in childhood CKD (Adapted from (Lalayiannis et al., 2019))

Authors, Year	Population (n=)	Age of population (yrs)	DXA	Key Findings	Biochemical Correlations	Limitations	Comments
Dialysis (Haemodialysis & Peritoneal Dialysis) & Chronic Kidney Disease							
Pluskiewicz et al, 2002 (Pluskiewicz et al., 2002)	HD&PD (30; 11 HD, 19 PD)	9-23	LS, TB	Low spine and TB BMD Z-scores (-1.47 & -1.53). These also correlated with each other (p<0.0001) and with dialysis vintage (p<0.05).	No correlation found between BMD and Ca, iPTH and P. iCa correlated with low spine BMD.	No longitudinal data Small number of participants	
Pluskiewicz et al, 2003 (Pluskiewicz et al., 2003)	CKD5, HD & PD (40; 15 CKD5, 9 HD, 16 PD)	7-19	LS, TB	Low spine and TB BMD Z-scores in all CKD Population. Dialysis vintage correlates with low TB-BMD in dialysis population (p<0.05)	High iPTH correlated with low TB-BMD Z-scores in predialysis patients (p<0.05).	Small number of participants	Study compared DXA with QUS also, with QUS parameters lower in CKD population
Bakr, 2004 (Bakr, 2004)	CKD5 &HD (65; 21 CKD5, 44 HD)	3-16	LS	61.9% of predialysis children had low LS BMD and 59.1% of HD patients	LS Z-scores of the osteopenic children negatively correlated with P (p=0.004), iPTH (p=0.03), and ALP (p=0.02). There was a positive correlation between LS Z-scores and 25OHD	Biochemical analysis only done in children with low Z-scores	
Pluskiewicz et al, 2005 (Pluskiewicz et al., 2005)	HD& PD (18; 9 HD, 9 PD)	8-21	LS, TB	Longitudinal data over 2 years showed TB Z-score was lower at end of study compared to baseline (p<0.05). Spine BMD was lower at end of study compared to baseline (p<0.01) in participants without GC use, and those with (p<0.05).	iPTH, Ca, iCa and P did not correlate with skeletal measures.	Small number of participants Comparisons are done in 2 groups; GC use and no GC use	Study compared DXA with QUS. Significant population overlap with the 2 aforementioned studies, as this study provides the longitudinal follow up.

Andrade et al, 2007 (Andrade et al., 2007)	HD&PD (20; 6 HD, 14 PD)	4-17	LS	25% had LS Z-scores <-2 SD, but these improved when adjusted for height. 60% of children has low-bone turnover disease.	No correlations found between bone turnover and Ca, P, PTH or ALP	Small number of participants. No comparison of DXA BMD with biochemical findings. Limited mineralisation reporting on bone biopsies	LS BMD z- scores improved when adjusted for height. BMD did not correlate with high or low bone turnover

Chronic Kidney Disease

van der Sluis et al, 2000 (van der Sluis et al., 2000)	CKD3-5 (33)	3-12	LS, TB	LS BMD increased with rhGH; ΔSDS 0.72/year (p<0.01) No change was seen with TB BMD	ALP increased in the growth hormone group significantly (p<0.05)	Study aimed at comparing GH use vs No GH use over 2 years	The study compared 18 children with CKD receiving rhGH vs 15 who did not over 2 years.
Van Dyck et al, 2001 (Van Dyck et al., 2001)	CKD 4-5 (10)	2-8	LS, TB	LS and TB BMD Z-scores increased after one year of rhGH treatment (p<0.01 and p<0.05)	After one year of rhGH, there was a significant rise in ALP from 308 u/L (124±621) to 720 u/L (226±1067)	Study aimed at comparing BMD before and after one year of rhGH treatment. Small cohort.	
Waller et al, 2007 (Waller et al., 2007)	CKD3-5 (64)	4-16	LS	The mean *Z-score* for BMD was normal [Z-score=0.0 (95% CI −0.29 to 0.28)]. Only 8% of the patients had a BMD *Z-score* of less than −2.0.	BMD *Z-score* did not correlate with any biochemical markers.	Only 2 participants had significantly raised PTH (>200pg/mL).	Strict PTH and MBD control in this population shows that maintenance of normal calcium, phosphate and PTH concentrations allows for normal LS BMD and good growth
Swolin-Eide et al, 2007	CKD2-5 (16)	4-18	TB, TH, LS	TB and TH BMD increased on average after 1 year (p<0.01).	There was a correlation between iPTH and LS BMD.	Small number of participants	All biochemical markers were within normal range. Strict MBD

(Swolin-Eide et al., 2007)				LS Z-scores did not change significantly.	PINP correlated with TB (P<0.05), LS (p<0.01)and TH BMD(p=0.05).	No healthy controls	control in this cohort may be the reason that only 44% had BMD Z-scores below zero and 38% for LS BMD. Also, severity of CKD must be factored in; median GFR was 46 (12–74) mL/min/1.73 m^2
Swolin-Eide et al, 2009 (Swolin-Eide et al., 2009)	CKD1-5 (15)	4-15	TB, TH, LS	Only 5 patients had TB Z-scores below 0 at start of study. On average, LS, TB and TH BMD increased over study period of 3 years	Most patients had raised PTH levels (Median 95, 23-407 ng/L).	Small number of participants. Wide range of GFR, with earlier stages of CKD included.	Median glomerular filtration rate of 48 (8-94 mL/min/1.73 m^2) may explain why the BMD Z-scores were good at baseline
Griffin et al, 2012* (Griffin et al., 2012)	CKD 4-5 (88)	5-21	LS, TBLH	Adjusting for lower height Z-scores in CKD population results in increased BMD Z-scores in LS and TB DXA scans.	LS BMD & TB BMC z-scores not associated with iPTH or P levels	No comparison to fracture events. Biochemical comparison did not include calcium. Cross-sectional data only. No comparison to bone histomorphometry.	pQCT showed lower tibial cortical density in CKD, but higher trabecular Z-scores
Post Renal Transplant							
Tsampalieros et al, 2014* (Tsampalieros et al., 2014)	Post renal Tx (56)	5-21	LS, TBLH	Children under 13 yrs had a significant reduction in LS BMD over 12 months (-0.65, -1.16 to -0.09); p=0.006)	iPTH reduction correlated with greater LS Z-score BMD reduction	No comparison to bone histomorphometry.	The Pearson correlations between tibia pQCT trabecular volumetric BMD and DXA LS BMD Z-scores

				Greater GC exposure correlated with greater LS and TBLH Z-score reduction. TBLH Z-scores were significantly lower in Tx recipients than controls (p=0.02).		No comparison to fracture events.	were 0.45 (p<0.01) and 0.36 (p=0.02) at baseline and 12 months.
Buyukkaragoz et al, 2016 (Buyukkaragoz et al., 2015)	Post renal Tx (33)	5-21	LS	There was no difference between pre-RTx BMD and BMD at the time of study (45.9 ± 30.9 months after RTx). Worst BMD scores were obtained at sixth month after RTx (0.2 ± 0.9) and best at fourth year (1.4 ± 1.3). There were no fractures during follow-up.	Ca, P, ALP, PTH, and 1,25-(OH)2 vitamin D levels were not different from controls (p > 0.05). 25-(OH) vitamin D levels were higher in the RTR compared to the controls (29.8 ±14.7 vs 19.2 ± 15.0, p < 0.001).	Small number of participants, retrospective data	The only parameter affecting BMD was the OPG (p < 0.001)

Children with CKD have lower aBMD by DXA compared to age and sex-matched peers. For example, a study of 65 children in CKD stage 5 and on haemodialysis showed that up to 62% had low BMD by lumbar spine DXA (Bakr, 2004). It is presumed that the biochemical dysregulation of Ca, P and PTH are reflected in the lower aBMD scores in CKD. Routine used biomarkers of ALP and iPTH are often found to have inverse correlations with aBMD. In a study with 40 children in CKD5 and on dialysis a correlation between high iPTH and low LS DXA z-scores was shown (Pluskiewicz et al., 2003). Waller et al suggested that maintaining calcium, phosphate and PTH within normal range was associated with normal lumbar BMD and growth in a pediatric cohort of 64 patients with CKD (Waller et al., 2007). A study in 56 children after renal transplantation found that changes in DXA lumbar spine aBMD were greatest in the children under 13 years over 12 months (-0.65, -1.16 to -0.09) and iPTH reduction correlated with greater LS z-score reduction (Tsampalieros et al., 2014).

In summary, the widespread availability of DXA makes it a popular tool in assessing BMD in CKD, but the pitfalls of overestimation of BMD in faltering growth and the superimposition of the two bone compartments are major drawbacks that need to be considered.

1.5.3.2 Assessing bone- Peripheral Quantitative CT

An imaging modality that circumvents the limitations of DXA is quantitative CT. QCT is an ionizing radiation imaging technique that provides quantitative measures

(BMC and BMD) for both bone compartments separately (Stagi et al., 2016). This can be deemed necessary, when studying diseases that affect the cortical and trabecular bone differently. Whilst regular whole body CT scanners can be used to obtain QCT images, smaller peripheral scanners are preferentially used on account of the much reduced radiation. The scanners usually work at speed, requiring around 1 minute per imaging 'slice' obtained (Adams et al., 2014).

The main advantage of the pQCT scanners is the fact that the bone BMD is provided in g/cm^3, thereby reflecting true volumetric bone density. Images or their density calculations do not have to be adjusted for size (Crabtree and Ward, 2015). Other measures obtained are bone area and other derived geometric measurements such as cross-sectional area, periosteal and endosteal circumferences and cross-sectional moment of inertia (Crabtree and Ward, 2015).

Due to its ability to distinguish between the bone compartments, pQCT has been used to study the effects of pathological processes on bone density and dimensions in a variety of diseases (Lalayiannis et al., 2021b), such as chronic kidney disease (Denburg et al., 2013, Tsampalieros et al., 2013b), cystic fibrosis (O'Brien et al., 2018), inflammatory bowel disease (DeBoer et al., 2018, Ward et al., 2017), arthritides (Baker et al., 2017), acute lymphoblastic leukaemia (Mostoufi-Moab et al., 2018), diabetes (Pham-Short et al., 2019), nephrotic syndrome (Tsampalieros et al., 2013a, Wetzsteon et al., 2009), anorexia nervosa (DiVasta et al., 2019, DiVasta et al., 2017) and Duchenne muscular dystrophy (Crabtree et al., 2018).

Any long bone can be scanned in the pQCT scanner but the radius or tibia are used most commonly. These long bones are easy to access, and they are more conducive to getting the patient to sit or lie comfortably, reducing motion artefact for the duration of the scanning. The operator selects the limb, and measures the length of the bone to be inputted into the software. This is usually the tibial plateau to the middle of the medial malleolus for the tibia, and from the olecranon of the ulna to the styloid process of the radius if the forearm is used.

Next, the loci to be scanned need to be selected. Usually a distal, metaphyseal site and a more proximal diaphyseal site are chosen at a minimum. This is because the trabecular BMD is best assessed at a metaphyseal site and the cortical BMD at a diaphyseal site. The cortex is too thin for meaningful analysis at the distal sites and similarly, the trabecular area is too small at the proximal sites. The scanning sites are expressed as percentages of the total length of the bone. Therefore, a 14% site would represent 14% of the length of the bone. A plethora of sites have been used in the literature, but most commonly, the 3% or 4% for trabecular bone measures (metaphyseal sites), 38% and 50% for cortical measures (diaphyseal sites), and 66% for muscle and fat area estimation for the tibia (Figure 1.5.3.2.). The 4% for trabecular measures and 50% or 66% for cortical measures are commonly used for the radius.

Figure 1.5.3.2. Dotted lines represent the commonly used sites for image acquisition on a tibia. The distal 3 & 4% sites are metaphyseal bone used for trabecular BMD estimation.

The 14, 38 & 50 % are diaphyseal sites used for cortical BMD. 66% is often used for fat and muscle area estimation. The solid line represents an example of where the reference line would be placed by the operator. (Adapted from (Lalayiannis et al., 2021b)).
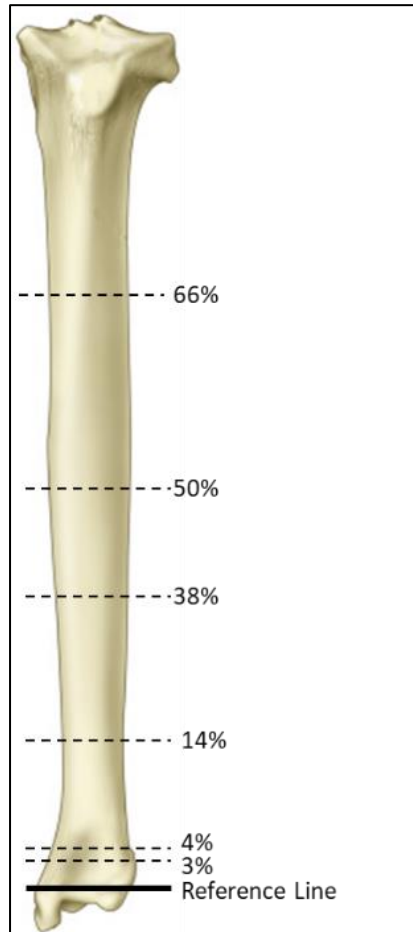
Other scanning parameters, such as scanner speed, voxel size, and image slice size need to be decided prior to scan initiation. These can be altered by the operator, but common settings are 15-25mm/s speed, 0.4-0.5mm voxel size and 2-2.3mm slice size. Smaller voxel and slice sizes and faster speeds (0.4mm voxel, 2mm slice, 25mm/s speed) reduce the radiation delivered, and as such are preferentially used in paediatric studies (Lalayiannis et al., 2021b).

The operator places the patients' limb to be imaged into the scanner and the scout view is obtained. The reference line is placed automatically by the software, but can be altered manually by the operator. The reference line placement is key after scout view acquisition and prior to scanning commencing. The positioning of the reference line can vary from study to study, and as it is used to calculate the distance from which the imaging slices will be taken, it is crucial that its placement is chosen carefully. This is important as image acquisition sites need to avoid bisphosphonate treatment lines, fracture healing calluses, or growth plates. Where consistency in imaging the same site, such as in longitudinal studies, is needed, this will provide the appropriate consistency. Finally, if z-scores are to be generated based on a healthy reference database, the same reference line placement methodology needs to be followed.

The commonest placement found in studies is at the proximal border of the distal endplate in post-pubertal young people with fused growth plates (Figure 1.5.3.2a) and at the proximal border of the distal tibia growth plate in children with open growth plates (Figure 1.5.3.2b).

Figures 1.5.3.2a &b. Screenshot pictures of the reference line (R) at the proximal border of the distal endplate in an adult with a fused growth plate (a), and at the proximal border of the distal tibia growth plate in a child with open growth plates (b). Dotted line (M1) denotes the first image acquisition point. (Adapted from (Lalayiannis et al., 2021b)).
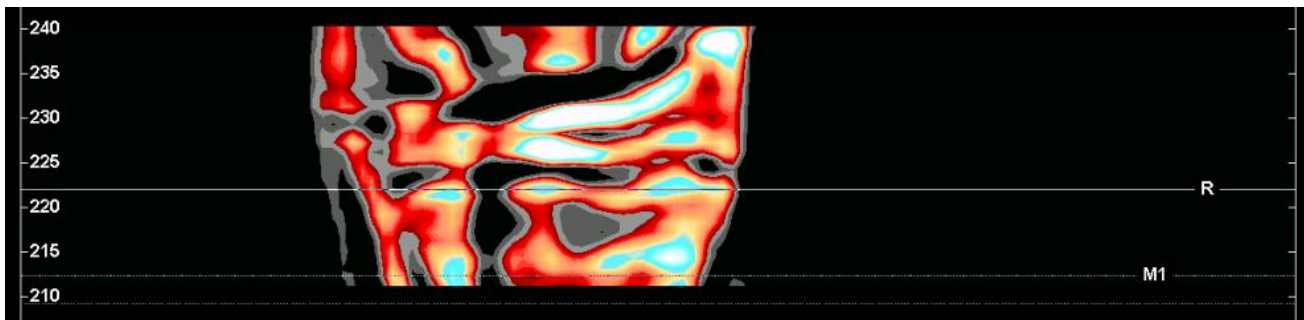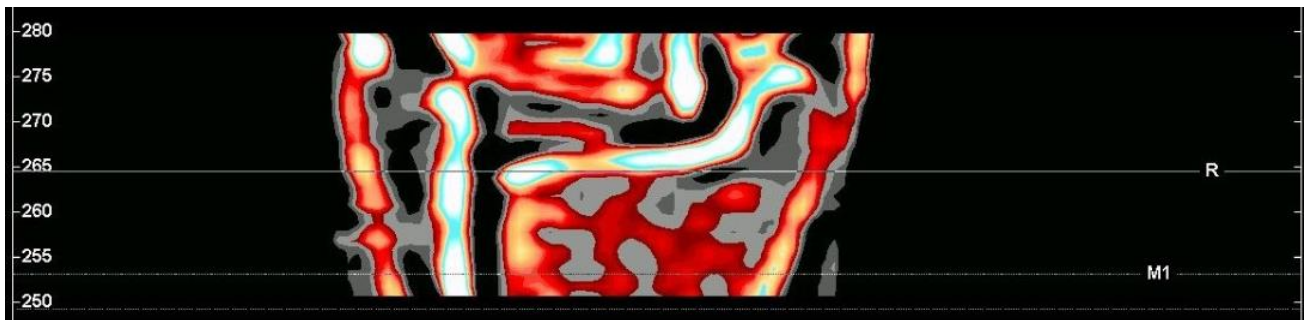
pQCT has been used to study different diseases' pathological influence on the two bone compartments. As bone is a metabolically active organ that grows in length/height and mineralizes during childhood and adolescence, it is important to express any measurements as z-scores. There are several healthy reference database studies published, which allow the calculation of age, height and sex matched z-scores of the radius or tibia (Adams et al., 2014) (Table 1.5.3.2.a.).

Table 1.5.3.2.a Key healthy reference database pQCT studies in children and young adults (Adapted from (Lalayiannis et al.,

2021b)).

Authors, Year	Population (n=)	Race (n=)	Age of population (years)	Software for Analysis (XCT 2000)	Skeletal Sites and long bone	Reference line Placement	Voxel size, Slice size and Speed	Trabecular analysis (Contour & Peel modes, density detection thresholds)	Cortical Analysis (Contour & Peel modes, density detection thresholds)	Comments
Radius										
Neu et al, 2001 (Neu et al., 2001)	371 children 107 adults	All Caucasian	6-23 29-40	v5.40	4%; non-dominant radius	Open growth plate: most distal portion of the growth plate; Fused growth plate: through the middle of the ulnar border of the articular cartilage	0.4mm; 2mm; 15mm/s	NR	NR	Only radial 4% site imaged so CortBMD analysed at 4% site, may be subject to partial volume effects
Rauch et al, 2008 (Rauch and Schoenau, 2008)	469	All Caucasian	6-40	v5.40	65%; non-dominant radius	Placed at the ulnar styloid process	0.4mm; 2mm; 15mm/s	NR	threshold 710 mg/cm^3	Age and sex dependent reference curves produced; This dataset is used by the software to produce Z-scores automatically
Ashby et al, 2009 (Ashby et al., 2009)	629	All Caucasian	5-25	v5.50	4%; 50% non-dominant radius	Open growth plate: Line to bisect the medial border of the distal metaphysis	0.4mm; 1.2mm or 2mm; 25mm/s	C2; P1,	C1; threshold 710 mg/cm^3	Centile plots produced for many bone measurement

						Fused growth plate: placed to bisect the medial border of the articular surface of the radius				indices based on the radial sites
Jaworski et al, 2018 (Jaworski and Graff, 2018)	221	NR	4-19	v6.20	4%;66% non-dominant radius	Open growth plate: through the most distal portion Fused growth plate: through the middle of the horizontal part of the articular surface of the radius	0.5mm; 2.3mm; 30mm/s	C1; P1; threshold 280 mg/cm^3	C1; threshold 711 mg/cm^3	Age and sex specific reference curves produced
Tibia										
Binkley et al, 2002 (Binkley et al., 2002)	231	Caucasian (226) Asian (3) Native American (2)	5-22	v5.40	20%; Left tibia	No scout view placed	0.4mm; 2mm; 20mm/s	C2; P2; threshold 400mg/cm^3	C1; P1; Threshold 710 mg/cm^3	Only 20% tibial site used
Moyer-Mileur et al, 2008 (Moyer-Mileur et al., 2008)	416	Caucasian (391) Hispanic (9) Pacific Islander (7) Asian (5) Black (4)	5-18	v5.4	4%; 66% non-dominant tibia	Open growth plate: most proximal line of the growth plate; Fused growth plate: through endplate	0.4mm; 2mm; 30mm/s	C1; P1; threshold 180 mg/cm^3	C1; P2; threshold 711 mg/cm^3	Height and gender specific curves reported Cortical parameters reported from the 66% site
Leonard et al, 2010 (Leonard	665	Caucasian (359) Black (306)	5-35	v5.50	38%; 66% non dominant tibia	NR	0.4mm; 2.3mm; 25mm/s	NR	C1; P2; Threshold 711 mg/cm^3	Largest cohort of healthy participants, including mix of Caucasian, Black,

et al., 2010)										Asian and Hispanic
Roggen et al, 2015 (Roggen et al., 2015b)	432	All Caucasian	5-19	v6.20	4%;14%; 38% dominant tibia	Open growth plate: proximal border of the distal growth plate; Fused growth plate: distal end plate	0.5mm; 2mm; 30mm/s	C1; P1; threshold 180 mg/cm^3	C1; P1; threshold 711 mg/cm^3	Gender specific centile curves produced for trabecular and cortical measures. All participants were Caucasian.
Baker et al, 2013 (Baker et al., 2013)	500	Black (255) Caucasian (221) Asian (20) Pacific Islander (3) Native American (1)	21-78	v6.00	3%;38%; 66% left tibia	Proximal border of the distal endplate	0.4mm; 2.3mm; 25mm/s	C3; P4; threshold 169 mg/cm^3	Threshold 710 mg/cm^3	Largest healthy adult cohort with mix of races
Jaworski et al, 2021 (Jaworski et al., 2021)	222	NR (All from Warsaw area)	4-19	v6.20	4%, 14%, 38%, 66%	Open growth plate: middle of growth plate; fused growth plate: middle of distal end plate	0.4mm; 2.3mm; 20mm/s	C1; P1; threshold 181 mg/cm^3	Threshold 710 mg/cm^3	LMS curves published to allow for z-score calculation Unknown if all cohort Caucasian

Due to the operator and scanning protocol differences of the image acquisition technique, however, there are several key discrepancies between studies. These include the long bone scanned (radius or tibia), loci of image slices (anatomical measurement sites reported include 4%, 20%, 30% and 66% in the radius and 3%, 4%, 14%, 20%, 38%, and 66% in the tibia from the distal end of the bone (Adams et al., 2014, Duff et al., 2017) and reference line placement (Neu et al., 2001, Binkley et al., 2002, Duff et al., 2017, Roggen et al., 2015b, Leonard et al., 2010, Moyer-Mileur et al., 2008). It is important that the correct reference dataset is used for the correct imaging protocol. The 2013 International Society of Clinical Densitometry (ISCD) Pediatric Official Positions (Crabtree et al., 2014) have called for standardization of pQCT methodology to enable between study comparisons, and wider reproducibility. This heterogeneity of scanning protocols has rendered pQCT largely a research tool, despite its great advantages over DXA.

Image analysis

Once the scanning has completed and all sites have been imaged, the acquired pictures are available immediately for analysis. The region of interest is selected in each image and the analysis is conducted automatically by the software to the specifications of the operator. Different analysis protocols have been used by different studies, and this needs to be taken into consideration. Apart from determining the region of interest, the operator can set the contour and peel modes to be used by the software.

The contour mode is the way in which soft tissue and bone are separated, thereby defining the outer contour of the bone. This outlines the total bone area. A 'threshold' density is set, above which pixels are defined as bone, and below which they are defined as soft tissue. This is set at 169mg/cm^3 for trabecular bone and 710mg/cm^3 for cortical bone (Lalayiannis et al., 2021b).

The peel mode employed subsequently is the way in which the software separates cortical and trabecular bone for analysis. The cortical bone is 'peeled away', leaving trabecular bone alone. There are a large number of different contour and peel modes available (Table 1.5.3.2).
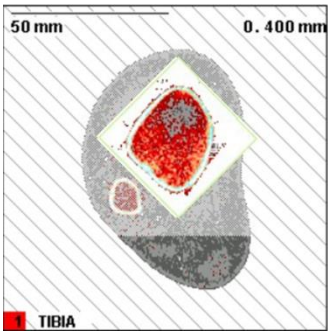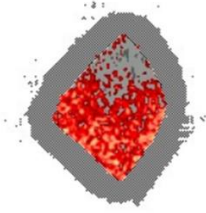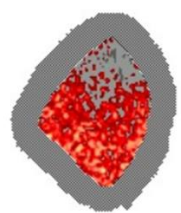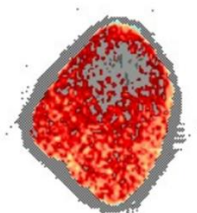
Table 1.5.3.2. Available contour and peel modes for the Stratec XCT2000, as summarized by Veitch et al (Veitch et al., 2004). All combinations of C and P modes can be used with each other.

Analysis	
Contour Mode	**Effect on image within ROI**
C1	*Threshold Algorithm*: allows the operator to select a threshold value which is used to separate the soft tissue from the outer edge of the bone – working from the outside inwards eliminating voxels above the set threshold (Threshold set at 169 mg/cm^3 for standard metaphyseal analysis)
C2	*Iterative Contour selection:* eliminates the soft tissue outside the bone. The threshold is automatically set by the software. The algorithm performs an iterative contour detection procedure by finding the first voxel of the outer bone edge. This voxel is

	compared to a set of neighbouring voxels using a set algorithm to determine the bone edge. This process continues all around the bone, returning to the starting point and thus defining the outer cortical shell
C3	As C2 but threshold operator defined (e.g. higher threshold of 710mg/cm^3 can be used to identify cortical bone only)
Peel Mode	
P1	*Default mode: w*orking from the outside edge of the bone the algorithm concentrically "peels" away a defined percentage of the outside area. A manually set percentage of cross-sectional area of trabeculum is used for analysis. This is usually set at 45%, to avoid the endosteum
P2	Operator defined inner threshold to separate trabecular and sub cortical bone. Voxels above the threshold are assigned as cortical and those lower than the threshold are assigned trabecular status.
P3	P2 combined with P1. If the amount of bone left after P2 is greater than the manually set percentage, then additional bone is peeled away. Used to eliminate the possibility of including sub cortical bone as trabecular bone.
P4	As per P3 but the operator defines a percentage of the detected bone area to be automatically peel off the trabecular area. Normally 5%
P5	Automatically detects threshold level from analysis of the steepest density gradient. Higher densities are defined as cortical, and lower densities as trabecular
P6	As per P5, but also 'peels' away cortical bone leaving a percentage of trabecular bone
P7	As per P5, but 'peels' away an extra 5% of the inner contour

P20	All pixels within a manually set percentage of the cross-sectional area in the ROI (e.g. 45%) analysed. Lowest densities defined as trabecular bone; higher densities defined as cortical

Table 1.5.3.2. Example of the same 4% metaphyseal tibial site image, with results produced under 3 different analyses (1,2,3) (Adapted from (Lalayiannis et al., 2021b)).

Tibial 4% metaphyseal site imaged	Analysis 1	Analysis 2	Analysis 3
Contour Mode	C1	C2	C1
Peel Mode	P1	P1	P4
Threshold (mg/cm^3)	180	169	200
Trabecular Area	45%	45%	95%
Trabecular bone mineral density (mg/cm^3)	197.2 (±3.0)	195.4 (±3.0)	218.7(±3.0)
Trabecular bone area (mm^2)	313.8	294.7	520.2

As any combination of contour and peel modes can be used with each other, as well as varying threshold levels can be set for total bone and cortical bone identification, this produces a near infinite number of combinations of the above. These variations can significantly affect image analysis and the results obtained. Table 1.5.3.2 displays the same 4% metaphyseal site analyzing the trabecular bone with 3 different analysis protocols. The resulting BMD and bone area differ significantly. With Analysis 3, the trabecular BMD is considerably higher. The 5% peel of the inner contour is not sufficient to remove all cortical bone (as can be seen in the image, with the outer rim of bright white colour). This increases the trabecular BMD as the software includes the cortical BMD, thereby increasing the average 'trabecular BMD'.

Cortical bone is identified at the diaphyseal site and defined as any bone above a certain threshold. This is usually set at $711mg/cm^3$. Figure 1.5.3.2 shows a screenshot example of a 38% tibial site image cortical BMD analysis.

Figure 1.5.3.2 The ROI (green box) has been set around the tibial bone in this 38% diaphyseal site. Contour mode: C1, which identified all pixels above the set threshold of 711mg/cm^3. All pixels above that density are designated as cortical bone. (Adapted from (Lalayiannis et al., 2021b))

.
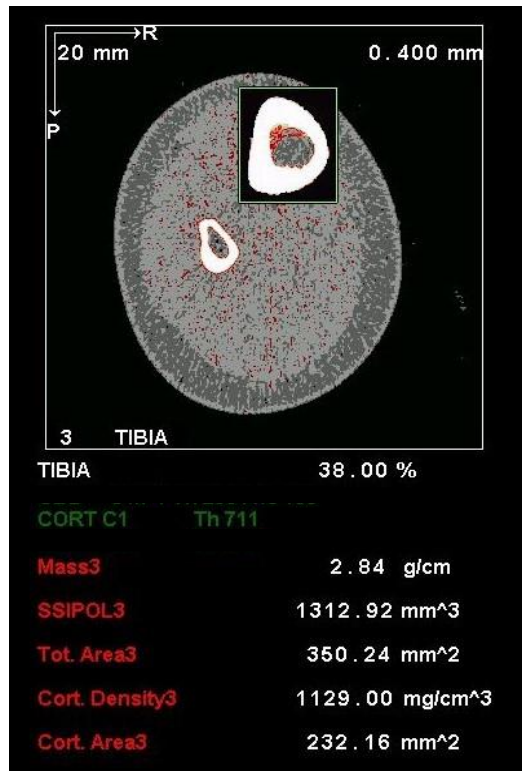
1.5.3.3 pQCT in Chronic Kidney Disease

As pQCT has the ability to distinguish and separate cortical and trabecular bone, it has proved a valuable tool in the study of childhood CKD-MBD (Table1.5.3.3). The separate effects of PTH on the bone compartments have been highlighted, with the anabolic effect on trabecular bone and catabolic effect on cortical bone that had been postulated previously (Parfitt, 1998).

Table 1.5.3.3 Key studies in childhood CKD employing pQCT (*Adapted from* (Lalayiannis et al., 2019))

Authors, Year	Population (n=)	Age of population (yrs)	pQCT site	Key Findings	Biochemical Correlations	Limitations	Comments
Dialysis (Haemodialysis & Peritoneal Dialysis) & Chronic Kidney Disease							
Wetzsteon et al, 2011 (Wetzsteon et al., 2011)	CKD 2-5, HD, PD (156; 120 CKD2-5, 36 24 HD, 12 PD)	5-20	Tibia	Trabecular BMD Z-scores were inversely associated with age and CKD severity (p<0.001). CKD 4-5 had the lowest cortical BMD (p=0.006)	Greater iPTH(p<0.01), BSAP (p<0.05), and β-CTX (p<0.02), were associated with lower cortical BMD Z-scores	No bone biopsy data No longitudinal follow up	
Griffin et al, 2012* (Griffin et al., 2012)	CKD 4-5 (88)	5-21	Left tibia	pQCT showed lower tibial cortical density in CKD patients, but higher trabecular Z-scores.	No analysis of pQCT vs biochemical markers was made	No comparison to fracture events. No comparison to bone histomorphometry.	Tibial cortical BMC was significantly correlated with TB BMC, and tibia trabecular BMD with LS BMC(p<0.0001)
Denburg et al, 2013 (Denburg et al., 2013)	CKD2-5, HD, PD (171; 109 CKD, 34 HD, 18 PD)	5-21	Tibia	Cortical BMD Z-scores were lower in CKD4-5 patients (p=0.002) A greater calcium increase over a year was associated with cortical BMD increases (p=0.002). Increases over a year of iPTH and 1,25OH$_2$D were associated with decreases in cortical BMD.	Higher Ca and 25OHD were associated with greater cortical BMD Z-scores. The opposite was true for P and iPTH.	No bone biopsy data No ionised calcium measurement	Important to note that 6.5% of participants suffered a fracture over one year, and this was associated with lower cortical BMD (HR 1.75; 95% CI 1.15-2.67)
Tsampalieros et al, 2013 (Tsampaliero	CKD3-5, HD, PD	5-21	Left tibia	Trabecular BMD did not change significantly over one year.	Higher iPTH values correlated with greater trabecular	No bone histomorphometry available.	

s et al., 2013b)	(103; 77 CKD, 16 HD, 10 PD)			Cortical BMD Z-scores decreased significantly over one year (p=0.02), although baseline Z-scores were no different to reference participants (p=0.06)	BMD changes (p<0.001). Baseline cortical Z-scores were inversely associated with iPTH levels.		
Post Renal Transplant							
Tsampalieros et al, 2014* (Tsampalieros et al., 2014)	Post renal Tx (56)	5-21	Tibia	The Pearson correlations between tibia pQCT trabecular volumetric BMD and DXA LS BMD Z-scores were 0.45 (p<0.01) and 0.36 (p=0.02) at baseline and 12 months. The decrease in pQCT trabecular volumetric BMD Z-score was significantly greater than the decrease in spine-BMD Z-score (−1.06 ± 1.29 vs. −0.43 ± 0.77, p<0.01)	pQCT not compared to biochemical markers.	pQCT used mainly as a comparator to DXA imaging.	Important to note that bone density values differed considerably between patients with high and low turnover lesions on bone biopsy.

A study of 156 children with CKD stages 2 to 5 including 36 on dialysis showed that higher iPTH levels were associated with higher trabecular BMD z-scores, but lower cortical BMD z-scores (p<0.01). Trabecular BMD was inversely associated with age and CKD stage (p<0.001) (Wetzsteon et al., 2011). Tsampalieros et al also showed in 103 CKD3-5 and dialysis patients that higher iPTH values correlated with greater trabecular BMD changes (p<0.001) and cortical BMD z-scores were inversely associated with iPTH levels.

Apart from BMD changes, pQCT has been used to show that low BMD is a predictor of fractures in the CKD population. A longitudinal study of 170 children and young people up to 21 years in CKD stages 2-5 and on dialysis identified lower cortical BMD as a significant predictor of fracture risk. Over the one year follow up (of 89 children), 6.5% suffered at least one fracture (incidence 556/10,000 person-years). Lower cortical BMD Z-score predicted future fractures [HR 1.75 (95% CI 1.15–2.67; p = 0.009) per SD decrease in baseline BMD] (Denburg et al., 2013).

In summary, pQCT is a very useful imaging modality to assess the two bone compartments separately examining true volumetric bone mineral densities. pQCT is reported to predict fracture risk in CKD, as well as show the likely opposing anabolic and catabolic effects on the trabecular and cortical bone compartments. Whilst it is affected by known limitations such as complex image acquisition and lack of standardised healthy reference databases, it provides a level of detail only superseded by bone biopsy.

1.5.4 Assessing bone- Other Modalities

Whilst the focus of this thesis is on DXA and pQCT as bone assessment modalities, it is important to mention other available imaging modalities that are being used solely in research studies, due to their lack of routine availability and lack of imaging protocol standardisation.

High Resolution peripheral quantitative CT

HR-pQCT offers a higher resolution than pQCT, although it is based on the same technology. This more detailed spatial resolution allows for the study of trabecular bone microarchitecture, trabecular numbers, thickness and separation (Crabtree and Ward, 2015, Mikolajewicz et al., 2020). These trabecular architecture features have been shown to correlate with bone biopsy findings (Marques et al., 2017), and some DXA findings (Ramalho et al., 2018). Mineralization abnormalities in children, may also be detectable by HR-pQCT (Pereira et al., 2016). HRpQCT has been used in 32 children aged 10-17 years with CKD stages 2-5 and an association of calcium and trabecular thickness with mean blood pressure was found (Preka et al., 2018).

HR-pQCT may have a role to play in future studies on fracture prediction and prevention in CKD. A recent meta-analysis of HR-pQCT studies in healthy people aged 11 to 85 years with no co-morbidities showed that radial and tibial parameters differed

significantly among fracture and control subjects. These included trabecular BMD, trabecular thickness and trabecular number (Mikolajewicz et al., 2020).

Magnetic Resonance Imaging

All the aforementioned imaging modalities involve ionizing radiation. Magnetic Resonance Imaging (MRI) has been explored as a more detailed way of non-invasively evaluating bone structure, without the use of ionizing radiation (Sharma et al., 2016).

MRI provides enough detail and information about the structure of the bone, including the trabecular microarchitecture, trabecular thickness and numbers, that it is considered a 'virtual biopsy' by some (Leonard, 2007). It allows for detailed visualisation of both cortical and trabecular compartments, and making it possible to see actual three dimensional views of the architecture. The sites reported so far in the literature to obtain images are the distal radius, calcaneus and distal tibia (Wehrli et al., 2004, Gomberg et al., 2004). MRI has been compared to bone histomorphometry in adult studies, showing good correlation of bone indices across the two modalities (Wehrli et al., 2004, Link et al., 2002, Sharma et al., 2018). There are no studies in children with CKD.

Bone Quantitative ultrasound

Quantitative Ultrasound (QUS) is the second modality not reliant on ionizing

radiation to assess bone mineral density. Apart from radiation-free it is fast, inexpensive and readily available. The bone indices are obtained based on the attenuation of the ultrasound wave or speed of sound as it passes through the bone structure. The relatively short penetration depth of the ultrasound waves means that only peripheral sites can be used. These tend to be the calcaneus, radius, phalanges or tibia. In children it is currently only used in research as an adjunct to other modalities (Stagi et al., 2013a).

There have been few studies of QUS in CKD in children. Adamczyk et al assessed seventy-six children with CKD and controls who had received glucocorticoid treatment by lumbar and total body DXA as well as phalange QUS. The CKD group had the lowest total body DXA z-scores and the QUS z-scores compared to controls (p<0.0001) (Adamczyk et al., 2018). Another study comparing lumbar spine DXA and radius and tibia QUS in 643 participants aged 5-20 years old (412 healthy, 117 with cystic fibrosis and 114 with a body mass index kg/m^2 above 95th centile), showed a good correlation of the two modalities in healthy children. However, in children with cystic fibrosis or high BMI there was a 6-31% disagreement of measurements. The authors of this study concluded that the two modalities are not yet interchangeable in their use or interpretation (Williams et al., 2012). The predictive value of QUS for fracture risk has yet to be explored.

Section III- Cardiovascular Disease in CKD

Chronic kidney disease is associated with a recognised disproportionate cardiovascular disease burden, and a resulting increased morbidity and mortality. CKD-MBD and the biochemical disturbance is closely linked to bone disease and extra-osseous calcification. This is reflected in the definition of CKD-MBD by KDIGO, where the aforementioned form the three pillars of CKD-MBD (Ketteler et al.).

In this chapter, the role of healthy vasculature will be outlined, and how preservation of the structure and function is crucial in maintaining health. The severity with which the CKD population is affected by CVD will be shown and how deposition of calcium and phosphate in the medial layer of the arteries is contributory to arterial stiffness, that in turn is detrimental to cardiovascular health.

1.6 Healthy vasculature

A healthy vasculature plays a key role in delivering blood to the tissues around the body. This is essential for oxygenation and nutrient distribution. In order to accommodate the large volume of the left ventricular output during each cardiac cycle and propagate the blood to the most distal parts of the body, the arteries have to act as a temporary reservoir for the cardiac output. Systole causes an increase in diameter of the arterial lumen, thereby effectively storing the increased blood volume in this enlarged space, followed by a diameter decrease in diastole, when the vessel walls

return to their normal size, thus creating a dynamic elastic propagation effect (Azukaitis et al., 2020). This leads to the needed continuous blood flow.

This dynamic elasticity occurs because arteries consist of three key layers. These are the tunica intima, tunica media and adventitia. The innermost tunica intima is formed of endothelial cells, fibrocollagenous tissue and the internal elastic lamina. The medial layer is composed of vascular smooth muscle cells, but also elastin fibres. The adventitia is formed of mainly fibrocollagenous tissue and the external elastic lamina (Shirwany and Zou, 2010). These structures give the arteries their elastic properties. Larger elastic arteries have a slightly higher elastin to VSMC ratio, compared to smaller muscular arteries (eg more distal arteries) which have more VSMCs in their medial layer. This is needed to alter the velocity of the pressure wave generated by the cardiac output and help propagate it. The relative impedance this pressure wave encounters downstream with the smaller lumens causes a 'reflected' back-pressure wave. This is key in the diastolic segment of the cardiac cycle as it helps maintain coronary artery flow at the root of the aorta (Shirwany and Zou, 2010).

Any pathological process that disrupts the normal elastic properties of the arteries can lead to alteration of this physiological process and have clinical implications with the ensuing arterial stiffness, poor coronary perfusion, thus causing cardiovascular morbidity. In CKD, the deleterious process is thought to be due to vascular calcification. In young people, this is mainly due to medial layer calcification.

1.7 Cardiovascular disease burden in CKD

The population with CKD is subjected to a disproportionate cardiovascular disease burden compared to their healthy peers.

In adult patients with CKD, reduced life expectancy is well recognised. In fact, Turin et al, examining the health records of all adults over the age of 30 years in Alberta, Canada (n=1,542,957) found that life expectancy decreased gradually as the CKD stage progressed; from 30.5 and 34.6 years at eGFR>60ml/min/1.73m^2 for men and women respectively, to 10.4 and 9.1 years at eGFR 15-29 ml/min/m^2 (Turin et al., 2012). This reduced life expectancy is due to CVD, and CVD-related morbidity. Navaneethan et al assessed the medical records of adults on a CKD registry in Ohio, USA (n=38,520) over a 2.3 year follow up period. They found that during this time, 17% of the cohort died. CVD was the leading cause (34.7%), over others such as malignancy (31.8%), chronic respiratory conditions (5%) and diabetes (3%). Within the CVD causes, ischaemic heart disease (53.9%), cerebrovascular events (11%) and heart failure (7%) were the most prevalent (Navaneethan et al., 2015). In other registry studies, as many as 50% of deaths are attributable to CVD in CKD (Saran et al., 2017).

Whilst the high CVD rates in 'older' adults may be expected on account of other comorbidities, including age, smoking, diabetes, obesity and other traditional Framingham risk factors, this increased morbidity and mortality is also seen in young adults (Modi et al., 2019). A registry study by Modi et al in the USA, found that over 20,000 young adults with CKD aged 22-29 years, had higher CVD hospitalisation rates

compared to children and adolescents [Haemodialysis (HR 14.24 [95% CI, 5.92-34.28]) and peritoneal dialysis (HR 8.47 [95% CI, 3.50-20.53]) were associated with a higher risk of CVD hospitalization compared with pre-emptive transplant]. These patients also had a high CVD cause of death (39.1%), a leading contributor to the overall 5- year mortality incidence of 7.3% (Modi et al., 2019).

Figure 1.7.1 Graph showing the 5-year cumulative mortality causes (Adapted from (Modi et al., 2019)).
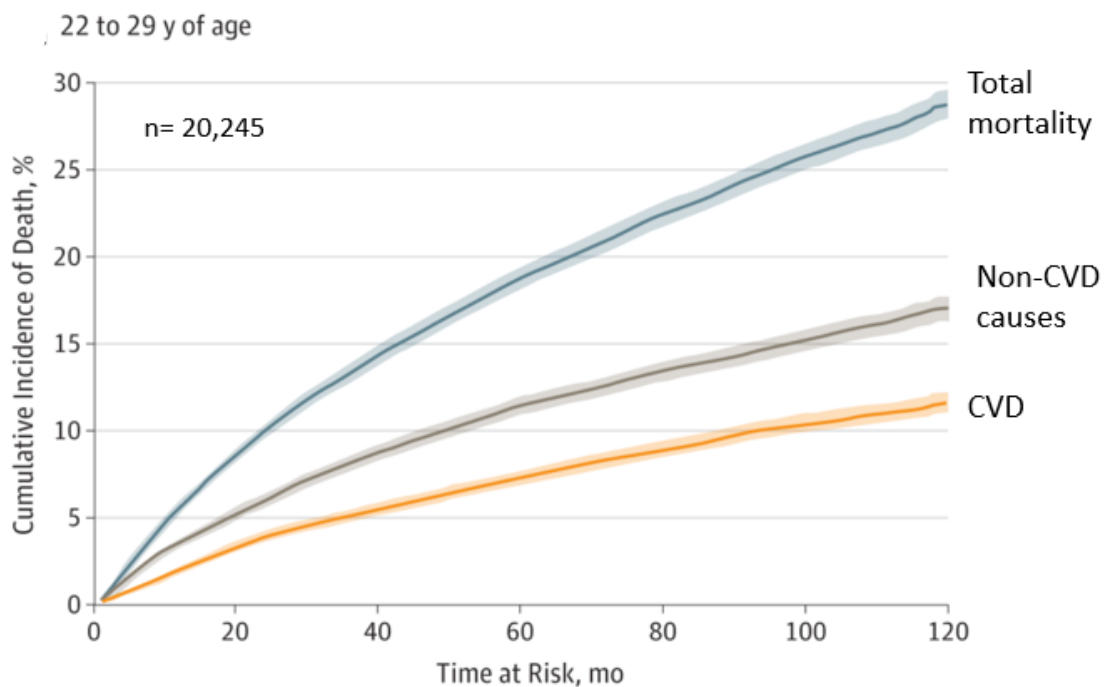
This same study found a lower 5-year cumulative mortality incidence in adolescents (4%; 12-21 years old) and children (1.7%; 1-11 years old) (Modi et al., 2019). Although there has been a gradual improvement in all-cause mortality risk in children and adolescents in the last 2 decades, cardiovascular disease remains the leading cause

of mortality and morbidity in children as well as young adults with CKD (Mitsnefes et al., 2013).

Children with kidney disease continue to have a distinct and marked decrease in life expectancy. In fact, cardiovascular disease can account for up to 30% of deaths of children on dialysis (Collins et al., 2015).

Figure 1.7.2 Figure from (Mitsnefes, 2012), showing leading causes of death in the general population and in children on RRT. Data is from US Renal Data System (2011).
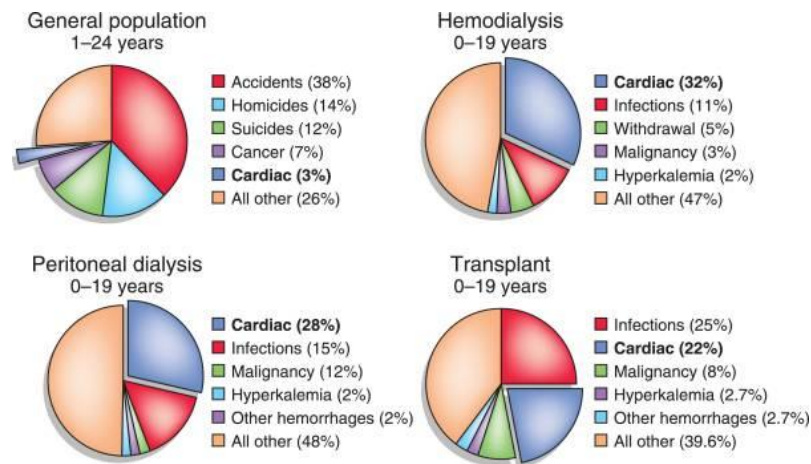
Even earlier stages of CKD such as stage 4 are associated with significantly higher death rates in young people compared to healthy peers (McDonald and Craig, 2004, Chesnaye et al., 2014). The most frequent cardiac events include arrhythmias (20%), valvular heart disease (12%), cardiomyopathy (10%) and acute cardiac death (3%) (Mitsnefes, 2012, Shroff et al., 2011, Chavers et al., 2002).

Cardiovascular mortality in the general population (NCHS) and in kidney failure treated by dialysis or transplant (USRDS)
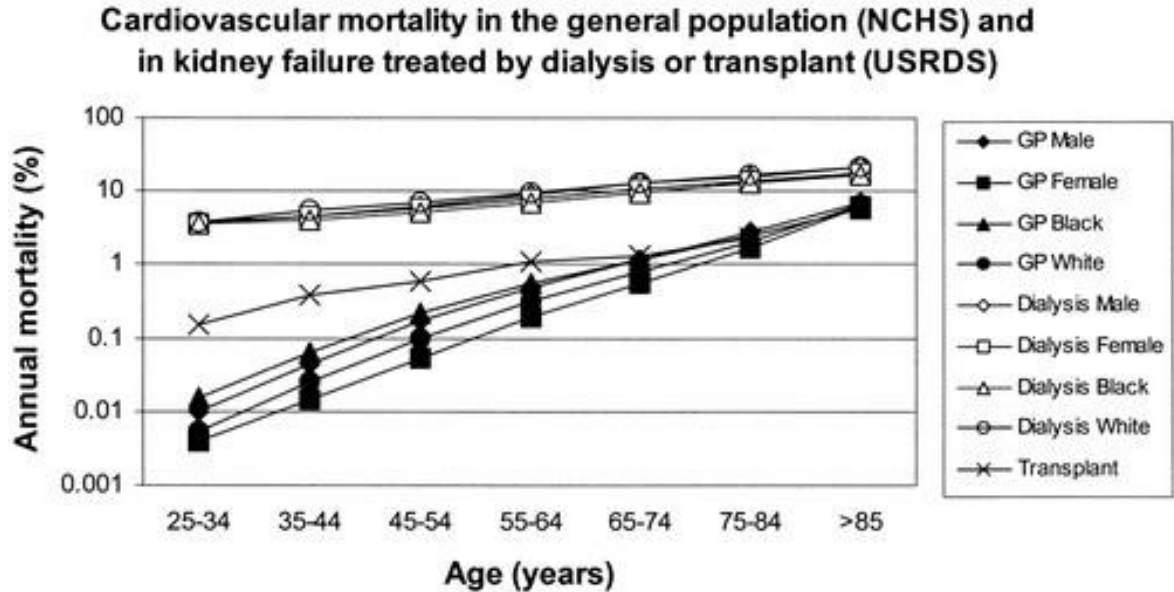
Figure from (Sarnak et al., 2003). Cardiovascular mortality in the general population, adults having received a kidney transplant and adults receiving RRT due to arrhythmias, cardiomyopathy, cardiac arrest, myocardial infarction, atherosclerotic heart disease, and pulmonary oedema.

Even in adulthood, the risk of cardiovascular mortality is not alleviated. In young adults on dialysis, the cardiovascular mortality rate is over 1000-fold higher than their healthy peers. In fact, the 25-34 age group have similar cardiovascular morbidity rates to 'healthy' octogenarians (Sarnak et al., 2003). Post transplantation, this risk does improve, but does not return to normal (Rees et al., 2007).

This exceptionally prevalent cardiovascular morbidity that is pervasive throughout the CKD population of all ages is caused by the extraskeletal calcification.

1.8 Vascular Calcification

Whilst extraskeletal calcification can happen in different tissues, such as with calciphylaxis, the vascular calcification that occurs throughout the arterial tree and the coronary arteries is the primary cause of the increased cardiovascular morbidity and mortality. Normal coronary artery blood flow is reliant on the reflected pulse wave during diastole in the cardiac cycle. When the heart contracts, it sends a pulse wave through to the aorta. As this wave progresses more distally, it meets an impedance due to the decreasing lumen size and vessel diameters. This propagates the forward motion of the wave, but also creates a reflected wave back that aids the diastolic blood pressure at the root of the aorta and formulates part of the coronary blood flow (Shirwany and Zou, 2010). A disruptive process such as calcification of the coronary arteries affects their ability to effectively perfuse the myocardium, leading to hypoxia of the muscle.

In adults, coronary calcification starts early in CKD and progresses as the kidney disease advances. It is found in as many as 40% of adult patients in CKD stages 3-4 (GFR 33.0 +/- 16.0 mL/min/1.73m^2) (Russo et al., 2004), increasing to 57% of patients starting haemodialysis (Spiegel et al., 2004), and up to 83% of patients on dialysis for a median of 3.6 years (Chertow et al., 2002). Although most studies showing coronary artery calcification in adults included older participants (Chertow et al., 2004, Spiegel et al., 2004, Cejka et al., 2014, Malluche et al., 2015), this has been shown in paediatric and young adult patients on dialysis as well (Shroff et al., 2007, Civilibal et al., 2006). In 39 patients aged up to 30 years old, 35% of patients had evidence of coronary artery

calcification (Goodman et al., 2000). Young adults with childhood onset CKD had a 92% prevalence of CAC (Oh et al., 2002). In fact, once coronary calcification is present, it seems to progress rapidly (Goodman et al., 2000), and is significantly associated with raised serum calcium and phosphate levels (Goodman et al., 2000, Civilibal et al., 2006, Shroff et al., 2007, Eifinger et al., 2000, Srivaths et al., 2010, Civilibal et al., 2009).

1.8.1 Medial layer calcification

Vascular calcification is not a uniform process. There are two areas in the vessel wall where vascular calcification can take place. Calcification of the innermost intimal layer is seen in the general population and is associated with increasing age, hypertension, smoking and dyslipidaemias. This is also known as 'atherosclerosis'. 'Arteriosclerosis', or Mönckeberg's sclerosis is seen in CKD, and this is calcification of the medial layer of the arterial wall as seen in blood vessel biopsy studies (Shroff et al., 2013). The processes that lead to eventual vessel calcification are varied and have probably not been explained in full to date, and there are likely several contributory pathways that lead to vascular calcification in CKD.

Medial vascular calcifications consist of calcium and phosphate deposits in the form of hydroxyapatite (Schlieper et al., 2010). It was previously though that the main driving force was passive hydroxyapatite deposition in the blood vessels due to the mineral dysregulation of calcium and phosphate in the serum in CKD (Ganesh et al., 2001, Shroff et al., 2008).

However, a complex cellular process is being identified as the main reason for calcification. Due to CKD, the normal calcification inhibiting factors are downregulated (such as Fetuin A), and VSMCs produce calcifying vesicles that contain hydroxyapatite (Shroff et al., 2013). Increasing phosphate levels have been shown to induce vascular smooth muscle cells (VSMCs) into an osteocytic phenotypic change. This is thought to be due to the uraemic state, with the presence of mineralization proteins upregulated locally (Shanahan et al., 1999). Once a calcification nodule is formed, the VSMC undergoes apoptosis, releasing the hydroxyapatite nanocrystals in matrix vesicles, which go on to form other areas of calcification (Reynolds et al., 2004). This process seems to produce an accelerated mechanism of calcification in the tunica media, particularly in the face of hyperphosphataemia and hypercalcaemia.

Other contributing factors have been proposed such as premature 'ageing' of the VSMCs, implicating DNA damage from prelamin A, a product of the LMNA gene being a driving force, as well as chronic inflammation and oxidative stress (Schlieper et al., 2016, Shanahan, 2013). There is a plethora of calcification promoter and inhibitor processes and proteins that have been identified (Schlieper et al., 2016, Moe and Chen, 2004, Nelson et al., 2020). In addition, inflammatory cytokines, expressed in the inflammatory state that is CKD (Viaene et al., 2016), likely contribute to VSMC calcification and apoptosis. This in turn may cause a further localised inflammatory response and contributes to the suppression of Fetuin-A (Ketteler et al., 2003). Inflammation may also increase expression of RANKL, stimulating bone resorption and promoting demineralisation (Ferreira et al., 2009).

Vitamin K deficiency has been implicated in vascular calcification and arterial stiffness in the general population (Shioi et al., 2020). Vitamin K is a cofactor in the carboxylation of G1a proteins. Incomplete carboxylation of the matrix G1a protein, which is a co-factor of Fetuin A, leads to a depletion of these mineralisation inhibitors, and therefore may promote vascular calcification (Shioi et al., 2020). A Vitamin K deficiency, identified in the majority of adult CKD patients may therefore be an additional co-contributor to vascular calcification (Krueger et al., 2009, Holden et al., 2010).

Certain bone signalling pathways, involved in bone mineral homeostasis, such as the Wnt-β catenin pathway are known to be affected in CKD, increasing bone resorption (Evenepoel et al., 2015). Sclerostin, a Wnt β catenin antagonist, is found to be elevated in CKD (Ishimura et al., 2014), and suppressed in the healthy population (Mödder et al., 2011). This pathway may be upregulated in calcifying vascular tissue, and sclerostin expression may represent an effort to halt the errant mineralisation.

In summary, the development of vascular calcification occurs early in CKD and accelerates as the disease progresses, and perhaps more so on dialysis. The precise processes behind the deposition of hydroxyapatite in the medial layer of the arteries are not fully understood, but are likely to be multifactorial and certainly related to the uraemic environment with exposure to the CKD mineral dysregulation.

1.9 Assessing Vascular Calcification

Clinical studies in adult patients with CKD use 'hard' and definitive endpoints such as death and cardiovascular events such as strokes or myocardial infarction when examining CVD in CKD. In children and adolescents, these events are much rarer and as such do not lend themselves to being study endpoints. Assessment of surrogate markers of vascular damage in CKD are more common. These can be subdivided into structural measures (Coronary artery calcification quantification & carotid intima media thickness measurement), examining the actual vascular calcification and functional measures, examining the functional effects of the structural changes (Pulse wave velocity reflecting arterial stiffness and pulse wave analysis/augmentation index).

Table 1.9 summarises some notable studies from the literature that have used surrogate markers of vascular changes in childhood CKD.

Table 1.9 Summary of some notable studies that have used coronary artery calcification (CAC), carotid intima media thickness (cIMT), and pulse wave velocity (PWV) to study vascular calcification and arterial stiffness in children with CKD, on haemodialysis (HD), peritoneal dialysis (PD) or post-transplant (Tx).

Authors, Year	Cohort (n=)	Age of population (yrs)	Surrogate Vascular Markers	Key Findings	Correlations	Comments
Goodman et al, 2000 (Goodman et al., 2000)	39 (HD 39)	7-30	CAC	CAC present in 14 of 16 patients over 20 years old. No CAC in patients younger than 20 years	CAC correlated with age, dialysis vintage, P, Ca and Ca intake from P binders. (p<0.001)	10 patients with CAC underwent follow up CT scanning, the CAC score doubled (p=0.02)
Eifinger et al, 2000 (Eifinger et al., 2000)	16 (CKD5d; mix of modalities)	14-39	CAC	CAC found in 37.5%	None drawn	Authors state that all but one participant had well controlled PTH, Ca and P.
Oh et al, 2002 (Oh et al., 2002)	39 (mix of modalities)	19-39	CAC, cIMT	CAC found in 92% of participants. cIMT increased compared to controls.	Both markers associated with dialysis vintage, CKD5 duration, Ca and P.	Participants with time averaged PTH >250pg/mL had 5-fold greater calcium scores than participants below this cut-off.
Groothoff et al, 2002 (Groothoff et al., 2002a)	130 (Tx 101, HD&PD 29)	20-41	cIMT	Participants had reduced arterial distensibility and increased stiffness compared to controls	Current systolic hypertension associated with findings.	Older cohort compared to the other studies, but included young adults
Litwin et al, 2005 (Litwin et al., 2005)	126 (CKD 55, HD&PD 37, Tx 34)	10-20	cIMT & femoral IMT	Significantly increased cIMT, femoral IMT, wall cross-sectional area and lumen cross-sectional area in all CKD patients, especially in dialysis patients	cIMT correlated with dialysis vintage, Ca, P, Ca intake from P binders and calcitriol dose	
Mitsnefes et al, 2005 (Mitsnefes et al., 2005)	60 (CKD 44, HD 16)	6-21	cIMT	All patients had increased IMT and greater arterial stiffness compared to controls.	cIMT correlated with dialysis vintage, Ca, P, Ca intake from binders and calcitriol dose	

Covic et al, 2006 (Covic et al., 2006)	14 (HD)	11-17	cIMT, PWV, PWA	Raised PWV and aortic augmentation index compared to controls (p<0001).	PWV correlated with Ca and P.	
Briese et al, 2006 (Briese et al., 2006)	40 (mix of modalities, Tx)	18-29	cIMT, CAC	10% of participants had coronary calcifications.	CAC and cIMT associated with dialysis vintage, Ca intake from binders, higher mean calcitriol dose	
Civibal et al, 2006 (Civilibal et al., 2006)	53 (15 HD, 24 PD, 14 Tx)	6-23	CAC	CAC seen in 15% of patients	Higher CAC scores associated with dialysis vintage, P, Ca and PTH levels.	
Civilibal et al, 2007 (Civilibal et al., 2007)	39 (15 HD, 24 PD)	11-18	cIMT	cIMT raised significantly compared to healthy controls (p<0.001)	cIMT associated with diastolic BP, Ca, P, and higher mean calcitriol dose.	
Shroff et al, 2007 (Shroff et al., 2007)	85 (21 HD, 64 PD)	5-18	cIMT, PWV, CAC	cIMT and PWV significantly greater in dialysis participants than controls. 20% of participants had CAC.	cIMT correlated with P, PTH, dialysis vintage. CAC with vit D dosage and PTH.	
Srivanths et al 2010 (Srivaths et al., 2010)	16 (HD)	9-21	CAC	31% had CAC.	Associated with P, dialysis vintage, malnutrition	
Chavarria et al 2012 (Chavarria et al., 2012)	60 (31 PD, 29HD)	9-16	cIMT	48% had raised cIMT.	Associated with dialysis vintage, calcitriol dose and HD vs PD	
Brady et al, 2012(Brady et al., 2012)	101 (CKD)	8-15	cIMT	Significantly higher IMT compared to controls	Correlated with hypertension and dyslipidaemia.	
Schaefer et al, 2017 (Schaefer et al., 2017)	688 (CKD)	6-17	cIMT, PWV	IMT increased in 41.6%, PWV increased in 20.1%	Both markers associated with systolic BP, P, time in CKD.	Largest paediatric cross-sectional cohort study of subclinical CVD in CKD population.

1.9.1 Coronary Artery Calcification on Cardiac CT

Calcification of the coronary arteries has been shown to be present both in adult (Chertow et al., 2004, Spiegel et al., 2004, Cejka et al., 2014, Malluche et al., 2015) and in paediatric patients (Shroff et al., 2007).

In adults coronary calcification starts early in CKD. A high prevalence of CAC with up to 94% in diabetic adult pre-dialysis patients and 59% in non-diabetic pre-dialysis patients was found by Merjanian et al with a mean GFR of 49.8 ± 6.1 mL/min/1.73 m^2. The multivariable linear regression modelling showed that increasing age, and the presence of diabetic kidney disease were significant predictors of CAC (Merjanian et al., 2003). Russo et al compared 85 adult patients with CKD (GFR 33.0 +/- 16.0 mL/min/1.73m^2) to 55 controls. 40% of patients with CKD had evidence of CAC compared to 13% of controls. Age was a significant predictor of CAC in this cohort. In ten patients, repeat CT showed progression of CAC after only 7.9 months (CAC score 383+/-627 to 682+/-890) (Russo et al., 2004).

Spiegel et al confirmed that calcification progresses through CKD as 57% of 129 adults newly commenced on haemodialysis had CAC. This cohort had not received dialysis or a kidney transplant prior to study enrollment. 34% of the overall cohort had CAC scores >90th centile for age and sex. Age (r=0.63, p<0.0001) and pulse pressure (r=0.25, p=0.004) were directly correlated with coronary artery calcification. On multivariable linear regression modelling, age, pulse pressure, diabetes, albumin, cholesterol and smoking were independent associates of CAC existence (Spiegel et al., 2004). It is suggested that calcification progresses on dialysis. Chertow et al conducted a randomised controlled trial of phosphate binders, but at study entry,

83% of patients (median age 56+/- 16 years) had CAC, with a preceding median dialysis vintage of 4.6 years. Progression of CAC was seen in the group receiving calcium based phosphate binders, and not in the group receiving sevelamer (a non-calcium based P-binder) (Chertow et al., 2002). The effect of calcium is also seen in adult patients on haemodialysis. Malluche and colleagues randomised 425 adult patients to receive dialysate with 1.25mmol/L or 1.75mmol/L concentration of calcium. The patients receiving the higher concentration of calcium showed a faster rate of progression of CAC (p=0.03) (Ok et al., 2016).

All the aforementioned clinical studies included adult patients with many confounding factors such as smoking and diabetes, that are not found in younger cohorts with CKD. The first seminal paper to show CAC in young people was published by Goodman et al in 2000. The authors showed that in 39 patients on dialysis aged 7 to 30 years old (mean age 19+/-7 years), 35% had evidence of CAC (Goodman et al., 2000). Interestingly, none of the patients aged under 20 years of age had CAC (n=23), whereas 14 of the 16 patients aged 20 to 30 years old had CAC. The participants with CAC were not only older (mean 26 vs 15 years, p<0.001), but they had also been treated with dialysis for longer (median 13 vs 2 years, p<0.001). Whilst the serum phosphate difference only approached significance (p=0.06), the calcium-phosphate product was ignificantly higher in the CAC group (65.0 vs 56.4 mg^2/dl^2, p=0.04). There was no statistical significance between the two groups' PTH levels (both were high at 361 and 445 pg/mL), but the oral calcium intake of the group with CAC was higher (6456 vs 3325 mg/d, p=0.02) (Goodman et al., 2000). CAC was found even in the 13 of 27 patients who had undergone transplantation, with previous dialysis vintage being the attributable factor for this (9 vs 3 years, p<0.001). The authors then

repeated the cardiac CT scans 22 months later at a follow up visit in 22 patients, and found that among the 12 patients with no CAC at baseline, 2 had evidence of CAC subsequently. Of the 10 patients with CAC at baseline, their CAC scores nearly doubled (125+/- 104 to 249 +/-216, p=0.02). Calcium-phosphate product correlated with this increase in CAC (Goodman et al., 2000).

The next important study that highlighted that CAC is indeed prevalent in the younger population with CKD, was published in 2002 by Oh et al. Thirty-nine patients (13 on dialysis, 26 post-transplant) aged 19 to 39 years, with childhood onset of CKD5 participated in the study. 92% of the patients had evidence of CAC. PTH, calcium-phosphate product and C-reactive protein were found to be independent predictors on linear regression modelling (Oh et al., 2002).

Eifinger et al in 2000 also found that in 16 children and young adults (up to 39 years) with CKD stage 5 or on dialysis, CAC was evident in 37.5% of the cohort. There were no control subjects however, and the authors state that all but one participants had well controlled PTH, Ca and P levels (Eifinger et al., 2000).

In another study which included 53 children with CKD (15 on haemodialysis, 24 on peritoneal dialysis, and 14 post-transplant), Civilibal et al showed that CAC was present in 15% of participants. The patients with CAC had a longer dialysis vintage (80.1 vs 47.3 months, p=0.005), had higher serum phosphate levels (p<0.001), calcium-phosphate product (p=0.012) and iPTH levels (542 vs 273 pg/mL, p=0.010). On logistic regression analysis phosphate (p=0.018) and the cumulative exposure to calcium-containing P-binders (p=0.016) were the most significant independent associations in the development of CAC in this cohort (Civilibal et al., 2006).

The largest paediatric study that included CAC was that by Shroff and colleagues in 2007. They examined 85 children aged 5 to 18 years, who had received dialysis for at least 6 months and had been in CKD stage 4 for at least 3 years. They split the cohort into those who had PTH below 2xULN and those with PTH above 2xULN. CAC was associated overall with iPTH levels (r=0.39, p=0.03) and serum phosphate (r=0.34, p=0.03). 12% of patients in the first group and 27% in the second group had evidence of CAC. The children in the second group had moderate and severe grades of calcification. On multiple regression analysis, vitamin D dose and iPTH levels were independent predictors of CAC (β 0.28, p=0.02 & β 0.53, p<0.001 respectively).

Cardiac CT scan is the only way currently that affords the researcher or clinician a direct quantification of calcification of the vasculature, in a tissue bed that is directly responsible for the increased morbidity and mortality in CKD. Another indirect way, is to measure the thickness of the medial layer of the arteries as a surrogate marker of calcification.

1.9.2 cIMT

Vascular calcification and hydroxyapatite deposition in the medial layer of the arteries causes an increase in the medial layer size. Ultra-high frequency ultrasound is able to differentiate between the different arterial layers (Dangardt et al., 2018). Due to this modality not being widely available or accessible, conventional US is used as its able to measure the combined intima and media thickness (cIMT). This

measurement is used as a surrogate marker of vascular calcification (Dangardt et al., 2018).

Many paediatric studies have used cIMT as their endpoint, in the absence of hard endpoints such as cardiovascular events or death. In fact, even in adult studies, such as that by Oh et al, where 39 patients (13 on dialysis, 26 post-transplant) aged 19 to 39 years, with childhood onset of CKD5 participated in the study, cIMT was elevated in dialysed and post-transplant patients compared to controls (p<0.01 and p<0.05 respectively). As perhaps expected the patients aged 28 to 43 years had higher cIMT compared to patients aged 19 to 27 years (p<0.05), although such a difference was not evident amongst the controls. Interestingly, cIMT did not correlate with CAC scores. On multiple regression analysis, serum calcium levels and dialysis vintage predicted IMT independently (Oh et al., 2002).

Another study by Groothoff et al showed that in adult patients aged 20 to 41 years, with childhood onset CKD (n=130; post-transplant 101, HD&PD 29), showed no difference in cIMT between patients and controls. Participants with CKD however, demonstrated higher BP measurements and increased measures of arterial stiffness (lower arterial wall distensibility and higher incremental modulus of elasticity) (Groothoff et al., 2002a).

Although adult studies have mostly shown increased cIMT in CKD and dialysis patients, these structural arterial calcification changes are seen as early as childhood and adolescence. Fifty-five children with CKD stages 2 to 4 (eGFR 51+/-31ml/min/1.73m^2; 37 HD, 34 post Tx) were compared to 270 control subjects. cIMT as well as wall cross-sectional area and lumen cross sectional areas were significantly

elevated in the CKD patients. In fact, cIMT was equal or exceeded the 95th centile in 89% of dialysed patients, 61% of pre-dialysis CKD and in 75% of the post Tx patients. The only independent predictor of cIMT in multivariable regression analysis was the cumulative previous phosphate binder dose (r=0.44, p=0.06). The lumen cross sectional area of the carotid artery was significantly increased in the dialysis and post-transplant groups. This study by Litwin et al provides the suggestion that the vascular damage begins early in the course of CKD and that there exists perhaps a remodelling or functional compensatory mechanism by which the structural alterations of the vessels are opposed (Litwin et al., 2005). This was further backed up by a study showing that although cIMT was higher in children on dialysis and with CKD stages 2-4, those on dialysis had significantly higher indices of arterial stiffness (p<0.0001) (Mitsnefes et al., 2005). In this cohort of 44 children cIMT was also associated with serum phosphate. Length of dialysis was a significant correlate (p<0.0001).

Shroff et al demonstrated in 85 children aged 5 to 18 years, who had received dialysis for at least 6 months that their cIMT was significantly raised compared to controls. Duration of dialysis was associated with cIMT (r=0.31, p=0.04), as was iPTH (r=0.71, p=0.0001) and phosphate (r=0.51, p<0.0001) (Shroff et al., 2007).

One of the larger cohorts in paediatric patients was published by the CKiD Study (Chronic Kidney Disease in Childhood study). One hundred and one children aged 2 to 18 years, with a median eGFR of 43ml/min/1.73m2 had hight cIMT measurement compared to healthy controls (p=0.03), and dyslipidaemia and hypertension were independent predictors on multivariable linear regression analysis. The absolute cIMT difference between CKD and healthy controls was not

very large (0.43 vs 0.41mm, p=0.03), but the fact that the children with CKD only had mild to moderate CKD, and yet the changes were already evident is significant (Brady et al., 2012).

The largest paediatric study to date to utilise cIMT has been the Cardiovascular Comorbidity in Children with CKD Study (4C Study), which is a pan-European, multicentre, prospective observational study of children aged 6 to 17 years old with eGFR of 10-60 ml/min/1.73m^2. The three year follow up results from 2009 to 2011 from 688 children were published in 2017 (Schaefer et al., 2017). The cIMT was elevated in 41.6% of patients above the 95th centile, with only 11% showing measurements below the 50th centile for age and sex. eGFR did not correlate with cIMT, highlighting the early commencement of calcification in CKD. Serum phosphate, systolic BP and BMI were independent predictors of cIMT overall(Schaefer et al., 2017).

All the aforementioned studies have validated the use of cIMT as a surrogate marker of vascular calcification, and have shown that cIMT is raised early in CKD, and probably increases as CKD progresses, and with dialysis. They have laid a solid foundation for use of cIMT in the absence of hard endpoints. Further research is needed however, for cIMT to be used as a target for treatments and therapies in the management of CKD-MBD.

1.9.3 PWV and PWA

Whilst cIMT and CAC are the anatomical, structural changes associated with vascular calcification, in a dynamic tissue such as a blood vessel, this may produce functional changes such as stiffness and reduced distensibility. This in turn increases the pulse wave velocity. Several studies have included PWV assessment and pulse wave analysis for augmentation index (AIx) in their protocols in attempt to characterise the effect of CKD-MBD on young blood vessels. It is noteworthy that an elevated arterial stiffness, as examined by PWV, is a predictor of future mortality and morbidity, independently of raised blood pressure in adult patients with CKD (Townsend et al., 2018, Ben-Shlomo et al., 2014). A study of 2795 adults, with a mean age of 60 years and mean eGFR of 44 mL/min/1.73m^2 showed that patients in the highest tertile of PWV (>10.3 m/s) were at a higher risk for progression to CKD stage 5 (HR 1.37 95% CI 1.05-1.80), or death (HR 1.72, 95% CI 1.24-2.38) (Townsend et al., 2018).

Covic et al studied PWV and augmentation index in 14 children on haemodialysis and found that PWV and Aix were significantly higher in children on dialysis compared to controls. Multiple linear regression modelling showed BP, age, height, Ca and P levels as independent associations of Aix (Covic et al., 2006). Shroff et al demonstrated that PWV was elevated in children on dialysis also, and that the arterial stiffness correlated with phosphate levels (r=0.39, p=0.03). Children with iPTH>2xULN had higher PWV values compared to controls and children with iPTH<2xULN (8.63 +/- 2.3 vs 5.81+/- 1.2m/s, p=0.03) (Shroff et al., 2007).

The 4C study showed that PWV is increased in 20% of children and adolescents with CKD, and that this is correlated with cIMT (r=0.23, p<0.001). The

implication of this is that the structural changes brought upon the blood vessels by CKD-MBD, affects the elasticity of the vessels and therefore the functional properties leading to the increased pulse wave velocity seen (Schaefer et al., 2017).

The number of large studies utilising PWV as a surrogate marker of arterial stiffness is small. Nevertheless, there is a clear signal that arterial stiffness is increased in CKD, and is likely to progress on dialysis. Ultimately, perhaps if the calcification could be arrested, the down-stream effects of increased arterial stiffness and cardiovascular morbidity could be prevented.

Section III- The link between Vascular Calcification and Bone Demineralisation

The co-existence of vascular calcification and bone mineral density reduction have been known to be a part of the CKD-MBD spectrum for some time. Osteoporosis and atherosclerosis were once thought to be unrelated diseases that are an inevitable part of the ageing process. Recent studies suggest that bone demineralization and vascular calcification may be closely linked processes(Kiel et al., 2001, Tankó et al., 2005).

CKD-MBD is defined as the triad of biochemical abnormalities, bone demineralisation and vascular calcification as stipulated by KDIGO ('KDIGO clinical practice guideline for the diagnosis, evaluation, prevention, and treatment of Chronic Kidney Disease-Mineral and Bone Disorder (CKD-MBD),' 2009). There seems to exist a "calcification paradox" (Khouzam and Wesseling-Perry, 2019) that occurs in patients with CKD, in which there is a process of mineral deposition in blood vessels and an opposite concurrent demineralization of bones over time. It is unknown whether the vascular abnormalities and the concurrent bone changes are separate and distinct processes or whether they occur in conjunction with each other. A small number of recent clinical studies in adult patients have attempted to examine this.

In the first longitudinal cohort study, Malluche et al followed up a group of 213 adults on haemodialysis over one year. CAC was assessed by cardiac CT, and bone mineral density was assessed by DXA and quantitative CT at three bony sites; the spine, femoral neck and total hip. One third (32.8%) of participants had low bone

mineral density and half of the participants had a high CAC score (>400 Agatston score) at baseline. The patients who had low BMD at the hip by QCT had more CAC compared to those with normal BMD [SQRV (Square root of volume of calcification); 33.8 vs 19.0, p<0.001). The same applied to the spine and femoral neck sites. One-hundred and twenty two patients were scanned a year later. A significant proportion of these patients lost more than 2% of their BMD at the different sites, both by QCT and DXA (39.2-57.6% of patients). There was also a significant increase in CAC AS from 353 to 552 (p<0.001). In fact, progression of SQRV CAC was higher in patients with low BMD at any site or by any imaging modality (7.5 vs 2.1, p=0.001). Progression of CAC correlated with PTH (r=0.24, p=0.02) but no other serum markers. In fact, after adjustment for age, low BMD and PTH were independent predictors of CAC progression (β=4.6, p=0.002 and β= 6.9, p=0.001) (Malluche et al., 2015).

Cejka et al studied the CAC and BMD in 66 adults aged 45 to 67 years on haemodialysis. Patients with higher CAC scores (≥100) were older compared to patients with lower CAC scores (<100) (p<0.001). However, in multivariate analysis adjusting for age, tibial density and bone volume/total volume (as assessed by HR-pQCT) were significantly lower in patients with higher CAC scores (p<0.05 for both) (Cejka et al., 2014).

Whilst the two studies above only recruited adult haemodialysis patients, a 2016 study by Chen et al recruited 231 adult participants aged 28-75 years (mean age 56 years, incident HD=95, PD=55, Tx=81). CAC was assessed by Cardiac CT, and BMD by vertebral body QCT and total body DXA. The spine BMD was used to split the cohort into tertiles. The lower tertile were older (65 vs 50, p<0.001) and had higher

CAC scores compared to the two higher tertiles (AS 960 vs 28, p<0.001). Age and CAC were independent predictors of lower BMD on regression analysis. During the 5 year follow up 19% of participants died, and these patients had higher CAC scores compared to those who did not (p<0.001). The all-cause mortality was in fact higher in the lower tertile for BMD compared to the middle and higher tertiles (p<0.001). In the final multivariate Cox proportional hazards analysis, low vertebral BMD was an independent predictor of all cause mortality even after adjusting for age, gender, diabetes, CVD and inflammation. On examining the ROC curve analysis for the ability of BMD, by QCT and by DXA, to predict CAC, QCT was associated with a higher CAC more strongly (AUC 0.75 vs 0.57). In summary, this study not only showed an independent association between CAC and BMD in adult patients with CKD, but also that low BMD was an independent predictor of CAC and all-cause mortality (Chen et al., 2016).

Apart from clinical observational studies, there have been studies examining coronary calcification in relation to bone biopsy findings. These have reported that both low and high turnover disease is associated with calcification. Asci et al, performed bone biopsies in 207 adult patients receiving haemodialysis (32-75 years). Of these patients, 69% had CAC. Higher CAC scores were associated with increasing age, dialysis vintage, and bone turnover (defined from the histological parameter of bone formation over bone surface area)(p=0.013). Low bone turnover was negatively associated with CAC (p=0.03) and high bone turnover was positively associated with CAC (p=0.01) (Asci et al., 2011).

Barreto et al have shown in adult dialysis patients that patients with both high and low turnover abnormalities showed calcification progression over one year of follow-up. Higher trabecular volume was independently associated with CAC at baseline (β= 0.83, p=0.006). The authors split the cohort into low and high turnover groups at baseline and at follow up. Logistic regression analysis revealed that low turnover at the 12-month bone biopsy was the only independent predictor for CAC progression (p= 0.04; β = 4.5; 95% CI, 1.04 to 19.39) (Barreto et al., 2008a).

The co-existence and association between bone demineralization and vascular calcification is not only seen in adult dialysis patients but also in pre-dialysis patients. Filgueira et al found that 50% of 72 pre-dialysis adults (age 52 ± 11.7 years, eGFR 40.4 ± 18.2 ml/min per 1.73 m^2) had coronary calcifications (severe calcification in 19%; >400 Agatston units). Coronary calcifications and vertebral body bone mineral density by QCT were inversely correlated (r=-0.31, p=0.01). When the vertebral body densities were split into tertiles, the lowest tertile had significantly higher CAC scores (p=0.04). Vertebral BMD was independently associated with CAC presence (β=1.43, 95% CI 1.18 to 14.9, p=0.03) (Filgueira et al., 2011).

All the aforementioned studies examined CAC association with bone demineralization in adult participants over the age of 30, with the average age being around 65 years old. A positive correlation and independent association between the two has been shown . However, we would be unable to extrapolate these results safely and confidently to children and young people. The adult cohorts involved many with diabetic kidney disease, smokers, pre-existing CVD and traditional Framingham risk factors such as hypercholesterolaemia.

There is a paucity of studies examining bone and cardiovascular calcification in children and young adults with CKD, and none have used direct examination of CAC by cardiac CT. There have been only two previous studies in children with CKD. The first, by Preka et al (n=32), demonstrated that trabecular thickness by HR-pQCT was positively associated with diastolic and mean arterial BP (r=0.54, p=0.002 and r=0.53, p=0.002 respectively) (Preka et al., 2018). The second, by Ziolkowska et al, showed that in 60 children with CKD, cIMT correlated with lumbar spine BMD (r=0.74, p<0.01) and total body less-head BMD (TBLH) by DXA (r=0.70, p<0.02) (Ziolkowska et al., 2008). There has been no longitudinal study looking at bone demineralization and vascular calcification simultaneously in children and young adults.

An additional major barrier that would prevent assumption that the adult studies' results be applied to a younger population is that the skeleton of younger people is in a different metabolic phase. In early life, the bones continue to mineralise and accrue calcium. Bone formation is the predominant driving force which aids bone lengthening and mineralisation. However, there comes a point at which the maximum genetic and environmentally determined amount of mineral is deposited, after which there is a gradual decline and the modelling/resorption cycle tips towards a negative state. This point in time is called peak bone mass (Weaver et al., 2016). After PBM is reached in the third or even early fourth decade of life, there is a natural very gradual decline in BMD. It may be that the pathological process of CKD in the 'older' adults in fact compounds this natural decline and renders them in an osteoporotic state, and thus with the associated bone morbidity of CKD. On the other hand, in young people, the growing skeleton is still in a predominantly formation

balance, with mineral accrual ongoing. It could, therefore, be suggested that a growing skeleton, with continuing mineralisation would be able to buffer and absorb excess calcium in CKD, thereby protecting blood vessels and preventing the initiation or progression of the vascular calcification process.

It becomes apparent that there is a gap in the knowledge of this relationship between bone and vessel in the younger population with CKD. Medical treatment of CKD-MBD includes dietary restriction of phosphate and use of phosphate binders. Phosphate binders can be calcium or non-calcium based. Calcium based phosphate binders -which are primarily used in childhood CKD- can lead to an increased calcium load, which may be of concern in the context of extra-skeletal calcification. Currently, the most challenging aspect in the management of CKD-MBD in the face of a growing skeleton, is the reconciliation of the need for calcium, phosphate and vitamin D by the bones and avoidance of any harm to the vessels and the heart. Calcium balance studies are needed in young people with CKD, as well as longitudinal cohort studies examining the bone and vascular link in young people under 30 years.

Section IV- Hypothesis and Project Design

As the ongoing mineralisation of the skeleton until the third or fourth decade of life, alongside and following the growth in childhood and adolescence, it can be postulated that the skeleton may form a buffer and acts as a protective element, thereby preventing or delaying vascular calcification initiation or progression in young people with CKD.

The hypothesis generated from the literature and I aimed to answer with this study therefore was that children and young people with increasing bone mineral density would not have any evidence of vascular calcification.

This thesis outlines the prospective, longitudinal, multicentre, clinical observational study and related work that examined the association between bone mineral density and vascular calcification in children and young adults with chronic kidney disease stages 4 to 5 and on dialysis.

PICO Summary of Study

Population	Children and young adults (5-30 years old) CKD 4/5 or on dialysis
Investigations	Bone health: • DXA Hips • DXA Lumbar spine • pQCT Tibia • pQCT Radius Vascular Health: • Ultrasound for Carotid Intima-Media Thickness • Pulse Wave Velocity and Pulse Wave Analysis • Cardiac CT for Coronary artery Calcification Serum Markers of CKD-MBD: Calcium, Phosphate, 25-hydroxyvitamin D, intact Parathyroid Hormone, Alkaline phosphatase
Comparison	N/A
Outcomes	Primary outcome: • To examine the association between bone mineral density and vascular calcification at baseline and during longitudinal follow up Secondary outcomes: • To compare tibial pQCT measurements from a sample of the local healthy population of young people to two of the largest pQCT reference databases • To examine the bone health, including bone pain and fracture history in a young cohort with CKD • To ascertain whether DXA is a useful tool in predicting BMD as assessed by pQCT • To determine whether routinely used serum biomarkers are good predictors of BMD • To characterise the prevalence of subclinical CVD in a young cohort with CKD • To examine the association between structural and functional changes in the blood vessels • To assess the progression of vascular calcification, if any, as examined by CT and cIMT over one year • Progression of bone demineralisation, if any, over one year
Design	Cross-sectional Study Longitudinal Follow up after 1 year minimum

Chapter 2- Methods

Introduction

This study aimed to examine the association of bone mineral density and vascular calcification in young people with CKD. Recent clinical studies have shown that the two processes of bone demineralisation and vascular calcification occur simultaneously in older adults. These results cannot be extrapolated to children on account of the skeleton of children being in a different physiological and metabolic state (with ongoing mineralisation and growth). There have been no longitudinal studies in children examining bone demineralisation and vascular calcification and their potential association.

In this methodology chapter, I have listed the investigations used in this study to assess bone mineral density and the investigations used to assess vascular calcification, including the structural and functional changes incurred by the vessels. I have outlined the rationale behind the techniques employed here and the analysis used.

All investigations, image acquisitions, and analysis were carried out by myself independently, unless otherwise stated. I am very grateful for all the training and help I received to be able to do this. I have acknowledged any and all additional aid I received in the corresponding sections below.

2.1- Inclusion and Exclusion Criteria

2.1.1 Inclusion Criteria

i)   **Age**: 5 to 30 years old

ii)   **CKD:** stages 4-5 (eGFR ≤30mls/min/1.73m^2) or on dialysis (Peritoneal dialysis or Haemodialysis)

I aimed to recruit children and young adults to the study. The age criteria were set at 5 years minimum to 30 years maximum. The lower limit was set at the age that it was thought some of the children would have the understanding to assent to the extra investigations on top of their routine care, but also be old enough to tolerate sitting still for the procedures. In addition, this is generally the lower limit and the youngest age in large healthy population databases of normal values of cIMT and PWV (Melk et al., 2015, Doyon et al., 2013). As these databases were going to be used to generate z-scores for our vascular measures, it seemed prudent to align the lower limit. The older age was set at 30 years old, as peak bone mass -the point at which the maximum genetic and environmentally determined amount of mineral is deposited in the skeleton- is reached by the fourth decade of life. The maximum mineral accrual happens around peak height velocity in adolescence but continues thereafter until it reaches its zenith (Weaver et al., 2016). This age range should be representative of a growing, mineralising skeleton in the context of CKD.

2.1.2 Exclusion Criteria

  i)   **Age**: under 5 years or over 30 years old

  ii)   **Genetic conditions affecting the bone structure**

  iii)   **Previous Bisphosphonate therapy**

  iv)   **Current functioning kidney transplant**

The age inclusion criteria are set out above. No patients above or below that age range were recruited.

There are certain nephrological conditions, genetic in nature, that affect bone microarchitecture and structure, thereby leading to an increased fracture burden. In primary hyperoxaluria, calcium oxalate crystals deposit in the bone causing alteration of the normal bone structure, leading to fractures, deformations, and oxalate osteopathy (Bacchetta et al., 2016). This can be seen in other genetic conditions, such as cystinosis, with bone being affected in a direct way, but also indirectly due to the effects of the disease (Machuca-Gayet et al., 2020). In cystinosis, there is probable impairment of osteoblasts and osteoclasts through the accumulation of cystine, but also an indirect effect on bone due to the renal Fanconi syndrome and mineral loss that is associated with the condition. As these conditions' pathophysiology is vastly different to normal CKD-MBD, we have excluded patients with these conditions from the study.

Whilst bisphosphonate use in childhood CKD is rare, we opted to exclude anyone with a prior treatment from the study. Bisphosphonate treatment is

associated with and can be visualised on plain fil radiography as it leaves a line of sclerosed non-decalcified cartilage in the metaphysis of the bone. These treatment lines can interfere and alter measurements obtained by BMD imaging. As pQCT is our main imaging modality, and it relies on specific loci for image acquisition, we would not be able to guarantee that these treatment areas would not be included. As such, prior bisphosphonate treatment was an exclusion criterion.

CKD-MBD remains an issue even post-transplant. In a prospective Finnish study of 196 children who had received a solid-organ transplant (n= 123 post kidney transplantation, 44 liver, 29 heart), followed up for 5 years, 38% of patients had at least one fracture (166 fractures in n=75 patients). This equated to a 6-fold higher fracture risk compared to the control population (All fracture incidence: 92 vs 14 fractures/1000 persons/year; $p<0.001$) and 160-fold higher vertebral fracture risk (57 vs 0.35 fractures/1000 persons/year; $p<0.001$) (Helenius et al., 2006a). Studying BMD in a post-transplant population becomes more challenging as the immunosuppressive regimens used can vary significantly, and can have differing effects on bone. In the aforementioned study the immunosuppressive agents used in the majority of the participants were glucocorticoids, that perhaps affected the outcomes. Although excluded from this study, a separate examination of CKD-MBD in a post-transplant population of young people is warranted, as it is still present and affecting the blood vessels and bones. A large, European registry study of 1237 children showed that 19% had hypocalcaemia and 40% had a high PTH three years after transplantation (IQR 1.1–6.2 years) (Bonthuis et al., 2015).

2.1.3 Participating Nephrology Centres

In order to recruit to target, I approached several paediatric and adult nephrology units. These are listed below.

<u>Paediatric Units</u>

Great Ormond St Hospital for Children NHS Foundation Trust, London, UK

Birmingham Women's and Children's NHS Foundation Trust, Birmingham, UK

Manchester University NHS Foundation Trust, Manchester, UK

Evelina Children's Hospital, Guy's and St Thomas' NHS Foundation Trust, London, UK

Athens General Children's Hospital "Panagiotis & Aglaia Kyriakou" (Παναγιώτης & Αγλαΐα Κυριακού), Athens, Greece

<u>Adult Units</u>

Royal Free London NHS Foundation Trust, London, UK

Imperial College Healthcare NHS Foundation Trust, London, UK

St George's University Hospitals NHS Foundation Trust, London, UK

University Hospitals Birmingham NHS Foundation Trust, Birmingham, UK

2.2 Assessing bone health and bone mineral density

Bone biopsy is the gold standard technique for bone assessment. Bone is a metabolically active organ that does not remain static and merely provide anchoring points for muscles and tendons. Bone undergoes formation, resorption and re-modelling continuously. Bone biopsy histomorphometry examines the dynamic process of bone formation and resorption. The histologic findings are categorised in terms of bone turnover, mineralisation and volume (the 'TMV' classification) ('KDIGO clinical practice guideline for the diagnosis, evaluation, prevention, and treatment of Chronic Kidney Disease-Mineral and Bone Disorder (CKD-MBD),' 2009). Bone biopsy is an invasive procedure and only a handful of nephrology centres around the world perform this even for research purposes. The procedure requires an anaesthetic and dosing with tetracycline, which has UV fluorescence properties, at two different time intervals to 'label' the bone for assessment of the dynamic features of bone formation (Torres et al., 2014). There is a paucity of histopathologists that would be available and experienced enough to interpret the histomorphometric findings. As a result, we required non-invasive, reproducible, accurate surrogate measures of bone mineral density and bone health. The ones employed in this project are outlined below.

i) **Dual Energy X-ray Absorptiometry** (DXA): Two sites were imaged for this study; the hips and lumbar spine. This modality is readily available and in regular clinical use. It allows for standardised z-score interpretations of hip areal BMD and lumbar spine areal BMD. The lumbar spine measurements

have to be adjusted for size either by height or by volume. I have employed the 'by volume' method that is in use in the UK. This provides bone mineral apparent density (BMAD) z-scores.

ii) **Peripheral quantitative CT** (pQCT) of non-dominant radius and tibia to measure cortical and trabecular volumetric bone mineral density (vBMD), bone dimensions (including cortical area, periosteal and endosteal circumference, cortical cross-sectional area, polar section modulus). pQCT was performed using a Stratec XCT-2000 machine.

iii) **Growth** – Height at the baseline and follow up visits were recorded. The height standard deviation score (SDS) was calculated cross-sectionally in all children, and any change in height was included in the analysis

iv) **Medical history** was obtained from direct questioning of the participant and/or guardian, as well as from the medical notes. Targeted questioning about fractures (number, site, impact- high or low energy, healing time), bone or joint pain as well as use of analgesia and effect on activities of daily living was undertaken.

2.2.1 Dual Energy X-Ray Absorptiometry (DXA)

DXA is a tool that is used for evaluating bone density in children and in adults (Wasserman et al., 2017). It uses low radiation to measure bone mineral content (BMC) and projected bone area (BA), from which the areal BMD is calculated as BMC/BA (Crabtree and Ward, 2015, Adams et al., 2014). Although measurements can be made at the spine, hip, forearm or whole body (Crabtree and

Ward, 2015), the common sites in paediatric practice include lumbar spine and 'total body less head' (Messina et al., 2018). Lumbar spine DXA is particularly useful in children because vertebrae are comprised of principally trabecular bone, and this site is readily influenced by any pathological processes, due to the rapid bone turnover (Wasserman et al., 2017). In adults, the recommended site is the femoral neck, as any possible aortic calcification can hinder interpretation of the lumbar region. Scanning lasts only a few seconds and is only vulnerable to motion artefact in very mobile children (Crabtree et al., 2014). The BMD score is produced automatically by the software and is expressed in age, sex and ethnicity matched z-scores (Gordon et al., 2014). Importantly, however, BMD reflects density in a two dimensional projection only. Therefore it may be misleading in shorter children or those with delayed growth, as the projected bone area will be smaller. To overcome this problem Bone Mineral Apparent Density (BMAD) is used to try and estimate the true density in g/cm^3.

Image acquisition

A DXA scanner produces X-rays that pass through the body of the subject and are detected on the opposite side by an electronic plate. The low level radiation (4-27microSv), at 2 different energies, enables the differentiation of soft tissue and bone (Crabtree and Ward, 2015, Adams et al., 2014). The hips and lumbar spine were chosen as sites due to being the commonest sites imaged in both children and adults. In general, the recommended imaging site in adults is the hips, as they are a major site for pathological fractures, and any possible aortic calcification can hinder the interpretation of the lumbar site imaging in the antero-posterior direction.

All DXA image acquisitions were undertaken using the standard operating procedure as required by the respective research site. This broadly included ensuring that the participant was not pregnant and then the lumbar spine and hips were imaged as per international guidelines(Crabtree et al., 2014).

I am very grateful to the radiographers at each site, and in particular Dr Nicola Crabtree (Consultant Clinical Densitometry Scientist; Birmingham Children's Hospital) and Katy Budhan-Mills (General superintendent Radiographer; Great Ormond Street Hospital) for helping me ensure all research patients were accommodated promptly and that the correct study procedures were followed.

The DXA imaging was performed at three hospitals in this study. This was for patient convenience as all investigations took place alongside a routine clinic visit or prior to a midweek haemodialysis session. The three sites were: Great Ormond St Hospital, Birmingham Children's Hospital and 'Aglaia Kyriakou' Children's hospital in Athens. The two DXA machines used were the Lunar iDXA (GE Healthcare; BCH and Athens) and the Lunar Prodigy (GE Healthcare). Each participant at follow up was scanned on the same machine as the first measurement. Both densitometers have been shown to produce highly correlated measurements of BMD, both at the L1-L4 spine and hip sites (Krueger et al., 2012)

Measurement analysis

It is important to note that aBMD represents a 2-dimensional image of a 3-dimensional structure. In growth restricted or short children, as the projected bone

area will be smaller it may provide a misleading overestimation of BMD (Figure 1.5.3.1) (Zemel et al., 2010) or underestimate BMD in a tall child (Crabtree and Ward, 2015).

To avoid overestimation of BMD, lumbar spine DXA aBMD results are therefore adjusted for bone size (ie growth or height of the child). The size-adjusted density measurements are known as Bone Mineral Apparent Density (BMAD). The aim of the size adjustment is to try and estimate the bone density in g/cm^3. This is consistent with the 2013 International Society of Clinical Densitometry (ISCD) Pediatric Official Positions (Crabtree et al., 2014). Reference data for lumbar spine BMAD in healthy children are available from 3598 healthy 4 to 20-year-olds from 7 UK centres (Crabtree et al., 2017). Other healthy reference datasets, adjusting for growth or height are also available (Kalkwarf et al., 2007, Ward et al., 2007, Zemel et al., 2011, Chastin et al., 2014).

BMAD was calculated as per Crabtree et al (Crabtree et al., 2017) using the :

$$\text{BMAD (g/cm}^3) = \frac{(\text{BMC1} + \text{BMC2} + \text{BMC3} + \text{BMC4})}{(\text{V1} + \text{V2} + \text{V3} + \text{V4})}$$

Where Vn is the volume of the nth individual vertebra. Vn= $APn^{1.5}$ (APn = projected vertebral area of the nth vertebra). BMCn is the bone mineral content of the nth vertebra.

BMAD z-scores were calculated from the UK reference data (Crabtree et al., 2017). This database is the main clinically used database.

This BMAD equation assumes that the vertebral bodies are a cube shape as published by Carter et al (Carter et al., 1992). There is a second widely used equation, published by Kröger et al (Kröger et al., 1992), which assumes the vertebral column being assessed is cylindrical in shape:

$$\text{BMAD (g/cm}^3) = \frac{BMC1,2,3,4}{\pi * (width/2) * (width/2) * (\frac{Area}{width})}$$

An analysis of both methods of BMAD calculation is presented in Chapter 4, of both children and young adults, thereby exploring any differences and uncovering potential confounding factors.

DXA scanning and measurement of aBMD are considered highly reproducible, on account of the standardised image acquisition techniques and the standardisation of the densitometers (Moreira et al., 2018, Leonard et al., 2009).

2.2.2 Peripheral Quantitative Computed Tomography

Quantitative CT (QCT) is a technique whereby CT images acquired are analysed by specific software to obtain quantitative measures such as volumetric bone mineral density and BMC in any bone compartment (Stagi et al., 2016). Some studies have used conventional CT scanners, but the scanners that are used in this project -across all research sites- are the XCT 2000 (Stratec Medizintechnik, Pforzheim, Germany). The advantage of using the pQCT scanner, as opposed to solely

DXA, is that it provides actual volumetric and density data in g/cm^3. It can distinguish between trabecular and cortical bone compartments independent of size of the subject (Crabtree and Ward, 2015).

In childhood CKD, pQCT has been used successfully to demonstrate the changes in bone demineralisation seen as the disease progresses. A study comparing 156 children with CKD (stages 2 to 5 including 36 on dialysis) to 831 healthy participants (ages 5-21yrs) using tibial pQCT showed that iPTH levels above the Kidney Disease Outcomes Quality Initiative (KDOQI) recommended target was associated with increased trabecular BMD Z-scores ($p<0.01$), but lower cortical BMD scores ($p<0.01$). Cortical BMD Z-scores were significantly lower in CKD stages 4-5 compared to healthy controls, and the duration of CKD also affected this ($p<0.05$) (Wetzsteon et al., 2011). Denburg et al have shown that per one SD lower baseline cortical BMD Z-score there was a 1.75 fold higher fracture risk (95%CI: 1.15-2.67, $p=0.009$) in children with CKD 2-5D (Denburg et al., 2013).

The predominant pQCT work in paediatric patients with CKD and other renal conditions has been done by Prof Leonard and her team at the The Children's Hospital of Philadelphia, Pennsylvania and latterly at the Stanford University in California (Denburg et al., 2013, Tsampalieros et al., 2013b, Tsampalieros et al., 2014, Wetzsteon et al., 2009, Wetzsteon et al., 2011), so we have adapted her pQCT methodology and protocol for this study (See SOP in Appendix) aquiring images at the 3%, 4%, 38% and 66% sites of the non-dominant tibia, and 4% and 66% sites of the non-dominant radius.

This is to allow generation of z-scores of the measurements against the largest standardised reference dataset, as published by Leonard et al (Leonard et al., 2010).

i)   The following measurements were collected from the tibial imaging:

3% metaphyseal site- analysed for trabecular volumetric BMD (mg/cm^3)

4% metaphyseal site-analysed for trabecular volumetric BMD (mg/cm^3)

38% diaphyseal site-analysed for cortical volumetric BMD (mg/cm^3), periosteal circumference (mm), endosteal circumference (mm), and cortical cross-sectional area (mm^2) within the region defined by the endosteal and periosteal surfaces, bone mineral content (mg/mm^3), polar section modulus (mm^3), and cross sectional moment of inertia.

66% diaphyseal site - Muscle and fat area (mm^3)

ii)   The following information was collected from the radial imaging:

4% metaphyseal site-analysed for trabecular volumetric BMD (mg/cm^3)

66% site-analysed for cortical volumetric BMD (mg/cm^3), periosteal circumference (mm), endosteal circumference (mm), and cortical cross-sectional area (mm^2) within the region defined by the endosteal and periosteal surfaces, bone mineral content (mg/mm^3), polar section modulus (mm^3) and cross-sectional moment of inertia.

My training and learning of the pQCT machine consisted of observing, then performing and being observed by Dr Shroff's Research Nurse Selmy Silva, trained in

the technique by Dr J. Willnecker of Stratec. I was also instructed by Dr Nicola Crabtree, Consultant Clinical Densitometry Scientist, from the Birmingham Women's and Children's NHS Foundation Trust. All pQCT scanning at Great Ormond St Hospital was undertaken by myself, at the Birmingham Women's and Children's hospital by Dr Nicola Crabtree and in Athens by Dr George Kiniklis. All scanning was based on the SOP of this study.

Image acquisition and protocol

For detailed description of the imaging protocol, please see the SOP for pQCT scanning in the Appendix. Prior to each use, the phantom limb associated with the particular machine was scanned. This ensures correct calibration for measurements, but also that the scanner is working correctly and the radiation dose is appropriate. This is a necessary step as the software requires it.

The non-dominant limb was chosen for scanning of both upper and lower limbs. Limbs with working or non-working fistulae were avoided. The dominant side can be established by asking which hand the participant writes with, and which leg the participant kicks a ball with.

Figure 2.2.2. Example of pQCT scanner, with left lower limb of participant inserted through the gantry prior to Scout View being obtained.
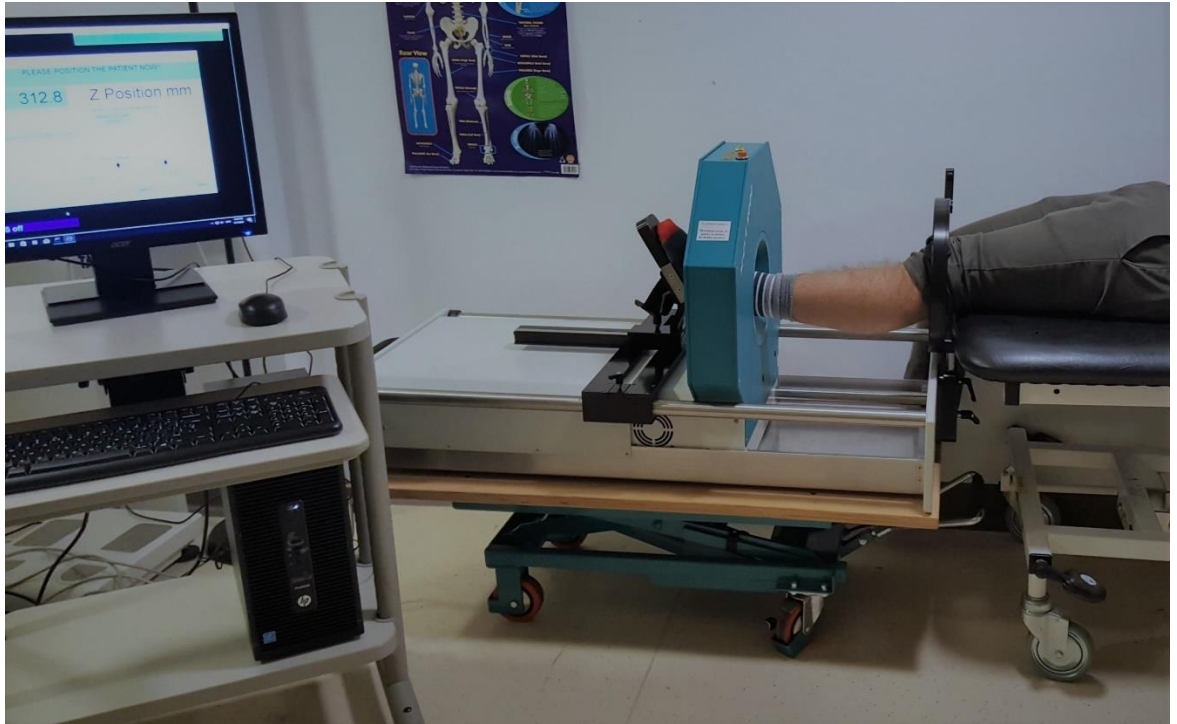
1. The participant was correctly identified with two pieces of information in addition to name (usually date of birth and address).

2. All females aged over 10 years old were asked directly whether they could be or were pregnant. If definitely not or within 2 weeks of last menstrual cycle, scanning proceeded.

3. Length of measurement: For tibial scans, the length from the intercondylar eminence (tibial plateau) to the middle of the medial malleolus was measured. For radial scans, the length from the head of the radius to the styloid process of the radius was measured. For each this was repeated 3 times for accuracy.

4. Settings: voxel size of 0.4 mm, slice thickness of 2.3 mm, and scan speed of 25 mm/sec were automatically selected.

5. Sites for measurement in the tibia:

3%, 4%, 38% and 66% of tibia length proximal to the reference line.

- 3% metaphyseal site - analysed for trabecular volumetric BMD (mg/cm3).

- 4% metaphyseal site- analysed for trabecular volumetric BMD (mg/cm3)

- 38% diaphyseal site – analysed for cortical volumetric BMD (mg/cm3), periosteal circumference (mm), endosteal circumference (mm), and cortical cross-sectional area (mm^2) within the region defined by the endosteal and periosteal surfaces, bone mineral content (mg/mm^3), and polar section modulus (mm^3).

- 66% diaphyseal site - Muscle and fat area (mm3)

6. Patient was asked to lie on the examination couch with the appropriate leg inserted through the gantry, or sat upright in chair with the appropriate arm through the gantry. The limb was secured by the Velcro holders.

7. The Scout View scan was initiated and the reference line placed:

-at the proximal border of the distal tibia growth plate in children with open growth plates

-at the proximal border of the distal endplate in participants with fused growth plates

8. The images were then acquired. The software calculates the distance to the loci of interest from the reference line and automatically moves the gantry to obtain the measurements.

Measurement Analysis

All scan results were available immediately after scanning. However, I analysed them in a semi-blinded fashion in batches of 50. With Dr Crabtree's help, I constructed a 'loop' whereby the software runs the analysis on the different image slices obtained with the pre-determined thresholds I had inserted. We used the analysis protocol as per Prof Leonard (Leonard et al., 2010). Namely this was Contour mode 1, Peel mode 4, threshold 600mg/cm3 for metaphyseal sites and Contour mode 1, Peel mode 2, threshold 711mg/cm^3 for diaphyseal bone sites.

Figure 2.2.2a An example of pQCT imaging of the left tibia of a 16 year old male with chronic kidney disease. The images have been obtained at 4 different sites along the tibia. The software then proceeds to automatic analysis of the bone parameters. In this example, the images are from the 3%, 4%, 38% and 6% sites.
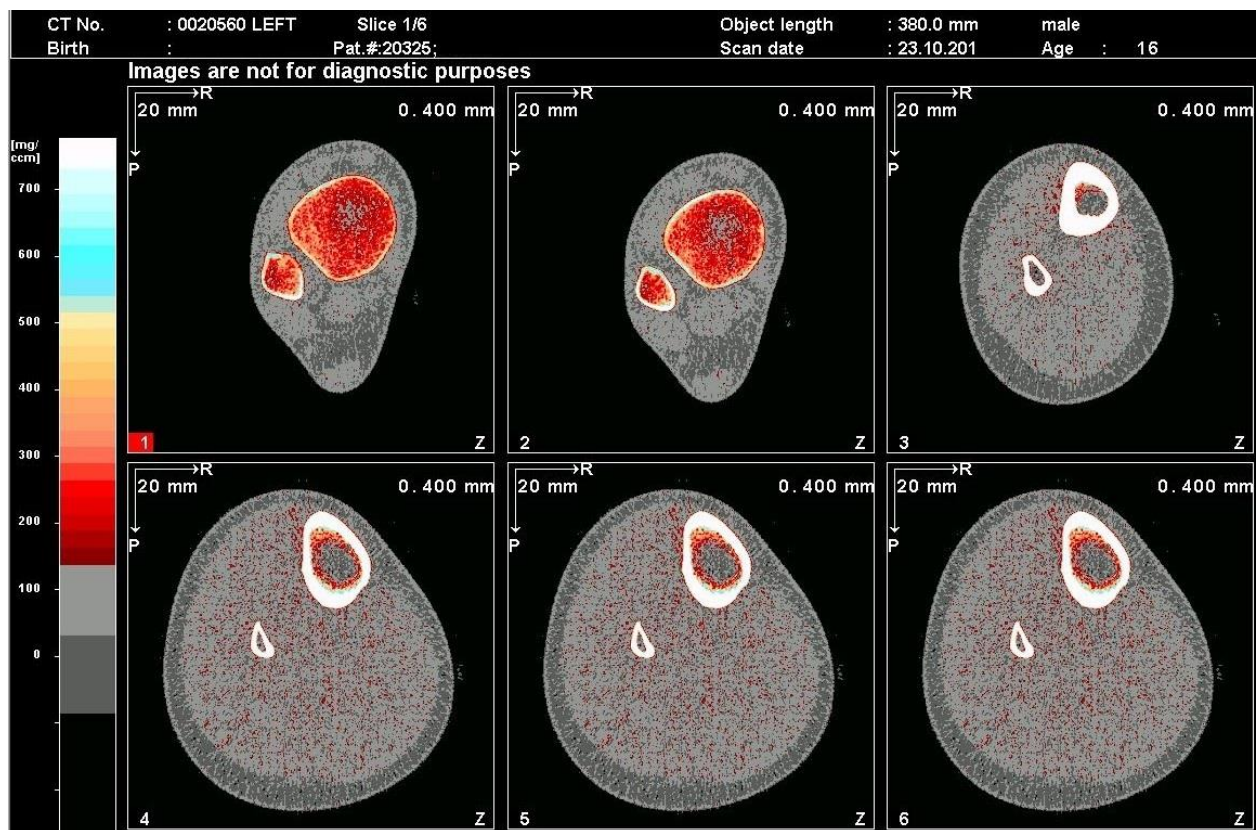
Figure 2.2.2b This is an example of the analysis of the 38% site of the left tibia of a 16 yearr old male with chronic kidney disease. In this particular analysis the total mass, total area, cortical area, and cortical density can be seen.
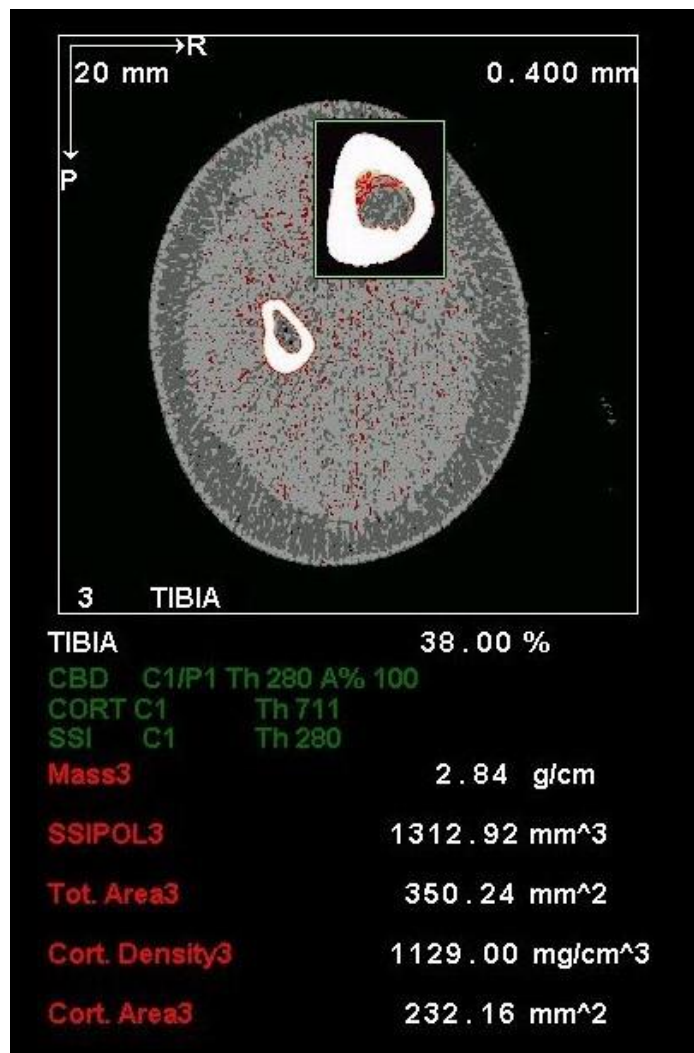
All pQCT scans were assessed in a blinded fashion by myself and Dr Nicola Crabtree to determine the quality. The scans were scored independently by both of us according to the Blew et al method (Blew et al., 2014). Some initial scans were disregarded due to motion artefact.

2.3.1 Assessing structural and functional vascular changes

2.3.1.1 Cardiac CT for coronary artery calcification

Calcification of the coronary arteries has been shown to be present both in adult (Chertow et al., 2004, Spiegel et al., 2004, Cejka et al., 2014, Malluche et al., 2015) and in paediatric patients with CKD (Shroff et al., 2007). CAC has been shown to start early in CKD and accelerate on dialysis (Russo et al., 2004, Spiegel et al., 2004, Goodman et al., 2000, Shroff et al., 2007). Cardiac CT scan is the only modality currently that affords the researcher or clinician a direct quantification of calcification of the vasculature, in a tissue bed that is directly responsible for the increased morbidity and mortality in CKD.

In this study, two CT scanners were used. A GE Discovery 750HD (64-slice) at the Birmingham Children's and the Somatom Force by Siemens (128-slice) at Great Ormond St Hospital, and 'Aglaia Kyriakou' Children's hospital in Athens. The slice number indicates the number of images the scanner obtains per rotation of the gantry. The high number of slices, the better quality of imaging.

To acquire images of the coronary arteries, the systole/diastole cycle of the heart needs to be taken into account. Simultaneous recording of the electrocardiogram (ECG) is needed, and the images can be obtained prospectively or retrospectively. Prospective ECG gating is a technique that uses forward-looking estimation of R wave timing, and retrospective ECG gating uses backward-looking estimation measurement of R wave timing. The main effect is that, with prospective gating, the x-ray beam is turned on for only a short portion of diastole, and it is turned

off during the rest of the R-R cycle, whereas with retrospective gating, the x-ray beam is on throughout the R-R cycle. This results in a significant difference is ionising radiation dose delivery. One study of 100 cardiac CT scans, with over 1200 segments of coronary arteries examined, showed that prospective gating delivered 77% lower radiation doses (Shuman et al., 2008). As this was a paediatric and young person study, prospective ECG gating was used to minimise ionising radiation.

Image acquisition and protocol

Coronary artery and valvular calcification were examined by CT (*Somatom Force; Siemens, Germany* or *GE Discovery 750HD, USA*) using the machines' standard Ca scoring protocol. Prospective ECG triggering was used to obtain images in diastole. Please see Appendix for SOP of Cardiac CTs for this study.

Protocol

I.   Type of Imaging

Non-contrast Prospective ECG-Gated Cardiac CT

II.   Devices

1.   GE Discovery 750HD at the Birmingham Children's Hospital

2.   Siemens Healthcare Somatom Force at Great Ormond Street and Aglaia Kyriakou Children's hospital, Athens.

III.   Patient position and preparation for examination.

Patient positioned feet first and three-lead ECG pads and leads applied

Requirement for breath holding explained and practised by the patient if required.

IV.   Site of measurements

Topogram carried out as per a normal Chest CT.

Plan the Scan range (Range of Interest) from the top of the Aortic Arch to Apex of

Heart. Lateral aspects should ensure the whole heart included.

V.   Measurements

DS Calcium Score Sequence	Ref. mAs	Ref. kVp	Tube Rotation time	Collimation	Slice scan width	Scan Time
Child	80	120	0.25s	1.2mm	3mm	0.14s

- If the heart rate was *below 75* trigger phase started at 70%

- If the heart rate was *above 75* trigger phase started at 40%

If heart rate was variable between the two 40% was selected

The scans were performed with Breathing Instructions on inspiration.

VI.   After the Scan

Images sent to electronic storage (PACS).

Images protected and locked on the work station when finished.

The scan was reviewed by a Named Consultant at each research site for governance reporting.

Radiation

The radiation effective dose equivalent from the cardiac CT scan is 0.6mSv. This radiation dose is well below the natural environmental radiation exposure in the UK (average 2.7 mSv/year), and less than the radiation exposure from a single transatlantic flight (0.8 µSv). This dose is lower than the average effective dose for an adult CT Chest of 7mSv, abdominal CT of 8mSv and much lower than the average effective dose of coronary angiography of 16mSv (Hirshfeld et al., 2018, Mettler et al., 2008).

The scanning protocol above and expected radiation dose were approved by the HRA and ethics committee (See Appendix).

Measurement Analysis

Calcification was expressed as Agatston score (Agatston et al., 1990) and analysed offline in a blinded fashion, confirmed independently by two observers (ADL and KHM) using Syngo Via software (*Siemens, UK*).

The Syngo Via software is an automatic method of scoring the coronary artery calcification. The cardiac CT to be analysed is selected and the program then identifies any tissue with a Hounslow score of 130 or above, and highlights it in pink (Figure 2.3.1.1a). The observer has to then label the areas of calcification as being of interest or to be disregarded (Figure 2.3.1.1b).

The software then produces an Agatston score from the mass and volume of the lesions selected. It summarises the findings in a table for further comprehension (Figure 2.3.1.1c).

There is no scope for the observer to increase or decrease the size of the lesions identified. The only variable open to change is the threshold of Hounslow units above which the calcification will be highlighted.

Figure 2.3.1.1a Single section of a cardiac CT of young person on haemodialysis. Evident are the calcifications in the coronary arteries as well as the haemodialysis central venous catheter.
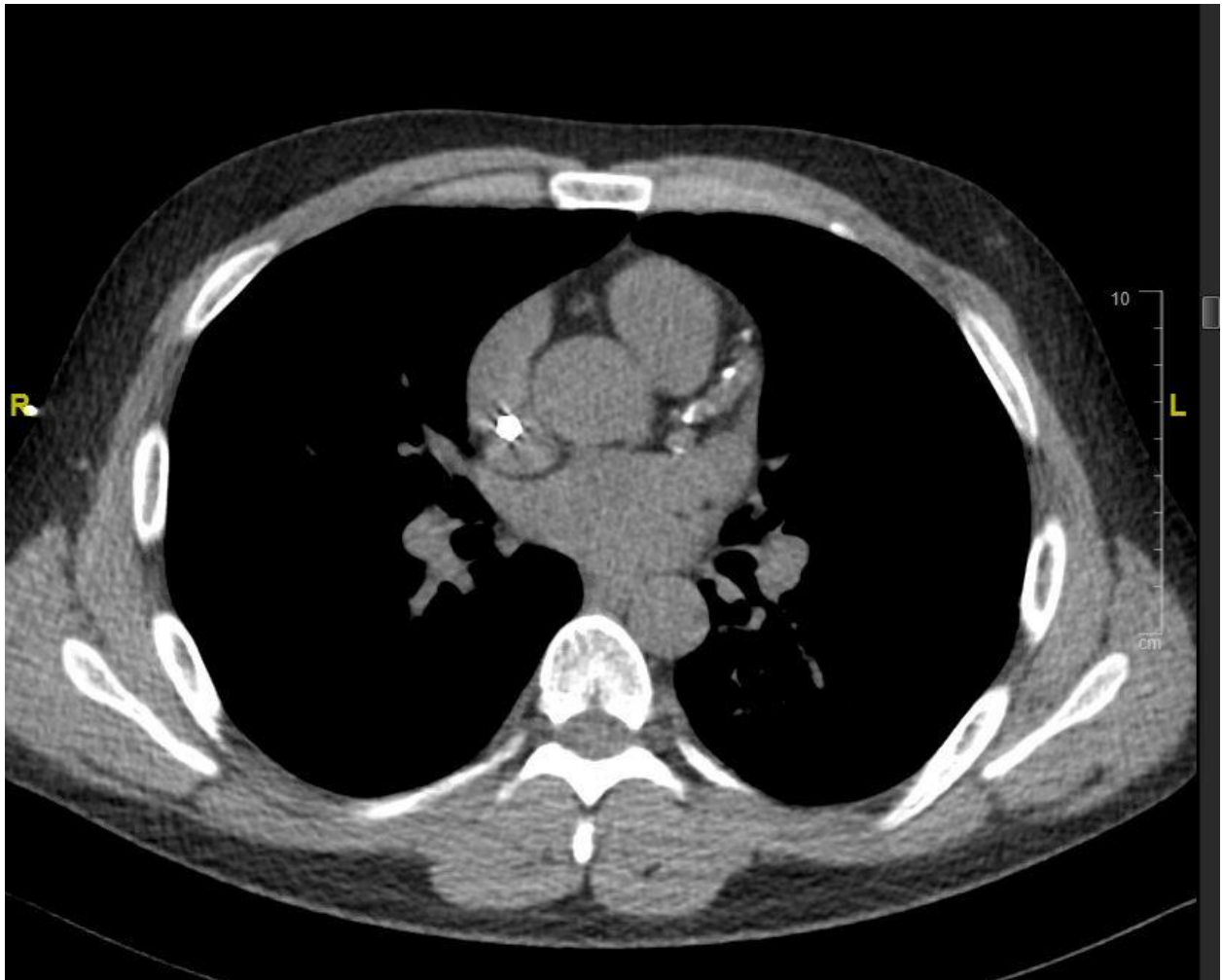
Figure 2.3.1.1b Same single section of a cardiac CT of a young person on haemodialysis. The Syngo Via software has highlighted in pink all areas of 130 Hounslow units or above. The observer has then labelled the haemodialysis catheter to be disregarded (in blue), and the coronary artery calcifications in green for the Left Main coronary artery and yellow for the Left Anterior Descending coronary artery.

Figure 2.3.1.1c Example of summary table produced by Syngo Via of an analysis of a cardiac CT scan. This participant had 3 calcification lesions identified. One in the left main coronary artery, 1 in the left anterior descending and one in the right coronary artery. The combined Agatston score is 19 in this patient.

Artery	Lesions	Volume / mm³	Equiv. Mass / mg	Score
LM	1	0.5	0.13	0.4
LAD	1	16.6	2.74	14.7
CX	0	0.0	0.00	0.0
RCA	1	6.7	0.88	3.8
Total	3	23.7	3.75	19.0
U1	0	0.0	0.00	0.0
U2	0	0.0	0.00	0.0

Settings
Score Type: User defined, Threshold: 130 HU (95.6 mg/cm³ CaHA)
Mass calibration factor: 0.736

2.3.1.2 Ultrasound for carotid intima-media thickness

Vascular calcification and hydroxyapatite deposition in the medial layer of the arteries causes an increase in the medial layer size. Ultra-high frequency ultrasound is able to differentiate between the different arterial layers (Dangardt et al., 2018), but due to this modality not being widely available or accessible, conventional US is routinely used to measure the combined intima and media thickness (cIMT). In adults, increase in cIMT has been used to stratify cardiovascular disease risk (Peters et al., 2012, Peters et al., 2011) as a surrogate measure of the extent of coronary artery disease (Amato et al., 2007). It has in turn been correlated with cardiovascular events, such as myocardial infarction (van der Meer et al., 2004, Szeto et al., 2007). Many paediatric studies have used cIMT as their endpoint, in the absence of hard endpoints such as cardiovascular events or death. It has been used as a sensitive marker of vascular damage, and to study the structural and functional changes of the carotid artery in CKD (Litwin et al., 2005, Mitsnefes et al., 2005, Shroff et al., 2007). Children and young adults with CKD have been shown to be at increased cardiovascular risk and they have been shown to have increased cIMT (Oh et al., 2002, Litwin et al., 2005, Brady et al., 2012, Chavarria et al., 2012, Delucchi et al., 2008, Groothoff et al., 2002a)

The largest paediatric study to date to utilise cIMT has been the Cardiovascular Comorbidity in Children with CKD Study (4C Study), which is a pan-European, multicentre, prospective observational study of children aged 6 to 17 years old with eGFR of 10-60 ml/min/1.73m^2 (Schaefer et al., 2017). The cIMT was elevated

in 41.6% of patients above the 95th centile, with only 11% showing measurements below the 50th centile for age and sex.

All the aforementioned studies have validated the use of cIMT as a surrogate marker of vascular calcification in the absence of hard endpoints.

Image acquisition and protocol

Please see Appendix for detailed SOP for this study.

With the increasing use of cIMT there have been increasing variations in practice. In an attempt to standardise image acquisition and measurement, the delegates of the 3rd and 4th Watching the Risk Symposiums and the 13th and 15th European Stroke Conferences in Mannheim, Germany published guidelines on best practice to measure cIMT (Touboul et al., 2012). The cIMT scanning protocol in this study is adapted from the Mannheim consensus (Touboul et al., 2012), and measurements obtained have been compared to reference values of healthy children for age and height (Doyon et al., 2013), to produce z-scores.

I undertook my scanning training on healthy volunteers at the Vascular Physiology Unit, UCL Institute of Cardiovascular Science, London and was instructed by Dr Scott Chiesa, PhD (Vascular and clinical scientist). I am very grateful to him for his help.

Analysis of the first ten participants with CKD was also done independently, and showed a r correlation coefficient of 0.93. Bland-Altman analysis showed that all measurements were within half a millimetre (Figure 2.3.1.2).

Figure 2.3.1.2a Bland-Altman analysis of the mean cIMT of the common carotid arteries by both myself and Dr Scott Chiesa (r=0.93). Any measurement differences of the mean of right and left carotid cIMT are within 0.05mm.
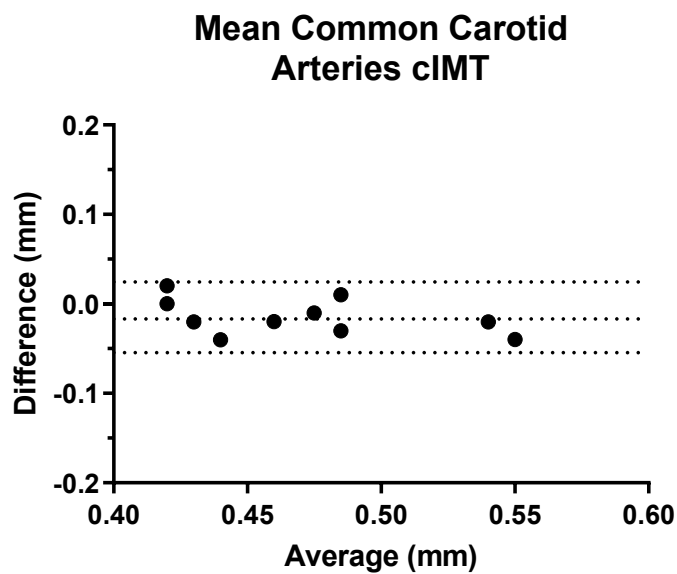
All scanning was undertaken by myself using a Vivid Iq scanner (GE Healthcare), kindly loaned to my by the Nephrology Department at the Birmingham Women's and Children's NHS Foundation Trust.

Figure 2.3.1.2b Vivid Iq (GE Healthcare) scanner used in this study. GE 12L-RS Linear probe pictured on the right.

Scanning protocol

I.   Device

1. Vivid Iq (GE Healthcare, USA).

2. Linear probe (12L-RS) 5 to 13 MHz

II.   Site of measurements

1. Common carotid arteries (CCA), 1 – 2 cm below bifurcation.

2. Measurements are taken from right and left arteries

III.   Patient position and preparation to examination.

1. Examination took place in a temperature controlled room, after 5 minutes

   rest

2. Supine position with slightly extended neck

3. Concurrent blood pressure measurement taken

IV.   IMT measurements

1. Three lead ECG electrodes connected, using general convention (Red lead to

   Right shoulder, Yellow lead to Left shoulder and Green lead to left/right side

   of abdomen)

2. Carotid function selected on software

3. Patient study number, sex and date of birth entered into software

4. CCA identified in transverse view

5. CCA identified in longitudinal view by rotating probe

6. Distance of CCA 1 – 2 cm below bifurcation identified

7. A minimum of 3x five second videos of this view obtained for each carotid.

8. Both the far wall of the CCA and the 'lead II' electrocardiogram were visible

   during recording. If they were not, recording repeated.

V.   Measurement of wall cross-sectional area

1. Longitudinal view of CCA in B-mode identified

2. Switch to M-mode to obtain vessel wall and electrocardiogram views

3. Concurrent BP measured on corresponding upper limb

4. A minimum of 3x 5 second video recordings obtained for each carotid

5. Offline and in a semi-blinded fashion: The video with the optimal views is frozen and the systolic internal diameter of CCA – the distance between two most distal points of near and far wall were measured. At least 5 – 6 measurements were taken and averaged for each carotid.

6. Then the diastolic internal diameter of the CCA was measured – using the smallest distance between near and far wall.

7. This process was repeated for the contra-lateral side.

Figure 2.3.1.2c Still image of a CCA with the software identifying the intima and media layers, as highlighted between the green lines

	Max	Mean	SD	QI	Points
Near	0.55 mm	0.47 mm	0.06 mm	0.26	41
Far	0.52 mm	0.43 mm	0.04 mm	0.94	150
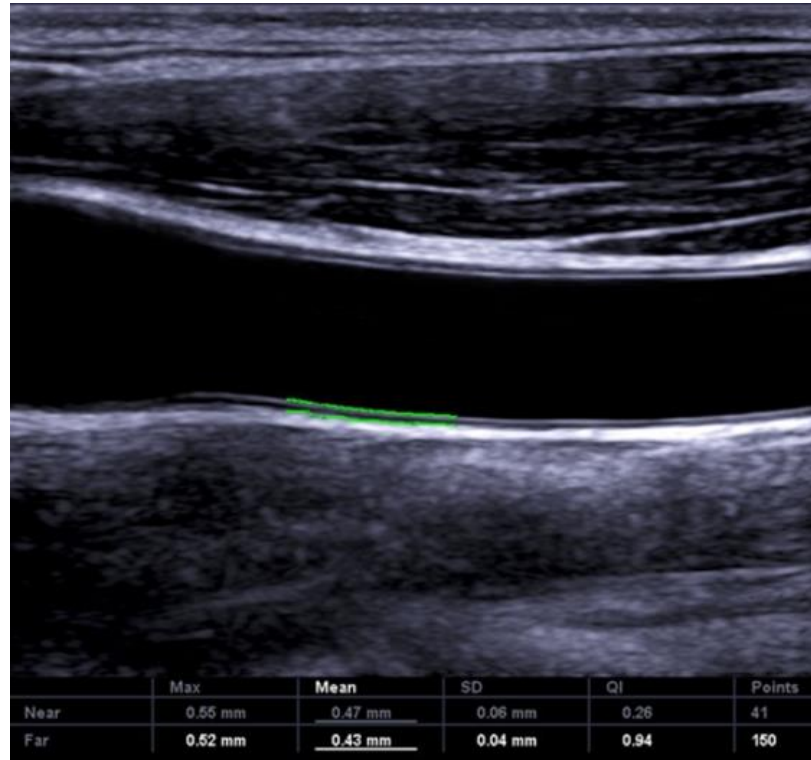
Figure 2.3.1.2d Still image of an M-Mode capture of a Left CCA. Visible are the B-mode transverse view of the vessel, the M-mode plain and the simultaneous 'lead II' electrocardiogram
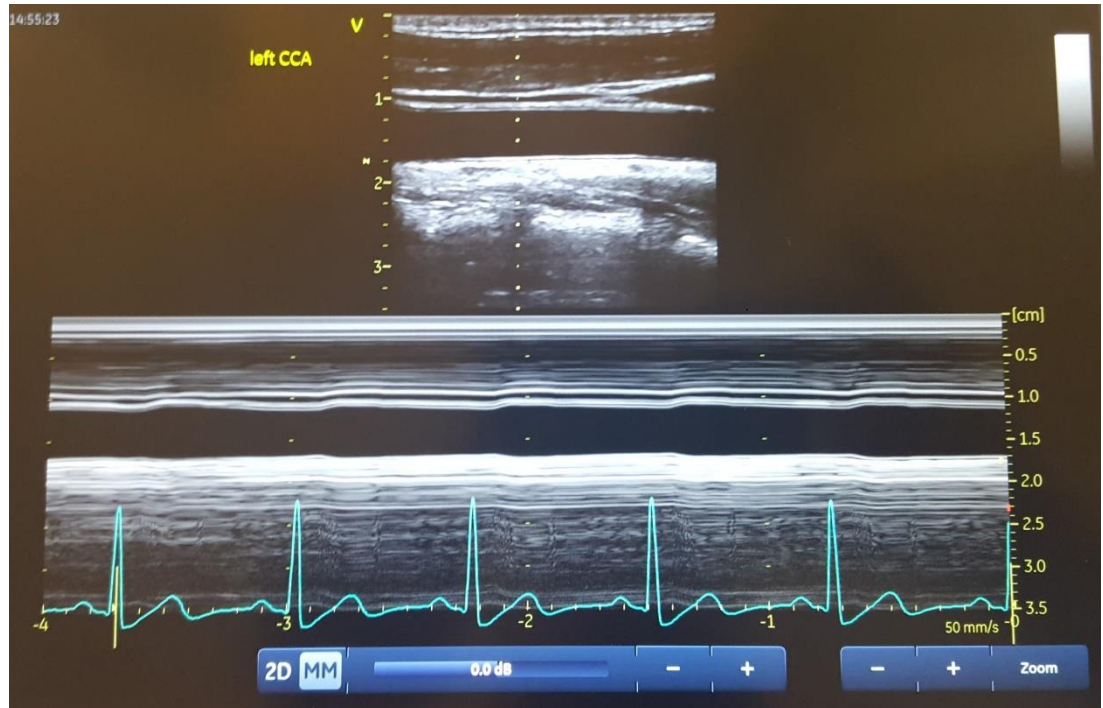
Measurement Analysis

As outlined above, all cIMT measurements were obtained on a single portable Vivid Iq (*General Electric, USA*) ultrasound machine according to the Mannheim consensus (Touboul et al., 2012). All measurements were obtained by myself. All images/video clips were stored on the machine in a digital, encrypted, password-protected way, and analyses were done offline, in a blinded fashion by myself.

cIMT was calculated semi-automatically with the Vivid Iq software. This software allows the operator to highlight a vessel wall length and automatically

identifies the intimal and medial layers. It then calculates the thickness in millimetres at 300 separate points and provides an average.

The recorded video to be analysed was frozen at the peak of the R wave and the area of interest highlighted. An area of 1cm was identified 1-2cm below the bifurcation of the carotid artery. This was repeated 3 times for each carotid and an average used.

Systolic and diastolic internal diameters of the common carotid artery were obtained from the M-mode transverse view recordings of each carotid. Five measurements of the carotid lumen diameter in systole and diastole were taken and the average of each used to determine systolic and diastolic diameter (Jourdan et al., 2005). In turn, these measurements were used to determine:

mean wall cross-sectional area (WCSA)

mean lumen cross-sectional area (LCSA)

their ratio (LCSA/WCSA; reflecting the ability of the vessel to dilate in relation to vessel wall thickening), distensibility coefficient (reflecting the functional properties of the carotid, and its ability to distend with each cardiac cycle)

and distensibility co-efficient.

The formulae for their calculations are presented in **Figure 2.3.1.2e** (Lalayiannis et al., 2021a).

Figure 2.3.1.2e. Adapted from (Lalayiannis et al., 2021a). Schematic figure

illustrating the layers of the carotid artery and the intima-media thickness.

Equations for calculation of the mean systolic and diastolic diameters, wall cross

sectional and lumen cross sectional areas and distensibility coefficient. Previously

published in (Jourdan et al., 2005)

Mean systolic diameter (sD) = (LsD + RsD)/2

Mean diastolic diameter (dD) = (RdD + LdD)/2

Wall cross sectional area (WCSA) = $\pi*(dD/2 + IMT)^2 - \pi*(dD/2)^2$

Lumen cross sectional area (LCSA) = $\pi *dD^2/4$

Distensibility coefficient = $2(\Delta D/dD)/(\Delta P/10*1.33*100)$

LsD = left common carotid artery systolic diameter
RsD = right common carotid artery systolic diameter
LdD = left common carotid artery diastolic diameter
RdD = right common carotid artery diastolic diameter
IMT = carotid intima media thickness
ΔD = sD - dD
ΔP = Systolic BP- Diastolic BP

cIMT measurements were expressed as z-scores according to Doyon et al

(Doyon et al., 2013). Adults' z-scores were calculated using interpolation of the

difference between 17 to 18 years old. The annual increase of absolute cIMT each

year to the age of 30 was assumed to be the same as the increase from 17 to 18

years. A comparison of the published healthy reference databases for z-score generation and further analysis of the interpolation method are provided in the results section of the thesis.

2.3.2 Pulse Wave Velocity (PWV) and Pulse Wave Analysis (PWA)

A healthy vasculature plays a key role in delivering blood, and thus oxygen to the tissues around the body. In order to accommodate the large volume of the left ventricular output during each cardiac cycle and propagate the blood to the most distal parts of the body, the arteries have to act as a temporary reservoir for the cardiac output. Systole causes an increase in diameter of the arterial lumen, thereby effectively storing the increased blood volume in this enlarged space, followed by a diameter decrease in diastole, when the vessel walls return to their normal size, thus creating a dynamic elastic propagation effect (Azukaitis et al., 2020). This leads to the needed continuous blood flow.

This dynamic elasticity occurs because arteries are composed of three key layers. The innermost tunica intima is formed of endothelial cells, fibrocollagenous tissue and the internal elastic lamina. The medial layer is composed of vascular smooth muscle cells and elastin fibres. The adventitia is formed of fibrocollagenous tissue and the external elastic lamina (Shirwany and Zou, 2010). Larger elastic arteries have a slightly higher elastin to VSMC ratio, compared to smaller muscular arteries (eg more distal arteries) which have more VSMCs in their medial layer. This is needed to alter the velocity of the pressure wave generated by the cardiac output and help propagate it. The relative impedance this pressure wave encounters downstream with the smaller lumens causes a 'reflected' back-pressure wave. This

is key in the diastolic segment of the cardiac cycle as it helps maintain coronary artery flow at the root of the aorta (Shirwany and Zou, 2010).

Any pathological process that disrupts the normal elastic properties of the arteries can lead to alteration of this physiological process and have clinical implications with the ensuing arterial stiffness and resulting poor coronary perfusion, thus causing cardiovascular morbidity. In CKD, the deleterious process is thought to be due to vascular calcification. The structural change associated with vascular calcification, in a dynamic tissue such as a blood vessel, may produce functional changes such as stiffness and reduced distensibility. This in turn increases the pulse wave velocity.

PWV is the speed of travel of the pulse along a segment of arterial vessel. Arterial stiffness can therefore be measured at any arterial site, but the carotid-femoral PWV includes the aorta and is considered the gold-standard and the most clinically relevant measurement used. CfPWV is determined by measuring the time delay between the pulse arriving at the carotid and femoral pressure sensors over the length of arterial vessel. It's a preferred marker of arterial stiffness as its non-invasive, simple to perform, reproducible and predicts cardiovascular outcomes in adult patients(Townsend et al., 2018).

Augmentation index (AIx) obtained from pulse wave analysis is the percentage by which the systolic blood pressure increases as a result of the wave reflection coming from distal blood vessels to the central blood vessels. Increased arterial stiffness causes an earlier return of the 'reflected wave', which arrives in systole instead of in diastole, causing a rise in systolic pressure and an increase in

pulse pressure (PP). This in turn increases left ventricular afterload and a decrease in diastolic blood pressure (BP) and impaired coronary perfusion. AIx increases with age, and it is calculated as AG (augmentation pressure) divided by PP ×100 to give a percentage (Fantin et al., 2007).

Figure 2.3.2a Central pressure waveform. Adapted from (Sharman et al., 2009). T_R is the timing of the reflected pressure wave. P1 and P2 are the systolic peaks. Augmentation index is the Augmented Pressure divided by the Pulse pressure x 100.
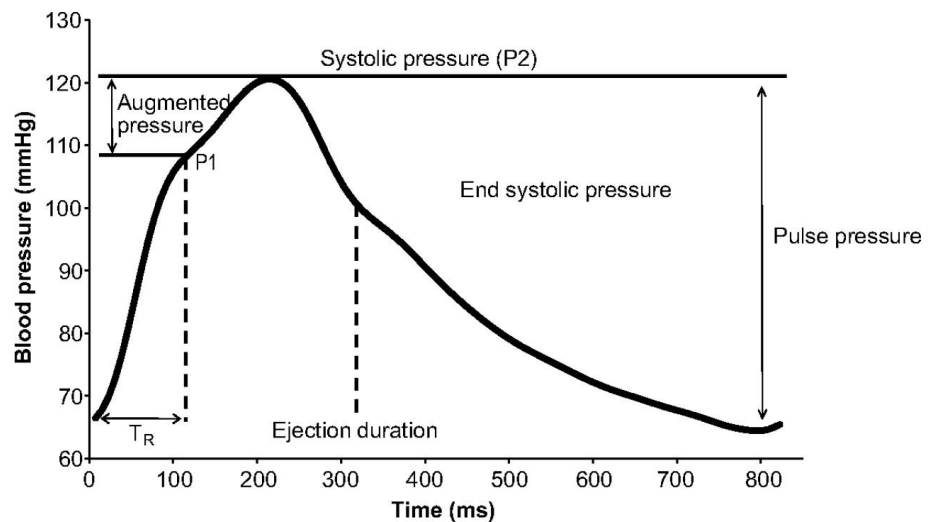
Several studies have included PWV assessment and pulse wave analysis for augmentation index (AIx) in their protocols in attempt to characterise the effect of CKD-MBD on young blood vessels. It is noteworthy that an elevated arterial stiffness, as examined by PWV, is a predictor of future mortality and morbidity, independently of raised blood pressure in adult patients with CKD (Townsend et al., 2018, Ben-Shlomo et al., 2014). Paediatric studies have shown that PWV and Aix are significantly higher in children on dialysis (Covic et al., 2006, Shroff et al., 2007). The

4C study showed that PWV is increased in 20% of children and adolescents with CKD, and that this is correlated with cIMT (r=0.23, p<0.001). The implication of this is that the structural changes brought upon the blood vessels by CKD-MBD, affects the elasticity of the vessels and therefore the functional properties leading to the increased pulse wave velocity seen (Schaefer et al., 2017).

The number of large studies utilising PWV as a surrogate marker of arterial stiffness is small. Nevertheless, there is a clear signal that arterial stiffness is increased in CKD, and is likely to progress on dialysis.

I undertook training in PWV and PWA technique with Dr Olga Panagiotopoulou, Clinical Research Fellow at the Cardiology Dept, King's College NHS Foundation Trust, as well as with Dr Dimitrios Chanouzas of the Institute of Inflammation and Ageing, University of Birmingham and University Hospitals Birmingham. I am very grateful for their support.

Image acquisition and protocol

Please see the Appendix for the detailed SOP for performing the PWV and PWA measurements in this study.

Protocol

I.   Devices

1. Oscillometric Vicorder system with Toshiba Laptop (Skidmore Medical, Bristol, UK; Software Version 8.1)

2. Neck cuff, femoral cuff (2 sizes available for <10 years and >10 years, judge by size)

II.   Positioning and cuff placement

1. Participants positioned in a quiet and air-conditioned room. The participant asked to lie in supine position with a 30° elevated head and shoulders. Measurements taken after at least 5 minutes of rest lying supine.

2. The neck cuff was placed around the neck, with the small inflatable pad placed above the right common carotid artery.

3. The femoral cuff was placed around the upper right thigh as close to the groin as possible. The air tubing was placed facing superiorly. If able, the participants were invited to help with this task. All items were removed from the right pocket prior to this.

III.   Distance measurement between cuffs

As per Kracht et al, 2011 (Kracht et al., 2011), the distances should be measured as:

Figure 2.3.2b Positioning of the cuffs and the distances measured to be

inputted as 'length' in the software
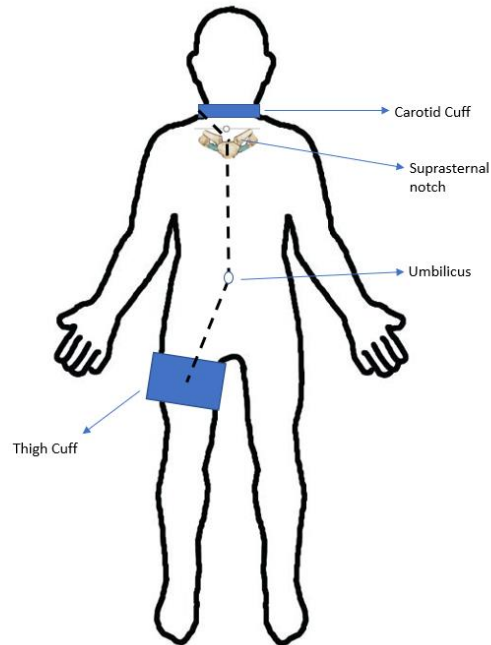
Suprasternal notch to umbilicus (SSN to Umb)

Umbilicus to mid thigh cuff (Umb to Tcuff)

Suprasternal notch to mid neck cuff (SSN to

Ncuff)

1. The 'length' to be entered for the PWV measurement should be calculated

    as:

    Length= (SSN to Umb)+ (Umb to Tcuff)- (SSN to Ncuff)

2. BP was measured in left upper arm with manual sphygmomanometer

    immediately prior to examination (or right upper arm if fistula present in left

    arm)

IV. PWV measurements

1. Cuffs inflated as per SOP and software requirement

2. At least 10 beats to be registered which are of adequate quality per

   measurement

3. If waveforms were erratic or of poor quality, the measurement was repeated

4. At least 3 measurements registered, each > 10 beats per recording.

Figure 2.3.2c Example of good quality reading:
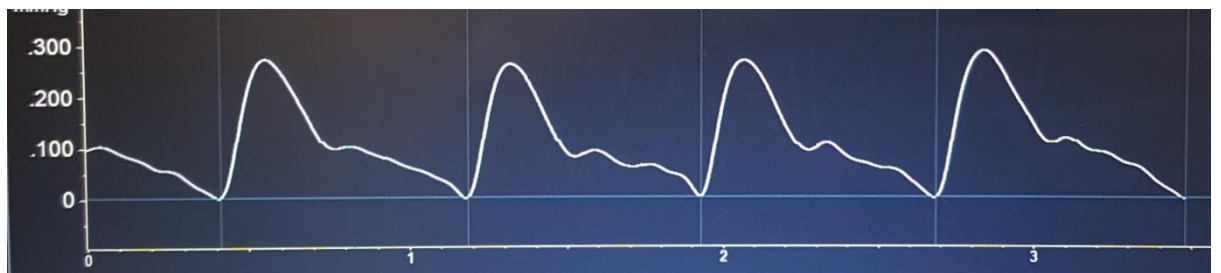
Figure 2.3.2d Example of poor quality reading:
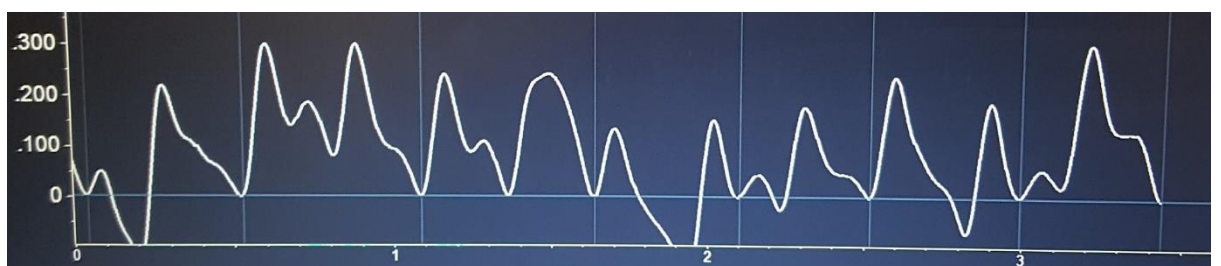
V. PWA & AIx measurements

1. Positioning of the participant was in the same as per PWV measurements

2. Auscultatory blood pressure with manual sphygmomanometer taken 3 times. The average reading of systolic and diastolic blood pressures were entered into relevant boxes.

3. Cuff placed on the right upper arm as high as possible to the shoulder. (Left arm used if fistula present in right arm)

4. Participant asked to relax and keep arm as still as possible

5. Measurement initiated and when at least 10 beats were registered and the software had calculated all parameters, measurement saved.

Figure 2.3.2e Example of adequate readings and calculated parameters:
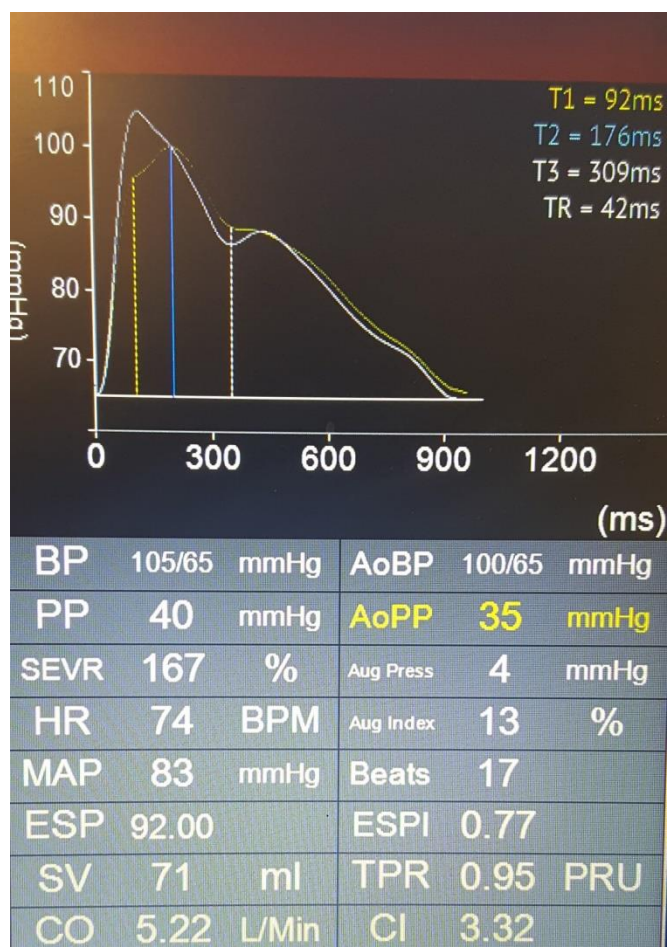
Measurement Analysis

All measurements of PWV and PWA were stored on the encrypted laptop and password protected. They were analysed in batches of at least 25 at a later date, off line, in a blinded fashion. The average of all measurements was taken and used as the PWV or AIx value for that participant, respectively. If there was an outlying value that was extremely low or high and out of keeping with the other values, it was disregarded and not included in the average calculation.

2.4 Serum Biomarkers

There are numerous serum biomarkers that have been utilised as surrogate measures of the metabolic cycle of the bone. They are grouped into bone formation markers, bone resorption markers and osteocytic markers.

Bone histomorphometric studies have shown that serum PTH is associated with both bone mineralisation and turnover. However, PTH can remain within normal levels in the early stages of CKD, despite bone biopsy studies showing that almost a third of children in CKD stage 2 have poor bone mineralisation (Bakkaloglu et al., 2010, Wesseling-Perry et al., 2012). Furthermore, PTH is not able to discriminate to a sufficient degree between low and high turnover bone disease, in the ranges where most patients' PTH values are found (100-1000 ng/L) (Barreto et al., 2008b). The combination of a high serum PTH and normal calcium value was 85% sensitive and 100% specific for identifying patients with high-turnover bone disease (Salusky et al., 1994). The optimal ranges for PTH and other biomarkers is heavily contested Maintaining PTH within normal levels up to 2x ULN seems to be associated with good

growth (Waller et al., 2008). The International Pediatric Peritoneal Dialysis Network Registry that followed up nearly 900 children on PD found that clinical and radiological symptoms markedly increased when PTH exceeded 300 pg/ml, the risk of hypercalcemia increased with levels below 100 pg/ml, and time-averaged PTH concentrations above 500 pg/ml were associated with impaired longitudinal growth (Borzych et al., 2010). In a prospective study of 171 children with CKD, high PTH was independently associated with a decline in tibial cortical BMD on annual follow-up (Denburg et al., 2013).

No biomarker individually or in combination, is sufficiently robust to diagnose bone mineralisation or turnover defects (Sprague et al., 2016, Behets et al., 2015). The bone biomarkers studied so far have not been sensitive or specific enough to be translated into an accurate clinical tool to predict bone turnover and mineralisation states. The 2017 KDIGO guidelines recommends using trends in PTH rather than absolute 'target' values when making decisions as to whether to start or stop treatments to lower PTH. The International Osteoporosis Foundation states that bone turnover markers may be useful in routine clinical practice to predict fracture risk and assess bone mineralisation, but they currently have significant drawbacks such as biological variability and inadequate evidence (Vasikaran et al., 2011). Furthermore, biomarkers vary depending on age, gender, pubertal stage, fasting status and circadian rhythms and assays are not always standardised (Glendenning, 2011, Fischer et al., 2012). Larger paediatric studies that correlate bone biomarkers with the gold standard of bone histomorphometry as well as patient level outcomes such as fractures are required.

In this study we have only included clinically routinely used serum biomarkers. Non-fasting blood samples were collected at the study visit or prior to a mid-week hemodialysis session and analysed in the patients' respective hospitals.

These included serum ionized calcium (iCa), total calcium (Ca), phosphate (P), magnesium (Mg), bicarbonate, intact PTH (iPTH), 25-hydroxyvitamin D [25OHD], and alkaline phosphatase (ALP). Due to different iPTH assays used (Immulite [*Siemens Healthcare Diagnostics*] and Elecsys 2010 [*Roche Diagnostics*]), results have been expressed in multiples of the upper limits of normal (ULN).

Extra serum was collected and was banked, as future studies are planned that will include more research based biomarkers and novel calcium isotope measurements.

2.5 Statistics

This section outlines broadly the statistical analysis used in this thesis. Each study in the chapters that follow has a more detailed outline of the statistical methods used.

All results are presented as median with interquartile range (IQR) as appropriate. SPSS 25 (IBM) was used for all statistical analyses. A p-value of <0.05 was considered statistically significant, and two-sided testing of the hypothesis was used. Spearman rank testing was used for correlations. Kruskal-Wallis ANOVA test for non-normally distributed data with appropriate corrections for unequal

variance, or Mann-Whitney U tests were used as required. Linear regression modelling was used to determine independent associations.

The Prism software program (Graphpad) was used to create graphs.

2.6 Ethical Approval

The project was registered with the UK Integrated Research Application System (IRAS) (#219269) and ethics approval was gained on 2/10/17 by the London-City and East Research Ethics Committee (Reference: 17/LO/0007).

Please see Appendix for Ethics Approval letter.

Chapter 3-

Studying Bone Mineral Density in Young People: The Complexity of choosing a pQCT Reference Database

In this chapter I have described how I came to choose the healthy reference database published by Leonard et al (Leonard et al., 2010) over other reference databases to generate z-scores for my participants. As the cohort age ranged from 5 to 30 years old, z-scores are vital to be able to compare participants BMD across the different ages, sexes and ethnicities as assessed by pQCT.

3.1 Abstract

Bone health is impacted by chronic illness, regardless of cause or organ system affected. This can be through metabolic abnormalities, physiologic processes or immobility. Chronic illness, therefore, often leads to mineralisation abnormalities in young people. Cortical and trabecular bone serve different purposes, with cortical bone acting as a calcium store and providing mechanical structure, and trabecular bone being the more metabolically active component of the skeleton. The two compartments can be affected differently in certain diseases. An imaging technique that allows for detailed study of the bone structure is required. Peripheral quantitative computed tomography (pQCT) overcomes the limitations of dual energy X-ray absorptiometry (DXA) and is perhaps more widely available for use in research than the gold-standard bone biopsy. There are no widely accepted healthy reference datasets for pQCT, unlike DXA.

Fifty-five children and young adults aged 7 to 30 years had the non-dominant tibia scanned at the 3% & 4% sites for trabecular bone mineral density and the 38% site for cortical bone mineral density and bone mineral content. Image acquisition and analysis was undertaken according to the protocols of two of the largest reference datasets for tibial pQCT. The z-scores generated were compared to examine the differences between protocols and the differences from the expected median of zero in a healthy population.

The trabecular bone mineral density and the cortical mineral content z-scores at the 38% site generated by the two protocols were similar. Cortical bone mineral density was significantly different between protocols, perhaps affected by

differences in the ethnicity of our cohort compared to the reference datasets. Only one reference dataset extended from childhood to young adulthood. Only trabecular bone mineral density, periosteal and endosteal circumference z-scores from one methodology were not significantly biased when tested for deviation of the median from zero.

pQCT is a useful tool for studying trabecular and cortical compartments separately. However, it is important to take into consideration that there are variations in pQCT scanning protocols, analysis methodology, and a paucity of reference data, which can significantly impact the generation of z-scores. Reference datasets may not be generalizable to local study populations, even when analysed using identical analysis protocols.

3.2 Introduction

Examining the effects of chronic disease on bone can be challenging. The two bone compartments, cortical and trabecular bone can be affected differently by chronic kidney disease (Parfitt, 1998). Bone biopsy for histomorphometry is considered the gold-standard method for assessing bone health in general. This is because it allows for study of all the dynamic, metabolic processes of the skeleton including the turnover, mineralisation and volume ('KDIGO clinical practice guideline for the diagnosis, evaluation, prevention, and treatment of Chronic Kidney Disease-Mineral and Bone Disorder (CKD-MBD),' 2009). Bone biopsy is not readily available, is invasive, requires a general anaesthetic in children, and histopathology experise

for interpretation. For these reasons, it is only performed in certain centres around the world.

Serum calcium, phosphate, alkaline phosphatase and parathyroid hormone, although used routinely in clinical practice as surrogate markers of bone metabolism, in fact correlate poorly with bone turnover and mineralization (Bakkaloglu et al., 2010). Currently, it is accepted that there is no combination of serum biomarkers that are sufficiently sensitive and specific enough for the accurate assessment of bone turnover or mineralisation state (Sprague et al., 2016, Behets et al., 2015).

Radiographic imaging is an accessible and reproducible way for estimation of bone mineral density clinically. Dual-energy Xray Absorptiometry (DXA) is widely available and clinically used for other disease entities. Normative data for age, sex, and race exist (Crabtree et al., 2017). There is a drawback to DXA in CKD however. DXA provides a two dimensional image of a three dimensional structure. It provides information over a projected area (g/cm^2). This may be misleading in shorter people or children with faltering growth (Fewtrell et al., 2005). Additionally, the image produced is a superimposition of trabecular and cortical bone, thus failing to explain changes in each bone compartment (Lalayiannis et al., 2019). An imaging modality that overcomes this problem is peripheral Quantitative Computed Tomography (pQCT).

pQCT examines a slice of the bone and measures volumetric bone mineral density (volumetric BMD in mg/cm^3) for both cortical and trabecular compartments separately (Stagi et al., 2016) without the need to adjust for body size during image

acquisition. Other parameters measured are bone mineral content, bone area and other derived geometric measurements (cross-sectional area, periosteal and endosteal circumferences, cross-sectional moment of inertia) (Crabtree and Ward, 2015). pQCT has been used to study the effects of chronic illness on bone density and dimensions in children with a variety of underlying diseases, such as chronic kidney disease (Denburg et al., 2013, Tsampalieros et al., 2013b), cystic fibrosis (O'Brien et al., 2018), inflammatory bowel disease (DeBoer et al., 2018, Ward et al., 2017), arthritides (Baker et al., 2017), acute lymphoblastic leukaemia survivors (Mostoufi-Moab et al., 2018), diabetes (Pham-Short et al., 2019), nephrotic syndrome (Tsampalieros et al., 2013a, Wetzsteon et al., 2009), anorexia nervosa (DiVasta et al., 2019, DiVasta et al., 2017) and Duchenne muscular dystrophy (Crabtree et al., 2018).

Our hypothesis was that the scanning protocol and analysis used can have a significant impact on the z-scores generated even in the same healthy population. Careful consideration of which reference dataset is applicable to the study population is needed in the planning stage of any project.

Our aim was to compare tibial pQCT measurements from a sample of the local healthy population of children, adolescents, and young adults to two of the largest reference datasets available.

3.3 Reference data

Many studies have developed normal reference data from a healthy population of children (Roggen et al., 2015b, Roggen et al., 2015a, Moyer-Mileur et al., 2008, Jaworski and Graff, 2018) or children and young adults (Neu et al., 2001, Rauch and Schoenau, 2008, Binkley et al., 2002, Ashby et al., 2009, Leonard et al., 2010, Baker et al., 2013). A detailed summary of the available healthy reference data has been set out in Chapter 1.

It is apparent that there is much variation in the measurement site, technique, software used, and population sample. The diversity is a major drawback to generalizing these results to local populations rendering results incomparable. The anatomical measurement sites reported using the Stratec XCT 2000 include the 4%, 20%, 50% and 66% loci in the radius and the 3%, 4%, 14%, 20%, 38%, and 66% loci in the tibia. In fact, the literature is so heterogenous, that the International Society of Clinical Densitometry (ISCD) published an Official Positions Statement in 2013 in an attempt to standardise the measurements obtained and techniques used (Adams et al., 2014).

3.4 Methods

3.4.1 Study Participants

Healthy children and young adults were recruited from our tertiary pediatric hospital. The cohort comprised children attending minor surgery lists (such as otolaryngology or plastic surgery) and their siblings who were confirmed to have no

underlying systemic illness or infections and were not on any medications, and healthcare staff.

Our inclusion criteria were: age from 5 to 30 years. Children under 5 were not included because of their inability to tolerate sitting still for the duration of the image acquisition. Also, this is generally the youngest age limit in the reference databases available. The older age limit was chosen as PBM is not achieved until the third decade of life. We excluded anyone with a pre-existing medical condition, or any conditions affecting growth, bone health or who would not have tolerated the scanning procedures.

A total of 72 people were identified and 65 agreed to participate. 10 were excluded after consenting due to inability to participate. 55 healthy volunteers underwent the investigations and were included in the analysis. Informed written consent was obtained from all parents or caregivers and adult participants. Assent was obtained from children when appropriate. The study was approved by the NHS Health Research Authority ethics committee (17/LO/0007).

3.4.2 Investigations Performed

3.4.2.1 Peripheral Quantitative Computed Tomography

A scan of the non-dominant tibia was obtained by pQCT as per manufacturer's instructions, and ISCD guidelines (Crabtree et al., 2014). The 3% and 4% metaphyseal sites as well as the 38% diaphyseal site were used for image acquisition of trabecular and cortical bone, respectively. This was to follow the

scanning protocols and image analyses as published by Roggen et al (Roggen et al., 2015b, Roggen et al., 2015a) and Leonard et al (Leonard et al., 2010, Baker et al., 2013).

All measurements from the 3% and 38% sites were expressed in age-, sex-, race- and height adjusted z-scores according to a healthy reference dataset (personal correspondence with Prof Leonard) (Leonard et al., 2010). All measurements from the 4% and 38% sites were expressed as age- or height-adjusted z-scores as published by Roggen et al (Roggen et al., 2015b, Roggen et al., 2015a).

3.4.2.2 Peripheral Quantitative Computed Tomography Procedure

The length of the tibia was measured from the tibial plateau to the middle of the medial malleolus. The tibial length and participant's height, weight, sex, and date of birth were inserted into the software when prompted. The participants were then scanned whilst supine on an examination couch, with the non-dominant lower limb extended into the pQCT scanner (XCT 2000, Stratec). Detailed scanning SOP in Appendix.

The reference line was placed in the scout view image at the proximal border of the distal tibia growth plate in children with open growth plates and at the proximal border of the distal endplate in young adults with fused growth plates (Wetzsteon et al., 2011, Roggen et al., 2015b). A voxel size of 0.4mm, slice thickness of 2.3mm, and scan speed of 25mm/s were utilized.

The Stratec hydroxyapatite phantom was scanned daily for quality assurance, as well as the super-added monthly 'cone' phantom scanning as required by the software.

All pQCT scans were undertaken by myself. All pQCT scans were scored independently and in a blinded fashion by Dr Nicola Crabtree (Consultant Clinical Densitometry Scientist, Birmingham Women's and Children's Hospital) and myself for scout view placement and movement as per Blew et al (Blew et al., 2014). None of the scans were deemed necessary to be excluded.

The pQCT measures obtained were the trabecular volumetric BMD (mg/cm^3) at the 3% and 4% sites, and the cortical volumetric BMD (mg/cm^3) at the 38% site. The 38% site also provided measures of cortical size such as periosteal circumference (mm), endosteal circumference (mm) and cortical bone mineral content. Whilst each research group has published more measurements, such as cross-sectional area of bone and cross-sectional moment of inertia, the above measurements are common to both protocols.

3.4.2.3 Anthropometry

Anthropometric measures were obtained at the study visit. Height was determined using a fixed wall stadiometer, and weight with a digital scale. Height, weight and BMI measurements are expressed as Z-scores using UK reference data (Cole et al., 1995, Freeman et al., 1995) .

3.5 Statistics

All results are presented as the median with interquartile range (IQR). SPSS 25 (IBM) was used for statistical analyses and Prism, Graphpad for figure design. Mann-Whitney non-parametric tests were used to compare groups. A p-value of <0.05 was considered statistically significant, and two-sided testing of the hypothesis was used in all tests were appropriate. The Bland-Altman method was used to compare z-scores for pQCT parameters generated using the two reference datasets, with a linear regression using the difference between measurements as the dependant variable, and the average of the measurements as the independent variable to analyse the correlation (Bland and Altman, 1986). Non-parametric Wilcoxon Signed Rank one sample T-testing was used to determine if the median (& its 95% confidence interval) of the Z-scores differed from a median of zero.

3.6 Results
3.6.1 Demographics of study population

Fifty-five people, aged 7 to 30 years, participated in the study. The median age was 16.5 years (13.3 to 24.3). Twenty-eight were female (50.9%). Twenty participants (36.3%) were aged 19 to 30 years. Most were Caucasian (76%, Black 15%, Asian 9%). The median height, weight and BMI z-scores were 0.13 (-0.44 to 0.78), 0.36 (-0.34 to 0.87) and 0.28 (-0.35 to 0.61) respectively.

3.6.2 pQCT measurement Z-scores

The Z-scores for the measurements for children and adults are shown in Tables 3.6.2a and 3.6.2b, respectively.

Table 3.6.2a. Median Z-scores of the pQCT measurements as calculated for each scanning protocol for children 7 to 18 years old. BMD; Bone mineral density

Bone Imaging measure		Z-score as per Roggen et al		Z-score as per Leonard et al	P-value for between group difference
		4%		**3%**	
Trabecular BMD		-0.29 (-0.94 to 0.17)		-0.17 (-1.11 to 0.62)	0.35
		38%			
Cortical BMD		0.71 (0.07 to 1.35)		-0.17 (-0.87 to 0.62)	**0.0005**
Cortical mineral content		-0.48 (-1.70 to 0.34)		-0.55 (-1.38 to 0.05)	0.85
Periosteal Circumference	Age adjusted	-1.94 (-2.88 to -0.41)	Age and height adjusted	-0.54 (-1.33 to 0.15)	**0.003**
	Height adjusted	-1.69 (-2.38 to -0.66)			**0.0008**
Endosteal Circumference	Age adjusted	-1.98 (-2.93 to -0.71)	Age and height adjusted	-0.22 (-0.92 to 0.68)	**<0.0001**
	Height adjusted	-2.15 (-3.09 to -0.90)			**<0.0001**

Table 3.6.2b Median Z-scores of the pQCT measurements for adults age ≥19 years old. Roggen et al database maximum age is 18.9, so unable to calculate adult Z-scores. BMD; Bone mineral density

Bone Imaging measure	Z-scores as per Leonard et al
	3%
Trabecular BMD	-0.10 (-0.85 to 0.36)
	38%
Cortical BMD	-0.91 (-1.77 to -0.02)
Cortical mineral content	-0.54 (-1.41 to 0.03)
Periosteal Circumference (Age and height adjusted)	-0.40 (-0.72 to 0.32)
Endosteal Circumference (Age and height adjusted)	0.24 (-0.47 to 0.74)

There was no significant difference for the TrabBMD at the 3% and 4% sites for the children, or the 38% bone mineral content. There was a significant difference for the CortBMD (Figure 5), with the Belgian derived Z-scores showing a higher median of 0.71 (0.07 to 1.35).

The Roggen et al database extends to 18.9 years old, so the Z-scores were calculated for the adults based on the Leonard et al database (Table 3.6.2b).

Figure 6.5.2. Median and IQR ranges for the bone measurements for healthy children as per each methodology. TrabBMD, Trabecular Bone Mineral Density; CortBMD, Cortical Bone Mineral Density

Healthy Children

p=0.35   p=0.0005

p=0.85

- Analysis as per Leonard et al
- Analysis as per Roggen et al

Z-score

2

0

-2

n=35   n=35   n=35

3%   4%   38%   38%

TrabBMD   CortBMD   Cort
Mineral
Content
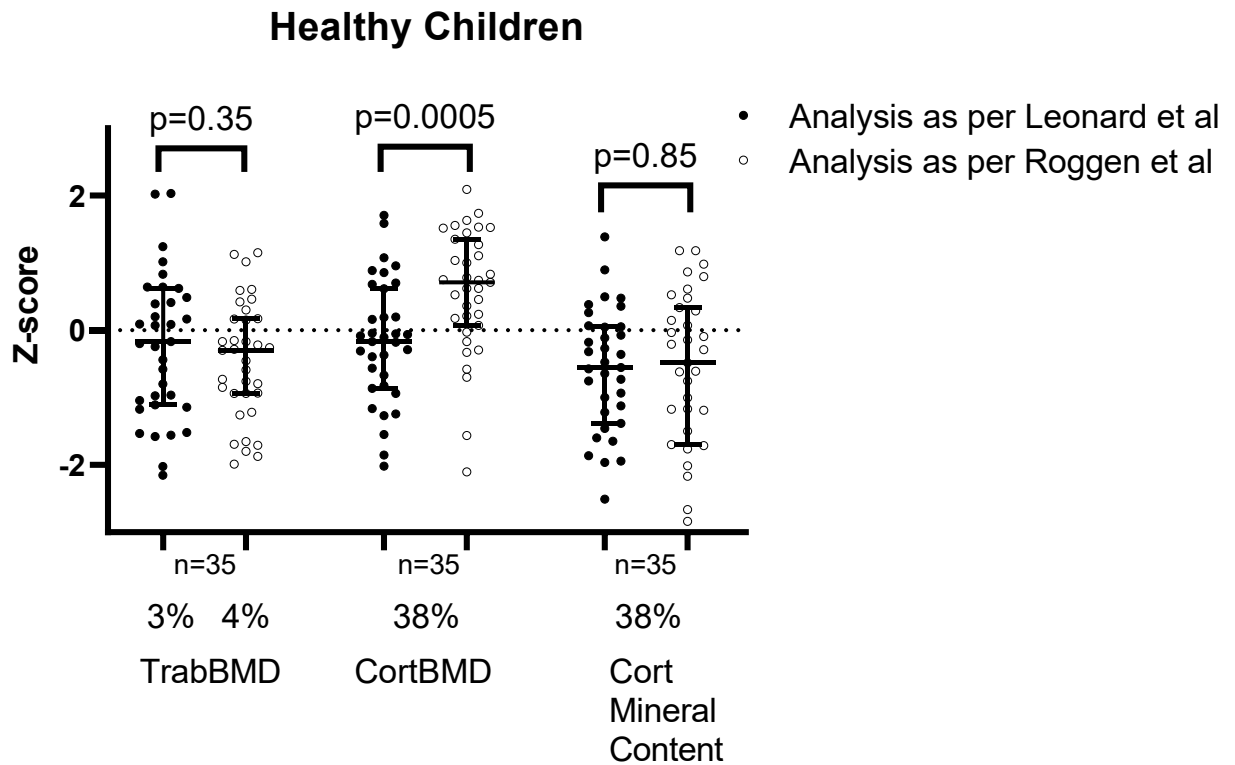
3.6.3 Bland-Altman method comparison of the two analysis protocols

The TrabBMD and cortical BMC Z-scores showed moderate correlation (R^2=0.26, p=0.002 and R^2= 0.19, p=0.008 respectively) with the majority of measurements within 1 Standard Deviation (SD) (Figure 3.6.3a &b). The CortBMD Z-scores did not show the same correlation (R^2=0.08, p=0.10) (Figure 3.6.3c), with significant offset and variation.

Figures 3.6.3a &b. Bland-Altman plots of Trabecular bone mineral density

(TrabBMD) and cortical mineral content Z-scores, with the bias depicted by the solid

line and the 1 standard deviation points (SD) by the dotted lines.

TrabBMD Z-scores

Cortical Mineral Con Content Z-scores
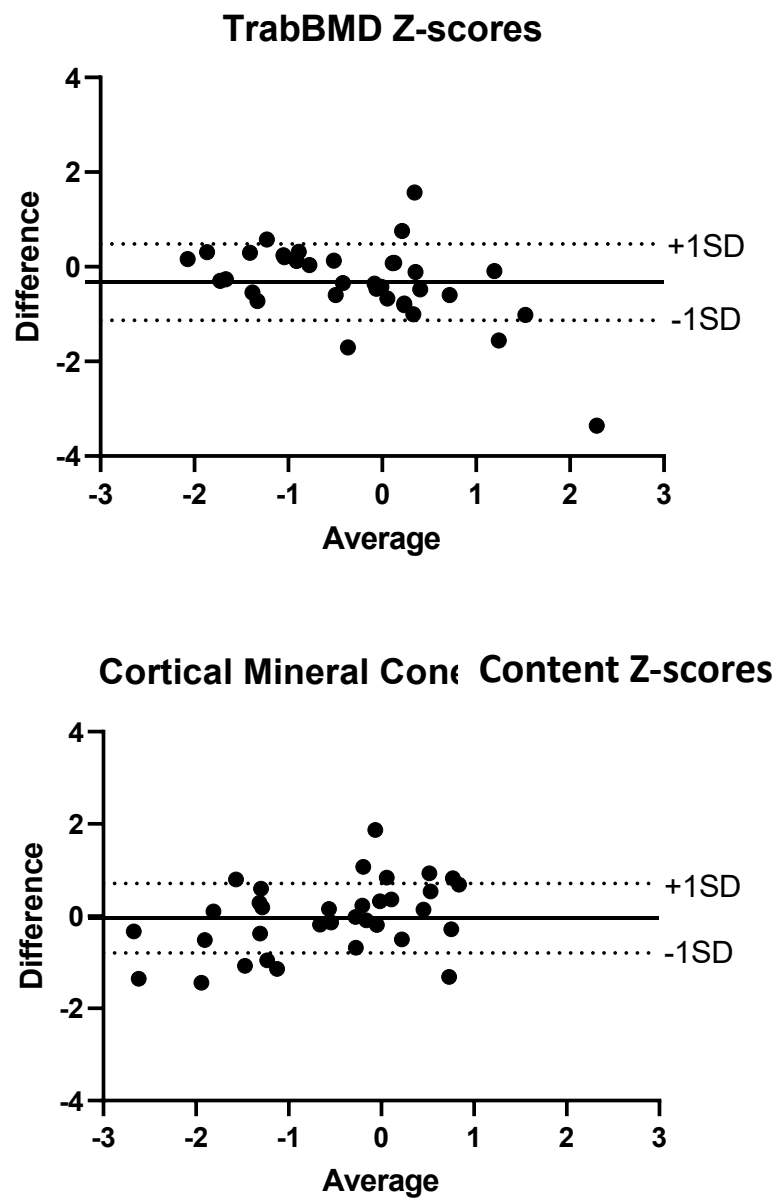
Figure 3.6.3c. Bland-Altman plot of cortical bone mineral density (CortBMD) with

the bias depicted by the solid line and the 1 standard deviation points (SD) by the

dotted lines. The dashed lines show the 2 SD points, highlighting the significant

variation of the difference.
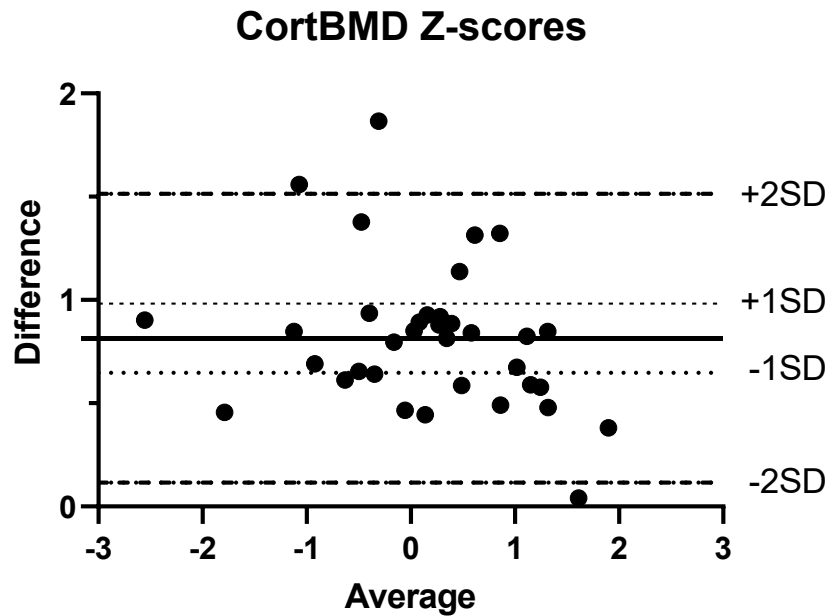
CortBMD Z-scores

3.6.4 Assessment of median Z-score deviation from zero

The assessment of deviation from a median of zero is displayed in Table

3.6.4. In our cohort the median z-score for trabBMD, cortBMD and endosteal

circumference by Leonard et al in children did not differ significantly from zero. In

adults, z-scores of trabBMD and measures of bone size did not differ significantly

from zero.

Table 3.6.4. Median (95% confidence interval of the median) of z-scores of measurements at each tibial site. Wilcoxon Signed Rank Testing (WSR) indicating if median discrepancy from a median of zero is statistically significant.

Bone Imaging measure Z-scores median (95%CI)		Roggen et al	WSR Test p value		Leonard et al	WSR Test p value	Leonard et al	WSR Test p value
		Children					**Adults**	
Site		4%			3%			
Trabecular BMD		-0.29 (-0.75 to -0.14)	**0.008**		-0.17 (-0.56 to 0.32)	0.36	-0.10 (-0.60 to 0.24)	0.33
Site		38%						
CortBMD		0.71 (0.26 to 0.89)	**0.0006**		-0.17 (-0.59 to 0.11)	0.2	-0.91 (-1.32 to -0.52)	**0.0004**
Cortical Mineral content		-0.48 (-1.17 to -0.23)	**0.01**		-0.55 (-1.02 to -0.30)	**0.0006**	-0.54 (-1.54 to -0.12)	**0.01**
Periosteal Circumference	Age adjusted	-1.94 (-2.69 to -0.17)	**<0.0001**	Age and height adjusted	-0.54 (-0.90 to -0.15)	**0.008**	-0.40 (-0.70 to 0.12)	0.12
	Height adjusted	-1.69 (-2.18 to 0.23)	**<0.0001**					
Endosteal Circumference	Age adjusted	-1.98 (-2.66 to -1.45)	**<0.0001**	Age and height adjusted	-0.22 (-0.54 to 0.30)	0.4	0.24 (-0.46 to 0.67)	0.39
	Height adjusted	-2.15 (-2.62 to -1.53)	**<0.0001**					

3.7 Discussion

I chose Leonard et al (Leonard et al., 2010, Baker et al., 2013) and Roggen et al (Roggen et al., 2015b, Roggen et al., 2015a) as the two databases closest to the population from which I would be recruiting from for my bone and vessel study in CKD. Each of these databases had the largest number of participants, from the available published studies. They have comparable scanning and analysis protocols with similar image acquisition sites. For the analysis of the healthy cohort, I separated it into ages under 19 and over 19, as the Roggen et al database extends up to 19 years old.

The trabecular BMD z-scores assessed at the 3% or 4% sites are similar and there is no difference between the methodologies. This is perhaps because the 3% and 4% sites do not differ by many millimetres and are thus essentially the same locus. For a 350mm measured tibia, for example, the 3% site would target an area 1.05 cm from the reference line placement, and the 4% would target a distance 1.4cm from the reference line. It is highly likely that these areas have a very similar composition, size and density of trabecular bone. In addition, these sites may overlap depending on the operator's measurement of the tibial length. This remains a potential source of confounding bias as the trabecular density decreases significantly along the metaphysis (Lee et al., 2007).

The cortBMD Z-scores at the 38% site differed significantly, with Roggen et al z-scores higher on average. This is perhaps as a result of having a proportion of Black and Asian participants in our cohort, whilst the Roggen et al database contains

only Caucasian participants. It is well established that Black and mixed race people have a higher bone mineral density (Laster et al., 2019, Ettinger et al., 1997, Bachrach et al., 1999, Zemel et al., 2011). The Bland-Altman analysis of the z-scores reflected the significant differences between the z-scores derived by the different image analysis protocols. Cortical mineral content z-scores were similar with each protocol and did not differ significantly. The z-scores of the peri- and endosteal circumferences (measurements of bone size with age *or* height adjustment for Roggen et al and age *and* height adjustment for Leonard et al) differed significantly, and this may be due to our cohort population differences. The voxel size, slice size and speed of scan varied from the Roggen et al methodology, which may have affected results or resulted in different volume effects.

Adult z-scores were not generated by the Roggen et al database as it extends to 19 years old only. It is assumed that normal bone mineralization continues until peak bone mass is reached in the late twenties or early thirties (Weaver et al., 2016). Any study assessing BMD in young people would need to carefully consider the age range of the reference database to be used, as assuming all young adults are aged 19 or interpolating the z-scores may provide misleading results.

As our cohort is representative of a healthy cohort, the median and mean values of the z-scores should be close to zero. When assessing the children's cohort's median z-scores bias from zero, the Leonard z-scores of TrabBMD, CortBMD and endosteal circumference did not differ significantly. The median cortical mineral content and median periosteal circumference differed significantly

from zero. This could be due to methodological constraints; it may be that the sample of 35 children is too small and may have contributed to this result. Equally, the cohort may differ in a significant way from the reference dataset in terms of regular diet, calcium intake, physical exercise, and dietary supplements. Sample size and lifestyle factor limitations apply to the 20 adults showing that their median Z-score for CortBMD and cortical mineral content differed significantly from zero.

Additional limitations include that the Roggen et al scanning protocol specifies use of the dominant tibia, whereas in this study the non-dominant tibia was used for all measurements. There is evidence that there are differences between the dominant and non-dominant limb bone measures, but the extent to which this is significant is debated (Haapasalo et al., 2000, Hildebrandt et al., 2016).

3.8.1 Overall limitations precluding pQCT from routine use

Peripheral QCT has many advantages and overcomes most of the criticisms encountered by DXA and also provides information on bone density, size and strength (Lalayiannis et al., 2019).

The variability in the literature of reference line placement and scanning protocol cannot be overlooked. Even if following the ISCD Official Positions Statement (Adams et al., 2014), there is still scope for sufficient human error in reference line placement and tibial length measurement to cause significant measurement error margins. There is also the challenge of standardisation between machines. Cross-calibration between scanners and research centres is vital to avoid

bias of the measurements. Reducing human error by training researchers to perform pQCT according to the same protocol and minimising the number of researchers performing the scans is important.

Furthermore, the most appropriate long bone for assessment has been debated. Whilst both the tibia and radius provide easy access to a metaphyseal and diaphyseal measurement, there is only now consensus on using the non-dominant limb. Imaging slice location on the tibia or radius for accurate and reproducible assessments is also varied. These need to be reproducible, not just between centres, but also longitudinally for patient follow up assessments. Currently, this overwhelming heterogeneity means there is a paucity of reference data for age, height and puberty staging for comparison and z-score generation. The lack of universally used or globally applicable reference data, and the variability in image acquisition techniques, currently limit the use of pQCT largely to research, with limited application in routine clinical practice.

3.8.2 High Resolution pQCT (HR-pQCT)

HR-pQCT is a newer, promising technology which is now becoming more widely available for research. First generation scanners were adept at scanning distal, metaphyseal sites (Whittier et al., 2020). Second generation scanners allow for image acquisition at distal sites as well, allowing for detailed cortical and trabecular analysis. It offers much more detail than QCT, showing trabecular bone microarchitecture, and enables measurement of trabecular number, thickness and separation (Crabtree and Ward, 2015). With reference databases being published

(Burt et al., 2016), the same heterogeneity of scanning protocols needs to be avoided (Mata-Mbemba et al., 2019). Image acquisition sites, analysis methods and guidelines for its use need to be standardized as suggested recently by Whittier et al (Whittier et al., 2020).

HR-pQCT was not available in any of my research sites to enable use in this project.

3.9. Conclusion

pQCT is a useful imaging tool in studying bone, especially in chronic illnesses that affect the bone compartments in different ways. It is, however, confined mainly to the research domain. The marked lack of methodology standardization and reference data further add to the limitations in its widespread clinical application. This study highlights the complexities and difficulties in choosing a reference dataset for conducting research with pQCT.

In the absence of bone biopsies, I chose to use pQCT and DXA as the imaging modalities most readily available to me. Each have their advantages and limitations, in a way complementing each other. I opted for use of the Leonard et al methodology, scanning protocol and image acquisition sites in my project, as this would allow comparison and z-score generation using one of the largest datasets. It would afford me the ability to compare my results with other studies examining bone health in CKD, having employed the same reference database.

Chapter 4

Bone health, routinely used bone mineral density imaging and serum biomarkers in children and young adults with CKD

In this chapter I have described the baseline bone health and biochemical data of the cohort. I have compared the utility of DXA and routinely used clinical serum biomarkers, in predicting bone mineral density in young patients with CKD and on dialysis.

The work in this chapter has been published in: Lalayiannis AD, Crabtree NJ, Ferro CJ, Askiti V, Mitsioni A, Biassoni L, Kaur A, Sinha MD, Wheeler DC, Duncan ND, Popoola J, Milford DV, Long J, Leonard MB, Fewtrell M, Shroff R. **Routine serum biomarkers, but not dual-energy X-ray absorptiometry, correlate with cortical bone mineral density in children and young adults with chronic kidney disease**. *Nephrol Dial Transplant*. 2021 Sep 27;36(10):1872-1881. (doi: 10.1093/ndt/gfaa199. PMID: 33094322).

In line with UCL policy, I declare that I collected and analysed the data and wrote the original manuscript. The co-authors very kindly helped with editing and proof-reading.

4.1 Abstract

Background

Biomarkers and Dual-energy X-ray Absorptiometry (DXA) are thought to be poor predictors of bone mineral density (BMD). KDIGO guidelines suggest using DXA if it will affect patient management, but this has not been studied in children or young adults in whom bone mineral accretion continues to 30 years of age. We studied the clinical utility of DXA and serum biomarkers against tibial cortical BMD measured by peripheral Quantitative CT (pQCT), expressed as a z-score (CortBMD), which predicts fracture risk.

Methods

Cross-sectional multicentre study in 26 patients with CKD 4-5 and 77 on dialysis.

Results

Significant bone pain that hindered activities of daily living was present in 58%, and 10% had at least one previous low-trauma fracture. CortBMD and cortical mineral content Z-scores were lower in dialysis compared to CKD patients (p=0.004 and p=0.02). DXA BMD hip and lumbar spine Z-scores did not correlate with CortBMD or biomarkers. CortBMD was negatively associated with parathyroid hormone (PTH; r=-0.44, p<0.0001) and alkaline phosphatase (ALP; r=-0.22, p=0.03) and positively with calcium (r=0.33, p=0.001). At PTH <3xULN (Upper Limit of Normal), none of the patients had a CortBMD below -2SD (OR 95%CI 7.331 to infinity).

On multivariable linear regression PTH (β-0.43, p<0.0001), ALP (β-0.36, p<0.0001) and calcium (β 0.21, p=0.005) together predicted 57% of variability in CortBMD. DXA measures did not improve this model.

Conclusions

Taken together, routinely used biomarkers, PTH, ALP and calcium, but not DXA, are moderate predictors of cortical BMD. DXA is not clinically useful and should not be routinely performed in children and young adults with CKD4-5D.

4.2 Introduction

Mineral bone disorder (MBD) is commonly seen in children and adults with chronic kidney disease (CKD). The biochemical abnormalities [of calcium (Ca), phosphate (P), parathyroid hormone (PTH) and 1,25-dihydroxyvitamin D], bone abnormalities (short stature, bone pain, deformities and increased risk of fractures) and extra-skeletal calcification (Wesseling-Perry and Salusky, 2013, Ketteler et al., 2018) together form the spectrum of CKD-MBD. This process starts early in CKD, with rising concentrations of the bone derived phosphaturic hormone, Fibroblast Growth Factor 23 (FGF23), and progresses as renal function declines (Portale et al., 2014, Portale et al., 2016, Wan et al., 2013). Mineral dysregulation leads to bone demineralization, that if untreated, leads to deformities and an increased fracture risk even in young CKD patients (Ketteler et al., Denburg et al., 2016, Yenchek et al., 2012).

Assessing bone health is a key element in the management of CKD. This relies on monitoring the trend in key serum biomarkers such as PTH, Ca, P and alkaline phosphatase (ALP). The 2017 KDIGO (Kidney Disease Improving Global Outcomes) guidelines suggest that in adults with CKD stages3 to 5 and on dialysis, dual energy x-ray absorptiometry (DXA) may be used if results are likely to impact patient management (Ketteler et al.). This recommendation relies on evidence gathered from older people with CKD (Yenchek et al., 2012, Iimori et al., 2012, Naylor et al., 2015, West et al., 2015). However, in children and young adults calcium accrual in the skeleton continues until the third decade of life when peak bone mass (PBM) is achieved (Weaver et al., 2016). It has been shown that if bone

mineral accretion is impaired by CKD or its treatment, this younger population is at a high risk of bone demineralization and associated fracture risk.

In a longitudinal follow up study of 89 patients (aged 5-21 years) in CKD stages 2-5 and on dialysis, the authors identified a higher fracture risk per 1 SD decrease in baseline BMD (HR 1.75, 95%CI 1.12-2.67,p=0.009) over a one year follow up. 6.5% suffered at least one fracture in the study's one year follow up period (incidence 556/10,000 person-years). The fractures occurred in distal long bones such as the clavicles, tibia, toes and radius. These fractures were sustained in low impact traumas, such as normal daily exercise and benign falls. A low serum Ca level was associated with a reduction in tibial cortical bone mineral density (BMD) on peripheral quantitative computed tomography (pQCT), and 1 SD decrease in BMD z-score was associated with a 2-fold increase in fracture risk (Denburg et al., 2013).

A detailed assessment of bone turnover and mineralization can only be achieved through bone biopsy (Ott, 2008). This gold-standard method however is invasive and seldom performed in routine clinical practice. In lieu of biopsies, serum biomarkers and radiological imaging are used as surrogate markers in assessing BMD, but have some limitations that need to be taken into account. Biomarkers may not reflect the true state of bone turnover or mineralization (Bakkaloglu et al., 2010, Barreto et al., 2008b), and no biomarker individually or in combination can reliably identify mineralization or turnover defects (Sprague et al., 2016). DXA produces a two dimensional image of a three dimensional bone structure, so that cortical and trabecular bones are superimposed. DXA measurements are affected by

bone and body size, and thus underestimates volumetric BMD (g/cm^3) in children

with short stature (Zemel et al., 2010). This makes its use challenging in the context

of young people with CKD, who do not achieve their height potential (Haffner et al.,

2000).

pQCT allows for measurement of volumetric BMD (g/cm^3), and clearly

distinguishes trabecular and cortical bone but is currently in use as a research tool

only. In CKD, it has been used to show progressive demineralization with CKD stage

(Wetzsteon et al., 2011).

Our hypothesis was that hip or lumbar spine DXA areal BMD (aBMD) was a

significant predictor of volumetric BMD as measured by tibial cortical pQCT

expressed as Z-score (referred to as CortBMD throughout) as determined by pQCT.

4.3 Methods

Study Participants

This cross-sectional element of the study included children and young adults

with CKD from 5 pediatric hospitals and 4 adult renal units. Our inclusion criteria

were: age from 5 to 30 years and CKD stages 4-5 (estimated glomerular filtration

rate (eGFR; by Schwartz formula (Schwartz et al., 2009)) <30ml/min/1.73m^2) or on

dialysis. This age group was selected because children under 5 years are too small

for the pQCT scanner and no reference data is available. Young adults up to 30 years

were included because bone mineral accretion is shown to continue up to the third

decade. We excluded any patient with malignancy, genetic or metabolic bone disease and those who would not have tolerated the scanning procedures.

A total of 145 patients were identified and 135 agreed to participate. 12 were excluded after consenting due to unwillingness to undergo some or all investigations. One-hundred and twenty three children and young adults with CKD were included. All pQCT scans were scored independently and in a blinded fashion by Dr Nicola Crabtree and myself for scout view placement and movement as per Blew et al (Blew et al., 2014), and any poor scans were excluded from this analysis a priori. One hundred and twenty one participants in total had a pQCT of the non-dominant tibia. Two children were too height restricted to obtain images of the diaphysis at the 38% site. Fifteen scans were excluded for poor reference line placement and five scans were excluded for significant movement artefact a priori to the analysis. In total, twenty were excluded prior to analysis due to poor quality scans.

A detailed medical history, with particular relevance to bone health, was taken for all participants using a set proforma (Table 4.3.1). Fracture history was self-reported and cross-referenced with the medical records. Participants were asked to record the severity of bone pain on a numeric rating scale (where 0 indicates no pain, 5 is pain affecting activities of daily living and 10 is disabling pain causing immobility) (Jensen et al., 1994).

Table 4.3.1 Study proforma used to complete medical history

Assessment	Date completed:

Height and weight (BMI/BSA)	
Waist	
Hips	
Blood pressure	
Tanner Stage/ LMP/ Contraception	
Bone pain- severity 0=nil, 5= affecting daily living, 10= debilitating How often? Details	
Renal Rickets? • signs	
Aseptic necrosis Any other bone disease	
Medical History • Diagnosis • Date eGFR <30 • Date started RRT • Any previous Tx?	
Fractures • Site • Severity of trauma • Healing (normal/prolonged, >6/52)	
Dialysis details • HD, HDF, HHD • Hrs per session • Times/week • Litres Processed • Dialysate Ca, HCO_3	
PD Dialysis • CAPD or APD • PD therapy regimen (prescription)	

• TVT Time • Initial drain • UF • LBF (extraneal)	
Bloods • Ca^{++}, iCa++, PO$_4$, Alk P, PTH, bicarb, Albumin, urea, creatinine • Parathyroidectomy	
Medication • Phosphate binders? • Alfacalcidol? • Vitamin D? • Any others?	
24 hrs urine collection & Spot Collection • Date • Nappies/ clean catch • volume	
Diet Diary • Oral/ NG/PEG • Any nutritional supplements (name)	
Birth History • Delivery Details • Birth Weight	

Investigations Performed

Serum Biomarkers

Routine serum biomarkers were measured on non-fasting blood samples collected at the study visit or prior to a mid-week hemodialysis session. These included serum ionized calcium (iCa), total Ca, P, magnesium (Mg), bicarbonate, intact PTH (iPTH), 25-hydroxyvitamin D [25(OH)D], and ALP. Due to different PTH

assays being used at different hospitals [Assays used: Immulite (Siemens Healthcare Diagnostics) and Elecsys 2010 (Roche Diagnostics)], PTH results have been expressed as upper limits of normal. As these biomarkers are measured as a part of routine clinical care, they were analysed in the patients' respective hospitals.

Dual Energy X-ray Absorptiometry

All DXA scans were undertaken by trained radiographers at the respective research centres according to the manufacturer's protocol. The lumbar spine (LS) and hips imaging were obtained according to the International Society for Clinical Densitometry (ISCD) guidelines using General Electric scanners (iDXA or Lunar) (Crabtree et al., 2014). Z-scores produced by either machine have been shown to be comparable (Crabtree et al., 2017).

To correct the LS aBMD measurements obtained in g/cm^2 for height, they were converted to bone mineral apparent density (BMAD) z-scores for participants under 20 years old. This provided age-, sex-, height- and race-specific z-scores (Crabtree et al., 2017), and avoids overestimating BMD in shorter individuals, or underestimating it in taller individuals. BMAD scoring is used routinely in the United Kingdom to correct DXA measurements for poor growth or height attainment in childhood and adolescence. Other methods for height adjustment have also been published (Zemel et al., 2011, Zemel et al., 2010).

There are two recognised and widely used equations to calculate BMAD, published in 1992 by Carter et al and Kroger et al (Carter et al., 1992, Kröger et al., 1992).

The first, by Carter et al, assumes that the vertebral bodies are a cube shape. The equation is:

$$\text{BMAD (g/cm}^3) = \frac{(BMC1+BMC2+BMC3+BMC4)}{(V1+V2+V3+V4)}$$

Where Vn is the volume of the nth individual vertebra. Vn is the projected vertebral area raised to the power of 1.5: $Vn = APn^{1.5}$ (APn = projected vertebral area of the nth vertebra). BMCn is the bone mineral content of the nth vertebra.

The second widely used equation, published by Kröger et al, assumes the vertebral column being assessed is cylindrical in shape:

$$\text{BMAD (g/cm}^3) = \frac{BMC1,2,3,4}{\pi * (width/2) * (width/2) * (\frac{Area}{width})}$$

DXA scanning and measurement of aBMD are considered highly reproducible, on account of the standardised image acquisition techniques and the standardisation of the densitometers (Moreira et al., 2018, Leonard et al., 2009). BMAD z-scores for young adult LS DXA aBMD measurements were calculated assuming a maximum age of 20 years, for the purposes of this analysis, and referred to as DXA z-scores throughout this chapter.

Peripheral Quantitative Computed Tomography

A scan of the non-dominant tibia was obtained by pQCT as per manufacturer's instructions and ISCD guidelines using measurement points recommended by Leonard et al (Crabtree et al., 2014, Leonard et al., 2010, Wetzsteon et al., 2011). A detailed protocol has been described in Chapter 2 and SOP is included in the Appendix. The 3% metaphyseal and 38% diaphyseal sites were used for image acquisition of trabecular and cortical bone respectively. The pQCT measures obtained and expressed as z-scores were the cortical volumetric BMD (mg/cm^3), trabecular volumetric BMD (mg/cm^3), periosteal circumference (mm), endosteal circumference (mm), cortical cross-sectional area (mm^2) and cross-sectional moment of inertia (CSMI). The CSMI is a mathematical calculation that tests the efficiency of a cross-sectional shape to resist bending caused by loading stress. All results were expressed in age-, sex-, race- and height adjusted z-scores derived from a reference dataset of 665 healthy children and young adults ages 5-35 years (Leonard et al., 2010).

Anthropometry

Height was determined using a fixed wall stadiometer, and weight with a digital scale. Height, weight and body mass index (BMI) measurements were expressed as z-scores. Young adults' z-scores were calculated assuming a maximum age of 20 years. Pubertal staging was determined by the children or their caregivers with a self-reported Tanner staging questionnaire (Marshall and Tanner, 1969, Marshall and Tanner, 1970).

4.4 Statistics

All results are presented as the median with interquartile range (IQR) as appropriate. SPSS 25 (IBM) and Prism (Graphpad) were used for all statistical analyses. A p-value of <0.05 was considered statistically significant, and two-sided testing of the hypothesis was used. Spearman rank testing was used for correlations. Kruskal-Wallis ANOVA test for non-normally distributed data with appropriate corrections for unequal variance, or Mann-Whitney U tests were used as required. Bland-Altman analysis was used to plot hip and LS DXA measurements and linear regression using the difference between measurements as the dependant variable, and the average of the measurements as the independent variable to analyse the correlation (Bland and Altman, 1986). Fischer's exact test was used to determine the cut-off value at which PTH levels (as a continuous variable expressed in ULN values) best predicted CortBMD below -2SD. All variable with univariate correlations of p≤0.15 were entered into a stepwise multivariable linear regression analysis where CortBMD was the dependent variable and serum biomarkers and DXA Z-scores were independent variables.

4.5 Results

Demographics of study population

The characteristics of the participants are shown in *Table 4.5.1*.

Table 4.5.1 Participant characteristics at 1st study visit

	CKD participants	Dialysis participants	Between group comparison
Total, n= (%)	n=26 (25%)	n= 77 (75%)	
Ages, years median (IQR[1])	11.9 (6.9-13.8)	14.2 (10.9-18.2)	p=0.008
5-19 years, n=(%)	26 (100%)	59 (76.6%)	NS
20-30 years, n=(%)	0 (0%)	18 (23.4%)	N/A
Sex, Female n=(%)	18 (69.2%)	38 (49.4%)	NS
Race, n= Caucasian/ Asian/ Black/ Other	20/ 2/ 4/ 0	35/ 24/ 17/ 1	p=0.01
Height Z-score[3]	-0.75 (-1.64 to 0.23)	-1.50 (-2.1 to -0.55)	p=0.02
Weight Z-score[3]	-0.21 (-1.01 to 0.86)	-0.95 (-1.96 to -0.04)	p=0.008
BMI[2] Z-score[3]	0.53 (-0.35 to 1.10)	0.01 (-0.95 to 0.85)	p=0.048
Renal disease aetiology, n= CAKUT[4]/ Nephrotic Syndromes/ Cystic Kidney Diseases/ Vasculitides/ Other	20/ 0/ 5/ 1/ 0	34/ 13/ 5/ 7/ 18	p=0.003
eGFR[5], ml/min/1.73m^2	13.3 (8.8 to 17.9)	N/A	
Dialysis modality, n= **HD/HDF/Home HD/PD**	N/A	44 / 12 / 4 / 17	
Years with eGFR<30, median (IQR)	3.8 (1.4-9.0)	6.1 (2.5 to 10.6)	NS
Dialysis vintage years, median (IQR)	N/A	2.5 (0.79- 5.09)	

Routine clinical serum biomarkers Calcium (mmol/L)	2.47 (2.41 to 2.52)	2.45 (2.33 to 2.58)	NS
Phosphate (mmol/L)	1.46 (1.29 to 1.62)	1.57 (1.29 to 1.90)	NS
25-hydroxyvitamin D [25(OH)D], (nmol/L)	94 (71 to 141)	63 (37 to 109)	0.02
Parathyroid Hormone (pmol/L)	6.90 (3.90 to 17.05)	21.60 (8.00 to 69.80)	0.0005
Phosphate binder therapy, **Calcium based/ Non-calcium** **based/ Both/ None (n=)**	19 / 1 / 0 / 6	23 / 22 / 5 / 27	
Calcium intake from binders **(mmol/kg/day)**	1.06 (0 to 2.13)	0 (0 to 1.46)	0.03
Other Medication **Vitamin D3 (Units/kg/day)**	0 (0 to 3.54)	0 (0 to 25.88)	0.33
Alfacalcidol[6] **(1α hydroxyvitamin D3) (mcg/day)**	0.50 (0.34 to 0.75)	0.75 (0.50 to 1.26)	0.08

[1]Interquartile range, [2]Body Mass Index (kg/m^2), [3]Height/Weight/BMI Z-scores calculated for participants aged 5-20 years. Any participants >20 years old, z-scores calculated assuming maximum age of 20 years, [4]Congenital abnormalities of the kidneys and urinary tract, [5]estimated Glomerular filtration rate, [6] Most participants were on alfacalcidol. Three participants in the dialysis group were on paricalcitol and were not included in the medication analysis, NS Not Significant

Bone Health: Bone Pain and Fractures

Bone pain was reported by 58% of patients with a median pain score of 4 out of 10 (IQR 0 to 5.75). The commonest sites were the lower limbs (38%), back (25%), knees (14.7%) and hips (10.3%). Most pain was reported to follow activities of daily living such as walking to school or doing housework, and required the

regular use of analgesics. Bone pain score correlated with hip DXA z-scores (p=0.04) only. It was not associated with a longer dialysis or CKD duration, serum biomarkers or other radiological measurements.

Ten (10%) participants reported at least one previous low-trauma fracture (See Table 4.5.2). Patients who had suffered a previous fracture had a longer dialysis vintage [4.5 (3.6 to 8.2) vs 2.1 (0.71 to 5.06) years respectively, p=0.04] and longer duration with a low eGFR [10.8 (6.5 to 13.3) vs 4.6 (1.9 to 9.6) years respectively, p=0.008] compared to patients with no fractures.

Table 4.5.2 Participant characteristics reporting a previous fracture

Age (years)	Number of Fractures	Fracture location	Mechanism	Prolonged healing	Years on Dialysis	Years with eGFR[1] <30 ml/min/1.73m^2
6	1	Metatarsal	Fall	yes	1.97	4.88
11	2	Distal phalanges	Fall whilst playing	no	4.75	10.8
11	1	Tibia	Fall	yes	8.28	11.27
14	1	Radius	Fall whilst playing	no	0.45	0.54
15	1	Radius	Fall from wheelchair	no	5.23	12
15	2	Clavicle & tibia	Fall from cot, fall from standing	no	n/a	8.81
16	1	Radius	Fall whilst playing	no	3.82	6
24	1	Tibia &	Trip/fall	yes	16.5	22.07

		Bilateral avascular necrosis of the femoral heads				
25	1	Tibia	Trip/fall	yes	4.48	8.11
30	1	Radius	Fall off swing	no	10.70	10.72

All mechanisms of injury were of low impact such as during play or falling from standing. Prolonged healing was defined as more than 6 weeks in a cast. Dialysis vintage and eGFR at time of participation in the study. [1]Estimated glomerular filtration rate ml/min/1.73m^2

Bone Imaging

At the outset of result analysis, an equation for estimation of BMAD needed to be determined. As I would be using the ALPHABET study (Crabtree et al., 2017) as the UK based healthy reference database for BMAD z-score estimation, the Carter equation was used for conversion of all patients' lumbar spine DXA measurements to BMAD z-scores. To ensure there was no discrepancy or confounding bias in the use of the Carter equation, I compared the adult machine generated LS DXA aBMD z-scores with Carter and Kröger estimated BMAD z-scores and the children's Carter with Kröger estimated BMAD z-scores.

Whilst the median value was higher when size adjusted, as would be expected, there was no significant difference between reported aBMD z-scores and Carter BMAD z-scores for the young adults [-1.05 (-2.78 to 0.18) vs -0.58 (-2.47 to 0.37), p=0.60)]. There was no difference between reported aBMD and Kröger estimated BMAD z-scores [-1.05 (-2.78 to 0.18) vs -0.52 (-2.24 to 0.33), p=0.71]. In

addition, there was also no difference between the two equations for BMAD [-0.58
(-2.47 to 0.37) vs -0.52 (-2.24 to 0.33), p=0.91](See Figure 4.5.1).

Figure 4.5.1 Young adult (n=20) lumbar spine DXA machine reported areal
bone mineral density (aBMD) z-scores, compared with Kröger and Carter equation
generated BMAD z-scores
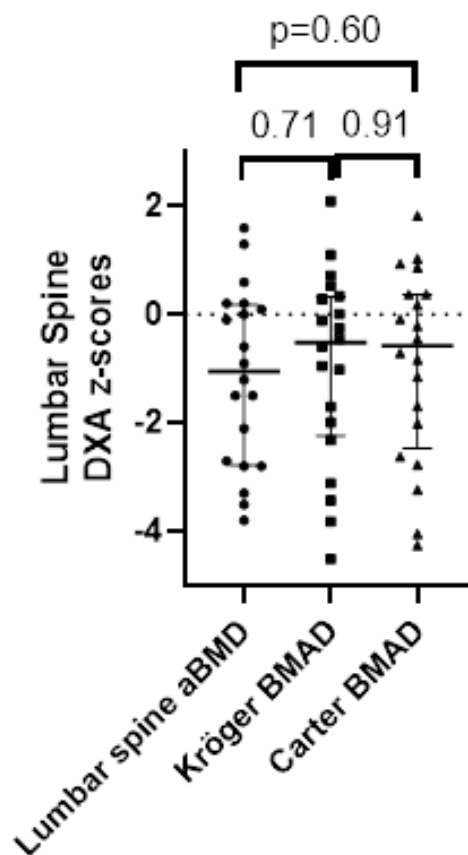
Comparing the children's aBMD z-scores and size adjusted BMAD z-scores
showed a significant difference. Machine generated aBMD z-scores significantly
underestimate the BMD when adjusting with the Carter equation [-0.30 (-1.20 to
0.5) vs 0.21 (-0.72 to 1.19), p=0.007)] as well as Kröger [-0.30 (-1.20 to 0.5) vs 0.24
(-0.66 to 1.19), p=0.006]. There was no difference between the two equations for

BMAD z-scores [0.21 (-0.72 to 1.19) vs 0.24 (-0.66 to 1.19), p=0.84] (See Figure

4.5.2).

Figure 4.5.2 Children's lumbar spine DXA machine reported areal bone

mineral density (aBMD) z-scores, compared with Kröger and Carter equation

generated BMAD z-scores
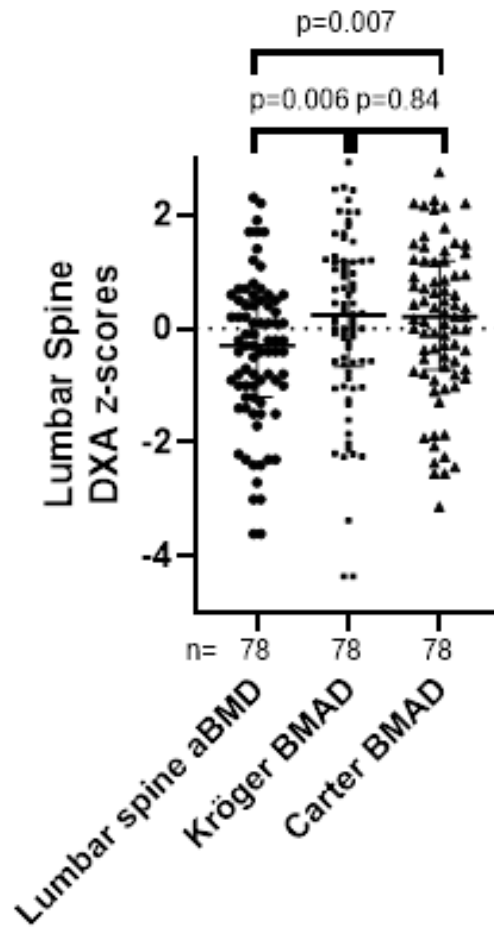
As the difference between the aBMD z-scores and the BMAD z-scores

in adults were not significant, and the two equation methods for BMAD estimation

in children were similar, the Carter method has been employed throughout this

thesis. From herein, BMAD refers to Carter equation calculated BMAD z-score for

both children and young adults.

Bland-Altman analysis (Bland and Altman, 1986) showed that there was very

weak agreement between the z-scores provided by hip and LS BMAD [R^2=0.06, β

0.25 (95% CI 0.05, 0.41), p=0.013]. (Figure 4.5.3)

Both DXA site z-scores were associated with weight SDS (BMAD r=0.23,

p<0.05 and Hip r=0.49, p<0.0001).

Figure 4.5.3 Bland-Altman plot of the mean and difference of agreement between

hip and lumbar spine BMAD z-score for the CKD and dialysis participants. +/- 1

standard deviation (SD) lines shown to illustrate the significant difference clinically
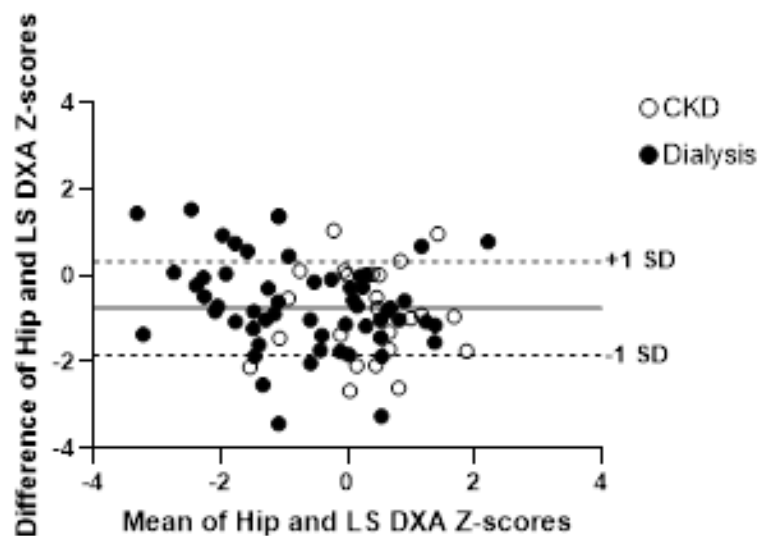
between the two measures

Comparing the pQCT BMD z-scores with the DXA z-scores, we found that TrabBMD correlated with both hip and LS BMAD (r=0.66, p<0.0001 and r=0.51, p<0.0001). CortBMD was not associated with hip or LS BMAD z-scores.

The dialysis group had significantly lower BMD z-scores compared to the CKD group, both for LS and hips (Figure 4.5.4 & Table 4.5.3).

Figure 4.5.4 Violin plot of the lumbar spine (BMAD) and hip z-scores of the CKD and dialysis groups of participants. Lines show the median and the interquartile range. p-value of between group comparison is shown.
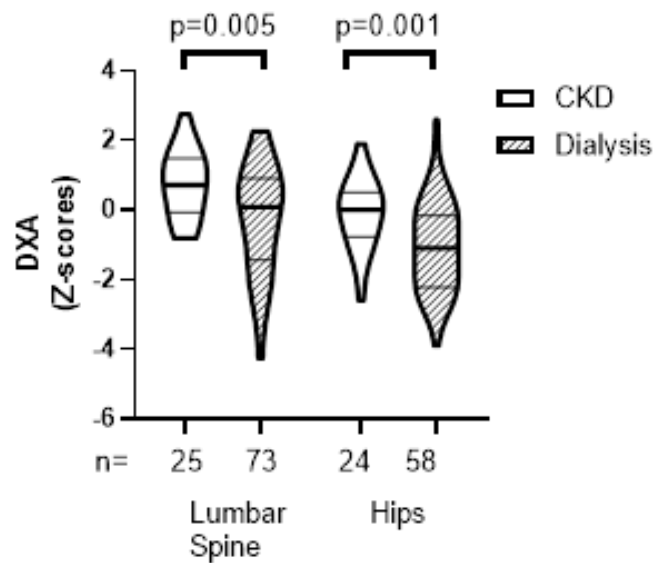
Table 4.5.3 Participant measures of bone size, mineral content and bone quality/strength

Bone Imaging measure Z-scores	CKD	Dialysis	Between group comparison
LS BMAD DXA	0.71 (-0.06 to 1.49) n=25	0.09 (-1.45 to 0.90) n=73	**p=0.005**
Hip BMD DXA	0.00 (-0.78 to 0.5) n=24	-1.10 (-2.25 to -0.18) n=58	**p=0.001**
Trabecular BMD[1]	1.23 (-0.15 to 2.20) n=25	-0.33 (-1.19 to 1.61) n=73	**p=0.013**
Cortical BMD	-0.18 (-0.58 to 0.34) n=25	-0.68 (-1.96 to 0.35) n=73	**p=0.004**
Cortical area	-0.43 (-1.32 to 0.10) n=25	-1.39 (-2.53 to -0.30) n=73	p>0.05
Periosteal circumference	-0.38 (-1.2 to 0.16) n=25	-0.82 (-1.67 to 0.31) n=73	p>0.99
Endosteal circumference	-0.13 (-1.38 to 0.41) n=25	0.2 (-0.52 to 0.97) n=73	p=0.38
Cortical mineral content	-0.39 (-1.13 to 0.19) n=25	-1.48 (-2.83 to -0.28) n=73	**p=0.02**
Total mineral content	-0.03 (-0.77 to 1.15) n=25	-0.65 (-1.96 to 0.39) n=73	p=0.17
Cross-sectional moment of inertia	-0.46 (-1.34 to 0.06) n=25	-1.10 (-1.85 to 0.08) n=73	p=0.25

[1]Bone Mineral Density

The dialysis group also had lower cortical and trabecular BMD as well as cortical mineral content compared to the CKD group (Figure 4.5.5) as measured by pQCT.

Figure 4.5.5 Violin plot of the cortical bone mineral density (CortBMD), trabecular BMD (TrabBMD), and cortical mineral content (CortCNT) as measured by pQCT in the CKD and dialysis groups. Lines show the median and the interquartile range. p-value between group significance shown.
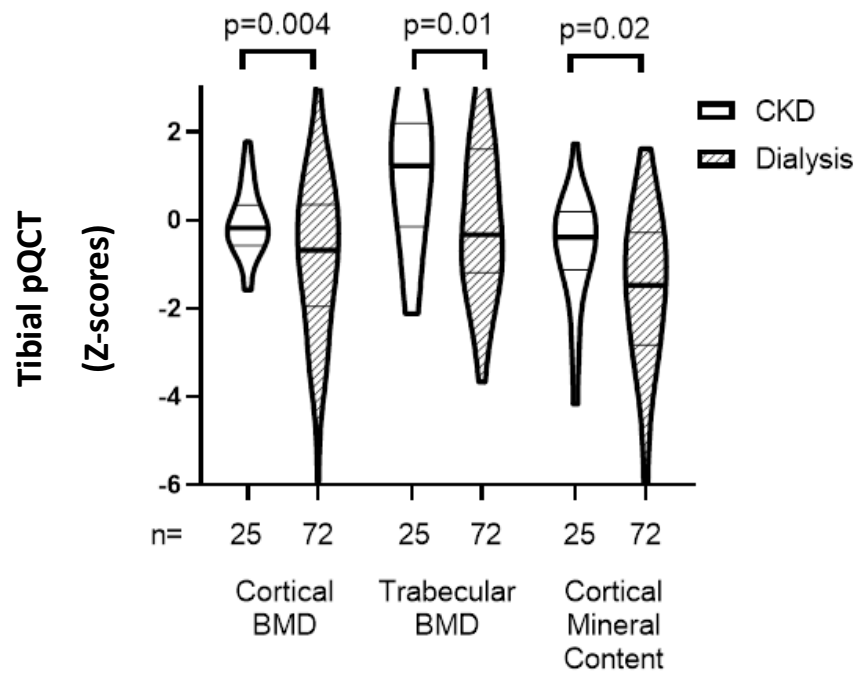
Patients who had a history of previous fractures had lower total mineral content [p=0.02, -2.15 (-3.17 to -0.54) vs -0.38 (-1.46 to 0.69)] and CSMI [p=0.048, -1.59 (-2.31 to -0.91) vs -0.83 (-1.65 to 0.13)] compared to patients without a previous fracture; this was despite the fact that the fractures preceded the study imaging by months or years. On multivariable linear regression, DXA and pQCT measures did not associate with a history of past fractures.

Serum biomarkers

The pairwise univariable correlations of serum biomarkers with imaging modalities are presented in the following tables (Tables 4.5.4 & 4.5.5).

Table 4.5.4 Participant correlation analysis of CKD & Dialysis participants' bone imaging and biomarkers

		CortBMD[1] z-score	TrabBMD z-score	Hip DXA z-score	LS BMAD z-score
SDS[2] Height	r	0.16	0.14	**0.50**	**0.22**
	p-value	0.11	0.18	**0.00**	**0.03**
SDS BMI	r	0.10	0.19	**0.30**	**0.26**
	p-value	0.35	0.06	**0.01**	**0.01**
SDS Weight	r	0.14	**0.22**	0.49	0.32
	p-value	0.18	**0.03**	0.00	0.00
CortBMD[1] Z-score	r	1.00	0.03	0.11	0.16
	p-value		0.77	0.33	0.12
TrabBMD Z-score	r	0.03	1.00	**0.66**	**0.51**
	p-value	0.77		**0.00**	**0.00**
Hip DXA z-score	r	0.11	**0.66**	1.00	0.69
	p-value	0.33	**0.00**		0.00
LS BMAD z-score	r	0.16	**0.52**	**0.67**	1.00
	p-value	0.13	**0.00**	**0.00**	
Total Ca	r	**0.33**	0.32	-0.02	0.17
	p-value	**0.00**	**0.00**	0.86	0.10

iCa[3]	r	**0.37**	0.07	0.05	0.08
	p-value	**0.00**	0.50	0.69	0.41
Phosphate	r	-0.06	0.12	0.11	0.15
	p-value	0.54	0.23	0.33	0.13
Mg	r	-0.16	0.06	-0.17	**-0.18**
	p-value	0.12	0.58	0.12	**0.07**
ALP	r	**-0.22**	0.15	-0.15	-0.15
	p-value	**0.03**	0.14	0.17	0.15
iPTH	r	**-0.44**	0.03	-0.04	-0.09
	p-value	**0.00**	0.80	0.73	0.40
Vitamin D	r	0.14	0.11	0.01	-0.05
	p-value	0.19	0.31	0.93	0.62
Bicarbonate	r	0.15	**-0.23**	**-0.23**	-0.07
	p-value	0.15	**0.02**	**0.04**	0.51

[1]Bone Mineral Density. [2]Standard Deviation Score, [3]Ionised Calcium

Table 4.5.5 Univariate correlation analysis of CKD & Dialysis participants' extended pQCT measure z-scores and serum biomarkers

		Cortical Area	Periosteal Circumference	Endosteal Circumference	CSMI[3]	Cortical Mineral Content	Total Mineral Content
SDS[1] Height	r	**0.47**	**0.33**	-0.05	**0.44**	**0.50**	**0.31**
	p-value	**0.00**	**0.00**	0.64	**0.00**	**0.00**	**0.00**
SDS BMI	r	**0.44**	**0.34**	-0.01	**0.38**	**0.45**	**0.34**
	p-value	**0.00**	**0.00**	0.93	**0.00**	**0.00**	**0.00**
SDS Weight	r	**0.63**	**0.50**	-0.01	**0.57**	**0.64**	**0.46**
	p-value	**0.00**	**0.00**	0.94	**0.00**	**0.00**	**0.00**
Total Ca	r	0.14	0.10	-0.07	0.12	0.19	**0.35**
	p-value	0.18	0.33	0.49	0.23	0.06	**0.00**
iCa[2]	r	**0.21**	0.11	**-0.21**	0.13	**0.26**	**0.31**
	p-value	**0.04**	0.30	**0.04**	0.22	**0.01**	**0.00**
Phosphate	r	**-0.25**	-0.10	0.15	-0.16	**-0.30**	-0.12
	p-value	**0.01**	0.32	0.16	0.12	**0.00**	0.25
Mg	r	-0.17	-0.15	0.12	-0.11	-0.15	-0.05
	p-value	0.09	0.13	0.24	0.28	0.14	0.60
ALP	r	**-0.26**	**-0.23**	-0.05	**-0.28**	**-0.26**	0.01
	p-value	**0.01**	**0.02**	0.60	**0.01**	**0.01**	0.91
PTH	r	-0.16	-0.08	0.18	-0.10	**-0.25**	-0.18
	p-value	0.12	0.44	0.08	0.32	**0.01**	0.08

		-0.02	-0.03	-0.17	-0.08	0.00	0.12
Vitamin D	r	-0.02	-0.03	-0.17	-0.08	0.00	0.12
	p-value	0.86	0.77	0.09	0.45	0.98	0.23
Bicarbonate	r	0.00	0.06	0.08	-0.02	0.00	-0.15
	p-value	0.99	0.57	0.46	0.88	0.97	0.15

[1]Standard Deviation Score, [2]Ionised Calcium, [3]Cross sectional moment of inertia.

Total serum calcium showed a positive association both bone compartments separately by pQCT; CortBMD (r=0.33, p=0.001; Figure 4.5.6a) and trabBMD (r=0.32, p=0.001). Ionised calcium correlated with cortical measures: CortBMD (r=0.37, p<0.001), cortical area (r=0.21, p=0.04) and cortical mineral content (r=0.26, p=0.01) . Both PTH and ALP showed inverse correlations with cortical measures: CortBMD (r=-0.44, p<0.0001 and r=-0.22, p<0.03 respectively) (Figures 4.5.6b and 4.5.6c) and cortical mineral content (r=-0.25, p=0.01 and r=-0.26, p=0.009 respectively). In addition, serum bicarbonate was significantly negatively associated with trabBMD (r=-0.23, p=0.02) and hip DXA z-scores (r=-0.23, p=0.04).

Figures 4.5.6a, b & c. Plot of cortical bone mineral density z-scores according to PTH, total calcium (Ca) and alkaline phosphatase (ALP) values. PTH plotted on a logarithmic scale- log2 (pmol/L). Solid line is linear regression best fit for all participants, with dotted lines showing the 95% CI. The Y axis of CortBMD z-scores has been curtailed at -6 for consistency. This leaves 3 value points outside the plotted areas as the participants had CortBMD z-scores lower than -6. These 3 dialysis participants although outliers, had consistently lower bone imaging z-scores across all modalities. [Multivariable regression associations for CKD participants only: R^2 0.24, Ca β=0.12, p=0.55; ALP β=-0.38, p=0.06; PTH β=-0.32, p=0.14; For

dialysis participants only: R^2 0.58, Ca β=0.22, p=0.01; ALP β=-0.37, p<0.0001; PTH

β=-0.41, p<0.0001]

a
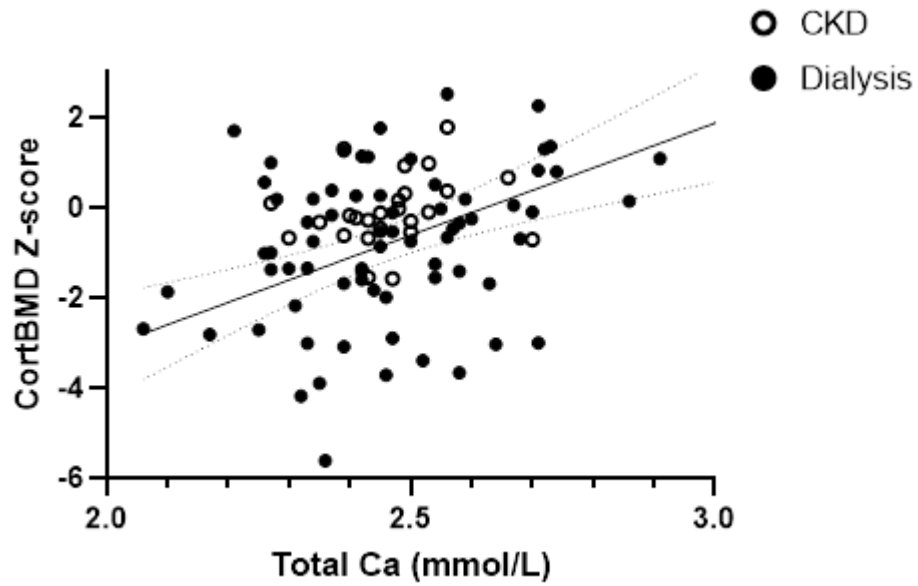
b
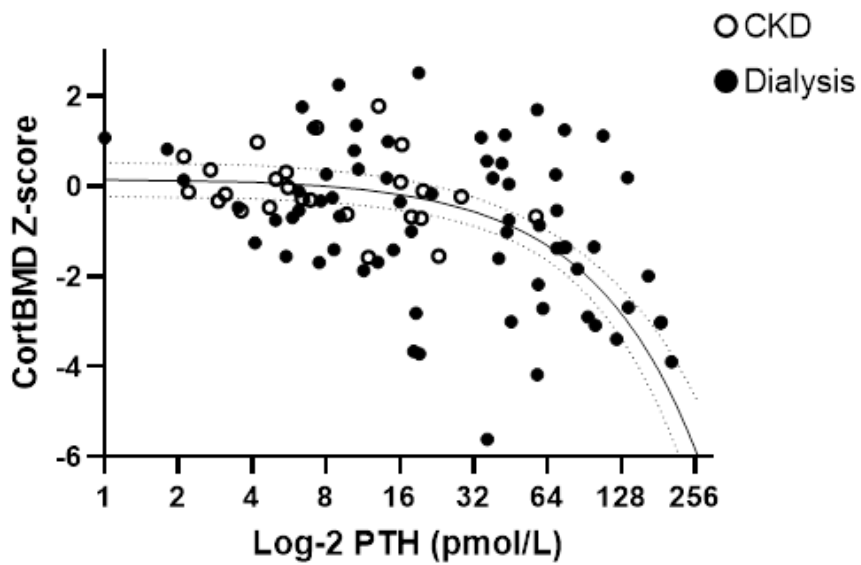
c
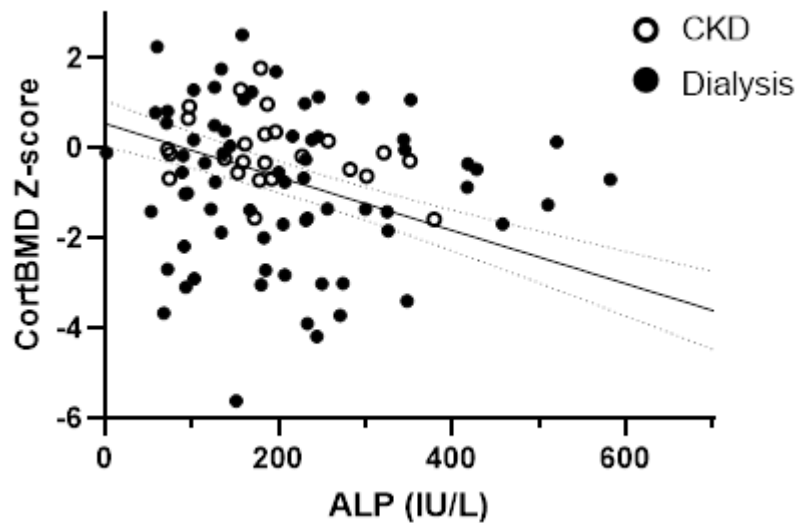
Given that different PTH levels are recommended by KDIGO (Ketteler et al.) and the European Pediatric Dialysis Working Group (EPDWG) (Klaus et al., 2006), I examined the different target PTH levels against CortBMD in the cohort. CortBMD was significantly lower in participants with PTH>9xULN (-1.92, -3.01 to -0.64), compared to 2-9xULN (-0.29, -1.56 to 0.52, p=0.03) (Figure 4.5.7a). However, there was no difference between PTH levels of <2xULN (-0.12, -0.56 to 0.69) and 2-9xULN (p=0.42) groups. When applying the EPDWG recommendations, PTH values less than 3xULN were associated with significantly higher cortical BMD compared to PTH values >3xULN (-0.11 [-0.56 to 0.79], vs -1.35 [-2.98 to 0.01], p<0.0001) (Figure 4.5.7b).

When PTH values were less than 3xULN none of the patients had a CortBMD below -2SD (OR 95%CI 7.33 to infinity) [sensitivity 100% (95% CI 93.1% to 100%) and specificity 36.9% (95%CI 24.5% to 51.4%)]. Further analysis confirmed that with increasing PTH levels the odds of having a CortBMD below -2SD increased, such that

with PTH >4xULN, the odds of a CortBMD below -2SD was 11-fold higher [OR 11.08

(95% CI 3.12 to 37.90), sensitivity 95% (95% CI 86.3% to 98.6%), specificity 36.8%

(95%CI 23.4% to 52.7%)].

Figures 4.5.7a &b. Scatter plots of the cortical BMD Z-scores, separated into

columns according to the PTH upper limit of normal (ULN) target in different

guidelines. Lines show the median and the interquartile range for all participants. p-

value between group significance shown.

a
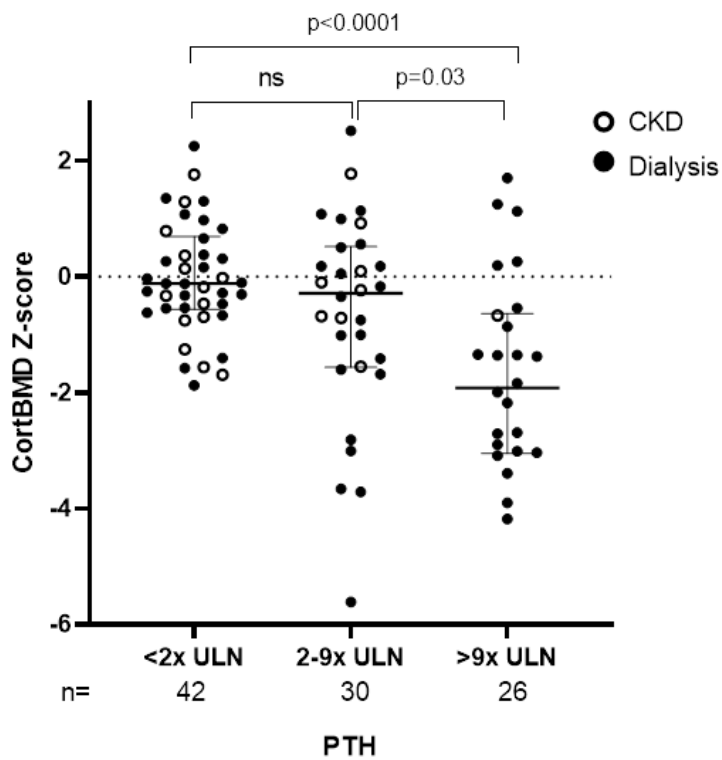
b
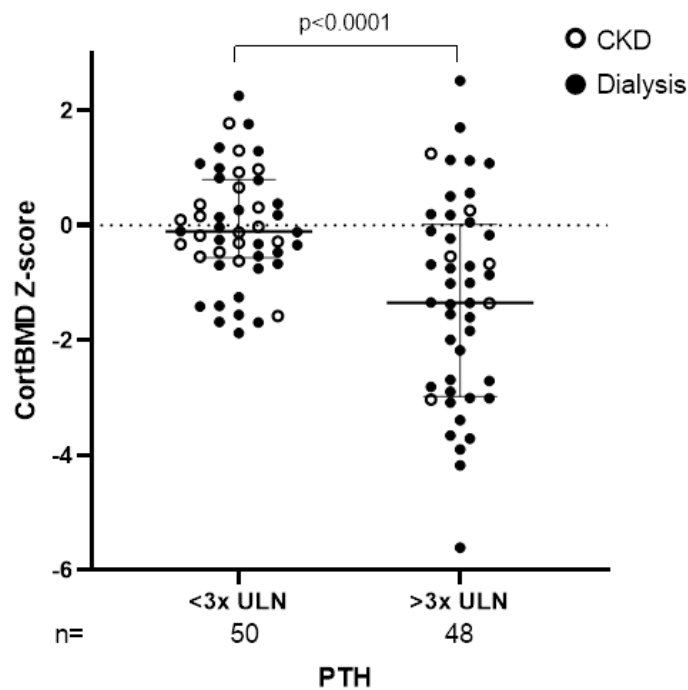
Medication and Supplements

More patients in the CKD cohort were on Ca-based phosphate binders compared to the dialysis group (73.1% vs 36.8%). Consequently, the elemental Ca intake from the binders was significantly higher in CKD compared to dialysis patients [p=0.03, 1.06 (0 to 2.13) vs 0 (0 to 1.46) mmol/kg/day]. There was no significant difference in alfacalcidol (1α hydroxyvitamin D3) treatment (p=0.08). On univariable analysis alfacalcidol was associated with TrabBMD (r=0.27, p=0.02), but was no longer significant on multivariable analysis. None of the medications were associated with CortBMD, or DXA Z-scores (Table 4.5.6).

Table 4.5.6. Univariate correlation analysis of CKD & Dialysis participants' bone imaging measures and medication

		CortBMD[1] z-score	TrabBMD z-score	Hip DXA z-score	LS BMAD z-score
Ca intake from binders	r	0.16	-0.11	0.11	0.001
	p-value	0.12	0.29	0.36	0.99
Vitamin D3	r	-0.82	0.11	0.06	-0.001
	p-value	0.42	0.27	0.57	1.00
Alfacalcidol (1α hydroxyvitamin D3)	r	0.01	**0.27**	-0.06	0.06
	p-value	0.93	**0.016**	0.62	0.57

[1]Bone Mineral Density

Multivariable regression analysis

We explored the ability of serum biomarkers and imaging tools used in routine clinical practice to predict CortBMD. We constructed stepwise multivariable linear regression models, including only those parameters with $p \leq 0.15$ on univariable analysis into the models (Table 4.5.7). Notably dialysis vintage, number of years with a low eGFR and dialysis/pre-dialysis status were not significant on univariable analysis. Model 1 included all serum biomarkers with $p \leq 0.15$ on univariable analysis. Model 2 included KDIGO recommended measures (Ca, ALP, and PTH) for monitoring CKD Mineral Bone Disease; phosphate and Vitamin D (25OHD) did not reach the pre-defined threshold on univariable analysis. Model 3 replaced total calcium with its co-dependent variable ionised calcium. Model 4 included lumbar spine DXA.

In the most robust model (model 2), independent predictors of CortBMD were total Ca (β 0.21, p=0.005), ALP (β -0.36, p<0.0001) and PTH (β-0.43, p<0.0001), accounting for 57% of the variability in CortBMD (R^2 0.57). When all significant variables from univariable analysis were included, bicarbonate was also a significant

independent predictor of CortBMD (β 0.16, p=0.03; model 1). Including LS BMAD

did not improve the predictive value of the model (model 4).

Table 4.5.7. Stepwise multivariable linear regression models used to find the

best serum biomarkers and/or DXA imaging to predict cortical BMD. All variables

with univariate correlations of p≤0.15 were entered into the analysis. Model 1

included all serum biomarkers meeting the univariate correlation threshold. Model

2 included KDIGO recommended measures (Ca, ALP, and PTH) for monitoring MBD.

Model 3 replaced total calcium with its co-dependent variable ionised calcium.

Model 4 included lumbar spine DXA.

Regression Model		B	95.0% Confidence Interval for B	Std. Error	Standardized β	p-value	Model R^2	Model Adjusted R^2
1	(Constant)	-7.75	-12.67, -2.82	2.48		0.002	0.53	0.51
	Total Ca	2.55	0.76, 4.35	0.90	0.22	**0.006**		
	Mg	-0.14	-2.04, 1.76	0.96	-0.01	0.884		
	ALP	-0.004	-0.01, -0.002	0.001	-0.37	**<0.0001**		
	PTH	-0.015	-0.02, -0.01	0.003	-0.38	**<0.0001**		
	Bicarbonate	0.09	0.01, 0.17	0.04	0.16	**0.03**		
2	(Constant)	-5.66	-10.11, -1.20	2.25		0.01	0.58	0.57
	Total Ca	2.57	0.79, 4.35	0.90	0.21	**0.005**		
	ALP	-0.004	-0.01, -0.002	0.001	-0.36	**<0.0001**		
	PTH	-0.02	-0.21, -0.10	0.003	-0.43	**<0.0001**		
3	(Constant)	0.58	-0.89, 2.04	0.74		0.44	0.57	0.56
	Ionized Ca	0.15	-1.03, 1.32	0.59	0.02	0.81		
	ALP	-0.003	-0.01, -0.002	0.001	-0.34	**<0.0001**		
	PTH	-0.02	-0.02, -0.01	0.003	-0.53	**<0.0001**		
4	(Constant)	-5.25	-9.68, -0.81	2.23		0.02	0.59	0.58
	Total Ca	2.36	0.59, 4.13	0.89	0.19	**0.01**		
	ALP	-0.003	-0.005, -0.002	0.001	-0.34	**<0.0001**		
	PTH	-0.02	-0.02, -0.01	0.003	-0.42	**<0.0001**		
	Lumbar spine DXA	0.14	-0.06, 0.34	0.10	0.09	0.18		

4.6 Discussion

Mineral and bone disorders of CKD account for a significant burden of pain and atraumatic fractures even in children and young adults with CKD and on dialysis. The data presented show that routinely measured serum biomarkers Ca, PTH and ALP taken together are moderate predictors of BMD, whereas DXA is not a useful additional measure, and should not be routinely performed in children and young adults with CKD4-5 or on dialysis.

In this cohort of young people under 30 years of age, morbidity from CKD-MBD is significant and prevalent. The pain was reported to affect daily activities, and required frequent use of analgesia. This is consistent with previous studies, showing that clinical symptoms of bone disease are present in children and adolescents on dialysis (Borzych et al., 2010). In a study reported almost 2 decades ago, young adults with childhood CKD had a heavy burden of bone disease ranging from bone pain to deformities, atraumatic fractures and impaired mobility from bone disease (Groothoff et al., 2003). With improved management, both prevalence and severity of MBD symptoms have reduced over the years, but remain a major concern for our patients (Tong et al., 2018). The CKiD study (CKD in Children) reported fracture rates of 2.4 and 3-fold higher in males and females respectively compared to their healthy peers (Denburg et al., 2016). 16% reported a prior fracture and over 3.9 years of follow up, 12.5% had a fracture (Denburg et al., 2016). 10% of our cohort had at least one previous low trauma fracture, consistent with the higher fracture risk in the young CKD population. In a study of 89 children with CKD stages 2-5D, 6.5% suffered a fracture during the one year follow-up, and

fracture risk doubled for every 1 SD decrease in CortBMD(Denburg et al., 2013). In this cohort, patients with a previous fracture had lower LS BMAD z-scores. However, the fractures preceded the bone imaging by months or years, and this association should be viewed with some caution. A long-term longitudinal study is required to establish the ability of BMD assessment by DXA or pQCT to predict fractures in the young CKD population.

In this cohort Ca, PTH and ALP, taken together, accounted for 57% of variability in CortBMD. The data are consistent with previous studies showing serum biomarkers are poor surrogate markers in assessing BMD, but as suggested by KDIGO, trends in Ca, P, PTH and ALP, taken together, are the best available measure for clinical management of MBD (Ketteler et al., 2018). Serum biomarkers do not reflect the true state of bone turnover or mineralisation (Bakkaloglu et al., 2010, Barreto et al., 2008b), and no biomarker individually or in combination can reliably identify mineralization or turnover defects (Sprague et al., 2016, Soeiro et al., 2020). Some markers vary significantly with age and stage of growth such as ALP (Zierk et al., 2017). Studies using bone histology have shown a mineralisation defect in over 80% of the dialysis population; this was associated with higher PTH and lower calcium levels (Wesseling-Perry et al., 2012, Bakkaloglu et al., 2010). In fact, mineralisation defects can begin early in children, with up to a third in CKD stage 2 having abnormal mineralisation (Wesseling-Perry et al., 2012), even though serum Ca, P and PTH levels may be normal. This is in sharp contrast with bone histology in older adults on dialysis wherein abnormal mineralisation is present in 3% of patients (Malluche et al., 2011). Other studies report higher ALP levels are associated with higher bone turnover rates by bone biopsy (Bakkaloglu et al., 2010), but also lower

CortBMD z-scores by pQCT (Wetzsteon et al., 2011), suggesting an uncoupling of osteoid formation and its mineralisation in CKD, as also shown by an inverse correlation of CortBMD and ALP in this cohort.

Alfacalcidol was associated with trabecular BMD on univariable analysis. Previous animal (Chen et al., 2008, Shiraishi et al., 2000) and clinical studies (Felsenberg et al., 2011, El-Agroudy et al., 2005) have shown that 1α-hydroxyvitamin D3 reduces bone resorption but maintains and/or stimulates bone formation by increasing osteoblast activity. None of the medication or supplements were independent predictors of cortical or trabecular BMD in this cross-sectional analysis of the cohort data.

The assessment of BMD in CKD remains challenging and fraught with technical difficulties. Bone biopsy, although considered the gold standard in assessing mineralisation changes, is highly invasive, requires skilled interpretation by a trained histopathologist, and is rarely performed in children or adults with CKD. DXA is widely available, inexpensive, observer independent, and provides aBMD data as well-validated age, sex and race matched z-scores (Gordon et al., 2014). As a two-dimensional image, DXA superimposes cortical and trabecular bone. PTH has an anabolic effect on trabecular bone and a catabolic effect on cortical bone (Parfitt, 1998), so effects of hyperparathyroidism cannot be studied with DXA (Weber and Mehls, 2010). In addition, DXA provides no information on bone microarchitecture, and trabecular thickness, spacing, connectivity and the ratio of plate- and rod-like structures all contribute to bone strength and quality (Mittra et al., 2005), apart from just BMD. Given that DXA measures areal BMD (g/cm^2) it can underestimate

volumetric BMD (g/cm^3) in children with short stature (Zemel et al., 2010) and overestimate BMD in a tall child (Crabtree and Ward, 2015), and make serial DXA scanning in growing children particularly challenging. There have been a few studies exploring the use of DXA in the young CKD population, and its association with biochemical markers, but none have examined the association of BMD with fractures (Pluskiewicz et al., 2003, Waller et al., 2007, Griffin et al., 2012).

Some of the limitations of DXA can be overcome by pQCT which distinguishes between cortical and trabecular bone, and is not affected by patient size. However, pQCT imaging is largely operator dependant, different protocols are used around the world, and the reference data to calculate age, height and sex adjusted z-scores for healthy people is limited (Adams et al., 2014, Leonard et al., 2010, Roggen et al., 2015b). These drawbacks have largely limited its use to research. Nevertheless, pQCT has been used in the young CKD population to show bone demineralisation (Wetzsteon et al., 2011) and correlated a reduction in cortical BMD z-score with a higher fracture risk in children with CKD 2-5D (Denburg et al., 2013). It has also shown that cortical BMD is inversely linked to higher PTH and ALP levels (Lima et al., 2003) as reported in this cohort.

Our data suggests that serum bicarbonate levels were significantly positively associated with CortBMD. There is evidence that acidosis impairs bone mineralisation (Raphael, 2018). Treatment with potassium citrate for 12 months improves cortical parameters on bone biopsy in post-transplant patients (n=19) (Starke et al., 2012). In vitro studies show that bone resorption increases with acidosis, through upregulation of osteoclast activity (Yuan et al., 2016). Buffering of

the acidosis with calcium carbonate released from the bone leads to further demineralisation ('K/DOQI clinical practice guidelines for bone metabolism and disease in chronic kidney disease,' 2003). Thus, it may be important to consider serum bicarbonate alongside routinely measured biomarkers of MBD.

The optimum target range for serum PTH levels to allow for bone mineralisation and normal bone turnover, whilst avoiding adynamic bone disease remains heavily debated, and often extrapolated from adult data (Ketteler et al.) or historic and highly confounded bone histology data (Ballanti et al., 1996, Salusky et al., 1994, Coen et al., 1998, Sprague et al., 2016). I examined the predictive value of the KDIGO recommended target range of 2-9xULN (although based on studies in adult CKD cohorts alone) and the significantly lower target of <3xULN suggested by the EPDWG. I found that there was a strong non-linear association between PTH and CortBMD such that when PTH was <3xULN none of the patients had CortBMD below -2SD. On the other hand, PTH target levels of <2xULN and between 2-9xULN were unable to differentiate normal CortBMD, implying a lack of sensitivity of such a wide PTH target. A review of bone biopsy studies in children with CKD suggests that high PTH levels are associated with high bone turnover, but the ability of serum PTH levels to distinguish between low and normal turnover bone disease is less clear (Rees, 2008). Of note, several bone biopsy studies included were either small, in older adults, on patients with long-standing hyperparathyroidism or those who had undergone parathyroidectomy, or patients on aluminium containing phosphate binders, making them less relevant to current practice. In untreated CKD, PTH levels increase early in the course of CKD and skeletal resistance develops requiring even higher PTH levels to maintain normal turnover (Rees, 2008, Ballanti et al., 1996).

The requirement to keep PTH levels above the upper limit of normal may now be less relevant.

Registry data (Borzych et al., 2010), prospective cohort studies examining fracture risk (Denburg et al., 2016), longitudinal studies examining cortical BMD using pQCT, growth data as well as vascular imaging studies suggest keeping PTH closer to the normal range. A study from the IPPN registry in over 900 children on peritoneal dialysis found that time-averaged PTH concentrations above 500 pg/ml were associated with impaired longitudinal growth, PTH levels exceeding 300 pg/ml increased clinical and radiological symptoms, but the risk of hypercalcemia increased with levels below 100 pg/ml, suggesting a PTH target range of 100–300 pg/ml in the pediatric age group (Borzych et al., 2010). Recently, the chronic kidney disease in childhood (CKiD) study has shown a lower fracture risk in children with lower PTH levels (Denburg et al., 2016). A prospective longitudinal follow-up study in children with CKD2-5D has shown that a greater increase in PTH was associated with greater declines in CortBMD z-scores over the 1-year follow-up period (Denburg et al., 2013).

A concern with a low PTH or suppression below the target range is the development of adynamic bone disease, as reported even in children (Ziolkowska et al., 2000). Indeed, in the presence of adynamic bone disease, a normal cortical or trabecular BMD does not necessarily imply normal structure and mechanical properties of the bone (Ng et al., 2016). However, others have challenged the concept of 'adynamic bone' as children with CKD in whom PTH was kept within normal limits had an above average rate of growth (Waller et al., 2003), suggesting

that normal PTH levels do not cause a low turnover bone state. Importantly, a paediatric dialysis cohort with PTH levels within 2-3xULN had normal carotid intima-media thickness, pulse wave velocity and lower coronary artery calcification scores compared to those with PTH >3xULN (Shroff et al., 2007). Taken together, these data suggest that PTH within 3xULN is associated with CortBMD above -2SD. Larger longitudinal studies are required to confirm this association.

In this paper we report the initial cross-sectional data examining bone health, and bone mineral density associations with routinely used serum biomarkers. We established that even a young cohort aged 5 to 30 years old suffer a high bone disease burden, with 10% reporting a previous fracture, and 58% reported pain that hindered activities of daily living. As bone biopsy is highly invasive, we used pQCT as the method of establishing CortBMD. pQCT has remained a research tool due to technical procedural constraints in obtaining the imaging as well as a lack of standardization of the measurement technique and lack of published reference data. We sought to alleviate these by having 2 observers independently score and evaluate the pQCT scans images as per Bleu et al (Blew et al., 2014).

4.7 Conclusion

In summary, we have shown that CKD-MBD leads to significant morbidity in young patients with a high prevalence of bone pain and atraumatic fractures. Assessment of CortBMD in the absence of bone biopsy is challenging, with routinely measured serum biomarkers Ca, PTH, ALP and bicarbonate being only moderate independent predictors of cortical BMD. DXA imaging does not correlate with CortBMD and should not be routinely performed in children and young adults with CKD4-5D. In this young cohort, PTH levels below 3xULN were associated with a normal cortical BMD.

Chapter 5

Clinical and Subclinical cardiovascular disease in children and young people with CKD stages 4-5 or on dialysis

In this chapter I have described the cross-sectional baseline vascular health and cardiovascular disease burden in this cohort of children and young adults with CKD or on dialysis. I have examined both the structural changes observed and the functional abnormalities of the vasculature.

The work in this chapter has been published in: Lalayiannis AD, Ferro CJ, Wheeler DC, Duncan ND, Smith C, Popoola J, Askiti V, Mitsioni A, Kaur A, Sinha MD, McGuirk SP, Mortensen KH, Milford DV, Shroff R. **The burden of subclinical cardiovascular disease in children and young adults with chronic kidney disease and on dialysis**. *Clinical Kidney Journal*. Volume 15, Issue 2, February 2022, Pages 287–294, https://doi.org/10.1093/ckj/sfab168

In line with UCL policy, I declare that I collected and analysed the data and wrote the original manuscript. The co-authors very kindly helped with editing and proof-reading.

5.1 Abstract

Background

Cardiovascular disease (CVD) is a common cause of morbidity and mortality even in young people with chronic kidney disease (CKD). Structural and functional cardiovascular changes in patients with CKD stages 4-5 and on dialysis under 30 years of age were examined.

Methods

Seventy-nine children and twenty-one young adults underwent cardiac computed tomography for coronary artery calcification (CAC), ultrasound for carotid intima media thickness (cIMT), carotid-femoral pulse wave velocity (cfPWV), and echocardiography. Differences in structural [CAC, cIMT z-score, left ventricular mass index] and functional [carotid distensibility z-score, cfPWV z-score] measures were examined between patients with CKD stages 4-5 and patients on dialysis.

Results

Overall the cIMT z-score was raised (median 2.17, IQR 1.14-2.86) and 10 (10%) had CAC. 16 of 23 (69.5%) with CKD 4-5 and 68 of 77 (88.3%) on dialysis had at least one structural or functional cardiovascular abnormality. There was no difference in the prevalence of structural abnormalities in CKD or dialysis cohorts, but functional abnormalities were more prevalent in patients on dialysis ($p<0.05$). The presence of >1 structural abnormality was associated with a 4.5-fold odds increase of >1 functional abnormality (95% CI 1.3 to 16.6, $p<0.05$). Patients with structural and functional abnormalities (cIMT z-score >2 standard deviations or distensibility <-2

standard deviations) had less carotid dilatation (lumen/wall cross sectional areas ratio) compared to those with normal cIMT and distensibility.

Conclusions

There is a high burden of subclinical cardiovascular disease in young CKD patients, with a greater prevalence of functional abnormalities in dialysis compared to CKD patients. Longitudinal studies are required to test these hypothesis generating data and define the trajectory of CV changes in CKD.

5.2 Introduction

Cardiovascular disease (CVD) is the most common cause of morbidity and mortality in young people with chronic kidney disease (CKD) (Mitsnefes, 2012, Modi et al., 2019). Mineral dysregulation in CKD - Mineral Bone Disorder (MBD) is causally linked with calcium (Ca) and phosphate (P) deposition in the medial layer of the arteries (Shroff et al., 2007), with an increase in arterial thickness and stiffening of the vessels (Shroff et al., 2008, Shroff et al., 2010, Shroff et al., 2013). Vascular damage and calcification may be present early in the course of CKD (Litwin et al., 2005, Schaefer et al., 2017) and progresses rapidly once dialysis is initiated (Shroff et al., 2007). It has been suggested that structural changes lead to arterial stiffness that in turn, causes an increased left ventricular pressure load (Litwin et al., 2005) and left ventricular hypertrophy (LVH), but correlations between structural and functional vascular changes and factors associated with these changes have not been fully examined.

In a cohort of children and young adults under 30 years of age I examined structural changes (including coronary artery calcification, cIMT and left ventricular mass), functional changes (carotid distensibility and arterial stiffness) and evidence of cardiovascular remodelling. The hypothesis was that young people with CKD stages 4-5 and on dialysis would have a high prevalence of subclinical CVD. I also examined the association of structural changes and functional abnormalities in this age group. This study is the baseline vascular cross-sectional element of the longitudinal, multicentre study examining bone and cardiovascular health in children and young adults with CKD. Young adults are included as the skeleton

continues to mineralise until the third or fourth decade of life (Weaver et al., 2016), accruing calcium and perhaps acting as a 'buffer' to prevent vascular calcification.

5.3 Methods

Study Participants

This cross-sectional element of the study included young people with CKD stages 4-5 or on dialysis from 5 pediatric and 4 adult nephrology units across the United Kingdom and Athens, Greece. The inclusion criteria were: age from 5 to 30 years and CKD stages 4-5 [estimated glomerular filtration rate (eGFR; by Schwartz formula (Schwartz et al., 2009)) <30ml/min/1.73m^2] or on dialysis. As skeletal mineralisation continues until 30 years of age when peak bone mass is reached, young adults up to 30 years of age were included (Weaver et al., 2016). Patients with a functioning kidney transplant and those who would not have tolerated the scanning procedures were excluded. Informed written consent was obtained from all parents or caregivers and adult participants. Assent was obtained from children where appropriate.

130 patients were identified and 112 agreed to participate. Twelve withdrew consent prior to taking part. One-hundred children and young adults with CKD completed the study and were included in the analyses.

Investigations Performed

Anthropometry

Height was measured using a fixed wall stadiometer, and weight recorded with a digital scale. Height, weight and body mass index (BMI) measurements were expressed as z-scores. Young adults' anthropometric z-scores were calculated assuming a maximum age of 20 years.

Manual blood pressure (BP) was recorded at a routine clinic visit or before a midweek haemodialysis session by myself and expressed as z-scores, adjusted for age, sex and height (Flynn et al., 2017). Hypertension (HTN) was defined as a systolic and/or diastolic measurement above the 95th centile for age and height as per the 2016 European Society of Hypertension (ESH) guidelines (Lurbe et al., 2016).

Given the age range of age of our patients, all age-related measures (including cardiovascular measures) are presented as z-scores. Z-scores reflect normative changes due to age, height and sex and allow for comparison of the vascular measures across all age-groups.

Serum Biomarkers

Routine serum biomarkers were measured on non-fasting blood samples collected at the study visit or prior to a mid-week hemodialysis session and analysed in the patients' respective hospitals. These included serum ionized calcium (iCa), total calcium (Ca), phosphate (P), magnesium (Mg), bicarbonate, intact PTH (iPTH), 25-hydroxyvitamin D [25OHD], and alkaline phosphatase (ALP). Due to different iPTH assays used (Immulite [*Siemens Healthcare Diagnostics]* and Elecsys 2010 [*Roche Diagnostics*]), results have been expressed in multiples of the upper limits of normal (ULN). Serum total cholesterol, triglycerides and glucose measurements were recorded where available.

Carotid Intima Media Thickness (cIMT) and carotid distensibility

cIMT measurements were obtained by ultrasound according to the Mannheim consensus (Touboul et al., 2012). The mean cIMT was calculated as the average IMT measurements of both carotids, 1-2 cm below the bifurcation using automatic software (Vivid iq, GE Healthcare, USA), and analysed offline in a blinded fashion. All measurements were obtained by myself.

All images/video clips were stored digitally, and analyses were done offline, in a blinded fashion by myself. cIMT was calculated semi-automatically with the GE Vivid Iq software. The recorded video was frozen at the peak of the R wave and the area of interest highlighted. An area of 1cm was identified 1-2cm below the bifurcation of the carotid artery. The software calculates an average cIMT from around 250 measurements. This was repeated 3 times for each carotid and an average used. Systolic and diastolic internal diameters of the common carotid artery were obtained from M-mode transverse views of the carotid. A 10-15 second clip was recorded of 5 consecutive heart cycles. Five measurements of carotid lumen diameter in systole and diastole were taken and the average of each used to calculate distensibility as published previously (Jourdan et al., 2005). M-mode was used for vessel systolic and diastolic diameter (See Appendix for SOP).

Mean wall cross-sectional area (WCSA), mean lumen cross-sectional area (LCSA) (Jourdan et al., 2005), their ratio (LCSA/WCSA; reflecting the ability of the vessel to dilate in relation to vessel wall thickening), distensibility coefficient (reflecting the functional properties of the carotid, and its ability to distend with each cardiac cycle) were also calculated (Figure 5.3.1) (Doyon et al., 2013).

Figure 5.3.1 Schematic representation of the constituent parts of the carotid wall and the carotid measure equations (Jourdan et al., 2005, Doyon et al., 2013). Adapted from (Lalayiannis et al., 2021a).

Mean systolic diameter (sD) = (LsD + RsD)/2

Mean diastolic diameter (dD) = (RdD + LdD)/2

Wall cross sectional area (WCSA) = $\pi*(dD/2 + IMT)^2 - \pi*(dD/2)^2$

Lumen cross sectional area (LCSA) = $\pi *dD^2/4$

Distensibility coefficient = $2(\Delta D/dD)/(\Delta P/10*1.33*100)$

LsD = left common carotid artery systolic diameter
RsD = right common carotid artery systolic diameter
LdD = left common carotid artery diastolic diameter
RdD = right common carotid artery diastolic diameter
IMT = carotid intima media thickness
ΔD = sD - dD
ΔP = Systolic BP- Diastolic BP

cIMT measurements were expressed as z-scores according to Doyon et al (Doyon et al., 2013). Adults' z-scores were calculated using interpolation of the difference between 17 to 18 years old (The annual increase of absolute cIMT each year to the age of 30 was assumed to be the same as the increase from 17 to 18 years). For this, I received help from UCL ICH statistician Dr Colette Smith, to whom I am very grateful. I compared these values with z-scores obtained from other healthy reference databases, and the comparison is presented in the results section.

Cardiac Computed Tomography

Coronary artery and valvular calcification were examined by CT (*Somatom Force; Siemens, Germany* or *GE Discovery 750HD, USA*) using the machines' standard Ca scoring protocol. Prospective ECG triggering was used to obtain images in diastole. Calcification was expressed as Agatston score (Agatston et al., 1990) and analysed offline in a blinded fashion, confirmed independently by two observers (myself and Dr Kristian H. Mortensen) using Syngo Via software (*Siemens, UK*). (See Appendix for detailed SOP)

Echocardiography

Left ventricular (LV) measures were collected from 2D echocardiography. The LV mass was calculated according to the Devereux equation (Devereux et al., 1986) and indexed to height$^{2.7}$(g/m$^{2.7}$) (LVMI) (Schaefer et al., 2017). Left ventricular hypertrophy (LVH) was defined as sex- and age- specific LVMI above the 95th percentile as defined by Khoury et al (Khoury et al., 2009). Evaluation of LV geometry (concentric vs eccentric hypertrophy) was done using the relative wall thickness (RWT) formula and normalised for age 10 years for participants under 18 years old and age 46 years for participants over 18 as described by de Simone et al (de Simone et al., 2005). The 95th percentile cut off values were used to define concentric geometry with 0.38 for children and 0.43 for adults (de Simone et al., 2005).

Carotid-Femoral Pulse Wave Velocity (cfPWV) & Pulse Wave Augmentation

cfPWV was measured with the Vicorder Oscillometric PWV device (*SMART Medical*, *UK*). The distance used in the calculations was from the suprasternal notch to the femoral recording point via the umbilicus minus the distance from the carotid to the suprasternal notch as described previously (Kracht et al., 2011). The measurements were taken as an average of 3 readings.

As the pulse wave propagates through the arteries, it is met with peripheral resistance from arterial branching and vessel diameter differences, which create a retrograde waveform. This retrograde wave returns to the aortic root during diastole. This reflected wave returns sooner, even during systole, as the arteries become more stiff. The antegrade and retrograde waves create two peaks in systole. The difference in pressure between these peaks is the augmentation pressure(Azukaitis et al., 2020). Pulse wave augmentation and augmentation index (AIx) measurements were obtained from the right brachial artery (providing no fistula present in that arm). A minimum of three measurements were taken, each at least 10 beats. The software maps the pulse wave form, determining the augmentation of the pulse wave (the absolute increase in pressure at the point a reflected pulse wave meets the forward moving waveform (Azukaitis et al., 2020)) and the augmentation index (AIx) is calculated automatically as the augmented pressure difference/pulse pressure and expressed as a percentage (Azukaitis et al., 2020). (Please see Appendix for detailed SOP)

cfPWV results were expressed as z-scores based on reference values normalised for height and age (for the et al., 2015). Adult z-scores were calculated using interpolation of the values between 17 and 18 years old, similar to the cIMT z-

scores. A comparison was made again with other healthy reference databases and presented in the results. Pulse wave augmentation and augmentation index (AIx) were obtained with the same Vicorder device (*SMART Medical, UK*).

cIMT and cfPWV healthy adult database z-score comparison

cIMT and cfPWV z-scores for the adults in the cohort were generated by interpolation of the difference in absolute measurement for the ages for 17 to 18 years in the databases used and extended through to 30 years old (Doyon et al., 2013, Melk et al., 2015). *This was done by Dr Colette Smith, and for this I am very grateful to her*. The Doyon et al database is henceforth referred to as the 4C database as they were done for the Cardiovascular Phenotypes in children with CKD: The 4C Study.

This provided the advantage of using the same database for the whole cohort. As these databases only included healthy participants up to the age of 18, this could also be considered a disadvantage. For this reason, I compared our z-scores (as per height and age) to z-scores generated for adults using other healthy reference databases (Table 5.3.1) (Engelen et al., 2015, Diaz et al., 2018). I have outlined this comparison below.

Twenty one adults aged 19.1 to 30.6 years of age (11 males), with a median age of 25.51 (23.9 to 29.0) were included. The absolute cIMT median was 0.52 mm (IQR 0.49 to 0.56).

Table 5.3.1. Median cIMT z-scores of 21 adults as calculated from the 3 different databases

Reference Dataset	cIMT Z-scores, Median (IQR)
4C (Age)	2.71 (2.15 to 3.53)
4C (Height)	2.73 (2.41 to 3.44)
Engelen et al	2.53 (1.99 to 3.36)
Diaz et al	0.92 (0.44 to 1.46)

The 4C study (Doyon et al., 2013) age and height adjusted z-scores did not differ (p>0.99) between each other. The Engelen et al (Engelen et al., 2015) values were the most similar with the 4C age and height z-scores (p=0.25 & p=0.14 respectively). The Diaz (Diaz et al., 2018) values were significantly different, with an overall lower median z-score (difference vs 4C p<0.0001 for age and height) (Figure 5.3.2).

Figure 5.3.2. Median and IQR cIMT z-scores of 21 adults as calculated from 3 different databases
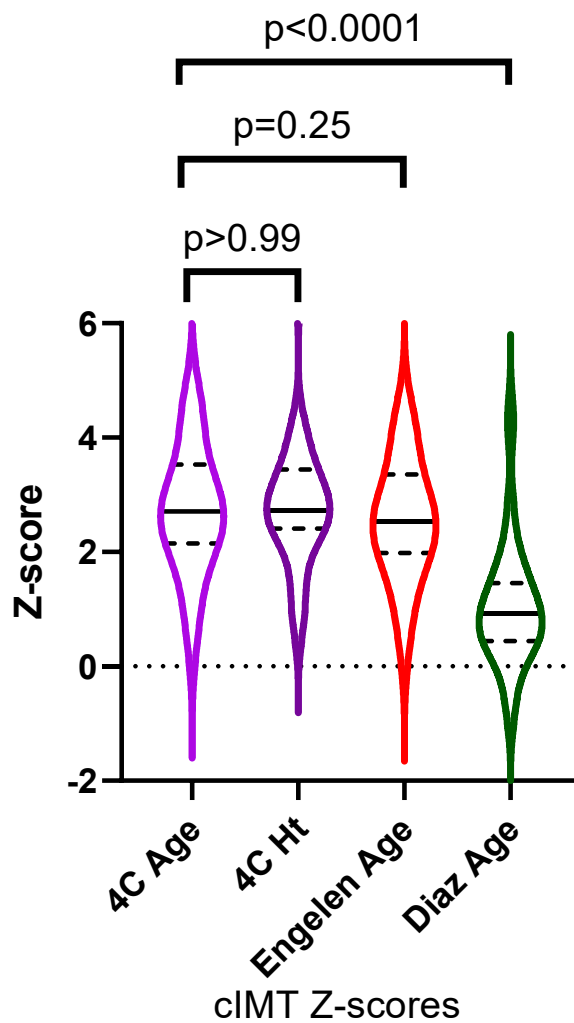
The Engelen et al dataset contains 4234 healthy participants with no underlying conditions or on chronic medications (females 52.9%). The age range was 15 to 90 years old. The publication however does not report the exact number of participants under 30 years old.

Diaz et al published a dataset of 1012 healthy participants aged 10 to 81 years, without reporting exactly how many were aged under 30. All participants were Argentinian, but there are no specific details about race, such as Caucasian or Native Andean, making the application to our cohort problematic. Z-scores for both these datasets were calculated on age alone. It is likely that the lower median z-score of our adult cohort is because the healthy dataset included young people from 10 years old.

cfPWV z-score comparison

The absolute value median for the adult participants was 7.27m/s (IQR 6.15 to 8.53). The medians and IQR of the z-scores according to the different databases are provided in the table (Table 5.3.2).

Table 5.3.2. Median cfPWV z-scores of 21 adults as calculated from 3 different databases

Reference Dataset	PWV Z-scores (Median, IQR)
4C (Age)	3.68 (0.91 to 5.89)
4C (Height)	4.24 (1.55 to 5.19)
RVASC	2.49 (1.00 to 4.18)
Diaz Age	2.16 (0.15 to 3.41)

The 4C age and height adjusted calculated z-scores were very similar. The 4C Age adjusted z-scores did not differ significantly from the RVASC z-scores. There were significant differences between the 4C height adjusted z-scores and the Diaz z-scores.

Figure 5.3.3. Median and IQR cfPWV z-scores of 21 adults as calculated from 3 different databases
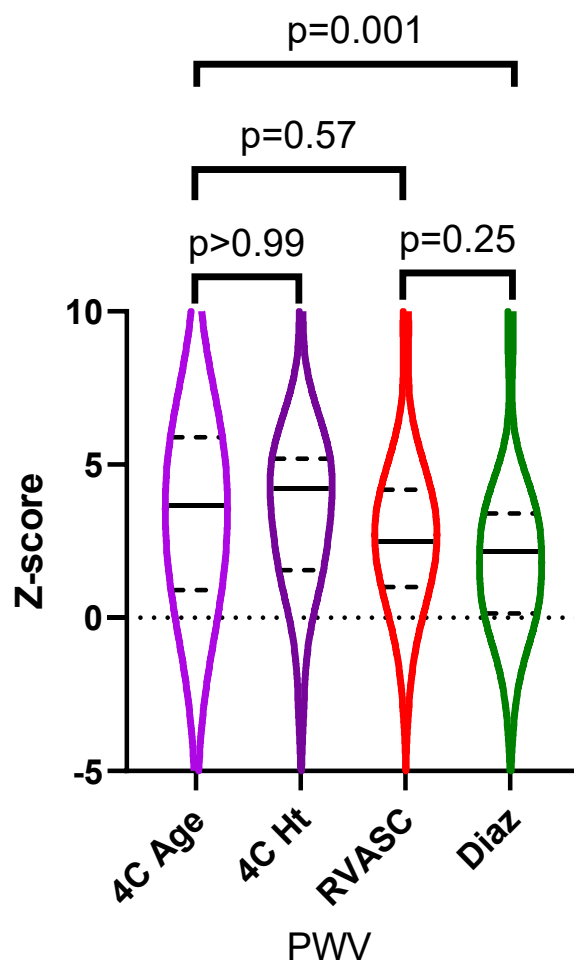
The European reference dataset from the Arterial Stiffness collaboration comprised 11,092 participants, aged 15 to 97 years. Of these participants, 1313 (11.8%) were under 30 years old. However, the LMS curves were derived from a specific subgroup of 1455 individuals with no co-morbidities or on regular

medication. These individuals were especially screened for normal blood pressure. It is unclear from the manuscript how many in this group with no co-morbidities were in fact under 30 years old.

The Diaz et al dataset provided normal reference centiles derived from 1722 participants, aged 9 to 87 years old. The exact number of participants under 30 years was not reported.

In the absence of a single healthy reference dataset to encompass the age range of all our participants, I opted therefore to use a single database and use interpolation to calculate adult z-scores. Reassuringly, these did not differ statistically from the healthy European adult database generated z-scores.

Z-scores vs absolute measurements

Z-scores were used in the analysis where able as well as absolute values of the different vascular measurements undertaken. I opted to present the z-score analyses, comparisons and associations in the thesis. The vascular tree is a dynamic tissue during childhood and adolescence. In healthy growing children, there is a gradual increase in the arterial wall diameter and total wall thickness. Total wall thickness increases due to the intima media layer, and is associated with the increasing blood pressure, age, sex and body dimensions (Sarkola et al., 2012). As such, z-scores reflecting normative changes due to age, height and according to sex are more accurate representations of deviation from the norm compared to

absolute measurements. Due to the relatively wide age range included in the study, z-scores allow for comparison across the age groups.

Cardiovascular abnormality scoring

For additional analysis and phenotyping of the cohort, CVD measures were split into structural (CAC, cIMT, LVMI) and functional (carotid distensibility & cfPWV) changes. I assigned one point for each measure above a z-score of 2 or above the 95th centile for all continuous data, and into presence or absence of CAC based on Agatston score. The total structural and functional scores for each patient were calculated.

5.4 Statistics

All results are presented as a median with interquartile range (IQR) or number and percentage. Spearman rank testing was used for univariable correlations. Kruskal-Wallis ANOVA test for non-normally distributed data with Dunn's correction for multiple comparisons was used. Mann-Whitney U tests were used for between group non-parametric comparisons. A series of linear regression models were performed, with the CVD measures (cIMT z-score, LVMI, distensibility, carotid dilatation, PWV z-score and augmentation) as the dependent variables. All independent variables with univariable associations of $p \leq 0.15$ were included in the multivariable models. All regression models included the CKD stage as a binary measure (CKD4-5 or dialysis) nominal category split. As z-scores are adjusted for age and sex, these were not included as a dependent variable. The association of structural and functional changes were expressed as odds ratios (OR) with 95%

confidence intervals, and an associated p-value was calculated using Fisher's exact test. SPSS 25 (IBM) was used for all statistical analyses and Prism (Graphpad) to create figures. A two-sided p value of ≤0.05 was considered to indicate a statistically significant difference.

5.5 Results

Demographics of the study population are shown in *Table 5.5.1*. Dialysis participants were older [median 14.3 (IQR 11.1 to 22.0) vs 11.5 (6.8 to 13.6) years, p=0.002], more likely to be of Asian (29.9% vs 17.4%) or Black (23.4% vs 8.7% respectively, p=0.03) race and more likely to have an underlying glomerular disease (16.9% vs 0%, p=0.001).

Table 5.5.1 Patient characteristics. All data presented as median (IQR). N/A, not applicable; CAKUT, Congenital abnormalities of the kidneys and urinary tract; eGFR, estimated glomerular filtration rate; ACEi, angiotensin-converting-enzyme inhibitor; ARB, angiotensin-receptor-blocker; ALP, Alkaline phosphatase; 25OHD, 25-Hydroxyvitamin D; PTH, parathyroid hormone; ULN, upper limit of normal. Serum total cholesterol, triglycerides and glucose measurements were recorded where available.

	Total	CKD	Dialysis	Between group comparison (p-value)
Total, n= (%)	**n=100**	n=23 (23%)	n= 77 (77%)	N/A
Age, years	13.82 (10.68, 16.46)	11.46 (6.80, 13.58)	14.25 (11.10, 21.95)	**0.002**
5-18 years, n=(%)	79 (79) 21 (21)	23 (100)	56 (73)	0.17
19-30 years, n=(%)		0	21 (27)	N/A
Sex, Female n=(%)	44	6 (26.1)	38 (49.4)	0.06

Race, n= Caucasian/ Asian/ Black/ Other	52/ 27/ 20/ 1	17/ 4/ 2/ 0	35/ 23/ 18/ 1	**0.03**
Height Z-score	-1.09 (-1.93, -0.36)	-0.84 (-1.6, 0.04)	-1.42 (-2.02, -0.43)	0.06
Weight Z-score	-0.56 (-1.67, 0.20)	-0.21 (-1.02, 0.64)	-0.78 (-1.77, 0.02)	**0.02**
BMI Z-score	0.14 (-0.88, 0.92)	0.52 (-0.66, 1.28)	0.01 (-0.95, 0.83)	0.06
SBP Z-score	0.89 (0.03, 1.67)	0.40 (-0.10, 1.13)	0.96 (0.12, 1.83)	**0.02**
DBP Z-score	0.72 (-0.14, 1.36)	0.50 (-0.18, 1.11)	0.87 (-0.04, 1.45)	0.30
Dialysis modality, n= HD/HDF/Home HD/PD	44/ 14/ 3/ 16	N/A	44/ 14/ 3/ 16	N/A
Phosphate binder therapy, n= Calcium based/ Non- calcium based/ Both/ None	39/ 23/ 5/ 33	16/ 1/ 0/ 6	23/ 22/ 5 / 27	**0.02**
Anti-hypertensive therapy, n= ACEi, ARB/ β-blocker/ Ca-channel blocker/ Diuretic/ combination	1/0/1/2/4	0/0/0/0/0	1/0/1/2/4	N/A
eGFR (ml/min/1.73m^2)	N/A	13.33 (9.72, 18.05)	N/A	N/A
Years with eGFR<30ml/min/1.73m^2	5.58 (2.02, 10.10)	3.68 (1.10, 8.81)	5.63 (2.50, 10.45)	0.09
Dialysis vintage, years	2.51 (0.75, 5.11)	N/A	2.51 (0.75, 5.11)	N/A
Serum biomarkers				
Total calcium (mmol/L)	2.47 (2.37 to 2.56)	2.48 (2.43 to 2.53)	2.47 (2.35 to 2.58)	0.99
Ionised calcium (mmol/L)	1.21 (1.12 to 1.29)	1.22 (1.16 to 1.27)	1.20 (1.11 to 1.29)	0.46
Phosphate (mmol/L)	1.53 (1.30 to 1.87)	1.46 (1.32 to 1.60)	1.58 (1.29 to 1.90)	0.20
ALP (IU/L)	183.50 (116.80 to 267.50)	184.00 (156.00 to 227.00)	183.00 (102.50 to 285.50)	0.93
25OHD (nMol/L)	78.00 (37.55 to 113.80)	94.00 (71.00 to 144.00)	61.00 (36.00 to 106.70)	**0.01**

PTH (x ULN)	x3 (x1 to x10)	x1 (<1 to x3)	x5 (x1 to x13)	**0.0005**
Total Cholesterol (mmol/L)	4.1 (3.5 to 4.9) n=35	4.4 (3.4 to 5.1) n=6	4.1 (3.6 to 4.9) n=29	0.80
Triglycerides (mmol/L)	1.5 (1.3 to 2.2) n=21	1.39 (1.26 to 1.61) n=4	1.52 (1.18 to 2.22) n=17	0.57
Glucose (mmol/L)	5.0 (4.4 to 5.4) n=22	5.3 (4.6 to 6.3) n=7	4.8 (4.2 to 5.3) n=15	0.26

As per the ESH guidelines, 28% of the cohort were hypertensive.

Hypertension was more prevalent in patients on dialysis (33.8% vs 8.6%, p=0.03).

There was no difference between those with glomerular vs non-glomerular (38.5% vs 26.4%, p=0.51) disease. 8% of the cohort were on anti-hypertensive medication, and of these, 50% had uncontrolled hypertension.

Patients on dialysis had lower 25OHD (61 vs 94 nmol/L, p=0.01) and higher PTH levels compared to CKD patients (x5 vs x1 ULN, p=0.0005).

Vascular measures

The structural and functional vascular measures for the total cohort as well as CKD stages 4-5 and dialysis groups are summarized in *Table 5.5.2*.

Univariable correlations between the vascular measures and the correlations with the serum biomarkers are presented in *Tables 5.5.3- 5.5.5*.

Table 5.5.2. Structural and functional cardiovascular measures in CKD and dialysis cohorts. All data presented as median (IQR), unless otherwise stated. Investigations performed in the entire cohort, except echocardiography, which was performed in 21/23 CKD patients, and 62/77 dialysis patients. CAC, coronary artery calcification; cIMT, carotid intima media thickness; LVMI, left ventricular mass index (Left ventricular mass/height$^{2.7}$), cfPWV, carotid femoral pulse wave velocity; WCSA, carotid wall cross sectional area; LCSA, carotid lumen cross sectional area. Adapted from (Lalayiannis et al., 2021a).

Vascular measures	Total	CKD	Dialysis	Between group comparison (p-value)
Structural Measures				
cIMT z-score	2.17 (1.14, 2.86)	2.46 (1.04, 2.76)	2.01 (1.14, 2.94)	0.72
CAC n=% (Agatston score range)	10% (0,412.6)	4.3% (0, 6.4)	12% (0, 412.6)	0.36
LVMI (g/m$^{2.7}$)	31.8 (28.0, 37.6)	30.23 (23.51, 33.44)	32.74 (29.48, 42.48)	**0.01**
Relative wall thickness	0.34 (0.29, 0.40)	0.32 (0.29, 0.38)	0.37 (0.30, 0.44)	0.08
Functional Measures				
Distensibility	-1.11 (-2.17, -0.15)	-0.39 (-1.34, 0.47)	-1.46 (-2.29, -0.30)	**0.009**
cfPWV z-score	1.45 (-0.16, 2.57)	0.61 (-0.78, 2.23)	1.52 (0.28, 2.81)	**0.03**
Augmentation (mmHg)	6.00 (4.00, 10.00)	6.33 (4.17, 9.5)	5.33 (3.33, 10.67)	0.60
Augmentation Index (%)	15.83 (10.67, 24.00)	16.00 (11.17, 22.50)	13.67 (9.00, 25.67)	0.73
Carotid dilatation (LCSA/WCSA)	3.06 (2.78, 3.36)	3.22 (3.03, 3.61)	2.98 (2.68, 3.29)	**0.006**

Table 5.5.3. Univariable correlation of structural changes showing Spearman correlation coefficient and p-value significance.

		LVMI (g/m$^{2.7}$)	Fractional Shortening	LV Ejection Fraction	Agatston Score	Z-Score cIMT	Distensibility z-score	Z-Score SBP	Z-Score DBP	Presence of Hypertension
cIMT Z-score	Correlation Coefficient	-0.134	-0.040	0.161	-0.046	1.000	.260[**]	0.044	0.071	-0.001
	Sig. (2-tailed)	0.229	0.750	0.183	0.653		**0.009**	0.661	0.481	0.991
	N	83	66	70	98	100	100	100	100	100
CAC (Agatston Score)	Correlation Coefficient	0.192	-0.070	-0.074	1.000	-0.046	-0.186	0.095	-0.073	0.098
	Sig. (2-tailed)	0.086	0.576	0.548		0.653	0.067	0.350	0.478	0.335
	N	81	66	68	98	98	98	98	98	98
LVMI (g/m$^{2.7}$)	Correlation Coefficient	1.000	-0.041	-0.190	0.192	-0.134	-.322[**]	.324[**]	0.144	.387[**]
	Sig. (2-tailed)		0.742	0.123	0.086	0.229	**0.003**	**0.003**	0.195	**0.000**
	N	83	66	67	81	83	83	83	83	83

Table 5.5.4. Univariable correlation of structural changes with routine serum biomarkers showing Spearman correlation coefficient and p-value significance.

		Total Ca (mmol/L)	iCa (mmol/L)	PO4 (mmol/L)	Mg (mmol/L)	ALP (IU/L)	PTH (pmol/L)	PTH ULN (x1->x9)	25OHD (nMol/L)	Bicarbonate (mmol/L)	Creatinine (umol/L)
cIMT z-score	Correlation Coefficient	0.193	0.159	0.052	0.121	.259[**]	-0.126	-0.092	0.154	-0.088	-0.106
	Sig. (2-tailed)	0.054	0.114	0.607	0.229	**0.009**	0.210	0.362	0.130	0.390	0.294
	N	100	100	100	100	100	100	100	98	98	100
CAC (Agatston Score)	Correlation Coefficient	-0.125	-0.098	-0.088	-0.034	0.010	0.124	0.091	-0.085	-0.018	0.171
	Sig. (2-tailed)	0.222	0.336	0.389	0.742	0.925	0.223	0.374	0.410	0.865	0.092
	N	98	98	98	98	98	98	98	96	96	98
LVMI (g/m2.7)	Correlation Coefficient	-0.116	-0.031	-0.017	0.140	-0.200	0.167	0.134	-0.143	-0.089	.257[*]
	Sig. (2-tailed)	0.296	0.778	0.878	0.208	0.069	0.131	0.226	0.199	0.429	**0.019**
	N	83	83	83	83	83	83	83	82	81	83

Table 5.5.5. Univariable correlation of structural changes showing Spearman correlation coefficient and p-value significance.

		Z-Score PWV	Augmentation (mmHg)	Augmentation Index (%)	LCSA/WCSA	Dialysis Vintage (yrs)	Years with eGFR <30	Alfacalcidol (mcg/day)	Vitamin D supp units/kg/day
cIMT Z-score	Correlation Coefficient	0.084	-0.037	0.008	-0.361	0.021	-0.080	0.016	0.133
	Sig. (2-tailed)	0.404	0.718	0.940	**<0.0001**	0.858	0.426	0.889	0.187
	N	100	100	100	100	77	100	82	100
CAC (Agatston Score)	Correlation Coefficient	-0.006	-0.028	-0.045	-0.061	0.149	0.029	0.104	-0.055
	Sig. (2-tailed)	0.956	0.782	0.659	0.549	0.201	0.776	0.358	0.589
	N	98	98	98	98	75	98	80	98

LVMI (g/m2.7)	Correlation Coefficient	0.179	0.120	0.111	-0.047	0.060	0.047	-0.031	0.026
	Sig. (2-tailed)	0.105	0.280	0.318	0.671	0.644	0.675	0.804	0.814
	N	83	83	83	83	62	83	67	83

Structural Measures

1. Carotid intima-media thickness

The cIMT z-scores were high across the entire study population, and there was no evidence of a difference between dialysis and CKD cohorts. Serum ALP levels correlated with cIMT z-scores (r=0.26, p=0.009). There were no independent associations of cIMT z-scores on multivariable analyses (Table 5.5.6).

Table 5.5.6. Summary of regression model with cIMT z-score as the dependent variable

Model Summary				
Model	R	R Square	Adjusted R Square	Std. Error of the Estimate
1	.215ᵃ	.046	.005	1.04

a. Predictors: (Constant), 25OHD (nMol/L), Alk P, Total Ca, CKD/Dial

Model		Unstandardized Coefficients		Standardized Coefficients	t	Sig.	95.0% Confidence Interval for B	
		B	Std. Error	Beta			Lower Bound	Upper Bound
1	(Constant)	-.147	1.636		-.090	.929	-3.395	3.101
	Total Calcium	.770	.653	.121	1.178	.242	-.528	2.068
	Alkaline Phosphatase	.000	.001	-.029	-.281	.780	-.001	.001
	25OHD (nMol/L)	.003	.002	.166	1.554	.124	-.001	.007
	CKD/Dial	.005	.261	.002	.019	.985	-.513	.523

a. Dependent Variable: Z-Score cIMT

2. Coronary artery calcification

Ten participants (9 on dialysis and 1 in CKD) had CAC; the Agatston score ranged from 0.8 to 412.6. There were no significant correlations between Agatston score and other vascular measures or serum biomarkers. There was no difference

between those with CAC and those without in terms of age, time on dialysis or

serum biomarkers, and the presence of CAC did not correlate with other vascular

measures (Table 5.5.7).

Table 5.5.7. Between group differences for the participants with and without coronary
artery calcification (CAC), in terms of characteristics, vascular measures and routinely
measured serum biomarkers.

	With CAC (n=10, median, IQR)	Without CAC (n=90, median, IQR)	Between group comparison (p-value)
Age (yrs)	18.94 (9.52 to 24.62)	13.5 (10.54 to 16.00)	0.16
Dialysis Vintage (yrs)	3.64 (1.22 to 10.18)	2.35 (0.70 to 5.06)	0.24
Years with eGFR<30 (yrs)	6.67 (1.06 to 13.25)	5.58 (2.06 to 10.01)	0.84
Vascular measures			
cIMT (z-score)	1.45 (1.01 to 3.06)	2.21 (1.12 to 2.88)	0.63
cfPWV (z-score)	0.89 (-0.30 to 2.93)	1.48 (-0.16 to 2.58)	0.84
Carotid distensibility (z-score)	-1.47 (-2.42 to -0.27)	-1.08 (-2.13 to -0.14)	0.51
Serum biomarkers			
Total calcium (mmol/L)	2.38 (2.18 to 2.65)	2.47 (2.39 to 2.56)	0.30
Ionized calcium (mmol/L)	1.16 (1.06 to 1.26)	1.21 (1.13 to 1.29)	0.42
Phosphate (mmol/L)	1.38 (1.19 to 1.76)	1.56 (1.34 to 1.87)	0.33
Magnesium (mmol/L)	1.03 (0.94 to 1.05)	1.03 (0.91 to 1.15)	0.66

ALP (IU/L)	168 (99 to 635)	184 (120 to 260)	0.89
PTH (pmol/L)	16.5 (7.25 to 204.30)	16.20 (6.05 to 48.55)	0.27
PTH ULN (x1 to >x9)	x3 (x2 to x9)	x3 (x1 to x8.25)	0.43

cfPWV (carotid femoral pulse wave velocity), cIMT (carotid Intima Media Thickness), ALP (Alkaline phosphatase), PTH (Parathyroid Hormone), ULN (Upper limit of normal)

3. Left ventricular mass index

LVMI was higher in dialysis patients compared to CKD (p= 0.01). LVMI correlated with HTN (r=0.39, p<0.001) and distensibility (r=-0.32, p=0.003). On multivariable regression, LV ejection fraction (β=-0.39, p=0.001), CAC Agatston score (β=0.25, p=0.02) and HTN (β=0.40, p<0.0001) were independent associations of LVMI (R^2 0.35) (Table 5.5.8).

Table 5.5.8. Summary of regression model with left ventricular mass index as the dependant variable

Model Summary				
Mode l	R	R Square	Adjusted R Square	Std. Error of the Estimate

1	.647[a]	.419	.347	10.09539

a. Predictors: (Constant), LVEF, Agatston Score, PWV z-score, distensibility z-score, Hypertension, Alkaline phosphatase, CKD/Dial

Model		Unstandardized Coefficients		Standardized Coefficients	t	Sig.	95.0% Confidence Interval for B	
		B	Std. Error	Beta			Lower Bound	Upper Bound
1	(Constant)	77.919	13.263		5.875	.000	51.361	104.477
	ALP	-.005	.005	-.095	-.920	.361	-.016	.006
	Agatston Score	.068	.029	.250	2.384	.020	.011	.126
	Distensibility (z-score)	1.192	1.007	.126	1.183	.242	-.825	3.209
	PWV (z-score)	-1.096	.751	-.161	-1.460	.150	-2.601	.408
	LVEF	-.665	.188	-.389	-3.531	.001	-1.043	-.288
	Hypertension	10.758	2.864	.400	3.757	.000	5.024	16.493
	CKD/Dial	3.032	3.249	.103	.933	.355	-3.474	9.537

a. Dependent Variable: LVMI (g/m$^{2.7}$)

21.7% of patients had an LVMI> 95th centile. In the participants with LVMI >95th centile, 61.1% showed concentric hypertrophy with RWT >95th centile, and 38.9% eccentric hypertrophy. 14.5% had RWT above the 95th centile. Of the patients with a high RWT, 58.3% had LVMI >95th centile. Therefore, 41.6% showed evidence of cardiac remodelling without a significant increase in LVMI.

Functional Measures

1. Carotid distensibility

The carotid distensibility z-score was lower in patients on dialysis compared to CKD [-1.46 (-2.29, -0.30) vs -0.39 (-1.34,0.47), p=0.009]. The carotid distensibility z-score correlated with the number of years with an eGFR below 30ml/min/1.73m^2 (r=-0.22, p=0.03), SBP z-score (r=-0.25, p=0.01), iCa (r=0.21, p=0.03) and 25OHD (r=0.28, p=0.006) (Tables 5.5.9 & 5.5.10).

Table 5.5.9 Univariable correlation of functional changes with each other, and medication

intake showing Spearman correlation coefficient and p-value significance

		PWV z-score	Distensibility z-score	LCSA/WCSA	Augment ation (mmHg)	Augme ntation Index (%)	Dialysis Vintage (yrs)	Years eGFR <30	Alfacalcidol (mcg/day)	VitD/kg /day	SBP z-score	DBP z-score	HTN
Z-Score PWV	Correlation Coefficient	1.000	-0.166	-0.011	-0.059	-0.094	0.004	-0.068	0.052	0.052	.412**	.391**	.260**
	Sig. (2-tailed)		0.100	0.916	0.561	0.351	0.973	0.504	0.646	0.611	**0.000**	**0.000**	**0.009**
	N	100	100	100	100	100	77	100	82	100	100	100	100
Distensibility z-score	Correlation Coefficient	-0.150	1.000	0.282	0.009	0.112	-0.021	-.217**	0.123	-0.054	-0.252	0.044	-0.049
	Sig. (2-tailed)	0.136		**0.004**	0.931	0.267	0.855	**0.030**	0.271	0.594	**0.011**	0.665	0.631
	N	100	100	100	100	100	77	100	82	100	100	100	100
Carotid dilatation	Correlation Coefficient	-0.011	.282**	1.000	-0.113	-0.134	-.230*	0.000	0.099	-0.074	0.047	0.164	0.245
	Sig. (2-tailed)	0.916	**0.004**		0.264	0.184	**0.045**	0.999	0.376	0.467	0.643	0.104	**0.014**
	N	100	100	100	100	100	77	100	82	100	100	100	100
Augmentation	Correlation Coefficient	-0.059	-0.063	-0.113	1.000	.935**	0.081	0.049	-0.034	-0.106	-0.113	.219*	.198*
	Sig. (2-tailed)	0.561	0.537	0.264		**0.000**	0.483	0.628	0.765	0.295	0.264	**0.029**	**0.048**
	N	100	100	100	100	100	77	100	82	100	100	100	100
Augmentation Index	Correlation Coefficient	-0.094	0.061	-0.134	.935**	1.000	0.105	-0.017	-0.011	-0.092	-0.134	0.117	0.157
	Sig. (2-tailed)	0.351	0.546	0.184	**0.000**		0.363	0.865	0.924	0.362	0.184	0.247	0.120
	N	100	100	100	100	100	77	100	82	100	100	100	100

Table 5.5.10 Univariable correlation of functional changes with routine serum biomarkers

showing Spearman correlation coefficient and p-value significance

		Total Ca (mmol/L)	iCa (mmol/L)	PO4 (mmol/L)	Mg (mmol/L)	Alk P (IU/L)	PTH (pmol/L)	PTH ULN (x1-x9)	25OHD (nMol/L)	bicarbonate (mmol/L)	creatinine (umol/L)
Carotid Dilatation	Correlation Coefficient	-0.167	0.010	0.042	-0.172	-0.113	-0.002	-0.031	0.160	0.054	-0.123
	Sig. (2-tailed)	0.097	0.923	0.676	0.087	0.265	0.981	0.756	0.117	0.597	0.224
	N	100	100	100	100	100	100	100	98	98	100
PWV z-score	Correlation Coefficient	-0.029	-0.049	0.123	-0.032	-0.054	0.068	0.072	-0.192	0.175	0.127
	Sig. (2-tailed)	0.775	0.631	0.225	0.749	0.597	0.499	0.478	0.058	0.085	0.209
	N	100	100	100	100	100	100	100	98	98	100
Distensibility z-score	Correlation Coefficient	0.166	.214*	-0.059	0.077	0.173	-0.172	-0.010	.276**	-0.077	-.312**

	Sig. (2-tailed)	0.099	**0.033**	0.561	0.445	0.086	0.088	0.918	**0.006**	0.450	**0.002**
	N	100	100	100	100	100	100	100	98	98	100
	Sig. (2-tailed)	0.801	0.273	0.248	0.821	0.153	0.408	0.293	**0.006**	0.093	**0.018**
	N	100	100	100	100	100	100	100	98	98	100
Augmentation (mmHg)	Correlation Coefficient	-0.175	0.034	0.023	0.027	0.067	.221[*]	0.206	-0.089	0.123	0.067
	Sig. (2-tailed)	0.081	0.738	0.823	0.791	0.508	**0.027**	**0.040**	0.382	0.228	0.505
	N	100	100	100	100	100	100	100	98	98	100
Augmentation Index (%)	Correlation Coefficient	-0.104	0.036	0.006	0.084	0.135	0.160	0.146	-0.044	0.069	0.024
	Sig. (2-tailed)	0.304	0.722	0.957	0.408	0.182	0.112	0.146	0.666	0.502	0.811
	N	100	100	100	100	100	100	100	98	98	100

On multivariable analysis, SBP z-score was the strongest independent predictor of distensibility (β=-0.33, p=0.002; Table 5.5.11). Being on dialysis (vs being in CKD4-5) was also an independent predictor of reduced distensibility (β= -0.22, p=0.03, Model 1 R^2= 0.27; Table 5.5.11). When replacing the binary CKD/Dialysis with years with a eGFR<30ml/min/1.73m2, this was also significant (β-0.26, p=0.01, Model 2 R^2 0.28).

Table 5.5.11 Regression model with distensibility z-score as the dependant variable

Model Summary				
Model	R	R Square	Adjusted R Square	Std. Error of the Estimate
1	.576[a]	.332	.272	17.73574
a. Predictors: (Constant), CKD/Dial, Alk P, Z-Score PWV, iCa++, carotid dilatation , 25OHD (nMol/L), Z-Score SBP, PTH (pmol/L)				
2	.589[a]	.346	.288	17.54037
a. Predictors: (Constant), Years with eGFR <30, Alk P, Z-Score PWV, iCa++, carotid dilatation , 25OHD (nMol/L), Z-Score SBP, PTH (pmol/L)				

Model		Unstandardized Coefficients		Standardized Coefficients	t	Sig.	95.0% Confidence Interval for B	
		B	Std. Error	Beta			Lower Bound	Upper Bound
1	(Constant)	5.625	16.590		.339	.735	-27.339	38.589
	SBP	-6.111	1.873	-.331	-3.263	.002	-9.833	-2.389
	PTH (pmol/L)	-.014	.039	-.039	-.349	.728	-.092	.064

		B	Std. Error	Beta	t	Sig.	Lower	Upper
	iCa++	4.653	7.671	.058	.607	.546	-10.589	19.894
	25OHD (nMol/L)	.038	.036	.105	1.070	.287	-.033	.110
	ALP	.005	.011	.047	.448	.655	-.016	.026
	Carotid dilatation	13.007	4.509	.263	2.884	.005	4.047	21.967
	PWV (z-score)	.352	.905	.036	.389	.698	-1.447	2.151
	CKD/Dial	-10.550	4.765	-.216	-2.214	.029	-20.018	-1.082
2	(Constant)	-5.064	15.041		-.337	.737	-34.951	24.822
	Z-Score SBP	-6.398	1.840	-.347	-3.477	.001	-10.054	-2.741
	PTH (pmol/L)	.005	.040	.013	.114	.909	-.076	.085
	iCa++	4.667	7.584	.058	.615	.540	-10.403	19.737
	25OHD (nMol/L)	.064	.035	.175	1.821	.072	-.006	.134
	Alk P	.010	.011	.096	.904	.368	-.011	.030
	LCSA/WCSA	15.004	4.360	.304	3.441	.001	6.341	23.667
	Z-Score PWV (age)	.139	.887	.014	.157	.876	-1.624	1.902
	Years eGFR <30	-1.047	.396	-.260	-2.647	.010	-1.833	-.261

a. Dependent Variable: Distensibility coefficient

2. *Carotid-femoral pulse wave velocity and pulse wave augmentation*

The median cfPWV z-score was 1.45 (-0.16 to 2.57) and higher in dialysis than CKD patients (1.52 vs 0.61; p=0.03). cfPWV z-scores correlated with SBP and DBP z-scores (r=0.41, p<0.0001 & r=0.39, p<0.0001 respectively), as well as presence of HTN (r=0.26, p=0.009). There were no independent associations of cfPWV z-scores on multivariable regression, with only DBP z-score approaching significance (β=0.26, p=0.056) (Table 5.5.12).

Table 5.5.12. Regression model with PWV z-score as the dependent variable

Model Summary				
Model	R	R Square	Adjusted R Square	Std. Error of the Estimate
1	.427[a]	.182	.127	2.01020

a. Predictors: (Constant), Z-Score DBP, Distensibility, bicarbonate, 25OHD (nMol/L), CKD/Dial, Z-Score SBP

Model		Unstandardized Coefficients		Standardized Coefficients	t	Sig.	95.0% Confidence Interval for B	
		B	Std. Error	Beta			Lower Bound	Upper Bound
1	(Constant)	-1.963	1.719		-1.142	.257	-5.378	1.453
	CKD/Dial	.434	.549	.087	.791	.431	-.656	1.525
	Distensibility	.002	.012	.020	.168	.867	-.022	.026
	25OHD (nMol/L)	-.003	.004	-.083	-.819	.415	-.011	.004
	bicarbonate (mmol/L)	.109	.062	.175	1.760	.082	-.014	.231
	Z-Score SBP	.253	.288	.129	.878	.382	-.320	.826
	Z-Score DBP	.605	.313	.263	1.935	.056	-.016	1.227

a. Dependent Variable: Z-Score PWV

There was no difference between dialysis and CKD stages 4-5 for augmentation or AIx. Augmentation was associated with DBP z-score (r=0.22, p=0.03) and HTN (r=0.20, p=0.048). Presence of HTN was an independent association of augmentation (β=0.28, p=0.02, R^2=0.05) (Table 5.5.13). AIx had no correlates or independent associations on multivariable regression.

Table 5.5.13. Regression model with Augmentation as the dependant variable

Model Summary				
Model	R	R Square	Adjusted R Square	Std. Error of the Estimate
1	.309[a]	.096	.048	5.58713

a. Predictors: (Constant), PTH (xULN), Z-Score DBP, CKD/Dial, Total Ca, Hypertension

Model		Unstandardized Coefficients		Standardized Coefficients	t	Sig.	95.0% Confidence Interval for B	
		B	Std. Error	Beta			Lower Bound	Upper Bound
1	(Constant)	11.006	9.737		1.130	.261	-8.326	30.339
	CKD/Dial	-1.972	1.524	-.146	-1.294	.199	-4.997	1.054
	Z-Score DBP	-.947	.699	-.158	-1.355	.179	-2.335	.440
	Hypertension	3.556	1.521	.280	2.338	.022	.536	6.576
	Total Ca	-1.496	3.820	-.044	-.392	.696	-9.080	6.088
	PTH (xULN)	.306	.214	.174	1.425	.158	-.120	.731

a. Dependent Variable: Augmentation

Prevalence of abnormal structural and functional CV measures

The percentages of CKD stages 4-5 and dialysis patients with structural and functional measures above 2SD are summarised in *Table 5.5.14*. There was no difference in the prevalence of structural abnormalities between the CKD and dialysis cohorts (p=0.43). Patients on dialysis had a higher functional abnormalities score compared to the CKD cohort (p=0.046). The odds of having any structural or functional abnormality was 17.3 times higher in the dialysis compared to CKD cohort (95% CI 5.28 to 53.52, p<0.0001; sensitivity 64.00% [44.52 to 79.75%],

specificity 90.67% [81.97 to 95.41%]). Overall, the presence of more than one

structural abnormality increased the odds of more than one functional abnormality

by 4.5-fold (95% CI 1.27 to 16.59, p=0.045; sensitivity 88.76% [80.54 to 93.78%],

specificity 36.36% [15.17 to 64.62%]).

Table 5.5.14. Structural and functional abnormalities scores depicting the proportion of

CKD and dialysis patients with vascular measures above 2 standard deviations from the

mean or the 95th centile

| Vascular measures	CKD (n=23)	Dialysis (n=77)	Between group comparison (p-value)
Structural Abnormalities			
cIMT	60.87%	50.65%	0.47
CAC (Presence of)	4.35%	11.69%	0.44
LVMI (g/m$^{2.7}$)	4.76%	27.42%	**0.03**
Total Structural Score 0/1/2/3 (%)	39.13/52.17/8.70/0.0	32.47/51.95/14.29/1.30	0.43
Functional Abnormalities			
Distensibility (< -2 SD)	13.04%	36.36%	**0.04**
cfPWV	30.43%	38.96%	0.47
Total Functional Score 0/1/2 (%)	60.87/34.78/4.35%	37.65/49.35/13.00%	**0.046**

CAC, coronary artery calcification; cIMT, carotid intima media thickness; LVMI, left ventricular mass index; RWT, relative wall thickness; cfPWV, carotid femoral pulse wave velocity; HTN, hypertension

The role of arterial dilatation

Carotid dilatation (LCSA/WCSA ratio) was lower in the dialysis cohort compared to those in CKD stages 4-5 (2.98 vs 3.22, p=0.006), and correlated with dialysis vintage (r=-0.23, p=0.045), cIMT z-scores (r=0.36, p<0.0001), HTN (r=0.25, p=0.01), and distensibility (r=0.28, p=0.004). Distensibility and HTN were independent associations (β=0.29, p=0.004 and β=0.25, p=0.03 respectively, R^2= 0.19)
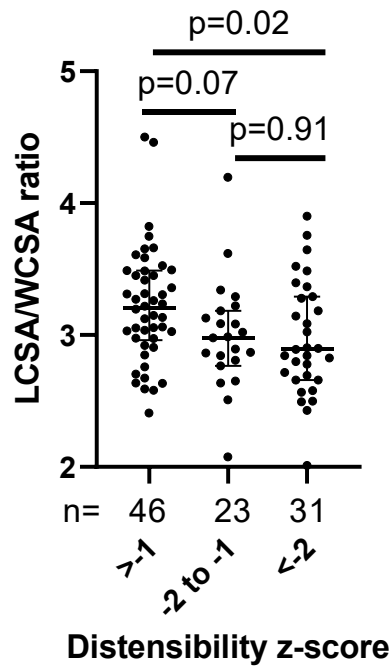
The carotid dilatation was lower in patients with cIMT z-scores >2 SD compared to <1 SD [2.91 (2.66 to 3.29) vs 3.33(2.95 to 3.72), p=0.003] (Figure 5.5.1). The same is true if comparing patients with cIMT z-scores <2SD and >2SD [3.18 (2.89 to 3.49) vs 2.91 (2.66 to 3.29), p=0.006]. Changes in carotid dilatation were not attributable to higher WCSA or lower LCSA in isolation, as there was no difference in LCSA or WCSA between those with cIMT<1, 1-2 and >2SD for either measure (p=0.07 and p=0.76 respectively).

Figure 5.5.1 LCSA/WCSA ratios for patients according to cIMT z-scores. Lines on figures depict median and IQR. cIMT, carotid intima media thickness; LCSA, carotid lumen cross sectional area; WCSA, carotid wall cross sectional area

Figure 5.5.2 LCSA/WCSA ratios for patients according to distensibility z-scores. Lines on figures depict median and IQR. LCSA, carotid lumen cross sectional area; WCSA, carotid wall cross sectional area
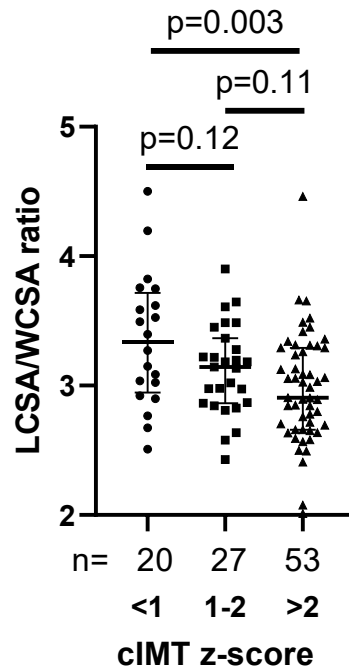
The carotid dilatation was significantly lower in patients with impaired arterial distensibility (below -2SD) than those with distensibility > -1 SD [2.89 (2.66 to 3.29) vs 3.21 (2.96 to 3.49), p=0.02] (Figure 5.5.2), without corresponding changes in cIMT z-score [1.80 (1.14 to 2.93) vs 2.31 (0.99 to 2.88), p=0.82]. Carotid dilatation was greater in those with HTN compared to those without HTN [3.30 (2.94 to 3.51) vs 2.98 (2.77 to 3.27), p=0.02. There was no difference in carotid dilatation between those with LVMI>95th centile and those without [3.14 (2.72 to 3.39) vs 3.08 (2.82 to 3.38), p=0.72].

Distensibility z-score

5.6 Discussion

In this chapter I have shown that subclinical CV abnormalities/changes are significantly prevalent in children and young adults with stages CKD4-5 and on dialysis, with up to 69.5% of CKD and 88.3% of dialysis patients having at least one structural or functional CV abnormality. This is the first study in a young CKD cohort, to the best of my knowledge, examining structural and functional CV abnormalities, with a comprehensive panel of surrogate vascular measures including CAC.

The prevalence of structural abnormalities did not differ between non-dialysis and dialysis cohorts, but functional abnormalities were more prevalent in patients on dialysis. The presence of more than one structural abnormality increased the odds of more than one functional abnormality 4.5-fold. These data highlight the burden of subclinical CVD even in a young cohort of CKD4-5 and

dialysis patients, stressing the importance of preventative strategies to halt the development or attenuate the progression of CVD in CKD. Also, the results suggest that there may be a temporal association between early structural changes that progress to functional CVD abnormalities when potential compensatory mechanisms, such as carotid dilatation that preserve vessel patency even in the presence of wall thickening, are overwhelmed; larger longitudinal studies are needed.

Substantial structural CV changes were evident in this cohort, with a high cIMT z-score in 53% and presence of CAC in 10%. The prevalence of CAC in this patient group is lower than previous published studies (Shroff et al., 2007, Civilibal et al., 2006, Oh et al., 2002), but the prevalence of CAC remains a concern as it is shown to be a significant predictor of major adverse cardiovascular events and mortality, due to its direct effect on myocardial perfusion (Mitchell et al., 2018, Bashir et al., 2015), and once coronary calcification is present, it progresses rapidly. In this young cohort, patients on dialysis had higher age-adjusted vascular stiffness measures compared to the CKD cohort, indicating a greater prevalence of functional CVD. Both the carotid distensibility z-score as well as cfPWV z-score were above normal, implying that arterial stiffness was present in multiple vascular beds. Whilst dialysis *per se* was independently associated with reduced distensibility, the years with a low eGFR (<30ml/min/1.73m^2) was also an independent predictor of vessel stiffness, implying cumulative cardiovascular damage due to prolonged exposure to the uraemic milieu or dialysis treatment may be deleterious. Aortic stiffness, as assessed by cfPWV, is an independent predictor of progression to dialysis and

mortality in adult patients with CKD stages 2 to 5 (Karras et al., 2012, Townsend et al., 2018).

We examined the structural and functional abnormalities separately, but the carotid dilatation (LCSA/WCSA ratio) offers a way of assessing structural and functional changes simultaneously. Here I have shown that the carotid dilatation was lower in patients with high cIMT z-scores (>2SD), but this was not due to WCSA increase or LCSA decrease alone. In fact, the LCSA did not differ between patients with cIMT z-scores of <1, 1-2 and >2 SD. This raises the possibility that vessel patency is maintained by arterial dilatation as a compensatory mechanism for increased cIMT early in the process of arterial wall thickening, but that there exists a physical limit, beyond which the capacity to dilatate is overwhelmed. This is also demonstrated by the fact that the patients with poor carotid distensibility (z-score below -2 SD) had lower dilatation compared to patients with distensibility above -1 SD. The cIMT z-scores did not correlate with distensibility, indicating that the dilatation is a separate mechanism to the structural changes that occur.

The arterial tree functions as a network of conduits, but it also acts as a temporary reservoir for the cardiac output (Azukaitis et al., 2020). Elastic properties of the arteries are due to the presence of elastin fibres. Elasticity of the vessels is a non-linear property however. At lower pressures, elastin-distensible fibres bear the tension but at higher pressures, elasticity is sustained by collagen fibres (which are less extendible) making the vessel progressively stiffer (London and Pannier, 2010). This loss of distensibility is compensated, in part, by dilatation of the arteries (London and Pannier, 2010). Above a certain threshold, at which distensibility is

significantly decreased and dilatation is no longer sufficiently compensatory, a rise

in PWV is seen. Arterial stiffening is also observed in the otherwise healthy ageing

population (Laurent et al., 2001) and in disease groups, such as William's syndrome,

wherein elastin mutations affect the elastic extracellular matrix structure of the

arteries (Kozel et al., 2014). Even in people with essential hypertension, arterial

eutrophic remodelling (increasing LCSA/WCSA with static WCSA), highlighting the

dilatation in the context of sustained increased pressure, is associated with vessel

stiffness and functional changes (Briet et al., 2006). In CKD, arterial stiffening is likely

to be a multifactorial process caused by the uraemic environment, inflammation,

oxidative stress, as well as hypertension which all contribute to direct vascular

damage (Azukaitis et al., 2020). The subsequent remodelling is hypertrophic, with

increasing WCSA due to cIMT changes, as well as increasing LCSA/WCSA (London,

2018). In turn, arterial stiffness increases the cardiac afterload, leading to LV

remodelling (Ohyama et al., 2016). The structural changes, such as cIMT increase

and subsequent stiffening begin in early CKD stages, and functional abnormalities

due to remodelling occur in later stages with progression of CVD (Litwin et al.,

2005). This may be evident in this cohort as years spent with a low eGFR was a

significant negative predictor of carotid distensibility.
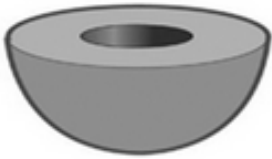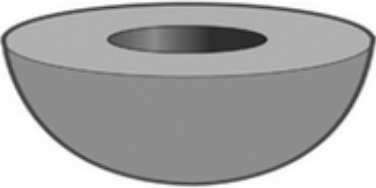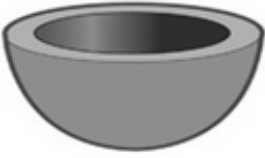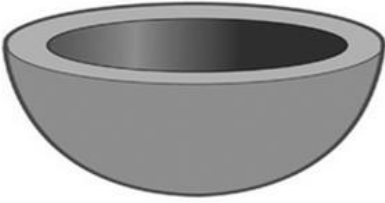
Few other studies have examined structural and functional abnormalities

separately in young people with CKD (Tawadrous et al., 2012). Litwin et al showed

that there is an increase in IMT in early stages of CKD preceding arterial stiffening

(Litwin et al., 2005). The authors compared 55 young people, aged 10 to 20 years

old, in CKD stages 2 to 4, 37 on dialysis and 34 post kidney transplant (GFR 73+/-

31ml/min/1.73/m^2) to 270 healthy controls. The cIMT, WCSA and LCSA were all

significantly increased in kidney patients, and particularly in dialysis patients, compared to controls. The cIMT was significantly lower in both CKD and post-transplant patients compared to young people on dialysis. Therefore, post renal transplantation, the cIMT potentially decreases, whereas the arterial dilatation does not, suggesting that the structural and functional changes are associated but not inextricably linked (Litwin et al., 2005). Briet et al studied 95 patients, aged 58 +/- 15 years, with CKD, 121 hypertensive patients (59 +/- 11 years) without CKD and 57 normotensive healthy controls. In adult patients with mild to moderate CKD, carotid diameter was larger than age and sex adjusted hypertensive and non-hypertensive controls (6.32±1.05, 5.84±0.74, and 5.50±0.64 mm^3, respectively; p<0.001) (Briet et al., 2006). The same was true of carotid compliance (compliance=arterial cross sectional area change/local pulse pressure), (CKD vs hypertensive patients, p<0.001) but carotid distensibility was lower, indicating that, in this study by Briet et al, arterial diameter increase appears to serve as a compensatory mechanism to maintain perfusion (Briet et al., 2006); This temporal association of structural changes with functional abnormalities needs to be elucidated further. It may serve as a potential surrogate marker for disease progression and effect monitoring, as well as a treatment target.

I collected echocardiography data for this cohort in order to examine the extent of the presence of LVH. The American Society of Echocardiography has a classification system for cardiac remodelling based on left ventricular mass and relative wall thickness (RWT; the posterior wall measurement times 2, divided by the LV end diastolic diameter)(Lang et al., 2005). The measurements can then be compared against the normal values for children and adults to determine if normal

or abnormal (de Simone et al., 2005, Devereux et al., 1986, Gjesdal et al., 2011).
Dependent on the left ventricular muscle mass and the RWT, the heart can be classified into having: normal geometry, concentric remodelling, concentric hypertrophy or eccentric hypertrophy (Figure 4.6.1). Cardiac remodelling has been associated with adverse cardiovascular events in the general population (Gjesdal et al., 2011), and it is known that abnormal LV geometry is common in CKD (Mitsnefes et al., 2003), with impaired systolic mechanical function in a significant proportion (Chinali et al., 2015).

Figure 5.6.1 Patterns of cardiac remodelling according to left ventricular mass and relative wall thickness. Adapted from (Gjesdal et al., 2011)

	No LV hypertrophy	LV hypertrophy
Increased Mass to Volume Ratio		
Normal Mass to Volume Ratio		

In this cohort, a fifth of patients had LVMI>95th centile (21.7%), of which almost 40% with present as eccentric hypertrophy. Over 40% of patients with evidence of cardiac remodelling did not meet criteria for LVH. In the 4C study, a prospective multicentre longitudinal follow-up of over 700 children with CKD stages 3-5 and on dialysis, a third of patients had LVH, but an additional 26% of the cohort showed cardiac remodelling even with normal LV mass (Schaefer et al., 2017). In a sub-study of 272 children, detailed echocardiographic analysis showed 55% had LVH, and concentric hypertrophy in 65% of those with LVH. Despite the high prevalence of cardiac geometric remodelling, all the patients had a normal ejection fraction (>56%); the authors speculate that concentric hypertrophy may not be a compensatory effect but a reflection of structural alterations of the myocardium showing impaired contraction (Chinali et al., 2015).

This study is limited by the absence of ambulatory assessment of BP. A single office-based manual BP measurement in clinic or prior to a dialysis session was taken (the best of three measurements as per Flynn et al (Flynn et al., 2017)). Even though masked hypertension is unlikely if 'office'/outpatient BP is in the low normal range (Mitsnefes et al., 2016), 28% of our cohort was defined as hypertensive. The cross sectional design of the study does not allow explanation of the role HTN in any detail as a cause or effect of structural and functional changes in this cohort. The likely bi-directional effect of HTN on arterial stiffness in the general as well as the CKD population has been explored extensively (Safar, 2018).

For this cross-sectional analysis I used only single time-point measurements of serum biomarkers, which may explain why there were no associations between

CKD-MBD biomarkers and vascular measures. All the young adults in this cohort were on dialysis, so CVD changes in adult onset CKD could not be studied. Z-scores were used to express all vascular measures, to enable comparison across the age range.

5.7 Conclusion

In summary, this cross-sectional element of the study shows a high prevalence of subclinical CVD in children and young adults with CKD and on dialysis. The prevalence of structural changes including cIMT increase and CAC were comparable in CKD and dialysis cohorts, but indices of arterial stiffness were higher in patients on dialysis, perhaps having developed when compensatory mechanisms such as arterial dilatation are overwhelmed. Further larger longitudinal studies will be required to define the trajectory of CV changes in children and young adults with CKD in order to identify early intervention strategies.

Chapter 6

Bone Mineral Density and Vascular Calcification in Children and Young Adults with CKD stages 4-5 or on dialysis

In this chapter I have described the longitudinal bone and vascular changes seen in the cohort of children and young adults with CKD or on dialysis. I have examined the relationship between bone, vessel and growth.

The work in this chapter has been published in: Lalayiannis AD, Crabtree NJ, Ferro CJ, Wheeler DC, Duncan ND, Smith C, Popoola J, Varvara A, Mitsioni A, Kaur A, Sinha MD, Biassoni L, McGuirk SP, Mortensen KH, Milford DV, Long J, Leonard MD, Fewtrell M, Shroff R. **Bone Mineral Density and Vascular Calcification in Children and Young Adults With CKD 4 to 5 or on Dialysis**. Kidney International Reports. 2022 Nov 2;8(2):265-273. doi: 10.1016/j.ekir.2022.10.023

In line with UCL policy, I declare that I collected and analysed the data and wrote the original manuscript. The co-authors very kindly helped with editing and proof-reading.

6.1 Abstract

Introduction

Older adults with chronic kidney disease (CKD) can have low bone mineral density (BMD) with concurrent vascular calcification. It is not known if mineral accrual by the growing skeleton protects young people with CKD from extraosseous calcification. My hypothesis was that children and young adults with increasing BMD do not develop vascular calcification.

Methods

This is a multicenter longitudinal study in children and young people (5-30 years) with CKD stages 4-5 or on dialysis. Cortical (Cort) and trabecular (Trab) BMD were assessed by peripheral quantitative Computed Tomography and lumbar spine BMD by DXA (Dual Energy X-ray Absorptiometry). Vascular calcification was assessed by cardiac CT for coronary artery calcification (CAC) and ultrasound for carotid intima-media thickness (cIMT). Arterial stiffness was measured by pulse wave velocity (PWV) and carotid distensibility. All measures are presented as age- and sex-adjusted z-scores.

Results

One hundred participants (median age 13.82 years) were assessed at baseline and 57 followed-up after a median of 1.45 years. TrabBMDz decreased (-0.26 to -0.38, p=0.01), and there was a non-significant decrease in CortBMDz (-0.47 to -1.13, p=0.09). Median cIMTz and PWVz showed non-significant increase (1.55 to 2.03; p=0.23 and 1.08 to 1.26, p=0.19 respectively). CAC was present in 10% at baseline

and in 10/18 (56%) at follow-up. Baseline TrabBMDz was independently associated with cIMTz (R^2=0.10, β=0.34, p=0.001). An annualised increase in TrabBMDz was an independent predictor of cIMTz increase (R^2=0.48, β=0.40, p=0.03), with 6-fold greater odds of an increase in ΔcIMTz in those with an increase in ΔTrabBMDz [(95%CI 1.88 to 18.35), p=0.003]. Young people that demonstrated statural growth (n=33) had lower ΔTrabBMDz and also attenuated vascular changes compared to those with static growth.

Conclusion

This hypothesis generating study suggests that children and young adults with CKD or on dialysis may develop vascular calcification even as BMD increases. A presumed buffering capacity of the growing skeleton may offer some protection against extraosseous calcification.

6.2 Introduction

The growing skeleton is uniquely vulnerable to impaired mineralisation in chronic kidney disease (CKD), manifesting as bone pain, deformities and a 3-fold higher risk of fractures compared to healthy peers (Moe et al., 2006, Ketteler et al., 2018, Denburg et al., 2016). Just as healthy individuals require calcium (Ca) for skeletal mineralisation (Weaver et al., 2016), young patients with CKD, particularly growing children, who have higher serum Ca levels are shown to have a greater increase in bone mineral density (BMD) (Denburg et al., 2013). On the other hand, patients with CKD, particularly those on dialysis, are at high risk of cardiovascular disease which typically manifests as vascular calcification. High calcium (Ca) intake and serum concentrations have been identified as key modifiable risk factors in the development and progression of vascular calcification (Block et al., 2004).

Decreasing bone mineral density is linked with increasing vascular calcification in older adults with CKD (Malluche et al., 2015, Chen et al., 2016, Cejka et al., 2014). It is not known if bone demineralisation is associated with vascular calcification in children and young adults with CKD. Our current practice is mostly based upon extrapolations from adult studies, but this can be particularly harmful in children, leading to inappropriate treatment with potentially lifelong increase in fracture risk as well as cardiovascular disease. There are no longitudinal studies looking at BMD and vascular calcification simultaneously in children and young adults with CKD. This longitudinal follow-up study, performing a comprehensive assessment of bone and cardiovascular measures in a cohort of children and young

adults with CKD stages 4-5 or on dialysis, aims to address this gap in the literature. My hypothesis was that patients with increasing BMD would not have evidence of vascular calcification.

6.3 Methods

Study Participants

I recruited young people (age 5 to 30 years) with CKD stages 4-5 (estimated glomerular filtration rate <30ml/min/1.73m^2) or on dialysis from 5 pediatric and 4 adult nephrology units. Given that bone mineral accrual continues until the third or fourth decade of life, when peak bone mass is reached (Weaver et al., 2016), young adults up to 30 years of age were included. I excluded patients with: a functioning kidney transplant, genetic bone disease, primary hyperoxaluria, previous bisphosphonate treatment or patients that would not have tolerated the scanning procedures. Informed written consent was obtained from all parents or caregivers and adult participants. Assent was obtained from children where appropriate. Cross-sectional data on bone health (Lalayiannis et al., 2020) and subclinical cardiovascular disease (Lalayiannis et al., 2021a) in this cohort have been published and are included in Chapters 4 and 5.

130 patients were identified and 112 agreed to participate. Twelve participants withdrew consent prior to taking part. One-hundred children and young adults with CKD entered the study and 57 were followed-up after an interval of at least one year.

Investigations Performed

Anthropometry

Height was determined using a fixed wall stadiometer, and weight with a digital scale. Height, weight and body mass index (BMI) measurements were expressed as z-scores.

Serum Biomarkers

Routine serum biomarkers were measured on non-fasting blood samples collected at the study visit or prior to a mid-week hemodialysis session and analysed in the patients' respective hospitals. In addition, monthly serum biomarker measurements were performed as part of routine clinical care. These included serum ionized calcium (iCa), total calcium (Ca), phosphate (P), magnesium (Mg), bicarbonate, intact PTH (iPTH), 25-hydroxyvitamin D (25OHD), and alkaline phosphatase (ALP). iCa was obtained by using Abbott iSTAT (USA) point of care analyser with EG7+ cartridges. Due to different iPTH assays being used (Immulite [*Siemens Healthcare Diagnostics]* and Elecsys 2010 [*Roche Diagnostics*]) at the participants' respective hospitals, results have been expressed and analysed in multiples of the upper limits of normal (ULN).

Bone and vascular imaging

Dual Energy X-ray Absorptiometry

All lumbar spine (LS) DXA scans were performed at the respective research centres according to the manufacturer's protocol. The imaging was obtained according to the International Society for Clinical Densitometry (ISCD) guidelines using General Electric scanners (iDXA or Lunar) (Crabtree et al., 2014). LS DXA z-

scores were expressed as bone mineral apparent density (BMAD z-scores) (Crabtree et al., 2017). As DXA can overestimate areal BMD in shorter people, it is necessary to adjust for height or bone size (Crabtree et al., 2014). BMAD is a widely used method to adjust for size based on bone volume (Crabtree et al., 2017). Young adults' LS DXA z-scores were also adjusted for size and presented as BMAD z-scores (Lalayiannis et al., 2020). Hip DXA was not performed in all participants as this imaging locus is not recommended for BMD estimation in growing children.

Peripheral Quantitative Computed Tomography

A scan of the non-dominant tibia was obtained by pQCT as per manufacturer's instructions and ISCD guidelines (Crabtree et al., 2014, Leonard et al., 2010, Wetzsteon et al., 2011). The 3% metaphyseal and 38% diaphyseal sites were used for image acquisition of trabecular and cortical bone respectively, with results expressed as age-, sex-, race- and height adjusted z-scores derived from a reference dataset of 665 healthy children and young adults ages 5-35 years (Leonard et al., 2010).

I would like to thank Professor Mary Leonard and Dr Jin Long of Stanford University, USA for their assistance in providing the pQCT z-scores.

Carotid Intima Media Thickness (cIMT) and distensibility

cIMT measurements were obtained by ultrasound according to the Mannheim consensus (Touboul et al., 2012). The mean cIMT was calculated as the average IMT measurements of both carotids, 1-2 cm below the bifurcation using automatic software (Vivid iq, GE Healthcare, USA), and analysed offline in a blinded

fashion. M-mode was used for vessel systolic and diastolic diameter. cIMT measurements were expressed as z-scores based on normative data from Doyon et al for children (Doyon et al., 2013) and the interpolation of the difference between 17 and 18 years for adults aged 18 to 30 years (Lalayiannis et al., 2021a).

Cardiac Computed Tomography

Coronary artery calcification was assessed by CT (*Somatom Force; Siemens, Germany* or *GE Discovery 750HD, USA*) using the machines' standard Ca scoring protocol. Prospective ECG triggering was used to obtain images in diastole. Calcification was expressed as Agatston score (Agatston et al., 1990) and analysed offline in a blinded fashion, confirmed independently by two observers (myself and Dr Kristian H. Mortensen, Consultant Cardiac Radiologist) using Syngo Via software (*Siemens, UK*). It was decided *a priori* that a repeat cardiac CT scan would be performed in all patients above 18 years of age but only in children <18 years who had evidence of CAC on their baseline scan in order to minimise radiation exposure to children.

Carotid-Femoral Pulse Wave Velocity (cfPWV) and Pulse Wave Augmentation

cfPWV and pulse wave augmentation index (AIx) were measured with the Vicorder Oscillometric PWV device (*SMART Medical*, *UK*).

Given the wide age range of participants, all age-related bone and cardiovascular measures are presented as z-scores and denoted by 'z' after the respective measure. Z-scores reflect adjustments for age, sex, and/or height based on the changes with growth in the healthy pediatric population, allowing for

comparison across all age groups. Where normative data for young adults was not available (anthropometry, systolic and diastolic BP), z-scores were calculated assuming a maximum age of 20 years. cIMTz and PWVz for young adults aged 18 to 30 were calculated using interpolation of the difference between 17 and 18 years in the reference dataset.

6.4 Statistics

All results are presented as a median with interquartile range (IQR) or number and percentage. All biomarker concentrations were expressed as time-averaged levels over the course of the study. As both the duration and extent of exposure above the ULN for phosphate has been associated with higher morbidity and mortality (Lopes et al., 2020), I chose to express serum phosphate concentrations as an area-under-the-curve (AUC), reflecting the time spent above ULN and the extent to which this threshold was exceeded (mmol*month/L) (Lopes et al., 2020). Bone and cardiovascular measures were expressed as annualised changes as follows:

$$\Delta\ change = \frac{\text{Final Visit Value} - \text{Baseline Visit Value}}{\text{Follow up Time in Years}}$$

As tibial pQCT was the main bone imaging modality, growth was defined as tibial lengthening (>0 cm) between visits. Spearman rank testing was used for univariable correlations and Kruskal-Wallis ANOVA test for non-normally distributed

data with Dunn's correction for multiple comparisons. Paired t-testing was used for 1st and 2nd visit comparisons. Paired Wilcoxon signed rank testing was used to compare the CAC change in Agatston score as these data are non-parametric. Mann-Whitney U tests were used for between group non-parametric comparisons. A series of multivariable linear regression models were built, with the dependent measure [ΔCortBMDz, ΔTrabBMDz, ΔcIMTz, Δdistensibility_z, ΔPWVz and Δaugmentation (Pulse wave augmentation) annualised changes] as the dependent variables. All independent variables with univariable associations of p≤0.15 were included in the multivariable models. Age and sex were not included as dependent variables as z-scores are adjusted for these. Being on dialysis or not was included as a binary dependent variable. Odds ratios (OR) with 95% confidence intervals, and an associated p-value were calculated using Fisher's exact test. SPSS 27 (IBM) was used for all statistical analyses and Prism (GraphPad) to create figures. A two-sided p value of <0.05 was considered to indicate a statistically significant difference.

6.5 Results

Characteristics of the participants

Demographics of the study population at baseline are shown in *Table 6.5.1*. Baseline bone and vascular measures have been presented in Chapters 4 and 5 and are summarised in Table 6.5.2.

Table 6.5.1. Patient characteristics at baseline

	Total (n = 100)	CKD (n = 23)	Dialysis (n = 77)	Between group comparison (p-value)
Age, years	13.82 (10.68, 16.46)	11.46 (6.80, 13.58)	14.25 (11.10, 21.95)	**0.002**
5-18 years, n=(%) 19-30 years, n=(%)	79 (79) 21 (21)	23 (100) 0	56 (73) 21 (27)	0.17 N/A
Sex, Female n=(%)	44	6 (26.1)	38 (49.4)	0.06
Race, n= Caucasian/ Asian/ Black/ Other	52/ 27/ 20/ 1	17/ 4/ 2/ 0	35/ 23/ 18/ 1	**0.03**
Height Z-score	-1.09 (-1.93, -0.36)	-0.84 (-1.60, 0.04)	-1.42 (-2.02, -0.43)	0.06
Weight Z-score	-0.56 (-1.67, 0.20)	-0.21 (-1.02, 0.64)	-0.78 (-1.77, 0.02)	**0.02**
BMI Z-score	0.14 (-0.88, 0.92)	0.52 (-0.66, 1.28)	0.01 (-0.95, 0.83)	0.06
Dialysis modality, n= HD/HDF/home HD/PD	44/ 14/ 3/ 16	N/A	44/ 14/ 3/ 16	N/A
Phosphate binder therapy, n= Calcium based/ Non-calcium based/ Both/ None	39/ 23/ 5/ 33	16/ 1/ 0/ 6	23/ 22/ 5 / 27	N/A
Calcium supplements (n=)	0	0	2	N/A
Total elemental Ca intake from medications (mg/kg/day)	0.00 (0.00, 1.53)	1.09 (0.00, 2.09)	0.00 (0.00, 1.47)	**0.03**
Vitamin D analogs (n=) alfacalcidol / paricalcitol/ calcitriol/ none)	69/6/1/24	21/0/1/1	48/6/0/23	N/A
eGFR (ml/min/1.73m^2)	N/A	13.33 (9.72, 18.05)	N/A	N/A

Years with eGFR<30ml/min/1.73m²	5.58 (2.02, 10.10)	3.68 (1.10, 8.81)	5.63 (2.50, 10.45)	0.09
Dialysis vintage, years	2.51 (0.75, 5.11)	N/A	2.51 (0.75, 5.11)	N/A

All data presented as median (IQR). N/A, not applicable; CAKUT, Congenital

abnormalities of the kidneys and urinary tract; eGFR, estimated glomerular filtration

rate estimated by Schwartz formula (Schwartz et al., 2009) in children under 18

years

Table 6.5.2. Patient bone and vascular measures at baseline

Z-score	Total (n=100)	CKD (n=23)	Dialysis (n=77)	Between group comparison (p-value)
Bone measures (Z-score)				
Lumbar Spine BMAD	0.37 (-0.83 to 1.04)	0.71 (-0.11 to 1.48)	0.20 (-1.21 to 0.93)	**0.01**
Trabecular BMD	0.57 (-1.01 to 1.91)	1.82 (-0.12 to 2.43)	-0.23 (-1.16 to 1.67)	**0.02**
Cortical BMD	-0.35 (-1.57 to 0.29)	-0.15 (-0.47 to 0.31)	-0.72 (-1.9 to 0.28)	**0.04**
Vascular measures (Z-score)				
SBP	0.89 (0.03 to 1.67)	0.40 (-0.10 to 1.13)	0.96 (0.12 to 1.83)	**0.02**
DBP	0.72 (-0.14 to 1.36)	0.50 (-0.18 to 1.11)	0.87 (-0.04 to 1.45)	0.30
cIMT	2.17 (1.14 to 2.86)	2.46 (1.04 to 2.76)	2.01 (1.14 to 2.94)	0.72
PWV	1.45 (-0.16 to 2.57)	0.61 (-0.78 to 2.23)	1.52 (0.28 to 2.81)	**0.03**

Distensibility	-1.11 (-2.17 to -0.15)	-0.39 (-1.34 to 0.47)	-1.46 (-2.29 to -0.30)	**0.009**
CAC (Agatston Score)	range 0 to 412.6 10% had CAC	range 0 to 6.4 mean 0.28 ± SD 1.3 n=1	range 0 to 412.6 mean 11.03± SD 63.4 n=9	0.36

BMAD; Bone mineral apparent density, BMD; bone mineral density, SBP; Systolic BP, DBP; Diastolic BP, cIMT; carotid intima media thickness, CAC; Coronary artery calcification. n=98 participants had Cardiac CT investigation at baseline.

One hundred participants were included at baseline, and fifty-seven patients were followed-up after a median of 1.45 (1.25, 1.81) years. Forty-three patients were not included in the follow-up due to transplantation (n=26, 60.5%), restrictions to research activities during the COVID-19 pandemic (n=16, 32.7%) or death (n=1, 2.3%). Table 6.5.3 outlines the differences between the group of participants followed up, and those lost to follow up. Those lost to follow-up were older (15.84 vs 12.71 years, p=0.003), but otherwise comparable to the cohort studied. Four patients with CKD at baseline visit were started on kidney replacement therapy (1 on home HD and 3 on PD) soon after their baseline visit.

Table 6.5.3. Demographics of patients who completed follow-up or were lost to follow-up

	Total	Follow-up performed	Lost to follow-up	Between group difference

Total, n= (%)	n=100	n=57	n=43	N/A
Age, years 5-19 years, n=(%) 20-30 years, n=(%)	13.82 (10.68, 16.46) 80 (80) 20 (20)	15.84 (12.56, 21.69) 42 (73.68) 15 (26.32)	12.71 (8.75, 15.99) 37 (86.05) 6 (13.95)	**p=0.003**
Sex, Female n=(%)	44 (44)	23 (40.35)	21 (48.84)	0.42
Race, n= Caucasian/ Asian/ Black/ Other	52/ 27/ 20/ 1	27/17/12/1	25/10/8/0	0.26
Renal disease aetiology, n= CAKUT/ Glomerular disease/ Cystic Kidney Diseases/ Vasculitides/ Other	50/ 13/ 10/ 8/ 19	28/9/6/4/10	23/4/4/3/9	0.94
Dialysis modality, n= CKD/HD/HDF/Home HD/PD	23/ 44/ 14/ 3/ 16	12/18/9/7/11	8/18/6/1/10	0.96
Years with eGFR<30ml/min/1.73m^2	5.58 (2.02, 10.10)	7.01 (1.99, 10.28)	4.80 (2.43, 10.00)	0.63
Dialysis vintage, years	2.51 (0.75, 5.11)	3.64 (0.58, 5.57)	2.43 (0.95, 4.72)	0.94

CAKUT; congenital abnormalities of the kidneys and urinary tract

Longitudinal changes in bone measures

On DXA scan there was a significant decrease in LS BMADz [-0.11 (-1.15, 0.76) to -0.60 (-2.04, 0.28), p=0.02]. On pQCT measures both TrabBMDz [-0.26 (-1.17, 1.93) to -0.38 (-1.47, 0.58), p=0.01] and CortBMDz [-0.47 (-1.87, 0.16) to -1.13 (-2.76, -0.13), p=0.26] decreased but the reduction in CortBMDz was not statistically significant (Table 6.5.4). On multivariable regression baseline BMADz (R^2 0.16, β -0.38, p=0.02) was an independent predictor of ΔBMADz (Table 6.5.5).

Table 6.5.4. Bone measures at baseline, follow-up, between visit comparison and annualised difference

Bone Imaging measure Z-scores	At Baseline (n=55)	At Follow-up (n=55)	Between visit difference (p-value)	Annualised difference (n=55)
LS BMAD	-0.11 (-1.15, 0.76)	-0.60 (-2.04, 0.28)	**0.02**	-0.30 (-0.95, 0.35)
Trabecular BMD z-score	-0.26 (-1.17, 1.93)	-0.38 (-1.47, 0.58)	**0.01**	-0.30 (-0.84, 0.40)
Cortical BMD z-score	-0.47 (-1.87, 0.16)	-1.13 (-2.76, -0.13)	0.26	-0.39 (-0.99, 0.56)

LS; Lumbar spine, BMAD; Bone mineral apparent density; BMD, Bone mineral density

Table 6.5.5. Multivariable linear regression with ΔBMAD as dependent variable

Model Summary				
Model	R	R Square	Adjusted R Square	Std. Error of the Estimate
1.00	0.49[a]	0.24	0.16	0.81

a. Predictors: (Constant), iPTH, Baseline BMAD, Mg, CKD/Dialysis

Model		Unstandardized Coefficients		Standardized Coefficients	t	Sig.	95.0% Confidence Interval for B	
		B	Std. Error	Beta			Lower Bound	Upper Bound
1.00	(Constant)	2.06	0.89		2.32	0.03	0.26	3.86

CKD/Dialysis	-0.56	0.34	-0.29	-1.65	0.11	-1.25	0.13
Baseline BMAD	-0.20	0.08	-0.38	-2.43	0.02	-0.37	-0.03
Mg	-1.35	0.90	-0.23	-1.50	0.14	-3.17	0.47
iPTH	0.00	0.01	-0.03	-0.18	0.86	-0.01	0.01

BMAD; Bone mineral apparent density, Mg; magnesium

ΔTrabBMDz inversely correlated with both total Ca (r=-0.37, p=0.006) and iCa (r=-0.45, p=0.01). ΔTrabBMDz correlated negatively with vitamin D analog treatment (r=-0.31, p=0.02). On multivariable regression, the only independent association with ΔTrabBMDz was TrabBMDz at baseline (R^2 0.53, β -0.69, p<0.0001; Table 6.5.6).

Table 6.5.6. Annualised trabecular bone mineral density z-score change multivariable linear regression

Model Summary				
Model	R	R Square	Adjusted R Square	Std. Error of the Estimate
1.00	0.80[a]	0.63	0.53	0.69
a. Predictors: (Constant), Alkaline phosphatase, Magnesium, Baseline Trabecular BMD, CKD/Dialysis, annualised Cortical BMD change, ionized Calcium				

Model		Unstandardized Coefficients		Standardized Coefficients	t	Sig.	95.0% Confidence Interval for B	
		B	Std. Error	Beta			Lower Bound	Upper Bound
1.00	(Constant)	5.28	3.82		1.39	0.18	-2.63	13.20

CKD/Dialysis	0.15	0.31		0.07	0.47	0.64	-0.50	0.79
Baseline Trabecular BMD	-0.31	0.06		-0.69	-5.04	<0.0001	-0.44	-0.18
Annualised cortical BMD change	0.29	0.17		0.28	1.72	0.10	-0.06	0.64
ionized Calcium	-4.87	2.92		-0.31	-1.67	0.11	-10.92	1.17
Magnesium	0.53	1.33		0.06	0.39	0.70	-2.24	3.29
Alkaline Phosphatase	0.00	0.00		-0.02	-0.12	0.91	0.00	0.00

ΔCortBMDz correlated positively with both total Ca (r=0.30, p=0.03) and iCa (r=0.37, p=0.04). iCa and baseline CortBMDz were significant independent predictors of ΔCortBMDz (R^2 0.23, β 0.68, p=0.01 and β -0.55, p=0.02 respectively; Table 6.5.7).

Table 6.5.7. Annualised Cortical bone mineral density z-score change multivariable linear regression modelling

Model Summary				
Model	R	R Square	Adjusted R Square	Std. Error of the Estimate
1.00	0.60[a]	0.37	0.23	0.87
a. Predictors: (Constant), Magnesium, Baseline Cortical BMD, Annualised trabecular BMD change, CKD/Dialysis, ionized Calcium				

Model	Unstandardized Coefficients		Standardized Coefficients	t	Sig.	95.0% Confidence Interval for B	
	B	Std. Error	Beta			Lower Bound	Upper Bound

1.00		B	Std. Error	Beta	t	Sig.	Lower	Upper
	(Constant)	-15.10	4.37		-3.46	0.00	-24.14	-6.06
	CKD/Dialysis	-0.34	0.41	-0.18	-0.85	0.41	-1.18	0.50
	Baseline Cortical BMD	-0.27	0.11	-0.55	-2.53	0.02	-0.48	-0.05
	Annualised trabecular BMD change	0.33	0.19	0.33	1.74	0.10	-0.06	0.71
	Ionized calcium	10.51	3.49	0.68	3.01	0.01	3.29	17.72
	Magnesium	2.21	1.57	0.26	1.41	0.17	-1.03	5.45
a. Dependent Variable: Annualised cortical Bone Mineral Density change								

Elemental Ca intake from phosphate binders and Ca supplements correlated with ALP (r=0.32, p=0.02), but did not correlate with any BMD measures.

Longitudinal changes in vascular measures

Both the cIMTz and PWVz showed a non-significant increase over the study period [1.55 (0.93, 2.66) to 2.03 (1.23, 2.97), p=0.10 and 1.08 (-0.42, 2.24) to 1.26 (0.25, 2.55), p=0.11 respectively; Table 6.5.8].

Table 6.5.8 Vascular measures at baseline, follow-up, between visit comparison and annualised difference

Vascular measure Z-scores	At Baseline N=57	At Follow-up N=57	Between visit comparison (p-value)	Annualised difference
cIMT	1.55 (0.93, 2.66)	2.03 (1.23, 2.97)	0.10	-0.06 (-0.50, 0.98)
PWV	1.08 (-0.42, 2.24)	1.26 (0.25, 2.55)	0.11	0.39 (-0.55, 1.15)

Distensibility Coefficient	-1.22 (-2.17, -0.02)	-1.69 (-2.98, -0.70)	**0.01**	-0.48 (-1.48, 0.01)
CAC (Agatston Score)	range 0 to 413 mean 8.10 ± SD 55.20	range 0 to 491 mean 42.61 ± SD 123.50 n=18	**0.002**	range 0 to 136.4 mean 12.68 ± SD 34.21 [4/10 had CAC previously 6/10 new CAC]
Augmentation (%)	6.83 (4.42, 10.00)	6.42 (4.08, 10.50)	0.89	-0.80 (-3.18, 3.02)
Augmentation Index	17.83 (11.42, 23.92)	16.50 (12.08, 24.00)	0.66	-0.97 (-4.94, 6.79)

cIMT; carotid intima media thickness, PWV; pulse wave velocity, CAC; coronary artery calcification

ΔcIMTz was higher in dialysis compared to the CKD cohort (r=0.38, p=0.004). iCa, total Ca and ALP showed inverse correlations with ΔcIMTz (r=-0.50, p=0.004, r=-0.50, p<0.0001 and r=-0.34, p=0.01 respectively), whereas iPTH showed a positive correlation (r=0.36, p=0.005) with ΔcIMTz. Patients with a positive ΔcIMTz change had higher iPTH values compared with those with a negative ΔcIMTz (6.7x ULN vs 2.8x ULN, p=0.02). On multivariable linear regression, phosphate AUC >ULN and serum Ca were independent predictor of ΔcIMTz (R^2 0.55, β 0.29, p=0.006 and β -0.45, p<0.001 respectively; Table 6.5.9, Figure 6.5.1).

Table 6.5.9 Annualised carotid intima media thickness Z-score change (ΔcIMT) multivariable linear regression model

			Unstandardized Coefficients		Standardized Coefficients	t	Sig.	95.0% Confidence Interval for B	
			B	Std. Error	Beta			Lower Bound	Upper Bound
Model 1	Adjusted R^2 0.48	(Constant)	5.12	5.11		1.00	0.33	-5.45	15.70
		CKD/Dialysis	-0.21	0.35	-0.10	-0.61	0.55	-0.92	0.50
		Baseline carotid intima media thickness z-score	-0.12	0.16	-0.11	-0.76	0.46	-0.46	0.21
		Ionized calcium	-4.75	3.80	-0.30	-1.25	0.22	-12.61	3.10
		Phosphate AUC >ULN	0.28	0.08	0.47	3.31	0.003	0.11	0.46
		Alkaline phosphatase	0.00	0.00	-0.09	-0.54	0.60	0.00	0.00
		iPTH	0.00	0.01	0.01	0.04	0.97	-0.02	0.02
		Positive/Negative annualised trabecular bone mineral density change	0.58	0.25	0.40	2.33	0.03	0.06	1.09
Model 2	Adjusted R^2 0.55								
		(Constant)	7.63	1.98		3.85	0.00	3.64	11.61
		CKD/Dialysis	0.36	0.30	0.13	1.22	0.23	-0.24	0.96
		Baseline carotid intima media thickness z-score	-0.16	0.13	-0.13	-1.21	0.23	-0.42	0.11
		Total calcium	-3.40	0.75	-0.45	-4.55	<0.001	-4.91	-1.90
		Phosphate AUC >ULN	0.14	0.05	0.29	2.85	0.006	0.04	0.25
		Alkaline phosphatase	0.00	0.00	-0.17	-1.71	0.09	0.00	0.00
		iPTH	0.00	0.00	0.12	1.09	0.28	0.00	0.01
		Positive/Negative annualised trabecular bone mineral density change	0.35	0.18	0.21	1.97	0.05	-0.01	0.72

Figure 6.5.1 ΔcIMT correlation with phosphate AUC.

R^2 0.55
β 0.29
p=0.0006

ΔcIMT (z-score/yr)

PO$_4$ AUC
[>ULN; (mmol*month)/L]

n=57
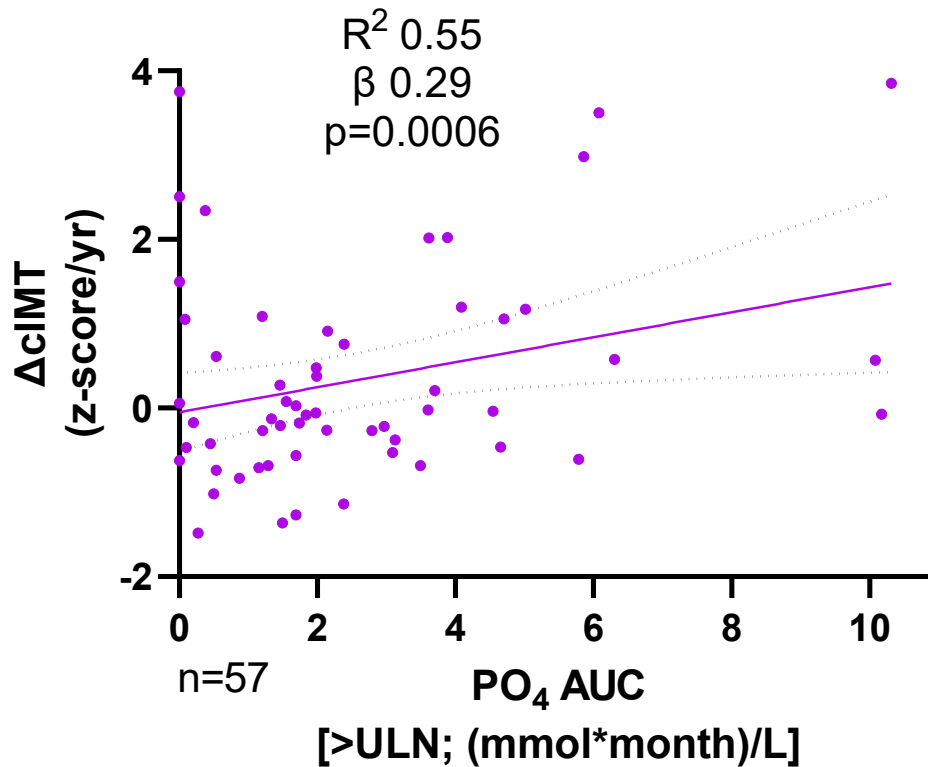
R^2, β and p values from multivariable regression modelling (See Supplemental Table 8). ΔcIMT; Annualised carotid intima media thickness z-score change, AUC; Area-under-the-curve

Vascular stiffness in different arterial beds was assessed by a reduction in carotid artery distensibility or an increase in the carotid-femoral PWV. There was a significant decrease in the distensibility_z [-1.22 (-2.17, -0.02) to -1.69 (-2.98, -0.70), p=0.01] over the study period (Table 6.5.8). Δdistensibility_z negatively correlated with an increase in ΔcIMTz (r=-0.37, p=0.005; Figure 6.5.2), and positively with diastolic BP (r=0.45, p<0.0001) and ALP (r=0.33, p=0.01). On multivariable regression analysis a decrease in Δdistensibility_z was predicted by increasing ΔcIMTz (R^2 0.58, β -0.26, p=0.04), ALP (β 0.26, p=0.01) and ΔBMADz (β -0.25, p=0.01) (Table 6.5.10).

Figure 6.5.2 ΔcIMT correlation with Δdistensibility.
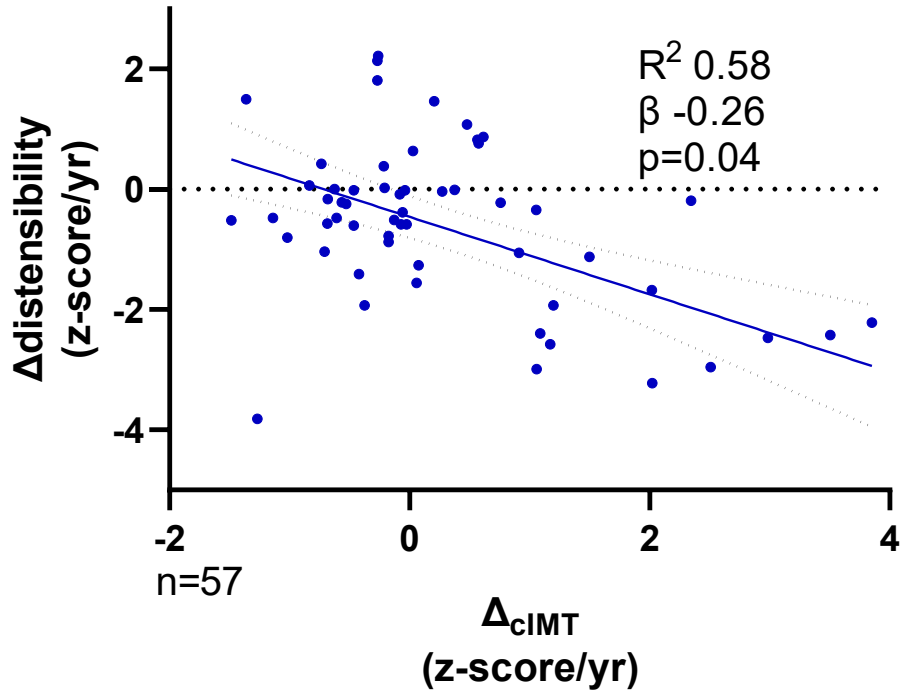
R^2, β and p values from multivariable regression modelling. ΔcIMT;

Annualised carotid intima media thickness z-score change, Δdistensibility;

Annualised carotid distensibility z-score change

Table 6.5.10 Annualised carotid distensibility z-score change multivariable linear regression model

Model Summary				
Model	R	R Square	Adjusted R Square	Std. Error of the Estimate

	1.00	.79[a]	0.63	0.58	0.97

a. Predictors: (Constant), Annualised bone mineral apparent density z-score change, Alkaline phosphatase, CKD/Dialysis, Total calcium, Baseline carotid distensibility z-score, Annualised carotid intima media thickness z-score change

Model		Unstandardized Coefficients		Standardized Coefficients	t	Sig.	95.0% Confidence Interval for B	
		B	Std. Error	Beta			Lower Bound	Upper Bound
1.00	(Constant)	-4.48	2.64		-1.70	0.10	-9.78	0.83
	CKD/Dialysis	-0.68	0.35	-0.20	-1.95	0.06	-1.39	0.02
	Baseline carotid distensibility z-score	-0.41	0.10	-0.39	-3.96	<0.001	-0.62	-0.20
	Total Calcium	1.67	1.04	0.19	1.60	0.12	-0.43	3.77
	Alkaline phosphatase	0.00	0.00	0.26	2.63	0.01	0.00	0.00
	Annualised carotid intima media thickness z-score change	-0.32	0.15	-0.26	-2.12	0.04	-0.61	-0.02
	Annualised bone mineral apparent density z-score change	-0.44	0.17	-0.25	-2.56	0.01	-0.79	-0.09

An increase in arterial stiffness measured by PWV correlated positively with an increase in systolic BP (r=0.44, p=0.001), and inversely with Mg (r=-0.34, p=0.02) and ALP (r=-0.28, p=0.04). The significant predictor of ΔPWVz was the annualised change in systolic BP (R^2 0.45, β 0.53, p=0.001; Table 6.5.11) and serum 25-hydroxyvitamin D (β 0.28, p=0.04). Δaugmentation correlated with ΔSBP (r=-0.35, p=0.008) and ΔDBP (r=-0.29, p=0.03), but there were no independent associations on linear regression.

Table 6.5.11 Annualised pulse wave velocity z-score change multivariable linear regression model

Model Summary				
Model	R	R Square	Adjusted R Square	Std. Error of the Estimate
1.00	0.75[a]	0.56	0.45	0.83

a. Predictors: (Constant), Vitamin D, Annualised SBP change, Annualised bone mineral apparent density z-score change, Annualised carotid Intima Media Thickness z-score change, Alkaline phosphatase, Magnesium, Baseline Pulse wave velocity z-score, CKD/Dialysis

Model		Unstandardized Coefficients		Standardized Coefficients	t	Sig.	95.0% Confidence Interval for B	
		B	Std. Error	Beta			Lower Bound	Upper Bound
1.00	(Constant)	0.11	1.11		0.10	0.93	-2.15	2.36
	CKD/Dialysis	0.42	0.36	0.18	1.17	0.25	-0.31	1.15
	Baseline pulse wave velocity z-score	-0.06	0.12	-0.07	-0.49	0.63	-0.29	0.18
	Annualised SBP change	1.08	0.30	0.53	3.63	0.001	0.47	1.68
	Annualised carotid intima media thickness z-score change	0.17	0.18	0.13	0.97	0.34	-0.19	0.54
	Annualised bone mineral apparent density z-score change	0.28	0.16	0.22	1.71	0.10	-0.05	0.61
	Magnesium	-1.00	1.09	-0.13	-0.92	0.36	-3.22	1.21
	Alkaline phosphatase	0.00	0.00	-0.11	-0.85	0.40	0.00	0.00
	Vitamin D	0.01	0.00	0.28	2.15	0.04	0.00	0.01

Ten percent (n=10) of the cohort had CAC at baseline, and 10/18 (56%) who had a CT scan at follow-up had CAC. The mean CAC score was 8.1 (range 0-412.6) at baseline and 42.61 (range 0-491.0) at follow-up. Of the patients with CAC at follow-up, 4 had CAC at baseline and 6 showed new onset calcification (Figure 6.5.3). The patients with an increase in CAC during follow-up had a higher phosphate AUC >ULN compared to those with no CAC (4.40 vs 0.79 mmol*month/L, p=0.04).

Figure 6.5.3 Coronary artery calcification (CAC; Agatston score) at baseline and follow-up visits

Agatston score in log-10 scale. P-value represents non-parametric paired t-testing.
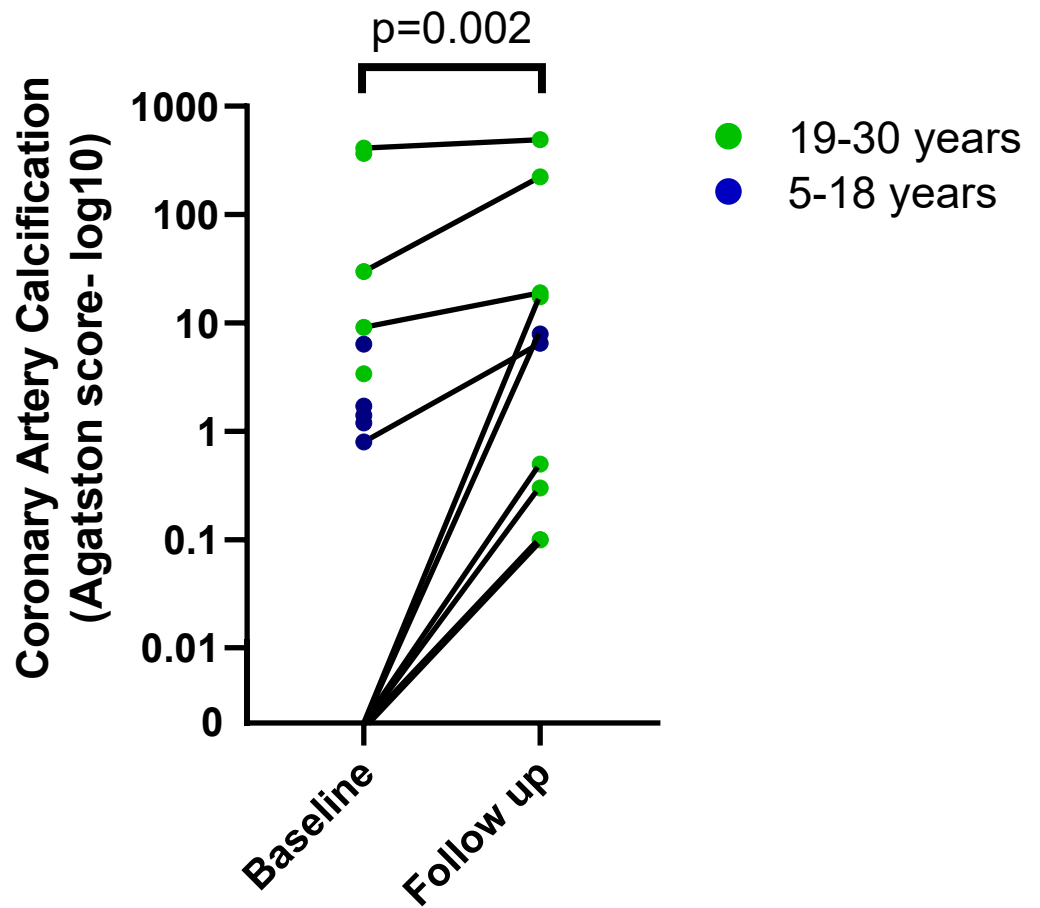
Total cardiac CT scans, n= (%)	98 (100)	18 (100)
Total with CAC n= (%)	10 (10)	10 (56)
Children (5-18 yrs) with CAC	5 (5)	2 (11)
Children (5-18 yrs) without CAC	72 (73)	1 (6)
Young adults (19-30 yrs) with CAC	5 (5)	8 (44)
Young adults (19-30 yrs) without CAC	16 (16)	7 (39)

Correlation between bone mineral density and vascular calcification

At baseline, cIMTz correlated with TrabBMDz (r=0.34, p<0.0001) (Figure 6.5.4a) and LS BMAD (r=0.22, p=0.03) (Figure 6.5.4b). On multivariable linear regression modelling, baseline TrabBMDz was an independent predictor of baseline cIMTz (R^2 0.10, β 0.34, p=0.001; Table 6.5.12). LS BMAD showed a similar but weaker correlation with cIMTz when substituted in the same model (R^2 0.06, β 0.26, p=0.01). The odds of patients with a TrabBMD z-score >2 having a cIMT z-score >2 was 4.2 times higher [(95%CI 1.44 to 11.09), sensitivity 77.27% (56.56 to 89.88%), specificity 55.26% (44.10 to 65.92), p=0.008]. Cortical BMDz did not correlate with cIMTz. There were no correlations seen with CAC.

Figure 6.5.4a. Baseline trabecular BMD and cIMT correlation
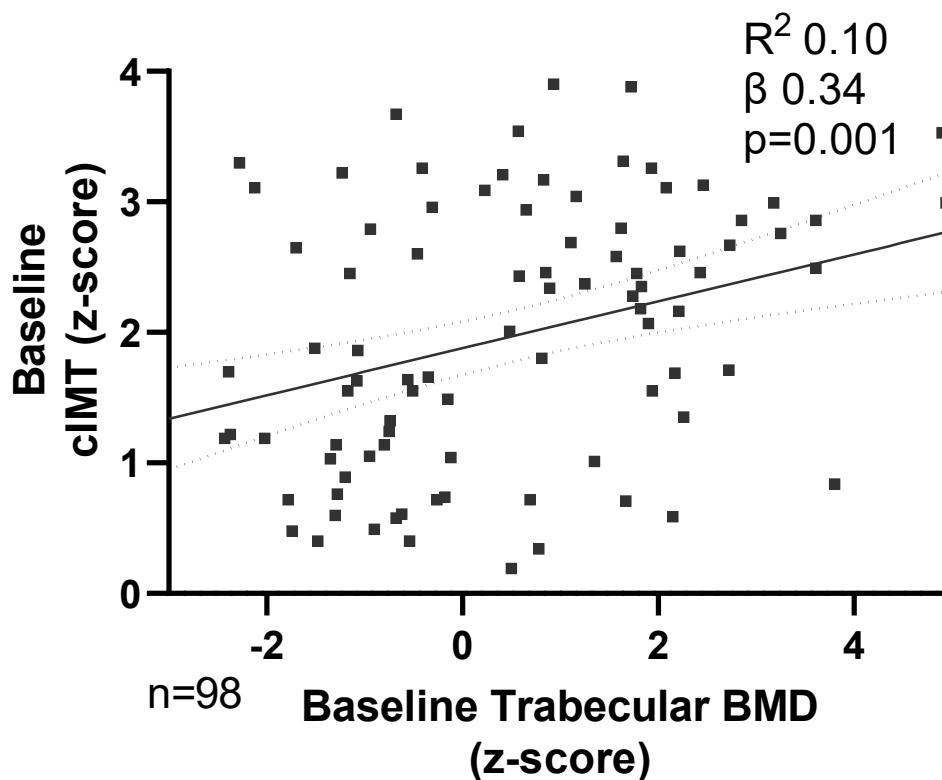
R^2, β and p values from multivariable regression modelling. BMD; Bone mineral density, cIMT; carotid intima media thickness, BMAD; bone mineral apparent density

Figure 6.5.4b. Baseline lumbar spine BMAD and cIMT correlation
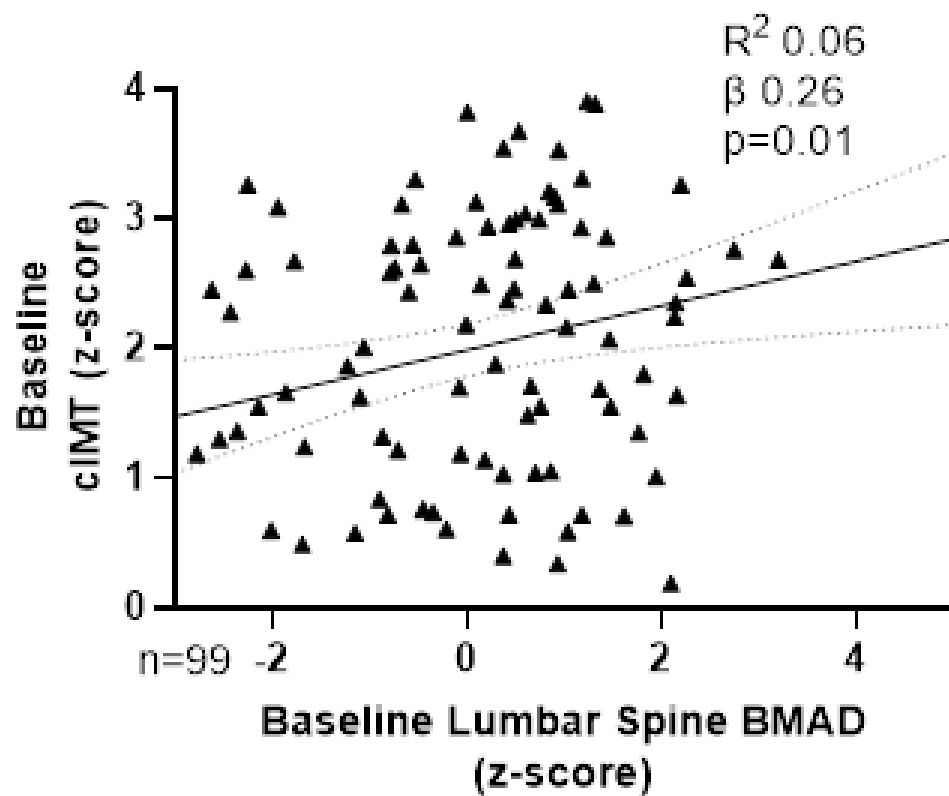
R^2, β and p values from multivariable regression modelling. cIMT; carotid intima media thickness, BMAD; bone mineral apparent density

Table 6.5.12 Multivariable linear regression model of baseline carotid intima media thickness z-score

Model		Unstandardized Coefficients		Standardized Coefficients	t	Sig.	95.0% Confidence Interval for B	
		B	Std. Error	Beta			Lower Bound	Upper Bound
Model 1 Adjusted R^2 0.10	(Constant)	1.15	1.60		0.72	0.47	-2.02	4.32
	Baseline trabecular bone mineral density z-score	0.17	0.05	0.34	3.39	0.001	0.07	0.27
	Total calcium	0.31	0.64	0.05	0.49	0.63	-0.96	1.58
	Alkaline phosphatase	0.00	0.00	-0.03	-0.29	0.77	-0.001	0.001
Model 2 Adjusted R^2 0.06	(Constant)	-0.09	1.55		-0.06	0.96	-0.09	1.55
	Baseline Lumbar Spine BMAD	0.17	0.07	0.26	2.51	0.01	0.17	0.07
	Total calcium	0.80	0.62	0.13	1.29	0.20	0.80	0.62
	Alkaline phosphatase	0.00	0.00	0.07	0.73	0.47	0.00	0.00

At follow up, ΔcIMTz correlated positively with ΔTrabBMDz (r=0.46, p<0.0001). An increase in ΔTrabBMDz was an independent predictor of ΔcIMTz increase (R^2 0.48, β 0.40, p=0.03), and those with a positive ΔTrabBMDz had a higher ΔcIMTz compared to those with no increase in ΔTrabBMDz [0.84(-0.05, 2.10) vs -0.26(-0.68, 0.29), p=0.005, Figure 6.5.5]. Patients who had an increase in ΔTrabBMDz had 6-fold greater odds of having a concurrent increase in ΔcIMTz [(95%CI 1.88 to 18.35), sensitivity 61.54% (42.53 to 77.57%), specificity 79.31% (61.61 to 90.15%), p=0.003].

Figure 6.5.5 Median and IQR comparison of ΔcIMT between patients with increasing and decreasing ΔTrabBMD z-score
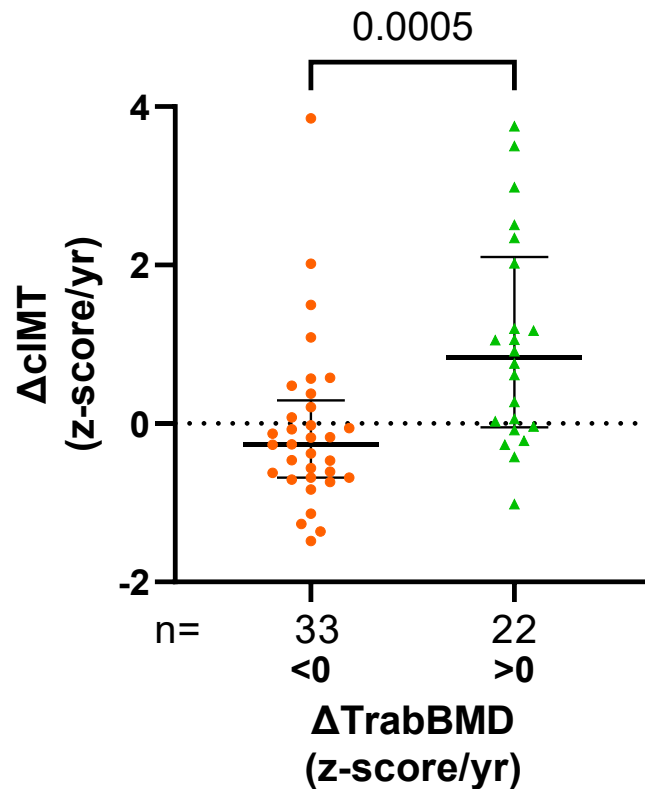
ΔcIMT; Annualised carotid intima media thickness z-score change, ΔTrabBMD; Annualised trabecular bone mineral density z-score change

Effect of linear growth on bone and vascular measures

Thirty-three (60%) patients demonstrated linear growth [>0 cm increase in tibial length; median growth 18.4 (15.9, 27.0) mm] during the study period. Annualised tibial length change correlated with annualised height change (r=0.76, p<0.0001) and higher ALP (r=0.52, p<0.0001). Patients with static growth were significantly older [25.5 (17.5, 28.0) vs 13.2 (10.8, 15.5) years, p<0.0001], and had lower serum ALP and Ca levels [112 (66, 139) vs 234 (168, 291), p<0.0001 and 2.40

(2.24, 2.49) vs 2.44 (2.41, 2.58), p=0.02 respectively] but there was no difference in

the other biomarkers or medication intake between groups (Table 6.5.13).

Table 6.5.13 Medication intake and serum biomarker comparison for participants
with tibial growth vs no growth

Medication intake/ Serum Biomarker	Linear growth (n=33)	Static growth (n=22)	Between group difference (p-values)
Elemental calcium intake from binders or supplements (mg/kg/day)	11.79 (0.00, 30.29)	4.23 (0.00, 17.84)	0.36
Alfacalcidol (ng/kg/day)	16.67 (2.67, 26.51)	10.46 (4.53, 15.06)	0.23
Vitamin D (units/kg/day)	0.00 (0.00, 37.34)	0.00 (0.00, 36.39)	0.92
Calcium (mmol/L)	2.44 (2.41, 2.58)	2.40 (2.24, 2.49)	**0.02**
Magnesium (mmol/L)	1.03 (0.91, 1.11)	0.94 (0.89, 1.05)	0.13
Phosphate (mmol/L)	1.55 (1.43, 1.75)	1.58 (1.37, 1.84)	0.95
Phosphate AUC (mmol*month/L)	1.69 (0.70, 3.32)	2.07 (0.43, 4.25)	0.61
Bicarbonate (mmol/L)	24.61 (21.71, 26.94)	23.00 (21.84, 25.86)	0.52

Alkaline Phosphatase (units/L)	233.9 (168.4, 291.3)	112.2 (66.1, 139.3)	**<0.0001**
Intact parathyroid hormone (xULN)	x3.1 (x1.5, x6.6)	x4.1 (x2.2, x12.9)	0.25
Serum Vitamin D (units/L)	96.50 (64.79, 127.80)	92.53 (71.98, 107.10)	0.57

Growth defined as >0 cm lengthening of tibia during follow up period. ULN; Upper limit of normal range

ΔTrabBMDz was lower in patients with linear growth compared to participants with no growth (-0.71 vs 0.11, p=0.0004), implying undermineralised osteoid. ΔCortBMDz did not differ between groups (-0.39 vs -0.48, p=0.31; Figure 6.5.6). Patients with linear growth had lower ΔcIMTz [-0.27 (-0.68, 0.04) vs 1.13 (0.05, 2.39), p<0.0001]), ΔPWVz [0.24 (-1.06, 0.72) vs 1.01 (-0.05, 1.39), p=0.02], and higher Δdistensibility z-scores [-0.17 (-0.59, 0.70) vs -1.81 (-2.67, -0.31), p<0.0001] compared to participants with static growth (Figure 6.5.7).

Figure 6.5.6. Comparison of bone mineral density changes (z-score/yr) for patients that demonstrated growth (tibial length increase) and no growth (static tibial length)
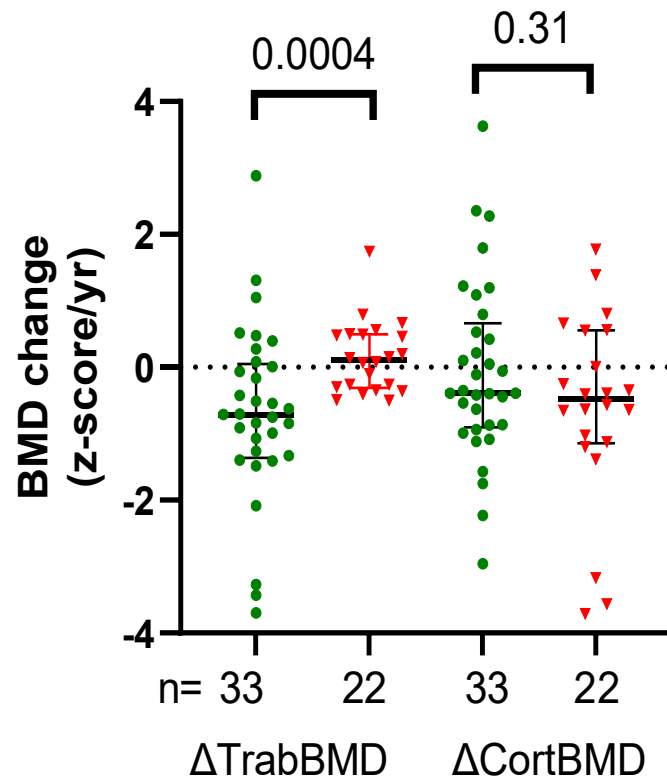
Figure 6.5.7. Comparison of vascular measure changes (z-score/yr) for patients that demonstrated growth (tibial length increase) and no growth (static tibial length)
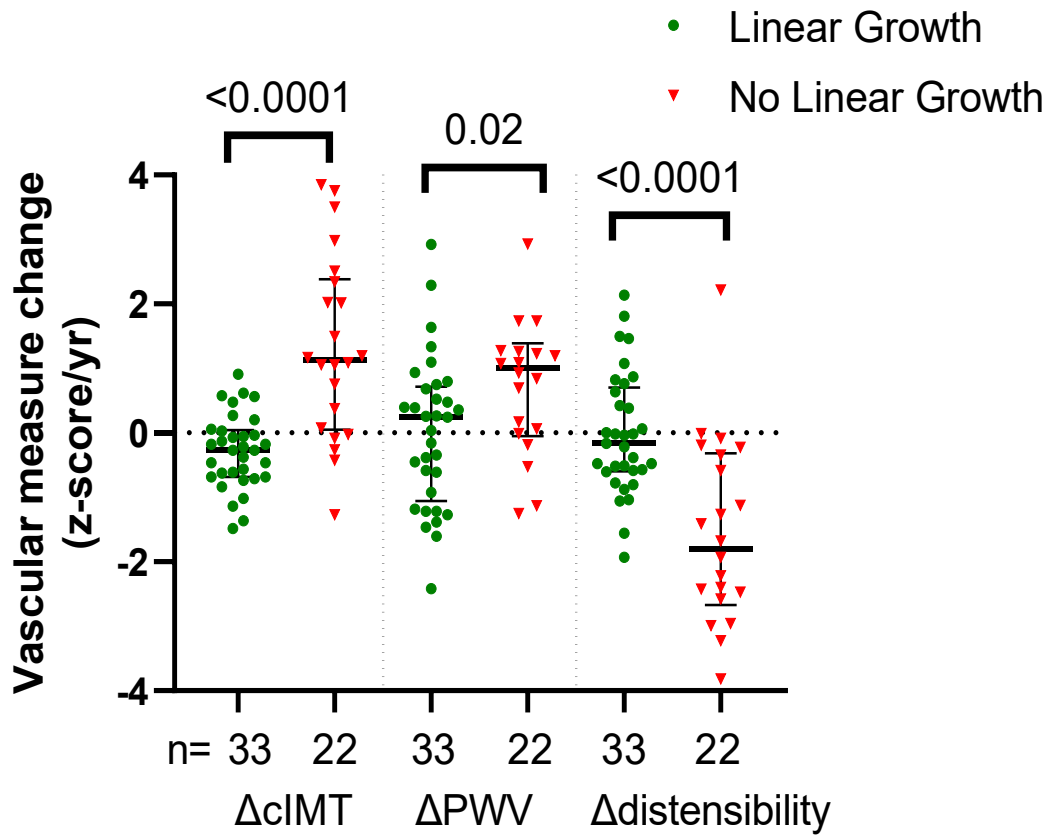
6.6 Discussion

To the best of my knowledge, this is the first prospective longitudinal study in a cohort of children and young adults with CKD stages 4-5 or on dialysis to concurrently examine changes in BMD alongside comprehensive measures of vascular calcification and stiffness. We have shown that even as BMD increases, vascular calcification can develop and progress in this young cohort with CKD: those with an increase in TrabBMDz were 6 times more likely to have an increase in cIMTz. Patients with linear growth showed an attenuated progression of all vascular measures, suggesting a buffering capacity of the growing skeleton. These hypothesis generating data suggest that despite Ca accrual by the skeleton, excess Ca is deposited in soft-tissues leading to vascular calcification. A biomarker of bone mineralisation that allows 'real time' evaluation of bone mineral balance, together with biomarkers of bone turnover, may determine the optimal Ca requirements of an individual, allowing normal bone mineralisation without extraosseous calcification.

Osteoporosis and atherosclerosis were once thought to be unrelated diseases that are an inevitable part of the ageing process. Recent studies suggest that bone demineralisation and vascular calcification may be closely linked processes (Kiel et al., 2001, Tankó et al., 2005). Older adults with CKD demonstrate a similar but exaggerated "calcification paradox" (Persy and D'Haese, 2009), demonstrating a concurrent progression of bone demineralisation and ectopic soft-tissue calcification (London, 2012). In a longitudinal study measuring CAC and BMD in older dialysis patients, Malluche et al showed that patients with the highest BMD loss had the greatest increase in CAC (Malluche et al., 2015). Similar, albeit cross-

sectional, studies have shown that both patients with CKD and on dialysis who have a lower BMD have higher CAC scores (Cejka et al., 2014, Chen et al., 2017, Filgueira et al., 2011, Toussaint et al., 2008, Adragao et al., 2009, Adragao et al., 2008, Kim et al., 2022), and a higher all-cause mortality (Chen et al., 2017). Importantly, the average age of patients in these studies was above 65 years, and therefore age-related osteoporosis may have contributed to these processes.

Unlike the predominant bone resorption activity in older adults, the growing skeleton avidly accrues Ca; the Ca content of the skeleton increases from ~25g at birth to ~1000 - 1200g in adult males and females (Matkovic and Heaney, 1992, Baxter-Jones et al., 2011). Bone mineral accretion continues into the 30s, when peak bone mass (the amount of bone acquired by the end of skeletal development) is reached (Baxter-Jones et al., 2011, Weaver et al., 2016). Bone histomorphometry studies in children have demonstrated that defective mineralisation was present as early as CKD stage 2, with the prevalence increasing to over 90% in children on dialysis (Bakkaloglu et al., 2010, Wesseling-Perry et al., 2012). In contrast, a mineralisation defect was observed in only 3% of adults on dialysis (Malluche et al., 2011). Hence, CKD-MBD studies in older adults cannot be extrapolated to children and young people. There have been only two small cross-sectional studies in children with CKD to date. Preka et al, demonstrated that trabecular thickness by High Resolution-pQCT (HR-pQCT) was positively associated with diastolic and mean arterial BP (Preka et al., 2018). The second, by Ziolkowska et al, showed that cIMT correlated with LS BMD and total body DXA (Ziolkowska et al., 2008). Both studies were cross-sectional, making it impossible to determine the causal effect of BMD on vascular calcification, if any.

These results suggest that linear growth may be a significant factor in the interplay between bone and blood vessels. The young people with linear growth had lower ΔTrabBMDz compared to those with no linear growth. Mineralisation of the osteoid scaffold lags behind formation of the bone matrix by osteoblasts by around 30 days (Katsimbri, 2017). During periods of rapid growth in childhood and adolesence, mineralisation follows the peak velocity of growth by 6-12 months (Stagi et al., 2013b). This leaves the bone compartment relatively undermineralised. In this cohort the higher ALP and negative ΔTrabBMDz demonstrated in growing children likely reflects this as yet unmineralised osteoid. The process of ongoing bone mineral deposition may be a protective factor, buffering the vasculature from high circulating Ca and phosphate. In adolescents, bone area increases rapidly around the time of and up to five years after peak height velocity and the bone mineral content continues to increase even after (Baxter-Jones et al., 2011). Perhaps once rapid linear growth ceases in late adolescence, the voracious absorption of minerals by the skeleton decreases, leading to increasing structural arterial wall changes.

This data and studies in adult dialysis patients suggest that trabecular (rather than cortical) BMD loss is associated with vascular calcification (Costa et al., 2020, Malluche et al., 2015, Chen et al., 2016). Trabecular bone is considered the more metabolically active bone compartment compared to cortical bone, accepting mineral ions from, and releasing them to, the circulation in response to hormonal

stimuli (Stagi et al., 2013b). This is reflected in the mineralisation process as new bone formation is completed in around 90 days in trabecular bone, but requires around 120 days in cortical bone (Katsimbri, 2017). Whilst cortical bone contains the majority of the bone mineral, the normal adult turnover rate is only 2-3% per year (Clarke, 2008). Equally, newly formed bone with relatively low mineral content has a larger surface-to-volume ratio that allows exchange of Ca and P with the extracellular fluid, highlighting the central role the trabecular compartment plays in maintaining Ca and phosphate homeostasis (Clarke, 2008). This may explain the inverse correlation between iCa and Ca with ΔTrabBMDz, suggesting a greater exchange of Ca from the trabecular compartment to maintain normal serum Ca levels.

With the exception of serum phosphate, the routinely used serum biomarkers did not correlate with BMD and vascular calcification changes. This is in keeping with earlier studies where we and others have shown that no biomarker individually or in combination is sufficiently robust to diagnose bone mineralisation or turnover defects (Bakkaloglu et al., 2010, Lalayiannis et al., 2020, Sprague et al., 2016). Serum Ca levels are currently our only tool for estimating bone mineral balance. However, serum Ca accounts for <0.1% of total body Ca, and due to tight negative feedback control, does not reflect the total body Ca (Bushinsky, 2010). Moreover, the mere presence of high serum Ca does not imply that it will be incorporated into bone, nor that it will be deposited in the vasculature. Instead, it is important to obtain a 'real time' estimation of bone mineral balance. Our group has shown that non-radioactive Ca isotopes that are naturally present in our food and water can be measured in serum, and their ratio (expressed as $\delta^{44/42}Ca_{serum}$) is a

significant and independent predictor of bone mineral balance in healthy children and young adults (Shroff et al., 2021). This work has been extended to children with CKD and on dialysis in whom $\delta^{44/42}Ca_{serum}$ values were the strongest predictor of total bone mineral content (Shroff et al., 2020b).

Although this is the first study to follow changes in BMD and vascular measures concurrently in a young CKD and dialysis cohort, several limitations of this work must be acknowledged. As with all paediatric studies where hard outcomes are relatively rare, surrogate measures of bone and cardiovascular outcomes were used. However, pQCT measurement of BMD has been associated with an increased fracture risk (Denburg et al., 2013), and cIMT is a well-established surrogate for the extent of coronary artery disease, correlating with hard endpoints such as myocardial infarction and stroke in adults without CKD (Lorenz et al., 2007) and cardiovascular events in CKD (Roumeliotis et al., 2019) and dialysis (Kouis et al., 2020) patients. These intermediate end-points must be interpreted with caution, and future studies must include key patient-level outcomes such as fractures that are commonly seen even in a young CKD cohort. In older adults, cIMT measurements may reflect both intimal thickening and atherosclerotic changes due to traditional Framingham risk factors. With the US imaging used, it is difficult to separate intimal and medial layers, but in children and young people, intimal thickening is rarely seen, so the cIMT increase can largely be attributed to medial layer changes (Shroff et al., 2008, Shroff et al., 2007). I was unable to perform bone biopsies, the current gold standard for determining mineralisation changes in bone. Patient follow-up was affected by the COVID-19 pandemic when research studies were abruptly halted; this together with a high transplantation rate, contributed to

significant loss to follow-up. As those lost to follow-up were younger, and the study

protocol dictated that only children with CAC at baseline and all adults should have

a cardiac CT at second visit, the true incidence and progression of CAC may have

been under- or over-estimated. In addition, all adults in the cohort were on

hemodialysis, limiting our ability to examine bone and vessel changes in adults with

CKD stages 4-5. Only 4 participants were on growth hormone treatment, so its

effects on bone mineralisation or vascular calcification in this cohort could not be

studied.

6.7 Conclusion

In this hypothesis generating study we have shown that children and young

adults with CKD or on dialysis develop vascular calcification even as BMD increases,

with the most significant vascular changes in young people with no linear growth.

One of the most challenging aspects of CKD-MBD management in young people is

to reconcile the need for Ca and phosphate for optimal skeletal mineralisation

whilst avoiding an excess Ca intake that can lead to vascular calcification. An

accurate estimation of the real time changes in bone mineral balance may guide

treatments based on the individual's state of bone turnover and mineralisation.

Chapter 7

Conclusions and Future Directions

In this thesis I present and discuss the findings of the multicentre longitudinal observational cohort study of children and young adults with CKD stages 4-5 or on dialysis. The rationale for including young adults alongside children and adolescents, is that the skeleton continues to mineralise until the 3rd, and perhaps 4th decade of life, at which point peak bone mass is reached. This ongoing early life skeletal mineral accrual is thought to prevent extraskeletal calcification in CKD.

My research has produced some hypothesis generating data in relation to the bone/vascular link in CKD in young people. The main conclusions are:

1. Mineral and bone disorders of CKD account for a significant burden of bone pain and atraumatic fractures in children as well as young adults with CKD stages 4 – 5 or on dialysis. There was significant reporting of daily bone pain, that affected daily activities, and required frequent use of analgesia. Ten percent of the cohort had suffered at least one atraumatic fracture, during their CKD journey (with an eGFR <30 ml/min/1.73m^2) (Lalayiannis et al., 2020). This correlates with previously published findings that even in earlier stages of CKD (Stages 2-3), young people suffer a very high burden of bone disease.

2. Calcium, parathyroid hormone and alkaline phosphatase, which are routinely measured to monitor patients' CKD-MBD and bone health, taken together are only moderate predictors of tibial cortical BMD as measured by peripheral quantitative Computed Tomography (pQCT). Addition of widely used and available DXA imaging for areal BMD estimation is not a useful additional measure, and should not be routinely performed in children and young adults with CKD4-5 or on dialysis (Lalayiannis et al., 2020). pQCT is considered advantageous in studying BMD as it provides a three dimensional slice for measurement and is able to quantify BMD in the two bone compartments- cortical and trabecular- separately. DXA superimposes cortical and trabecular bone, and underestimates BMD in growth stunted bones(Lalayiannis et al., 2019). Choosing the correct pQCT healthy database for z-score calculation is important consideration in any study (Lalayiannis et al., 2021b).

3. The optimum target range for serum PTH levels to allow for bone mineralisation and normal bone turnover, whilst avoiding adynamic bone disease remains unclear. I compared the predictive value of the KDIGO recommended target range of 2-9xULN and the significantly lower target of <3xULN suggested by the European Pediatric Dialysis Working Group. I found that there was a strong but non-linear association between PTH and cortical BMD such that when PTH was

<3xULN none of the patients had cortical BMD below 2 standard deviations. On the other hand, PTH target levels of between 2-9xULN were unable to differentiate normal CortBMD, implying a lack of sensitivity of such a wide PTH target.

4. I examined structural and functional cardiovascular changes in this cohort and found that they are significantly prevalent in children and young adults with stages CKD 4-5 or on dialysis, with up to 69% of CKD and 88% of dialysis patients having at least one structural or functional cardiovascular abnormality. Structural changes included carotid intima media thickness, coronary artery calcification and left ventricular hypertrophy. Functional changes examined were carotid-femoral pulse wave velocity, and carotid distensibility. We noted a possible temporal association between structural changes and functional abnormalities , with compensatory vessel dilatation following the early structural changes. This high burden of vascular disease highlights the need for early intervention and treatment strategies to prevent vascular calcification (Lalayiannis et al., 2021a).

5. Phosphate emerged as the most important routinely used biomarker in relation to structural vascular changes. The extent of hyperphosphataemia and the time spent with a high phosphate together were a significant independent predictor of carotid intima media

thickness increase. Other routinely used biomarkers were less sensitive or specific and showed weaker correlations.

6. As tibial bone mineral density increased, vascular calcification also developed and progressed, even in a young cohort with CKD. Those with an increase in Trabecular BMD z-score were 6 times more likely to have an increase in cIMT z-score.

7. Stature growth during childhood and adolescence (using tibial length as a proxy for height) may be a significant factor in the bone-vascular link in CKD. Young people with tibial growth had static vascular measures compared to their peers with no growth, who demonstrated progression and worsening of their subclinical vascular changes.

In conclusion, this study has generated the hypothesis that bone demineralisation and vascular calcification are are closely inter-related in early life CKD and not just in later adulthood. The pathophysiological mechanisms that underpin this relationship requires further exploration. It is likely a complex bidirectional relationship, that is also temporal in nature, with the early life accelerated growth playing a major role in attenuating vascular changes.

I will continue to try and answer some of the questions that have arisen through this work. I have started the following projects aiming to address the gap in knowledge in the field of CKD-Mineral Bone Disorder in childhood:

1. **Fractures in young people with CKD, on dialysis or post transplantation**

   An increased risk of fractures was seen in this cohort and confirms the findings of the CKiD study (Denburg et al., 2016, Laster et al., 2021). Working closely with the European Society of Pediatric Nephrology CKD-MBD Working group, I have initiated a European, multi-centre, retrospective survey with additional prospective data collection in children with CKD, on dialysis or port transplant who have suffered a pathological, atraumatic fracture. The aims of the two-part study will be to determine the prevalence of fractures in European children with CKD, and to determine the potential risk factors for the fractures (age, growth velocity, medications, dialysis vintage, eGFR, CKD-MBD biochemistry). This has been set out as one of the recommendations for future research by the ESPN CKD-MBD working group in the Clinical Practice Points publication in 2020 (Bakkaloglu et al., 2020).

2. **Radial BMD vs Tibial BMD**

   pQCT is a bone imaging tool I am now very familiar with as a result of employing it in this study. Despite its many benefits and attributes, it remains a research tool and I do not envisage it becoming a widely

available imaging modality for the practicing clinician. In this thesis, I have extensively described how I set about using pQCT to examine the cortical and trabecular bone compartments in the tibia separately. It is not known however, if the tibia is the best long bone for assessment. BMD is affected by many variables, not least by weight bearing and exercise. I have collected data on radial cortical and trabecular BMD. I aim to analyse these data to see how the two long bones (radius and tibia) compare in absolute values, but also by z-score generation. I will examine if the radial BMD values correlate with any of the routinely used serum biomarkers.

3. **Research Biomarker Study**

The routinely used serum biomarkers of calcium, phosphate, parathyroid hormone and alkaline phosphatase only correlated modestly with the bone mineral density measured by pQCT and the surrogate markers of vascular calcification. This is probably because the bone and vascular changes occur over many months and years, and the follow-up period of around a year may not have been sufficient to uncover more significant correlations. In addition, it has been shown by Bakkaloglu et al that PTH and ALP are only moderate predictors of bone histomorphometric indices (namely turnover and mineralisation) (Bakkaloglu et al., 2010). I have banked serum of the participants in this study for the purpose of analysing research biomarkers of bone formation [bone specific alkaline phosphatase, osteocalcin, procollagen type 1 N-terminal propeptide

(P1NP) and carboxy-terminal procollagen type 1 propeptide (P1CP)],

bone resorption [carboxyterminal cross-linking telopeptide of bone

collagen (CTX) and tartrate-resistant acid phosphatase (TRAP5b)], and

osteocytic markers such as Endopeptidases on X chromosome (PHEX),

Dentin Matrix Protein-1 (DMP1), sclerostin and FGF23. I will also include

other normal calcification inhibiting factors such as Fetuin A, to assess

the correlations with the vascular calcification markers. Perhaps these

more specific biomarkers of bone turnover will be better performers in

identifying demineralising bone and/or vascular calcification.

4. **Natural Calcium Isotope ratios as a biomarker**

It is widely accepted that biomarkers such as calcium, phosphate and

alkaline phosphatase and imaging modalities such as DXA and pQCT do

not perform well in quantifying bone mineralisation in the general

population and in disease states such as osteoporosis or CKD. A novel

biomarker being studied by my supervisor Prof R. Shroff, is naturally

occuring calcium isotopes and their ratio ($\delta^{44/42}$ Ca) in the serum and

urine. It has so far shown good positive correlation with bone formation

markers and negative correlation with bone resorption markers in

healthy children, children and young adults with CKD(Shroff et al., 2022)

and older women with osteoporosis (Shroff et al., 2020a, Eisenhauer et

al., 2019). I will be examining the $\delta^{44/42}$ Ca ratio in the banked serum

samples of this cohort and comparing it to the extensive bone and

vascular imaging obtained during this PhD. An accurate, non-invasive and easily reproducible biomarker of bone and vascular health is needed in patients with CKD in order to target treatments appropriately.

I hope these projects will add to the evidence base in the field of CKD-MBD, and increase awareness of the importance of addressing bone and vascular health in childhood CKD. I hope I can play a small role in the effort to alleviate our patients' bone and cardiovascular disease burden.

Appendix A

List of publications during my research studies

Original Research Articles

1. **Lalayiannis AD**, Crabtree NJ, Ferro CJ, et al. Routine serum biomarkers, but not dual-energy X-ray absorptiometry, correlate with cortical bone mineral density in children and young adults with chronic kidney disease. *Nephrology Dialysis Transplantation*. 2020; doi:10.1093/ndt/gfaa199

2. **Lalayiannis AD**, Fewtrell M, Biassoni L, et al. Studying bone mineral density in young people: The complexity of choosing a pQCT reference database. *Bone*. 2021/02/01/ 2021;143:115713. doi: 10.1016/j.bone.2020.115713

3. **Lalayiannis AD**, Ferro CJ, Wheeler DC, et al. The burden of subclinical cardiovascular disease in children and young adults with CKD and on dialysis. *Clinical Kidney Journal*. 2021; doi:10.1093/ckj/sfab168

4. **Lalayiannis AD**, Crabtree NJ, Ferro CJ, et al. Bone mineral density and vascular calcification in young people with CKD4-5 or on dialysis. Kidney International Reports. *Submitted May 2022-under review*

Review Article

5. Lalayiannis AD, Crabtree NJ, Fewtrell M, et al. Assessing bone mineralisation in children with chronic kidney disease: what clinical and research tools are available? *Pediatr Nephrol*. Jun 25 2019; doi:10.1007/s00467-019-04271-1

Other publications involved with during PhD

6. Bakkaloglu SA, Bacchetta J, **Lalayiannis AD**, et al. Bone evaluation in paediatric chronic kidney disease: Clinical practice points from the European Society for Paediatric Nephrology CKD-MBD and Dialysis working groups and CKD-MBD working group of the ERA-EDTA. *Nephrol Dial Transplant*. Nov 2 2020; doi:10.1093/ndt/gfaa210

7. Shroff R, Fewtrell M, Heuser A, **Lalayiannis AD** et al. Naturally Occurring Stable Calcium Isotope Ratios in Body Compartments Provide a Novel Biomarker of Bone Mineral Balance in Children and Young Adults. *J Bone Miner Res*. Aug 12 2020; doi:10.1002/jbmr.4158

8. Shroff R, **Lalayiannis AD**, Fewtrell M, et al. Naturally occurring stable calcium isotope ratios in body compartments: a novel biomarker of bone calcium balance in children with chronic kidney disease. Kidney International. 2022 May 27:S0085-2538 doi: 10.1016/j.kint.2022.04.024. (Epub ahead of print)

Funding Obtained

Appendix B- Ethics Approval

NHS
Health Research Authority

London - City & East Research Ethics Committee

Tel: 02071048033/53

> **Please note: This is the favourable opinion of the REC only and does not allow the amendment to be implemented at NHS sites in England until the outcome of the HRA assessment has been confirmed.**

02 October 2017

Ms Emma Pendleton
Deputy Director of
Research &
Innovation GOSH/
UCL ICH R&D Office
30 Guildford Street,
Bloomsbury, London
WC1N 1EH

Dear Ms Pendleton

Study title:	**Assessing calcium balance in children with chronic kidney disease to optimise treatment strategies**
REC reference:	**17/LO/0007**
Protocol number:	**1**
Amendment number:	**1**
Amendment date:	**11 August 2017**
IRAS project ID:	**219269**

The above amendment was reviewed by the Sub-Committee in correspondence.

Ethical opinion
The members of the Committee taking part in the review gave a favourable ethical opinion of the amendment on the basis described in

the notice of amendment form and supporting documentation.

Approved documents

The documents reviewed and approved at the meeting were:

Document	Version	Date
Notice of Substantial Amendment (non-CTIMP) [AmendmentForm_ReadyForSubmission (1)]	1	11 August 2017
Participant consent form [CVDBone - Assent Form - V2 - 10.08.2017]	2	10 August 2017
Participant consent form [CVDBone - Consent Form - 16+ age - V2 - 10.08.2017]	2	10 August 2017
Participant consent form [CVDBone- Consent Form Parents - V2]	2	10 August 2017
Participant information sheet (PIS) [CVDBone - PIS 5 - 8 yrs - V3 - 10.08.2017]	3	10 August 2017
Participant information sheet (PIS) [CVDBone - PIS 9 - 15 yrs - V3 - 10.08.2017]	3	10 August 2017
Participant information sheet (PIS) [CVDBone - PIS 16+ young adults - V4 - 10.08.2017]	4	10 August 2017
Participant information sheet (PIS) [CVDBone - PIS parents - V4 - 10.8.2017]	4	10 August 2017
Research protocol or project proposal [CVD-Bone - Study Protocol - V3 - 21.08.2017]	3	21 August 2017

Membership of the Committee

The members of the Committee who took part in the review are listed on the attached sheet.

Working with NHS Care Organisations

Sponsors should ensure that they notify the R&D office for the relevant NHS care organisation of this amendment in line with the terms detailed in the categorisation email issued by the lead nation for the study.

Statement of compliance

The Committee is constituted in accordance with the Governance Arrangements for Research Ethics Committees and complies fully with the Standard Operating Procedures for Research Ethics Committees in the UK.

We are pleased to welcome researchers and R & D staff at our Research Ethics Committee members' training days – see details at http://www.hra.nhs.uk/hra-training/

17/LO/0007:   **Please quote this number on all correspondence**

Yours sincerely

pp Dr John Keen Chair

E-mail: nrescommittee.london-cityandeast@nhs.net

London - City & East Research Ethics Committee Attendance at Sub-Committee of the REC meeting in correspondence

Committee Members:

Name	Profession	Present	Notes
Dr Ayse Baxter	Pharmaceutical Physician	Yes	
Dr John Keen	GP (REC Chairman)	Yes	

Also in attendance:

Name	Position (or reason for attending)
Mr Rajat Khullar	REC Manager

Appendix C- Peripheral Quantitative Computed Tomography (pqCT) Standard Operating Procedure

VI.   Device

1.   Stratec Medizintechnik GmbH XCT 2000

2.   Holders available: phantom limb quality assurance and calibration, tibial and radial scanning holders.

3.   Software version 6.0

VII.   Quality Assurance and Calibration

1.   Prior to each use, the phantom limb associated with this particular machine should be scanned. This ensures correct calibration for measurements, but also that the scanner is working correctly and the radiation dose is appropriate.

2.   Turn on socket at the wall.

3.   Turn on Computer and Scanner.

4.   Open pqCT software and enter Username and Password as supplied.

5.   Software will prompt for calibration scan.

6.   NOTE: You will need to undertake this as you will not be allowed to scan a patient/participant otherwise.

7.   Attach the phantom limb scanning holder. Insert phantom limb and start scan.

8.   Report will state whether parameters are within acceptable range and radiation dose is correct. Click OK when prompted to save QA scan to log. This is important for audit purposes.

9.   If QA report shows any issue, you will be unable to continue with scanning. Discontinue scanning and inform Dr Shroff/Radiology department.

VIII. Site of measurements for CVDBone

1. **Tibia**. Left tibia should be scanned unless left is dominant side. If this is the case, scan right tibia.

2. **Radius**. Left radius should be scanned unless left is dominant side. If this is the case, scan right radius.

The dominant side can be established by asking which hand the participant writes with, and which leg the participant kicks a ball with.

IX. Identification of Participant

1. The participant must be correctly identified. The healthcare worker must actively match at least two pieces of information on the referral to the presenting individual in addition to name. Usually date of birth and address will suffice. Ask patient for name regardless of age. If child <10 years, ask DOB and address, but confirm with parent.

2. This must be done by the healthcare worker undertaking the scanning.

3. If there is a mismatch, abandon procedure until source of error identified.

X. Excluding Pregnancy

1. All females aged 10 to 65 years old must be asked directly whether they are pregnant. If definitely not or within 2 weeks of last menstrual cycle, scanning can proceed (ie The patient must be asked whether her period is overdue. If not, then the test can go ahead). Radiation risk and exposure is minimal, but can be delayed until after pregnancy if scan needed for research purposes solely.

2. If any female participants breastfeeding: scanning can proceed. If purely for research purposes, consider delaying until breastfeeding discontinued.

XI. Preparation for examination

4. Select 'New Patient' on computer

5. Insert demographic details accurately (Name, First Name, DOB, GOSH ID number). This should include height and weight measured on the day of the scan.

6. Length of measurement: For tibial scan measure length from intercondylar eminence (tibial plateau) to middle of medial malleolus. For radial scan measure from head of radius to styloid process of radius. For each this should be repeated 3 times for accuracy.

XII.   Commencing pqCT measurements

9. Press F2 to select which 'scan mask' (scanning protocol) to undertake. Choose **TIBIA4VS** for tibia or **RADIUS2VS** for radius for **CVDBone** study.

   Settings: voxel size of 0.4 mm, slice thickness of 2.3 mm, and scan speed of 25 mm/sec. These will be set automatically, do not change.

   Sites for measurement in tibia:

   3%, 4%, 38% and 66% of tibia length proximal to the reference line.

   - **3% metaphyseal site** - analysed for trabecular volumetric BMD (mg/cm^3).

   - **4% metaphyseal site**- analysed for trabecular volumetric BMD (mg/cm^3)

   - **38% diaphyseal site** – Settings: cortmode 2 (threshold, 711 mg/cm^3).

   Analysed for cortical volumetric BMD (mg/cm^3), periosteal circumference (mm), endosteal circumference (mm), and cortical cross-sectional area (mm^2) within the region defined by the endosteal and periosteal surfaces, bone mineral content (mg/mm^3), and polar section modulus (Zp, mm^3).

   - **66% diaphyseal site** - Muscle and fat area (mm^3)

10. You will be prompted to move scanner gantry. Follow on-screen instructions.

11. Once gantry fully withdrawn, insert appropriate holders for tibial or radial scanning.

12. Patient should lie on examination couch with appropriate leg inserted through gantry, or sat upright in chair with appropriate arm through gantry.

13. The inserted limb should be secured with the holders. Ensure patient comfortable.

14. Start Scout View scan. See attached images in Appendix for choice of reference line placement.

15. Select appropriate reference line placement

    -at the **proximal border of the distal tibia growth plate** in children with open growth plates

    -at the **proximal border of the distal endplate** in participants with fused growth plates

16. Start Scan. This will continue and complete automatically. Software will show seconds to end of examination. The yellow light on top of gantry indicates live radiation administration.

17. Image acquisition is very sensitive to movement. All patients should be actively encouraged to keep as motionless as possible.

18. If at any stage you need to abandon the procedure, press SPACEBAR or F4.

XIII.   Relatives

8. A parent, guardian, carer or relative can be present in the room. Maximum number is 1 other person.

9. They must sit in the chairs furthest from the scanner by the wall. Radiation risk is minimal, but as will be sat 2 meters away this decreases potential radiation exposure by >4-fold.

XIV.   Analysis of Results.

1. All scan results are available immediately after the scan. Run AUTO analysis. Select
    Tables. Cortical and trabecular bone mineral density, endosteal circumference,
    periosteal circumference, bone mineral content will be available by pressing page up or
    page down.

2. Also run 'NICLOOP' for analysis for CVDBone Study

Appendix
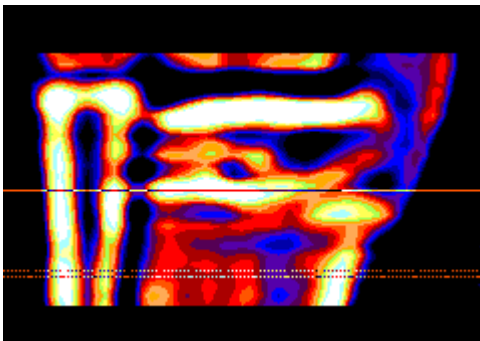
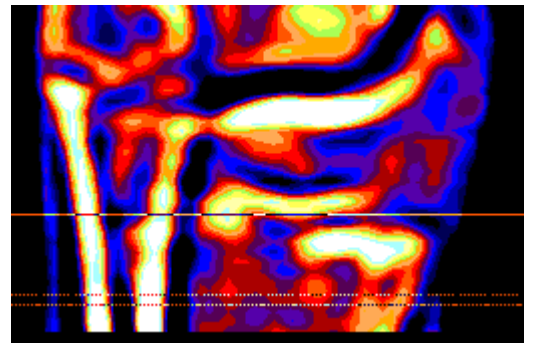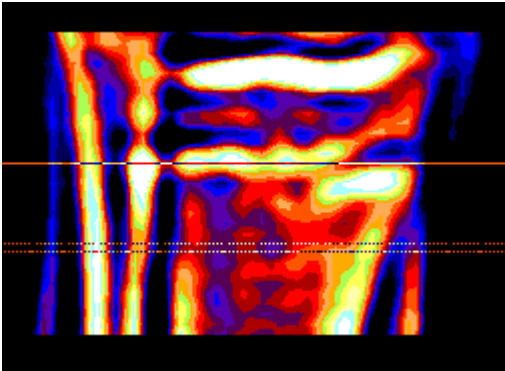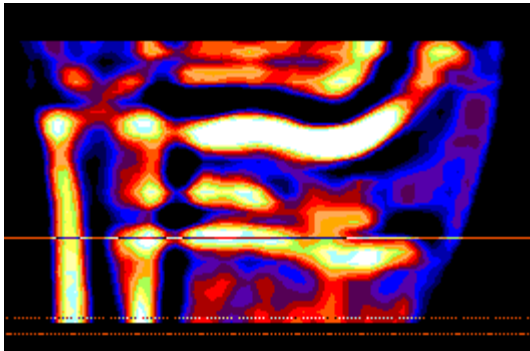1. Scout View Reference line placement examples

Males
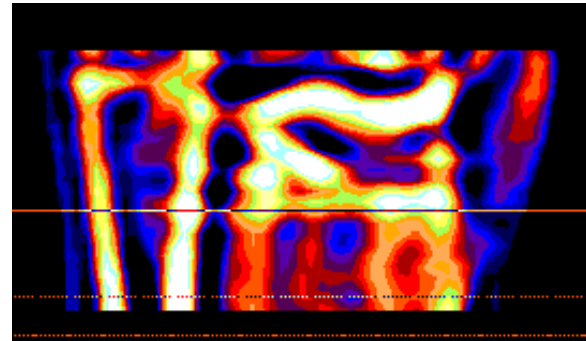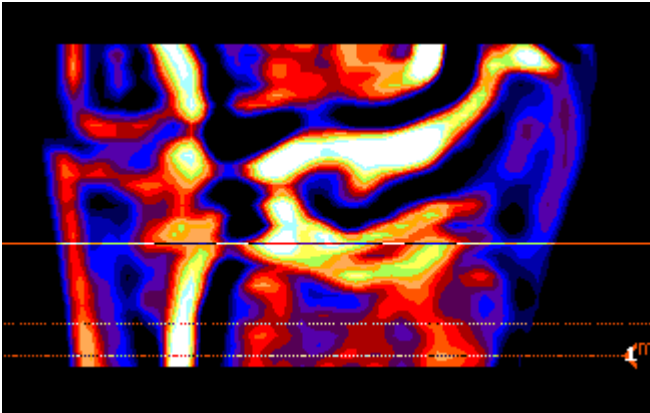
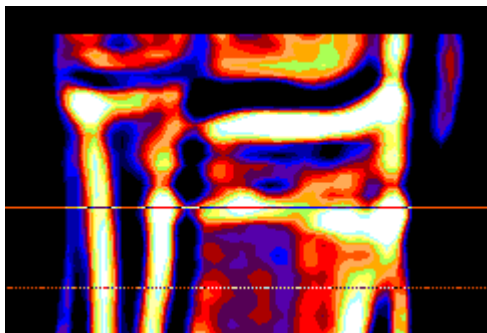5 years
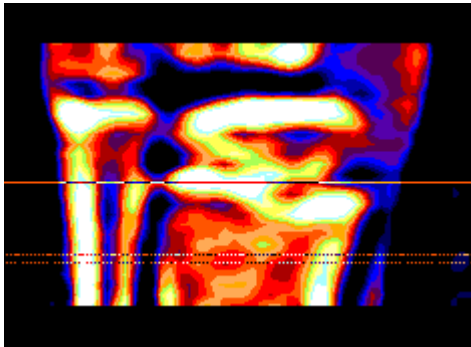
6 years
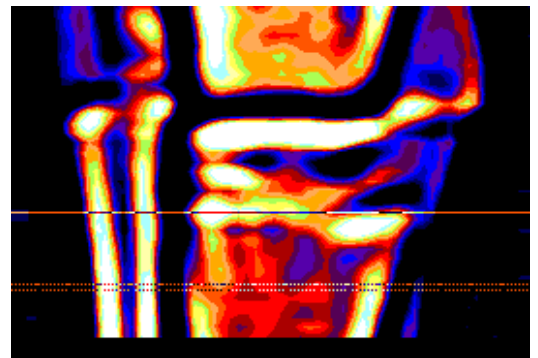
7 years
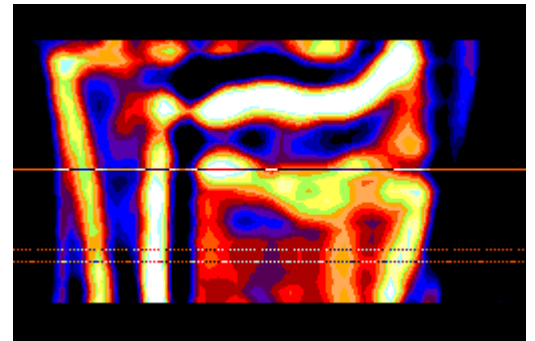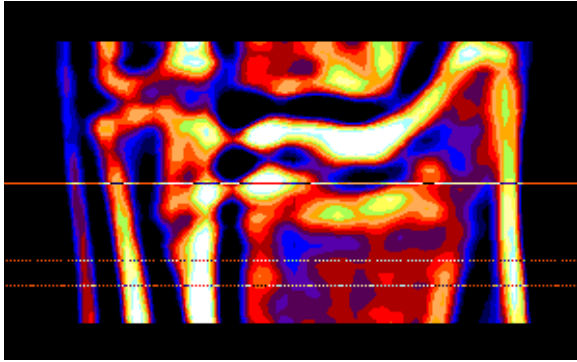

8 years

9 years
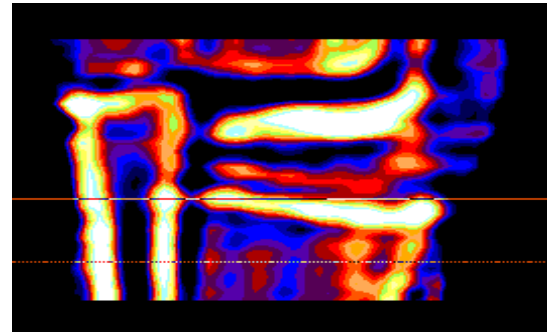
10 years

11 years
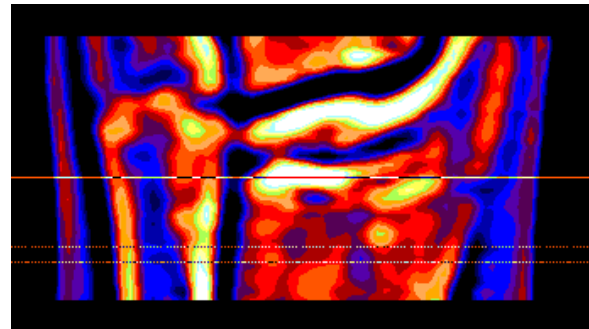
12 years

13 years
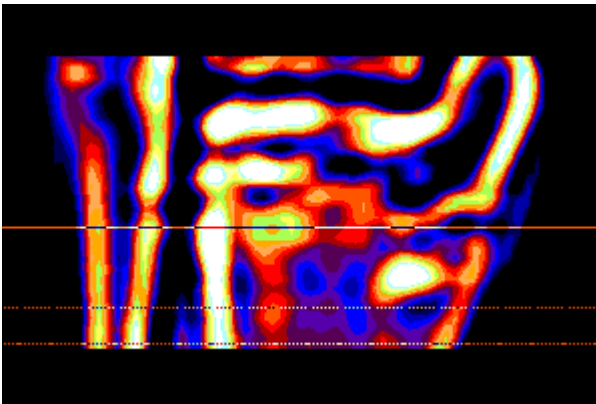
14 years
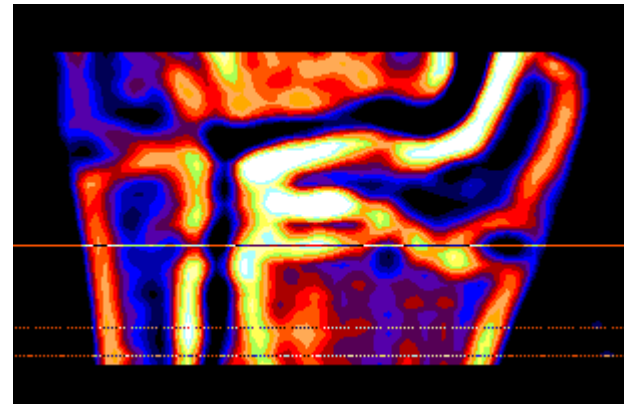
≥15 years

Females

7 years

8 years

9 years
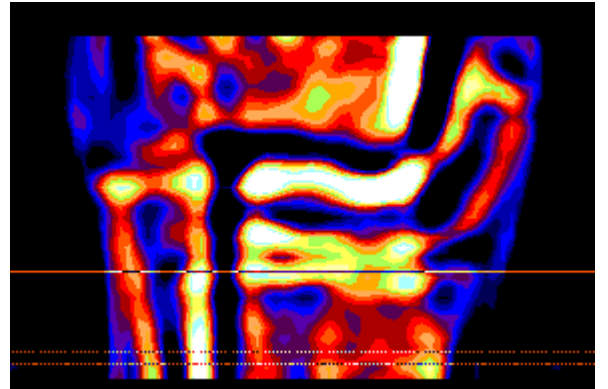
10 years
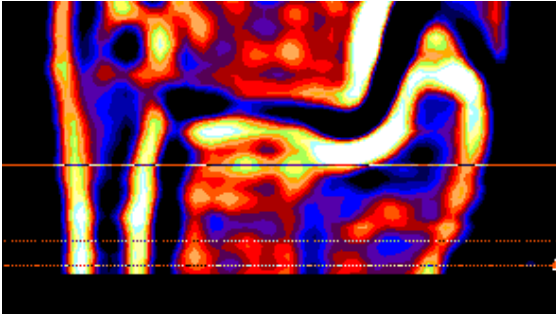
13 years
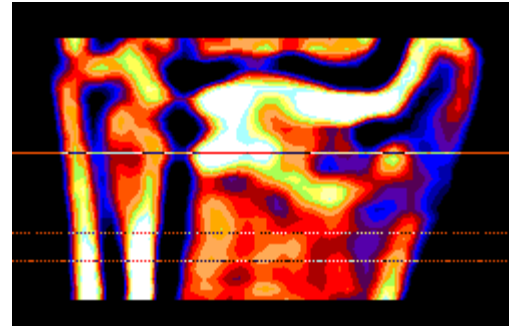
14 years
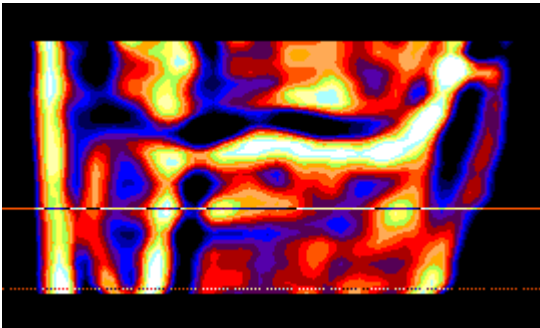
15 years
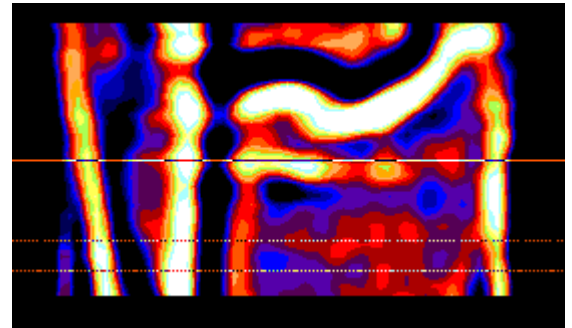
≥16 years

pQCT images
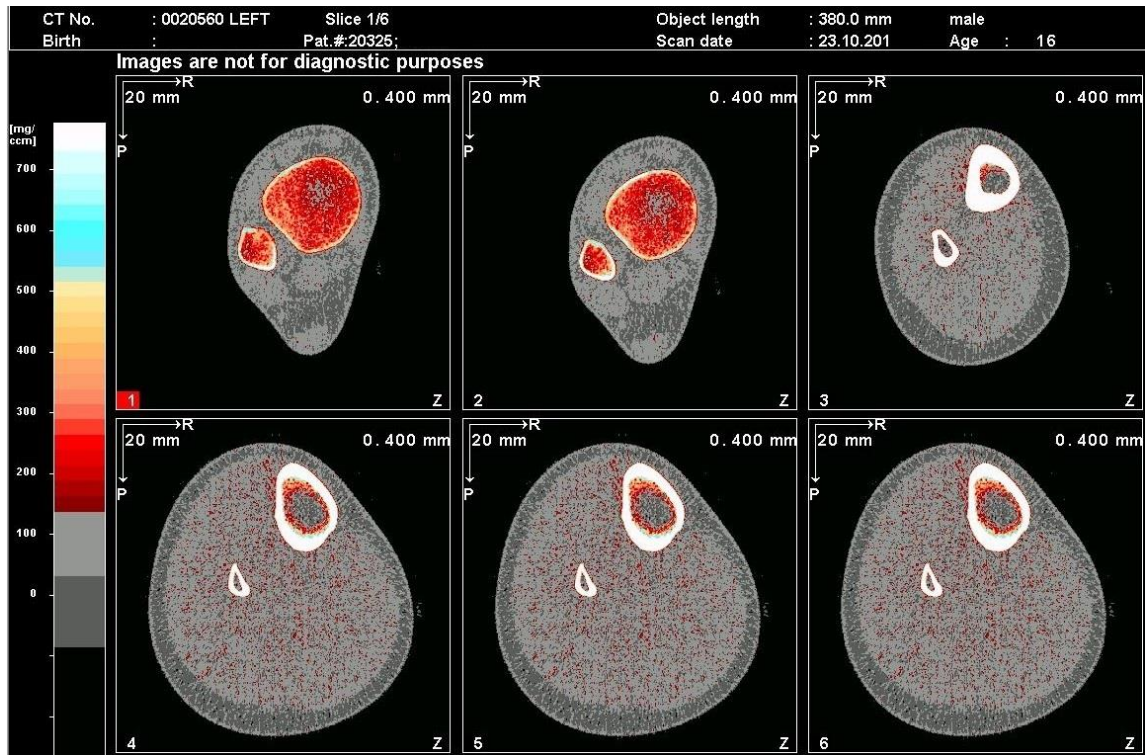
This is an example of pQCT imaging of the left tibia of a 16 year old male with chronic kidney disease. The images have been obtained at 4 different sites along the tibia. The software then proceeds to automatic analysis of the bone parameters. In this example, the images are from the 3%, 4%, 38% and 66% sites.
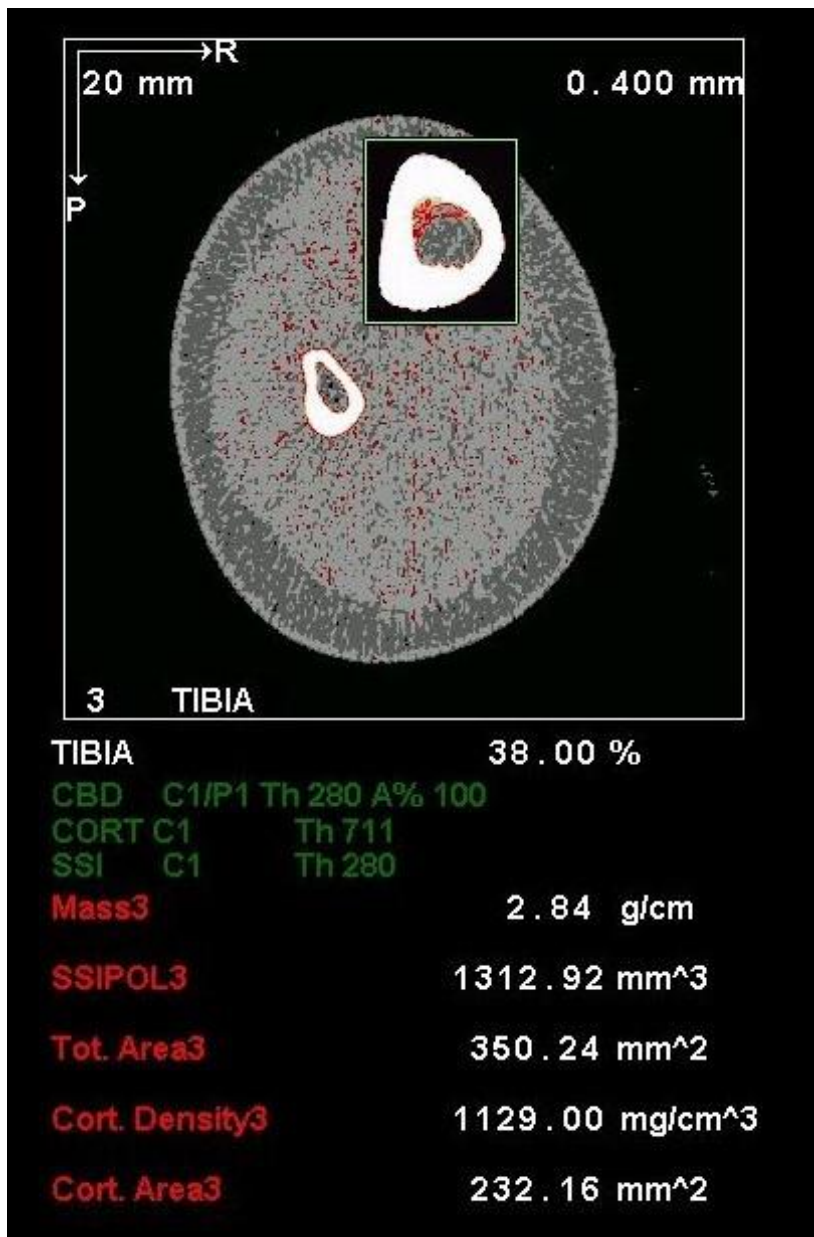
This is an example of the analysis of the 38% site of the left tibia of a 16 yr old male with chronic kidney disease. In this particular analysis the total mass, total area, cortical area, and cortical density have been given.

Appendix D- Standard Operating Procedure of carotid intima-media thickness (IMT) measurements for CVDBone

XV.   Device
3.   Use Vivid Iq (GE Healthcare, USA) ultrasonographic device.
4.   Linear probe (12L-RS)5-13 MHz

XVI.   Site of measurements
3.   Common carotid artery (CCA), 1 – 2 cm below bifurcation.
4.   Measurements are taken from right and left arteries.

XVII.   Patient position and preparation to examination.
7.   Use temperature controlled room, with 10 mins rest prior to examination
8.   Supine position with slightly extended neck
9.   Concurrent BP measurement on the ipsilateral upper limb to the carotid to be measured. ***Avoid that limb if fistula present***
10. Open new patient examination on software. Insert patient study ID (CALBAL###), date of birth and sex. No other identifiable information to be entered.

XVIII.   IMT measurements
1.   Three lead ECG electrodes connected, using general convention (Red lead to Right shoulder, Yellow lead to Left shoulder and Green lead to left/right side of abdomen)
2.   Carotid function selected on software
3.   Patient study number, sex and date of birth entered into software
4.   CCA identified in transverse view
5.   CCA identified in longitudinal view by rotating probe
6.   Distance of CCA 1 – 2 cm below bifurcation identified
7.   A minimum of 3x five second videos of this view obtained for each carotid.
8.   Both the far wall of the CCA and the 'lead II' electrocardiogram were visible during recording. If they were not, recording repeated.

XIX.   Measurement of wall cross-sectional area
1.   Obtain longitudinal view of CCA in B-mode
2.   Switch to M-mode to obtain vessel wall and electrocardiogram views
3.   Concurrent BP should be measured on corresponding upper limb
4.   A minimum of 3x 5 second video recordings should be obtained for each carotid
5.   Offline and in a semi-blinded fashion: The video with the optimal views to be frozen and the systolic internal diameter of CCA – the distance between two most distal points

of near and far wall were measured. At least 5 – 6 measurements were taken and averaged for each carotid.

6. Then the diastolic internal diameter of the CCA to be measured – using the smallest distance between near and far wall.
7. This process to be repeated for the contra-lateral side.

XX.   Calculations.

3. All IMT results should be averaged (sum of all recordings divided by the number of measurements) for each side. Then add results of right and left IMT and divide by 2. The result will be mean IMT.
4. The same for internal systolic and diastolic diameters.
5. Calculate WCSA, LCSA for left and right side.
6. Calculate mean WCSA.
7. Calculate distensibility coefficient (See Figure Below)

Figure 1. Schematic representation of cIMT, and calculations to be used

Mean systolic diameter (sD) = (LsD + RsD)/2

Mean diastolic diameter (dD) = (RdD + LdD)/2

Wall cross sectional area (WCSA) = $\pi*(dD/2 + IMT)^2 - \pi*(dD/2)^2$

Lumen cross sectional area (LCSA) = $\pi *dD^2/4$

Distensibility coefficient = $2(\Delta D/dD)/(\Delta P/10*1.33*100)$

LsD = left common carotid artery systolic diameter
RsD = right common carotid artery systolic diameter
LdD = left common carotid artery diastolic diameter
RdD = right common carotid artery diastolic diameter
IMT = carotid intima media thickness
ΔD = sD - dD
ΔP = Systolic BP- Diastolic BP

Figure 2 Still image of a CCA with the software identifying the intima and media layers, as highlighted between the green lines

	Max	Mean	SD	QI	Points
Near	0.55 mm	0.47 mm	0.06 mm	0.26	41
Far	0.52 mm	0.43 mm	0.04 mm	0.94	150
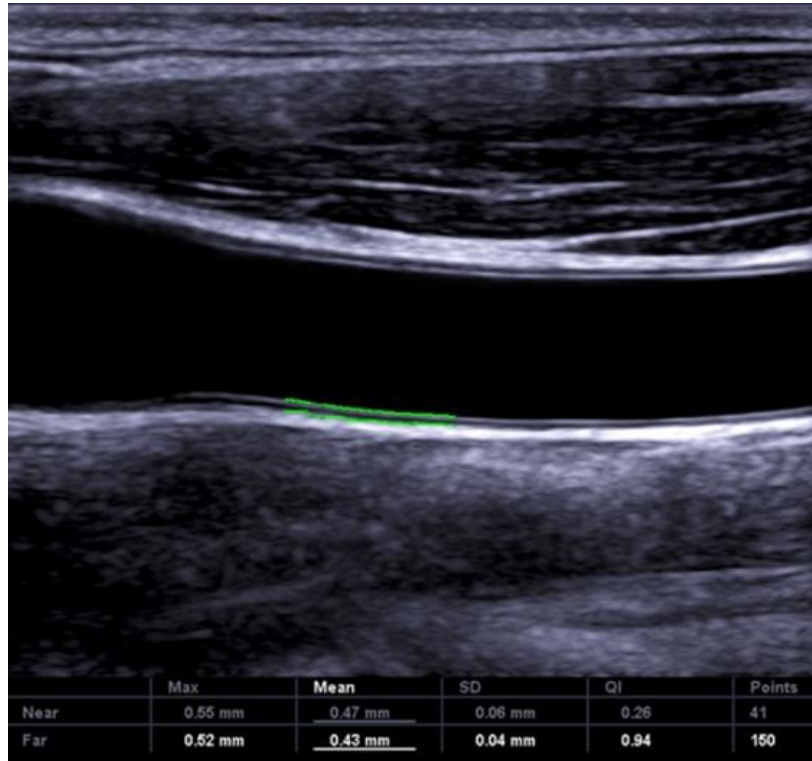
Figure 3 Still image of an M-Mode capture of a Left CCA. Visible are the B-mode transverse view of the vessel, the M-mode plain and the simultaneous 'lead II' electrocardiogram
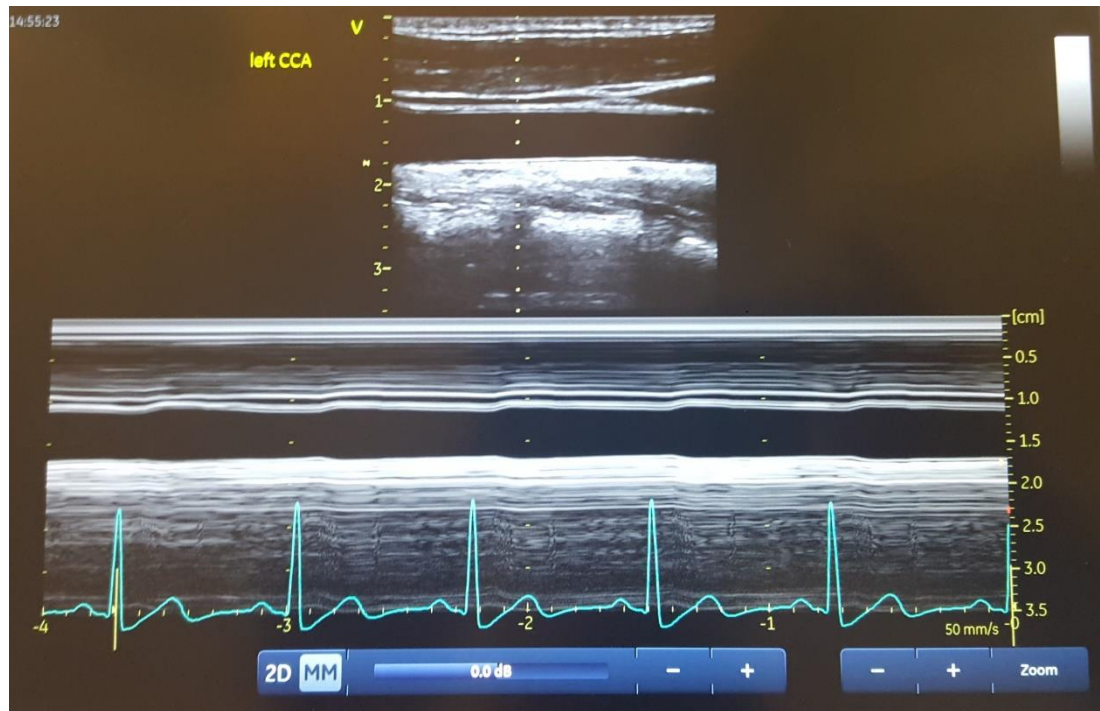
Appendix E- Pulse Wave Velocity (PWV), Pulse Wave Analysis (PWA), and Augmentation Index (AI) measurements Standard Operating Procedure

As per (Kracht et al., 2011)

VI. Device
5. Oscillometric Vicorder system with Toshiba Laptop (Skidmore Medical, Bristol, UK; Software Version 8.1)
6. Neck cuff, femoral cuff

VII. Entering a new Participant
1. Turn on laptop once Vicorder device connected
2. Double-click Vicorder Software
3. Click on 'New Patient'
4. Enter CALBAL as last name
5. Enter study number (xyz) as first name
6. Enter CALBALxyz as ID number
7. Enter weight, height and Save

VIII. Positioning and cuff placement
4. Participant should be in a quiet and air-conditioned room. Measurements should be taken after at least 5 minutes of rest lying supine. The participant should be asked to lie in supine position with a 30° elevated head and shoulders.
5. The neck cuff should be placed around the neck, with the small inflatable pad placed above the right common carotid artery.
6. The femoral cuff should be placed around the upper right thigh as close to the groin as possible. The air tubing should be facing superiorly. If able, the participants should help with this task. All items should be removed from the right pocket prior to this.

IX.   Distance measurement between cuffs
As per Kracht et al, 2011 (Kracht et al., 2011), the distances should be measured as:

Suprasternal notch to umbilicus (SSN to Umb)

Umbilicus to mid thigh cuff (Umb to Tcuff)

Suprasternal notch to mid neck cuff (SSN to Ncuff)

Carotid Cuff

Suprasternal notch

Umbilicus

Thigh Cuff
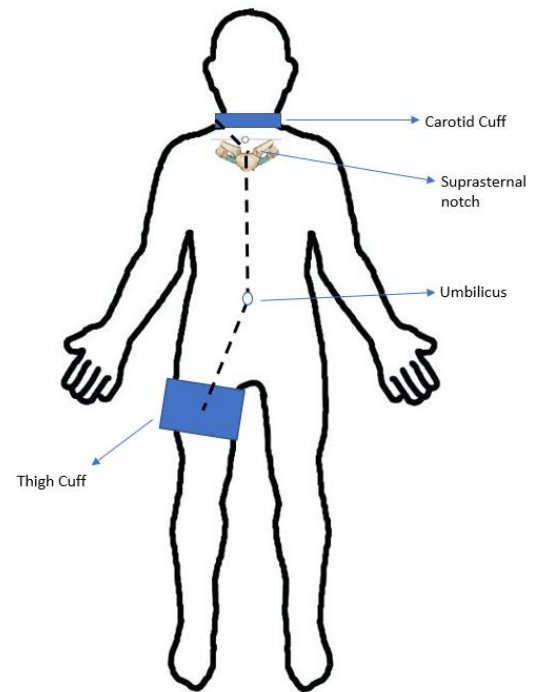
3. The 'length' to be entered for the PWV measurement should be calculated as:

Length= (SSN to Umb)+ (Umb to Tcuff)- (SSN to Ncuff)

4. Measure BP in left upper arm with manual sphygmomanometer immediately prior to examination (or right upper arm if fistula present in left arm)

X.   PWV measurements
5. Select participant to be measured and under the 'Quick Launch' menu, select 'PWV'.
6. Enter the 'length' as described above
7. Ensure the file will be saved under C:/Desktop/CVDBone/Hospital/xyz
8. Click 'OK'
9. Press Spacebar to inflate cuffs
10. Once at least 10 beats have registered which are of adequate quality, press Spacebar again.
11. Press Enter to save
12. If waveforms are erratic or of poor quality, don't save, but repeat with Spacebar
13. Repeat this for a total of 3 times, each > 10 beats per recording.

Example of good quality reading:
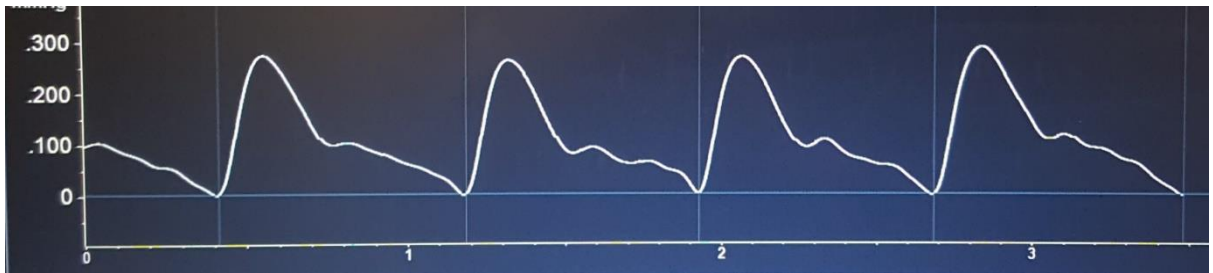
Example of poor quality reading:
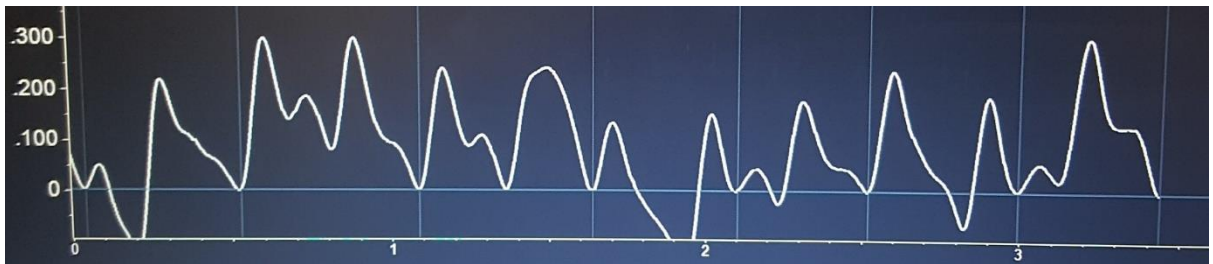
XI.   PWA & AI measurements
1. Positioning of the participant is the same as per PWV
2. Under quick launch menu select PWA
3. Take auscultatory blood pressure with manual sphygmomanometer 3 times. Take average reading of systolic and diastolic blood pressure and enter into relevant boxes.
4. Place the cuff on the right upper arm as high as possible to the shoulder. (Use left arm if fistula present in right arm)
5. Connect red wire to the arm cuff
6. Ask participant to relax and keep arm as still as possible
7. Press spacebar to inflate cuff
8. When at least 10 beats have registered and the software has calculated all parameters, press spacebar again to freeze
9. Press enter to save to file

Example of adequate readings and calculated parameters:

BP	105/65	mmHg	AoBP	100/65	mmHg
PP	40	mmHg	AoPP	35	mmHg
SEVR	167	%	Aug Press	4	mmHg
HR	74	BPM	Aug Index	13	%
MAP	83	mmHg	Beats	17	
ESP	92.00		ESPI	0.77	
SV	71	ml	TPR	0.95	PRU
CO	5.22	L/Min	CI	3.32	

T1 = 92ms
T2 = 176ms
T3 = 309ms
TR = 42ms
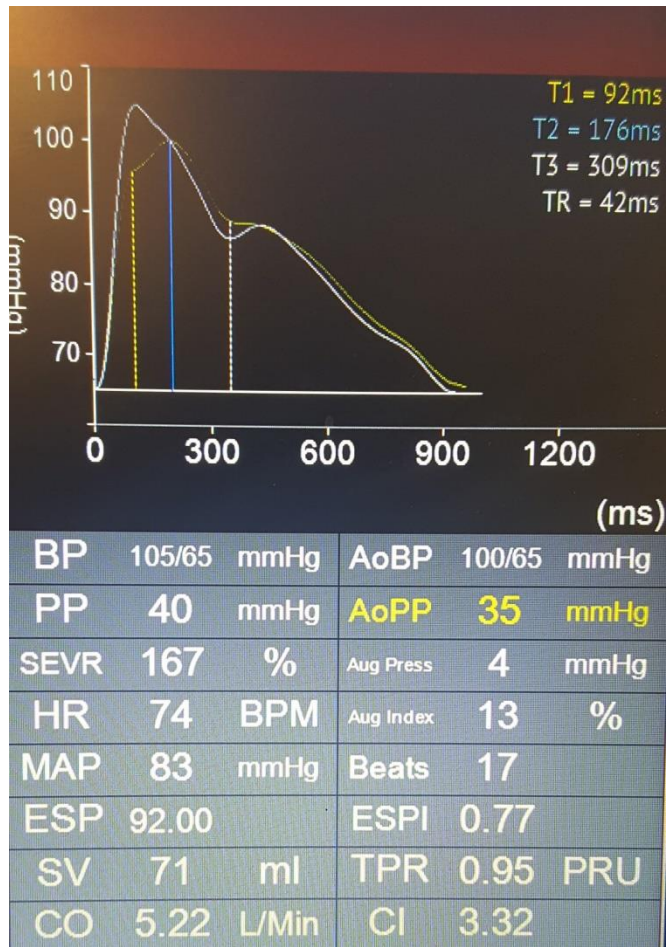
Ensure the C:/Desktop/CVDBone file is regularly backed up onto an external hard drive.

Appendix F- Standard Operating Procedure for Cardiac CTs for Calcium Scoring

The scans are for research purposes for the CVDBone Study looking at calcium, bone health and cardiovascular health in children and young adults with chronic kidney disease.

The purpose of this scan is to look for calcium deposits in the coronary vessels.

I.   Type of Imaging
     Non-contrast Prospective ECG-Gated Cardiac CTs

II. Devices
     7. GE Discovery 750HD at the Birmingham Children's Hospital
     8. Siemens Healthcare Somatom Force at Great Ormond Street

III. Patient position and preparation to examination.
     Position patient feet first (the same as a Chest CT) and apply ECG pads and leads correctly

IV. Site of measurements
     Carry out the Topogram as per a normal Chest CT.

     Plan the Scan range (Range of Interest) from the top of the Aortic Arch to Apex of Heart.

V.   Measurements
     The protocol you must use is in Child option and then in the Cardiac Section.

     Please select **DS_CaScore_AdaptSeq (Child)**
     This scan uses dose modulation (Care kV and Care Dose 4D)

DS Calcium Score Sequence	Ref. mAs	Ref. kVp	Tube Rotation time	Collimation	Slice scan width	Scan Time
Child	80	120	0.25s	1.2mm	3mm	0.14s

Select 'Cardiac Trigger Tab':

   - If the heart rate is **below** 75 trigger phase start at 70%

   - If the heart rate is **above** 75 trigger phase start at 40%

If heart rate is jumping between the two select 40%

The scans should be performed with Breathing Instructions on Inspiration.

VI.   After the Scan

Send images to PACs

Please protect the study on the work station when finished.

The scan will be reviewed by the Named Consultant at each research site for governance reporting.

Calcium scoring will be done by Dr Kristian Mortensen, Consultant Radiologist at Great Ormond Street.

References

Abrams, S. A. (1999) 'Using stable isotopes to assess mineral absorption and utilization by children', *Am J Clin Nutr,* 70(6), pp. 955-64.

Abrams, S. A., Esteban, N. V., Vieira, N. E. and Yergey, A. L. (1991) 'Dual tracer stable isotopic assessment of calcium absorption and endogenous fecal excretion in low birth weight infants', *Pediatr Res,* 29(6), pp. 615-8.

Adamczyk, P., Szczepanska, M. and Pluskiewicz, W. (2018) 'Skeletal status assessment by quantitative ultrasound and bone densitometry in children with different renal conditions', *Osteoporos Int*.

Adams, J. E., Engelke, K., Zemel, B. S. and Ward, K. A. (2014) 'Quantitative computer tomography in children and adolescents: the 2013 ISCD Pediatric Official Positions', *J Clin Densitom,* 17(2), pp. 258-74.

Adragao, T., Branco, P., Birne, R., Curto, J. D., de Almeida, E., Prata, M. M. and Pais, M. J. (2008) 'Bone mineral density, vascular calcifications, and arterial stiffness in peritoneal dialysis patients', *Perit Dial Int,* 28(6), pp. 668-72.

Adragao, T., Herberth, J., Monier-Faugere, M. C., Branscum, A. J., Ferreira, A., Frazao, J. M., Dias Curto, J. and Malluche, H. H. (2009) 'Low bone volume--a risk factor for coronary calcifications in hemodialysis patients', *Clin J Am Soc Nephrol,* 4(2), pp. 450-5.

Agatston, A. S., Janowitz, W. R., Hildner, F. J., Zusmer, N. R., Viamonte, M., Jr. and Detrano, R. (1990) 'Quantification of coronary artery calcium using ultrafast computed tomography', *J Am Coll Cardiol,* 15(4), pp. 827-32.

Alem, A. M., Sherrard, D. J., Gillen, D. L., Weiss, N. S., Beresford, S. A., Heckbert, S. R., Wong, C. and Stehman-Breen, C. (2000) 'Increased risk of hip fracture among patients with end-stage renal disease', *Kidney Int,* 58(1), pp. 396-9.

Amato, M., Montorsi, P., Ravani, A., Oldani, E., Galli, S., Ravagnani, P. M., Tremoli, E. and Baldassarre, D. (2007) 'Carotid intima-media thickness by B-mode ultrasound as surrogate of coronary atherosclerosis: correlation with quantitative coronary angiography and coronary intravascular ultrasound findings', *Eur Heart J,* 28(17), pp. 2094-101.

Andrade, M. C., Carvalhaes, J. T., Carvalho, A. B., Lazarretti-Castro, M. and Brandao, C. (2007) 'Bone mineral density and bone histomorphometry in children on long-term dialysis', *Pediatr Nephrol,* 22(10), pp. 1767-72.

Asci, G., Ok, E., Savas, R., Ozkahya, M., Duman, S., Toz, H., Kayikcioglu, M., Branscum, A. J., Monier-Faugere, M. C., Herberth, J. and Malluche, H. H. (2011) 'The link between bone and coronary calcifications in CKD-5 patients on haemodialysis', *Nephrol Dial Transplant,* 26(3), pp. 1010-5.

Ashby, R. L., Ward, K. A., Roberts, S. A., Edwards, L., Mughal, M. Z. and Adams, J. E. (2009) 'A reference database for the Stratec XCT-2000 peripheral quantitative computed tomography (pQCT) scanner in healthy children and young adults aged 6-19 years', *Osteoporos Int,* 20(8), pp. 1337-46.

Azukaitis, K., Jankauskiene, A., Schaefer, F. and Shroff, R. (2020) 'Pathophysiology and consequences of arterial stiffness in children with chronic kidney disease', *Pediatr Nephrol*.

Bacchetta, J., Boivin, G. and Cochat, P. (2016) 'Bone impairment in primary hyperoxaluria: a review', *Pediatr Nephrol,* 31(1), pp. 1-6.

Bacchetta, J., Harambat, J., Cochat, P., Salusky, I. B. and Wesseling-Perry, K. (2012) 'The consequences of chronic kidney disease on bone metabolism and growth in children', *Nephrol Dial Transplant,* 27(8), pp. 3063-71.

Bachrach, L. K., Hastie, T., Wang, M. C., Narasimhan, B. and Marcus, R. (1999) 'Bone mineral acquisition in healthy Asian, Hispanic, black, and Caucasian youth: a longitudinal study', *J Clin Endocrinol Metab,* 84(12), pp. 4702-12.

Baker, J. F., Davis, M., Alexander, R., Zemel, B. S., Mostoufi-Moab, S., Shults, J., Sulik, M., Schiferl, D. J. and Leonard, M. B. (2013) 'Associations between body composition and bone density and structure in men and women across the adult age spectrum', *Bone,* 53(1), pp. 34-41.

Baker, J. F., Long, J., Mostoufi-Moab, S., Denburg, M., Jorgenson, E., Sharma, P., Zemel, B. S., Taratuta, E., Ibrahim, S. and Leonard, M. B. (2017) 'Muscle Deficits in Rheumatoid Arthritis Contribute to Inferior Cortical Bone Structure and Trabecular Bone Mineral Density', *J Rheumatol,* 44(12), pp. 1777-1785.

Bakkaloglu, S. A., Bacchetta, J., Lalayiannis, A. D., Leifheit-Nestler, M., Stabouli, S., Haarhaus, M., Reusz, G., Groothoff, J., Schmitt, C. P., Evenepoel, P., Shroff, R. and Haffner, D. (2020) 'Bone evaluation in paediatric chronic kidney disease: Clinical practice points from the European Society for Paediatric Nephrology CKD-MBD and Dialysis working groups and CKD-MBD working group of the ERA-EDTA', *Nephrol Dial Transplant*.

Bakkaloglu, S. A., Wesseling-Perry, K., Pereira, R. C., Gales, B., Wang, H. J., Elashoff, R. M. and Salusky, I. B. (2010) 'Value of the new bone classification system in pediatric renal osteodystrophy', *Clin J Am Soc Nephrol,* 5(10), pp. 1860-6.

Bakr, A. M. (2004) 'Bone mineral density and bone turnover markers in children with chronic renal failure', *Pediatr Nephrol,* 19(12), pp. 1390-3.

Ball, A. M., Gillen, D. L., Sherrard, D., Weiss, N. S., Emerson, S. S., Seliger, S. L., Kestenbaum, B. R. and Stehman-Breen, C. (2002) 'Risk of hip fracture among dialysis and renal transplant recipients', *Jama,* 288(23), pp. 3014-8.

Ballanti, P., Wedard, B. M. and Bonucci, E. (1996) 'Frequency of adynamic bone disease and aluminum storage in Italian uraemic patients--retrospective analysis of 1429 iliac crest biopsies', *Nephrol Dial Transplant,* 11(4), pp. 663-7.

Barreto, D. V., Barreto Fde, C., Carvalho, A. B., Cuppari, L., Draibe, S. A., Dalboni, M. A., Moyses, R. M., Neves, K. R., Jorgetti, V., Miname, M., Santos, R. D. and Canziani, M. E. (2008a) 'Association of changes in bone remodeling and coronary calcification in hemodialysis patients: a prospective study', *Am J Kidney Dis,* 52(6), pp. 1139-50.

Barreto, F. C., Barreto, D. V., Moysés, R. M. A., Neves, K. R., Canziani, M. E. F., Draibe, S. A., Jorgetti, V. and Carvalho, A. B. (2008b) 'K/DOQI-recommended intact PTH levels do not prevent low-turnover bone disease in hemodialysis patients', *Kidney International,* 73(6), pp. 771-777.

Bartosh, S. M., Leverson, G., Robillard, D. and Sollinger, H. W. (2003) 'Long-term outcomes in pediatric renal transplant recipients who survive into adulthood', *Transplantation,* 76(8), pp. 1195-200.

Bashir, A., Moody, W. E., Edwards, N. C., Ferro, C. J., Townend, J. N. and Steeds, R. P. (2015) 'Coronary Artery Calcium Assessment in CKD:

Utility in Cardiovascular Disease Risk Assessment and Treatment?', *American Journal of Kidney Diseases,* 65(6), pp. 937-948.

Baxter-Jones, A. D., Faulkner, R. A., Forwood, M. R., Mirwald, R. L. and Bailey, D. A. (2011) 'Bone mineral accrual from 8 to 30 years of age: an estimation of peak bone mass', *J Bone Miner Res,* 26(8), pp. 1729-39.

Behets, G. J., Spasovski, G., Sterling, L. R., Goodman, W. G., Spiegel, D. M., De Broe, M. E. and D'Haese, P. C. (2015) 'Bone histomorphometry before and after long-term treatment with cinacalcet in dialysis patients with secondary hyperparathyroidism', *Kidney Int,* 87(4), pp. 846-56.

Ben-Shlomo, Y., Spears, M., Boustred, C., May, M., Anderson, S. G., Benjamin, E. J., Boutouyrie, P., Cameron, J., Chen, C. H., Cruickshank, J. K., Hwang, S. J., Lakatta, E. G., Laurent, S., Maldonado, J., Mitchell, G. F., Najjar, S. S., Newman, A. B., Ohishi, M., Pannier, B., Pereira, T., Vasan, R. S., Shokawa, T., Sutton-Tyrell, K., Verbeke, F., Wang, K. L., Webb, D. J., Willum Hansen, T., Zoungas, S., McEniery, C. M., Cockcroft, J. R. and Wilkinson, I. B. (2014) 'Aortic pulse wave velocity improves cardiovascular event prediction: an individual participant meta-analysis of prospective observational data from 17,635 subjects', *J Am Coll Cardiol,* 63(7), pp. 636-46.

Binkley, T. L., Specker, B. L. and Wittig, T. A. (2002) 'Centile curves for bone densitometry measurements in healthy males and females ages 5-22 yr', *J Clin Densitom,* 5(4), pp. 343-53.

Bland, J. M. and Altman, D. G. (1986) 'Statistical methods for assessing agreement between two methods of clinical measurement', *Lancet,* 1(8476), pp. 307-10.

Blew, R. M., Lee, V. R., Farr, J. N., Schiferl, D. J. and Going, S. B. (2014) 'Standardizing evaluation of pQCT image quality in the presence of subject movement: qualitative versus quantitative assessment', *Calcified tissue international,* 94(2), pp. 202-211.

Block, G. A., Klassen, P. S., Lazarus, J. M., Ofsthun, N., Lowrie, E. G. and Chertow, G. M. (2004) 'Mineral metabolism, mortality, and morbidity in maintenance hemodialysis', *J Am Soc Nephrol,* 15(8), pp. 2208-18.

Bonewald, L. F. (2011) 'The amazing osteocyte', *J Bone Miner Res,* 26(2), pp. 229-38.

Bonjour, J. P., Carrie, A. L., Ferrari, S., Clavien, H., Slosman, D., Theintz, G. and Rizzoli, R. (1997) 'Calcium-enriched foods and bone mass growth in prepubertal girls: a randomized, double-blind, placebo-controlled trial', *Journal of Clinical Investigation,* 99(6), pp. 1287-1294.

Bonthuis, M., Busutti, M., van Stralen, K. J., Jager, K. J., Baiko, S., Bakkaloğlu, S., Battelino, N., Gaydarova, M., Gianoglio, B., Parvex, P., Gomes, C., Heaf, J. G., Podracka, L., Kuzmanovska, D., Molchanova, M. S., Pankratenko, T. E., Papachristou, F., Reusz, G., Sanahuja, M. J., Shroff, R., Groothoff, J. W., Schaefer, F. and Verrina, E. (2015) 'Mineral Metabolism in European Children Living with a Renal Transplant: A European Society for Paediatric Nephrology/European Renal Association–European Dialysis and Transplant Association Registry Study', *Clinical Journal of the American Society of Nephrology : CJASN,* 10(5), pp. 767-775.

Borzych, D., Rees, L., Ha, I. S., Chua, A., Valles, P. G., Lipka, M., Zambrano, P., Ahlenstiel, T., Bakkaloglu, S. A., Spizzirri, A. P., Lopez, L., Ozaltin, F., Printza, N., Hari, P., Klaus, G., Bak, M., Vogel, A., Ariceta, G., Yap, H. K., Warady, B. A. and Schaefer, F. (2010) 'The bone and mineral disorder of children undergoing chronic peritoneal dialysis', *Kidney Int,* 78(12), pp. 1295-304.

Brady, T. M., Schneider, M. F., Flynn, J. T., Cox, C., Samuels, J., Saland, J., White, C. T., Furth, S., Warady, B. A. and Mitsnefes, M. (2012) 'Carotid intima-media thickness in children with CKD: results from the CKiD study', *Clin J Am Soc Nephrol,* 7(12), pp. 1930-7.

Briese, S., Wiesner, S., Will, J. C., Lembcke, A., Opgen-Rhein, B., Nissel, R., Wernecke, K. D., Andreae, J., Haffner, D. and Querfeld, U. (2006) 'Arterial and cardiac disease in young adults with childhood-onset end-stage renal disease-impact of calcium and vitamin D therapy', *Nephrol Dial Transplant,* 21(7), pp. 1906-14.

Briet, M., Bozec, E., Laurent, S., Fassot, C., London, G. M., Jacquot, C., Froissart, M., Houillier, P. and Boutouyrie, P. (2006) 'Arterial stiffness and enlargement in mild-to-moderate chronic kidney disease', *Kidney International,* 69(2), pp. 350-357.

Burt, L. A., Liang, Z., Sajobi, T. T., Hanley, D. A. and Boyd, S. K. (2016) 'Sex- and Site-Specific Normative Data Curves for HR-pQCT', *J Bone Miner Res,* 31(11), pp. 2041-2047.

Bushinsky, D. A. (2010) 'Contribution of intestine, bone, kidney, and dialysis to extracellular fluid calcium content', *Clin J Am Soc Nephrol,* 5 Suppl 1, pp. S12-22.

Buyukkaragoz, B., Bakkaloglu, S. A., Kandur, Y., Isiyel, E., Akcaboy, M., Buyan, N. and Hasanoglu, E. (2015) 'The evaluation of bone metabolism in children with renal transplantation', *Pediatr Transplant,* 19(4), pp. 351-7.

Cadogan, J., Eastell, R., Jones, N. and Barker, M. E. (1997) 'Milk intake and bone mineral acquisition in adolescent girls: randomised, controlled intervention trial', *BMJ : British Medical Journal,* 315(7118), pp. 1255-1260.

Carrillo-Lopez, N., Panizo, S., Alonso-Montes, C., Roman-Garcia, P., Rodriguez, I., Martinez-Salgado, C., Dusso, A. S., Naves, M. and Cannata-Andia, J. B. (2016) 'Direct inhibition of osteoblastic Wnt pathway by fibroblast growth factor 23 contributes to bone loss in chronic kidney disease', *Kidney Int,* 90(1), pp. 77-89.

Carter, D. R., Bouxsein, M. L. and Marcus, R. (1992) 'New approaches for interpreting projected bone densitometry data', *J Bone Miner Res,* 7(2), pp. 137-45.

Carvalho, C. G., Pereira, R. C., Gales, B., Salusky, I. B. and Wesseling-Perry, K. (2015) 'Cortical and trabecular bone in pediatric end-stage kidney disease', *Pediatr Nephrol,* 30(3), pp. 497-502.

Cejka, D., Weber, M., Diarra, D., Reiter, T., Kainberger, F. and Haas, M. (2014) 'Inverse association between bone microarchitecture assessed by HR-pQCT and coronary artery calcification in patients with end-stage renal disease', *Bone,* 64, pp. 33-8.

Chan, G. M., Hoffman, K. and McMurry, M. (1995) 'Effects of dairy products on bone and body composition in pubertal girls', *J Pediatr,* 126(4), pp. 551-6.

Chastin, S. F., Mandrichenko, O. and Skelton, D. A. (2014) 'The frequency of osteogenic activities and the pattern of intermittence between periods of physical activity and sedentary behaviour affects bone mineral content: the cross-sectional NHANES study', *BMC public health,* 14, pp. 4-4.

Chavarria, L. A., Aguilar-Kitsu, A., Rosas, P., Fajardo, A., Mendoza-Guevara, L., Sanchez, L., Zepeda, C., Ibarra, P., Luna, A., Lindholm, B. and

Garcia-Lopez, E. (2012) 'Intima media thickness in children undergoing dialysis', *Pediatr Nephrol,* 27(9), pp. 1557-64.

Chavers, B. M., Li, S., Collins, A. J. and Herzog, C. A. (2002) 'Cardiovascular disease in pediatric chronic dialysis patients', *Kidney Int,* 62(2), pp. 648-53.

Chen, H., Tian, X., Liu, X., Setterberg, R. B., Li, M. and Jee, W. S. (2008) 'Alfacalcidol-stimulated focal bone formation on the cancellous surface and increased bone formation on the periosteal surface of the lumbar vertebrae of adult female rats', *Calcif Tissue Int,* 82(2), pp. 127-36.

Chen, J., Budoff, M. J., Reilly, M. P., Yang, W., Rosas, S. E., Rahman, M., Zhang, X., Roy, J. A., Lustigova, E., Nessel, L., Ford, V., Raj, D., Porter, A. C., Soliman, E. Z., Wright, J. T., Jr., Wolf, M. and He, J. (2017) 'Coronary Artery Calcification and Risk of Cardiovascular Disease and Death Among Patients With Chronic Kidney Disease', *JAMA Cardiol,* 2(6), pp. 635-643.

Chen, Z., Qureshi, A. R., Ripsweden, J., Wennberg, L., Heimburger, O., Lindholm, B., Barany, P., Haarhaus, M., Brismar, T. B. and Stenvinkel, P. (2016) 'Vertebral bone density associates with coronary artery calcification and is an independent predictor of poor outcome in end-stage renal disease patients', *Bone,* 92, pp. 50-57.

Chertow, G. M., Burke, S. K. and Raggi, P. (2002) 'Sevelamer attenuates the progression of coronary and aortic calcification in hemodialysis patients', *Kidney Int,* 62(1), pp. 245-52.

Chertow, G. M., Raggi, P., Chasan-Taber, S., Bommer, J., Holzer, H. and Burke, S. K. (2004) 'Determinants of progressive vascular calcification in haemodialysis patients', *Nephrol Dial Transplant,* 19(6), pp. 1489-96.

Chesnaye, N., Bonthuis, M., Schaefer, F., Groothoff, J. W., Verrina, E., Heaf, J. G., Jankauskiene, A., Lukosiene, V., Molchanova, E. A., Mota, C., Peco-Antic, A., Ratsch, I. M., Bjerre, A., Roussinov, D. L., Sukalo, A., Topaloglu, R., Van Hoeck, K., Zagozdzon, I., Jager, K. J. and Van Stralen, K. J. (2014) 'Demographics of paediatric renal replacement therapy in Europe: a report of the ESPN/ERA-EDTA registry', *Pediatr Nephrol,* 29(12), pp. 2403-10.

Chinali, M., Matteucci, M. C., Franceschini, A., Doyon, A., Pongiglione, G., Rinelli, G. and Schaefer, F. (2015) 'Advanced Parameters of Cardiac

Mechanics in Children with CKD: The 4C Study', *Clinical Journal of the American Society of Nephrology,* 10(8), pp. 1357.

Civilibal, M., Caliskan, S., Adaletli, I., Oflaz, H., Sever, L., Candan, C., Canpolat, N., Kasapcopur, O., Kuruoglu, S. and Arisoy, N. (2006) 'Coronary artery calcifications in children with end-stage renal disease', *Pediatr Nephrol,* 21(10), pp. 1426-33.

Civilibal, M., Caliskan, S., Kurugoglu, S., Candan, C., Canpolat, N., Sever, L., Kasapcopur, O. and Arisoy, N. (2009) 'Progression of coronary calcification in pediatric chronic kidney disease stage 5', *Pediatr Nephrol,* 24(3), pp. 555-63.

Civilibal, M., Caliskan, S., Oflaz, H., Sever, L., Candan, C., Canpolat, N., Kasapcopur, O., Bugra, Z. and Arisoy, N. (2007) 'Traditional and "new" cardiovascular risk markers and factors in pediatric dialysis patients', *Pediatr Nephrol,* 22(7), pp. 1021-9.

Clarke, B. (2008) 'Normal Bone Anatomy and Physiology', *Clin J Am Soc Nephrol,* Suppl 3(3), pp. S131-139.

Coco, M. and Rush, H. (2000) 'Increased incidence of hip fractures in dialysis patients with low serum parathyroid hormone', *Am J Kidney Dis,* 36(6), pp. 1115-21.

Coen, G., Ballanti, P., Bonucci, E., Calabria, S., Centorrino, M., Fassino, V., Manni, M., Mantella, D., Mazzaferro, S., Napoletano, I., Sardella, D. and Taggi, F. (1998) 'Bone markers in the diagnosis of low turnover osteodystrophy in haemodialysis patients', *Nephrol Dial Transplant,* 13(9), pp. 2294-302.

Cole, T. J., Freeman, J. V. and Preece, M. A. (1995) 'Body mass index reference curves for the UK, 1990', *Arch Dis Child,* 73(1), pp. 25-9.

Collins, A. J., Foley, R. N., Gilbertson, D. T. and Chen, S.-C. (2015) 'United States Renal Data System public health surveillance of chronic kidney disease and end-stage renal disease', *Kidney International Supplements,* 5(1), pp. 2-7.

Cooper, C., Dennison, E. M., Leufkens, H. G., Bishop, N. and van Staa, T. P. (2004) 'Epidemiology of childhood fractures in Britain: a study using the general practice research database', *J Bone Miner Res,* 19(12), pp. 1976-81.

Costa, L. R., Carvalho, A. B., Bittencourt, A. L., Rochitte, C. E. and Canziani, M. E. F. (2020) 'Cortical unlike trabecular bone loss is not associated

with vascular calcification progression in CKD patients', *BMC Nephrol,* 21(1), pp. 121.

Covic, A., Mardare, N., Gusbeth-Tatomir, P., Brumaru, O., Gavrilovici, C., Munteanu, M., Prisada, O. and Goldsmith, D. J. (2006) 'Increased arterial stiffness in children on haemodialysis', *Nephrol Dial Transplant,* 21(3), pp. 729-35.

Crabtree, N. and Ward, K. (2015) 'Bone Densitometry: Current Status and Future Perspective', *Endocr Dev,* 28, pp. 72-83.

Crabtree, N. J., Adams, J. E., Padidela, R., Shaw, N. J., Hogler, W., Roper, H., Hughes, I., Daniel, A. and Mughal, M. Z. (2018) 'Growth, bone health & ambulatory status of boys with DMD treated with daily vs. intermittent oral glucocorticoid regimen', *Bone,* 116, pp. 181-186.

Crabtree, N. J., Arabi, A., Bachrach, L. K., Fewtrell, M., El-Hajj Fuleihan, G., Kecskemethy, H. H., Jaworski, M. and Gordon, C. M. (2014) 'Dual-energy X-ray absorptiometry interpretation and reporting in children and adolescents: the revised 2013 ISCD Pediatric Official Positions', *J Clin Densitom,* 17(2), pp. 225-42.

Crabtree, N. J., Shaw, N. J., Bishop, N. J., Adams, J. E., Mughal, M. Z., Arundel, P., Fewtrell, M. S., Ahmed, S. F., Treadgold, L. A., Hogler, W., Bebbington, N. A. and Ward, K. A. (2017) 'Amalgamated Reference Data for Size-Adjusted Bone Densitometry Measurements in 3598 Children and Young Adults-the ALPHABET Study', *J Bone Miner Res,* 32(1), pp. 172-180.

Dangardt, F., Charakida, M., Chiesa, S., Bhowruth, D., Rapala, A., Thurn, D., Schaefer, F., Deanfield, J. and Shroff, R. (2018) 'Intimal and medial arterial changes defined by ultra-high-frequency ultrasound: Response to changing risk factors in children with chronic kidney disease', *PloS one,* 13(6), pp. e0198547-e0198547.

Daniels, M. W., Wilson, D. M., Paguntalan, H. G., Hoffman, A. R. and Bachrach, L. K. (2003) 'Bone mineral density in pediatric transplant recipients', *Transplantation,* 76(4), pp. 673-8.

de Simone, G., Daniels, S. R., Kimball, T. R., Roman, M. J., Romano, C., Chinali, M., Galderisi, M. and Devereux, R. B. (2005) 'Evaluation of concentric left ventricular geometry in humans: evidence for age-related systematic underestimation', *Hypertension,* 45(1), pp. 64-8.

DeBoer, M. D., Lee, A. M., Herbert, K., Long, J., Thayu, M., Griffin, L. M., Baldassano, R. N., Denson, L. A., Zemel, B. S., Denburg, M. R.,

Herskovitz, R. and Leonard, M. B. (2018) 'Increases in IGF-1 After Anti-TNF-alpha Therapy Are Associated With Bone and Muscle Accrual in Pediatric Crohn Disease', *J Clin Endocrinol Metab,* 103(3), pp. 936-945.

Delanaye, P., Souberbielle, J. C., Lafage-Proust, M. H., Jean, G. and Cavalier, E. (2014) 'Can we use circulating biomarkers to monitor bone turnover in CKD haemodialysis patients? Hypotheses and facts', *Nephrol Dial Transplant,* 29(5), pp. 997-1004.

Delucchi, A., Dinamarca, H., Gainza, H., Whitttle, C., Torrealba, I. and Iniguez, G. (2008) 'Carotid intima-media thickness as a cardiovascular risk marker in pediatric end-stage renal disease patients on dialysis and in renal transplantation', *Transplant Proc,* 40(9), pp. 3244-6.

Denburg, M. R., Kumar, J., Jemielita, T., Brooks, E. R., Skversky, A., Portale, A. A., Salusky, I. B., Warady, B. A., Furth, S. L. and Leonard, M. B. (2016) 'Fracture Burden and Risk Factors in Childhood CKD: Results from the CKiD Cohort Study', *Journal of the American Society of Nephrology : JASN,* 27(2), pp. 543-550.

Denburg, M. R., Tsampalieros, A. K., de Boer, I. H., Shults, J., Kalkwarf, H. J., Zemel, B. S., Foerster, D., Stokes, D. and Leonard, M. B. (2013) 'Mineral Metabolism and Cortical Volumetric Bone Mineral Density in Childhood Chronic Kidney Disease', *The Journal of Clinical Endocrinology and Metabolism,* 98(5), pp. 1930-1938.

Devereux, R. B., Alonso, D. R., Lutas, E. M., Gottlieb, G. J., Campo, E., Sachs, I. and Reichek, N. (1986) 'Echocardiographic assessment of left ventricular hypertrophy: comparison to necropsy findings', *Am J Cardiol,* 57(6), pp. 450-8.

Diaz, A., Bia, D., Zócalo, Y., Manterola, H., Larrabide, I., Lo Vercio, L., Del Fresno, M. and Cabrera Fischer, E. (2018) 'Carotid Intima Media Thickness Reference Intervals for a Healthy Argentinean Population Aged 11-81 Years', *International journal of hypertension,* 2018, pp. 8086714-8086714.

DiVasta, A. D., Feldman, H. A., O'Donnell, J. M., Long, J., Leonard, M. B. and Gordon, C. M. (2017) 'Effect of Exercise and Antidepressants on Skeletal Outcomes in Adolescent Girls With Anorexia Nervosa', *J Adolesc Health,* 60(2), pp. 229-232.

DiVasta, A. D., Feldman, H. A., O'Donnell, J. M., Long, J., Leonard, M. B. and Gordon, C. M. (2019) 'Impact of Adrenal Hormone Supplementation

on Bone Geometry in Growing Teens With Anorexia Nervosa', *J Adolesc Health,* 65(4), pp. 462-468.

Doyon, A., Kracht, D., Bayazit, A. K., Deveci, M., Duzova, A., Krmar, R. T., Litwin, M., Niemirska, A., Oguz, B., Schmidt, B. M., Sozeri, B., Querfeld, U., Melk, A., Schaefer, F. and Wuhl, E. (2013) 'Carotid artery intima-media thickness and distensibility in children and adolescents: reference values and role of body dimensions', *Hypertension,* 62(3), pp. 550-6.

Duff, W. R. D., Björkman, K. M., Kawalilak, C. E., Kehrig, A. M., Wiebe, S. and Kontulainen, S. (2017) 'Precision of pQCT-measured total, trabecular and cortical bone area, content, density and estimated bone strength in children', *Journal of Musculoskeletal & Neuronal Interactions,* 17(2), pp. 59-68.

Eifinger, F., Wahn, F., Querfeld, U., Pollok, M., Gevargez, A., Kriener, P. and Gronemeyer, D. (2000) 'Coronary artery calcifications in children and young adults treated with renal replacement therapy', *Nephrol Dial Transplant,* 15(11), pp. 1892-4.

Eisenhauer, A., Müller, M., Heuser, A., Kolevica, A., Glüer, C. C., Both, M., Laue, C., Hehn, U. V., Kloth, S., Shroff, R. and Schrezenmeir, J. (2019) 'Calcium isotope ratios in blood and urine: A new biomarker for the diagnosis of osteoporosis', *Bone Rep,* 10, pp. 100200.

El-Agroudy, A. E., El-Husseini, A. A., El-Sayed, M., Mohsen, T. and Ghoneim, M. A. (2005) 'A prospective randomized study for prevention of postrenal transplantation bone loss', *Kidney Int,* 67(5), pp. 2039-45.

Engelen, L., Bossuyt, J., Ferreira, I., van Bortel, L. M., Reesink, K. D., Segers, P., Stehouwer, C. D., Laurent, S. and Boutouyrie, P. (2015) 'Reference values for local arterial stiffness. Part A: carotid artery', *J Hypertens,* 33(10), pp. 1981-96.

Ettinger, B., Sidney, S., Cummings, S. R., Libanati, C., Bikle, D. D., Tekawa, I. S., Tolan, K. and Steiger, P. (1997) 'Racial differences in bone density between young adult black and white subjects persist after adjustment for anthropometric, lifestyle, and biochemical differences', *J Clin Endocrinol Metab,* 82(2), pp. 429-34.

Evenepoel, P., D'Haese, P. and Brandenburg, V. (2015) 'Sclerostin and DKK1: new players in renal bone and vascular disease', *Kidney Int,* 88(2), pp. 235-40.

Fantin, F., Mattocks, A., Bulpitt, C. J., Banya, W. and Rajkumar, C. (2007) 'Is augmentation index a good measure of vascular stiffness in the elderly?', *Age and Ageing,* 36(1), pp. 43-48.

Felsenberg, D., Bock, O., Borst, H., Armbrecht, G., Beller, G., Degner, C., Stephan-Oelkers, M., Schacht, E., Mazor, Z., Hashimoto, J., Roth, H. J., Martus, P. and Runge, M. (2011) 'Additive impact of alfacalcidol on bone mineral density and bone strength in alendronate treated postmenopausal women with reduced bone mass', *J Musculoskelet Neuronal Interact,* 11(1), pp. 34-45.

Ferrari, S. L., Chevalley, T., Bonjour, J. P. and Rizzoli, R. (2006) 'Childhood fractures are associated with decreased bone mass gain during puberty: an early marker of persistent bone fragility?', *J Bone Miner Res,* 21(4), pp. 501-7.

Ferreira, A., Saraiva, M., Behets, G., Macedo, A., Galvão, M., D'Haese, P. and Drüeke, T. B. (2009) 'Evaluation of bone remodeling in hemodialysis patients: serum biochemistry, circulating cytokines and bone histomorphometry', *J Nephrol,* 22(6), pp. 783-93.

Fewtrell, M. S. (2003) 'Bone densitometry in children assessed by dual x ray absorptiometry: uses and pitfalls', *Archives of Disease in Childhood,* 88(9), pp. 795.

Fewtrell, M. S., Gordon, I., Biassoni, L. and Cole, T. J. (2005) 'Dual X-ray absorptiometry (DXA) of the lumbar spine in a clinical paediatric setting: does the method of size-adjustment matter?', *Bone,* 37(3), pp. 413-9.

Filgueira, A., Carvalho, A. B., Tomiyama, C., Higa, A., Rochitte, C. E., Santos, R. D. and Canziani, M. E. F. (2011) 'Is Coronary Artery Calcification Associated with Vertebral Bone Density in Nondialyzed Chronic Kidney Disease Patients?', *Clinical Journal of the American Society of Nephrology,* 6(6), pp. 1456.

Fischer, D. C., Mischek, A., Wolf, S., Rahn, A., Salweski, B., Kundt, G. and Haffner, D. (2012) 'Paediatric reference values for the C-terminal fragment of fibroblast-growth factor-23, sclerostin, bone-specific alkaline phosphatase and isoform 5b of tartrate-resistant acid phosphatase', *Ann Clin Biochem,* 49(Pt 6), pp. 546-53.

Flynn, J. T., Kaelber, D. C., Baker-Smith, C. M., Blowey, D., Carroll, A. E., Daniels, S. R., de Ferranti, S. D., Dionne, J. M., Falkner, B., Flinn, S. K., Gidding, S. S., Goodwin, C., Leu, M. G., Powers, M. E., Rea, C.,

Samuels, J., Simasek, M., Thaker, V. V. and Urbina, E. M. (2017) 'Clinical Practice Guideline for Screening and Management of High Blood Pressure in Children and Adolescents', *Pediatrics,* 140(3), pp. e20171904.

for the, C. S. C., Melk, A., Thurn, D., Doyon, A., Wühl, E., Schaefer, F., Sözeri, B., Bayazit, A. K., Canpolat, N., Duzova, A., Querfeld, U. and Schmidt, B. M. W. (2015) 'Aortic Pulse Wave Velocity in Healthy Children and Adolescents: Reference Values for the Vicorder Device and Modifying Factors', *American Journal of Hypertension,* 28(12), pp. 1480-1488.

Freeman, J. V., Cole, T. J., Chinn, S., Jones, P. R., White, E. M. and Preece, M. A. (1995) 'Cross sectional stature and weight reference curves for the UK, 1990', *Archives of disease in childhood,* 73(1), pp. 17-24.

Frost, H. M. (2002) 'Emerging views about "osteoporosis", bone health, strength, fragility, and their determinants', *J Bone Miner Metab,* 20(6), pp. 319-25.

Gabel, L., Macdonald, H. M. and McKay, H. A. (2017) 'Sex Differences and Growth-Related Adaptations in Bone Microarchitecture, Geometry, Density, and Strength From Childhood to Early Adulthood: A Mixed Longitudinal HR-pQCT Study', *J Bone Miner Res,* 32(2), pp. 250-263.

Ganesh, S. K., Stack, A. G., Levin, N. W., Hulbert-Shearon, T. and Port, F. K. (2001) 'Association of elevated serum PO(4), Ca x PO(4) product, and parathyroid hormone with cardiac mortality risk in chronic hemodialysis patients', *J Am Soc Nephrol,* 12(10), pp. 2131-8.

Gjesdal, O., Bluemke, D. A. and Lima, J. A. (2011) 'Cardiac remodeling at the population level--risk factors, screening, and outcomes', *Nat Rev Cardiol,* 8(12), pp. 673-85.

Glendenning, P. (2011) 'Markers of bone turnover for the prediction of fracture risk and monitoring of osteoporosis treatment: a need for international reference standards: osteoporos int 2011;22:391-420', *Clin Biochem Rev,* 32(1), pp. 45-7.

Gomberg, B. R., Wehrli, F. W., Vasilic, B., Weening, R. H., Saha, P. K., Song, H. K. and Wright, A. C. (2004) 'Reproducibility and error sources of micro-MRI-based trabecular bone structural parameters of the distal radius and tibia', *Bone,* 35(1), pp. 266-76.

Goodman, W. G., Goldin, J., Kuizon, B. D., Yoon, C., Gales, B., Sider, D., Wang, Y., Chung, J., Emerick, A., Greaser, L., Elashoff, R. M. and Salusky, I. B. (2000) 'Coronary-artery calcification in young adults

with end-stage renal disease who are undergoing dialysis', *N Engl J Med,* 342(20), pp. 1478-83.

Goodman, W. G., Ramirez, J. A., Belin, T. R., Chon, Y., Gales, B., Segre, G. V. and Salusky, I. B. (1994) 'Development of adynamic bone in patients with secondary hyperparathyroidism after intermittent calcitriol therapy', *Kidney Int,* 46(4), pp. 1160-6.

Gordon, C. M., Leonard, M. B. and Zemel, B. S. (2014) '2013 Pediatric Position Development Conference: executive summary and reflections', *J Clin Densitom,* 17(2), pp. 219-24.

Goulding, A., Jones, I. E., Williams, S. M., Grant, A. M., Taylor, R. W., Manning, P. J. and Langley, J. (2005) 'First fracture is associated with increased risk of new fractures during growth', *J Pediatr,* 146(2), pp. 286-8.

Griffin, L. M., Kalkwarf, H. J., Zemel, B. S., Shults, J., Wetzsteon, R. J., Strife, C. F. and Leonard, M. B. (2012) 'Assessment of dual-energy X-ray absorptiometry measures of bone health in pediatric chronic kidney disease', *Pediatr Nephrol,* 27(7), pp. 1139-48.

Groothoff, J. W., Gruppen, M. P., Offringa, M., de Groot, E., Stok, W., Bos, W. J., Davin, J. C., Lilien, M. R., Van de Kar, N. C., Wolff, E. D. and Heymans, H. S. (2002a) 'Increased arterial stiffness in young adults with end-stage renal disease since childhood', *J Am Soc Nephrol,* 13(12), pp. 2953-61.

Groothoff, J. W., Gruppen, M. P., Offringa, M., Hutten, J., Lilien, M. R., Van De Kar, N. J., Wolff, E. D., Davin, J. C. and Heymans, H. S. (2002b) 'Mortality and causes of death of end-stage renal disease in children: a Dutch cohort study', *Kidney Int,* 61(2), pp. 621-9.

Groothoff, J. W., Offringa, M., Van Eck-Smit, B. L., Gruppen, M. P., Van De Kar, N. J., Wolff, E. D., Lilien, M. R., Davin, J. C., Heymans, H. S. and Dekker, F. W. (2003) 'Severe bone disease and low bone mineral density after juvenile renal failure', *Kidney Int,* 63(1), pp. 266-75.

Haapasalo, H., Kontulainen, S., Sievanen, H., Kannus, P., Jarvinen, M. and Vuori, I. (2000) 'Exercise-induced bone gain is due to enlargement in bone size without a change in volumetric bone density: a peripheral quantitative computed tomography study of the upper arms of male tennis players', *Bone,* 27(3), pp. 351-7.

Haffner, D., Schaefer, F., Nissel, R., Wuhl, E., Tonshoff, B. and Mehls, O. (2000) 'Effect of growth hormone treatment on the adult height of

children with chronic renal failure. German Study Group for Growth Hormone Treatment in Chronic Renal Failure', *N Engl J Med,* 343(13), pp. 923-30.

Helenius, I., Remes, V., Salminen, S., Valta, H., Mäkitie, O., Holmberg, C., Palmu, P., Tervahartiala, P., Sarna, S., Helenius, M., Peltonen, J. and Jalanko, H. (2006a) *Incidence and Predictors of Fractures in Children After Solid Organ Transplantation: A 5-Year Prospective, Population-Based Study.*

Helenius, I., Remes, V., Tervahartiala, P., Salminen, S., Sairanen, H., Holmberg, C., Palmu, P., Helenius, M., Peltonen, J. and Jalanko, H. (2006b) 'Spine after solid organ transplantation in childhood: a clinical, radiographic, and magnetic resonance imaging analysis of 40 patients', *Spine (Phila Pa 1976),* 31(18), pp. 2130-6.

Hildebrandt, E. M., Manske, S. L., Hanley, D. A. and Boyd, S. K. (2016) 'Bilateral Asymmetry of Radius and Tibia Bone Macroarchitecture and Microarchitecture: A High-Resolution Peripheral Quantitative Computed Tomography Study', *J Clin Densitom,* 19(2), pp. 250-4.

Hirshfeld, J. W., Jr., Ferrari, V. A., Bengel, F. M., Bergersen, L., Chambers, C. E., Einstein, A. J., Eisenberg, M. J., Fogel, M. A., Gerber, T. C., Haines, D. E., Laskey, W. K., Limacher, M. C., Nichols, K. J., Pryma, D. A., Raff, G. L., Rubin, G. D., Smith, D., Stillman, A. E., Thomas, S. A., Tsai, T. T., Wagner, L. K. and Wann, L. S. (2018) '2018 ACC/HRS/NASCI/SCAI/SCCT Expert Consensus Document on Optimal Use of Ionizing Radiation in Cardiovascular Imaging-Best Practices for Safety and Effectiveness, Part 1: Radiation Physics and Radiation Biology: A Report of the American College of Cardiology Task Force on Expert Consensus Decision Pathways', *J Am Coll Cardiol,* 71(24), pp. 2811-2828.

Holden, R. M., Morton, A. R., Garland, J. S., Pavlov, A., Day, A. G. and Booth, S. L. (2010) 'Vitamins K and D status in stages 3-5 chronic kidney disease', *Clin J Am Soc Nephrol,* 5(4), pp. 590-7.

Holloway, K. L., Brennan, S. L., Kotowicz, M. A., Bucki-Smith, G., Timney, E. N., Dobbins, A. G., Williams, L. J. and Pasco, J. A. (2015) 'Prior fracture as a risk factor for future fracture in an Australian cohort', *Osteoporos Int,* 26(2), pp. 629-35.

Hruska, K. A., Seifert, M. and Sugatani, T. (2015) 'Pathophysiology of the chronic kidney disease-mineral bone disorder', *Current opinion in nephrology and hypertension,* 24(4), pp. 303-309.

Iimori, S., Mori, Y., Akita, W., Kuyama, T., Takada, S., Asai, T., Kuwahara, M., Sasaki, S. and Tsukamoto, Y. (2012) 'Diagnostic usefulness of bone mineral density and biochemical markers of bone turnover in predicting fracture in CKD stage 5D patients--a single-center cohort study', *Nephrol Dial Transplant,* 27(1), pp. 345-51.

Isakova, T., Wahl, P., Vargas, G. S., Gutiérrez, O. M., Scialla, J., Xie, H., Appleby, D., Nessel, L., Bellovich, K., Chen, J., Hamm, L., Gadegbeku, C., Horwitz, E., Townsend, R. R., Anderson, C. A. M., Lash, J. P., Hsu, C.-Y., Leonard, M. B. and Wolf, M. (2011) 'Fibroblast growth factor 23 is elevated before parathyroid hormone and phosphate in chronic kidney disease', *Kidney international,* 79(12), pp. 1370-1378.

Ishimura, E., Okuno, S., Ichii, M., Norimine, K., Yamakawa, T., Shoji, S., Nishizawa, Y. and Inaba, M. (2014) 'Relationship between serum sclerostin, bone metabolism markers, and bone mineral density in maintenance hemodialysis patients', *J Clin Endocrinol Metab,* 99(11), pp. 4315-20.

Jadoul, M., Albert, J. M., Akiba, T., Akizawa, T., Arab, L., Bragg-Gresham, J. L., Mason, N., Prutz, K. G., Young, E. W. and Pisoni, R. L. (2006) 'Incidence and risk factors for hip or other bone fractures among hemodialysis patients in the Dialysis Outcomes and Practice Patterns Study', *Kidney Int,* 70(7), pp. 1358-66.

Jarvinen, T. L., Sievanen, H., Jokihaara, J. and Einhorn, T. A. (2005) 'Revival of bone strength: the bottom line', *J Bone Miner Res,* 20(5), pp. 717-20.

Jaworski, M. and Graff, K. (2018) 'Peripheral quantitative computed tomography of the distal and proximal forearm in children and adolescents: bone densities, cross-sectional sizes and soft tissues reference data', *J Musculoskelet Neuronal Interact,* 18(2), pp. 237-247.

Jaworski, M., Kobylińska, M. and Graff, K. (2021) 'Peripheral quantitative computed tomography of the lower leg in children and adolescents: bone densities, cross-sectional sizes and muscle distribution reference data', *J Musculoskelet Neuronal Interact,* 21(2), pp. 215-236.

Jensen, M. P., Turner, J. A. and Romano, J. M. (1994) 'What is the maximum number of levels needed in pain intensity measurement?', *Pain,* 58(3), pp. 387-92.

Johnston, C. C., Jr., Miller, J. Z., Slemenda, C. W., Reister, T. K., Hui, S., Christian, J. C. and Peacock, M. (1992) 'Calcium supplementation and increases in bone mineral density in children', *N Engl J Med,* 327(2), pp. 82-7.

Jourdan, C., Wuhl, E., Litwin, M., Fahr, K., Trelewicz, J., Jobs, K., Schenk, J. P., Grenda, R., Mehls, O., Troger, J. and Schaefer, F. (2005) 'Normative values for intima-media thickness and distensibility of large arteries in healthy adolescents', *J Hypertens,* 23(9), pp. 1707-15.

'K/DOQI clinical practice guidelines for bone metabolism and disease in chronic kidney disease', (2003) *Am J Kidney Dis,* 42(4 Suppl 3), pp. S1-201.

Kalkwarf, H. J., Laor, T. and Bean, J. A. (2011) 'Fracture risk in children with a forearm injury is associated with volumetric bone density and cortical area (by peripheral QCT) and areal bone density (by DXA)', *Osteoporos Int,* 22(2), pp. 607-16.

Kalkwarf, H. J., Zemel, B. S., Gilsanz, V., Lappe, J. M., Horlick, M., Oberfield, S., Mahboubi, S., Fan, B., Frederick, M. M., Winer, K. and Shepherd, J. A. (2007) 'The bone mineral density in childhood study: bone mineral content and density according to age, sex, and race', *J Clin Endocrinol Metab,* 92(6), pp. 2087-99.

Karras, A., Haymann, J. P., Bozec, E., Metzger, M., Jacquot, C., Maruani, G., Houillier, P., Froissart, M., Stengel, B., Guardiola, P., Laurent, S., Boutouyrie, P. and Briet, M. (2012) 'Large artery stiffening and remodeling are independently associated with all-cause mortality and cardiovascular events in chronic kidney disease', *Hypertension,* 60(6), pp. 1451-7.

Katsimbri, P. (2017) 'The biology of normal bone remodelling', *Eur J Cancer Care (Engl),* 26(6).

'KDIGO clinical practice guideline for the diagnosis, evaluation, prevention, and treatment of Chronic Kidney Disease-Mineral and Bone Disorder (CKD-MBD)', (2009) *Kidney Int Suppl,* (113), pp. S1-130.

Ketteler, M., Block, G. A., Evenepoel, P., Fukagawa, M., Herzog, C. A., McCann, L., Moe, S. M., Shroff, R., Tonelli, M. A., Toussaint, N. D.,

Vervloet, M. G. and Leonard, M. B. 'Executive summary of the 2017 KDIGO Chronic Kidney Disease–Mineral and Bone Disorder (CKD-MBD) Guideline Update: what’s changed and why it matters', *Kidney International,* 92(1), pp. 26-36.

Ketteler, M., Block, G. A., Evenepoel, P., Fukagawa, M., Herzog, C. A., McCann, L., Moe, S. M., Shroff, R., Tonelli, M. A., Toussaint, N. D., Vervloet, M. G. and Leonard, M. B. 'Executive summary of the 2017 KDIGO Chronic Kidney Disease–Mineral and Bone Disorder (CKD-MBD) Guideline Update: what's changed and why it matters', *Kidney International,* 92(1), pp. 26-36.

Ketteler, M., Block, G. A., Evenepoel, P., Fukagawa, M., Herzog, C. A., McCann, L., Moe, S. M., Shroff, R., Tonelli, M. A., Toussaint, N. D., Vervloet, M. G. and Leonard, M. B. (2018) 'Diagnosis, Evaluation, Prevention, and Treatment of Chronic Kidney Disease-Mineral and Bone Disorder: Synopsis of the Kidney Disease: Improving Global Outcomes 2017 Clinical Practice Guideline Update', *Ann Intern Med,* 168(6), pp. 422-430.

Ketteler, M., Bongartz, P., Westenfeld, R., Wildberger, J. E., Mahnken, A. H., Böhm, R., Metzger, T., Wanner, C., Jahnen-Dechent, W. and Floege, J. (2003) 'Association of low fetuin-A (AHSG) concentrations in serum with cardiovascular mortality in patients on dialysis: a cross-sectional study', *Lancet,* 361(9360), pp. 827-33.

Khoury, P. R., Mitsnefes, M., Daniels, S. R. and Kimball, T. R. (2009) 'Age-specific reference intervals for indexed left ventricular mass in children', *J Am Soc Echocardiogr,* 22(6), pp. 709-14.

Khouzam, N. and Wesseling-Perry, K. (2019) 'Pathophysiology and treatment of cardiovascular disease in pediatric chronic kidney disease', *Pediatr Nephrol,* 34(1), pp. 1-10.

Kiel, D. P., Kauppila, L. I., Cupples, L. A., Hannan, M. T., O'Donnell, C. J. and Wilson, P. W. (2001) 'Bone loss and the progression of abdominal aortic calcification over a 25 year period: the Framingham Heart Study', *Calcif Tissue Int,* 68(5), pp. 271-6.

Kim, H., Lee, J., Lee, K. B., Kim, Y. H., Hong, N., Park, J. T., Han, S. H., Kang, S. W., Choi, K. H., Oh, K. H. and Yoo, T. H. (2022) 'Low bone mineral density is associated with coronary arterial calcification progression and incident cardiovascular events in patients with chronic kidney disease', *Clin Kidney J,* 15(1), pp. 119-127.

Kini, U. and Nandeesh, B. (2012) 'Physiology of Bone Formation, Remodeling and Metabolism', in Fogelman, I., Gnanasegaran, G. & van der Wall, H.E. (eds.) *Radionuclide and Hybrid bone Imaging*: Springer, pp. 29-57.

Klaus, G., Watson, A., Edefonti, A., Fischbach, M., Ronnholm, K., Schaefer, F., Simkova, E., Stefanidis, C. J., Strazdins, V., Vande Walle, J., Schroder, C., Zurowska, A. and Ekim, M. (2006) 'Prevention and treatment of renal osteodystrophy in children on chronic renal failure: European guidelines', *Pediatr Nephrol,* 21(2), pp. 151-9.

Kouis, P., Kousios, A., Kanari, A., Kleopa, D., Papatheodorou, S. I. and Panayiotou, A. G. (2020) 'Association of non-invasive measures of subclinical atherosclerosis and arterial stiffness with mortality and major cardiovascular events in chronic kidney disease: systematic review and meta-analysis of cohort studies', *Clin Kidney J,* 13(5), pp. 842-854.

Kozel, B. A., Danback, J. R., Waxler, J. L., Knutsen, R. H., de Las Fuentes, L., Reusz, G. S., Kis, E., Bhatt, A. B. and Pober, B. R. (2014) 'Williams syndrome predisposes to vascular stiffness modified by antihypertensive use and copy number changes in NCF1', *Hypertension,* 63(1), pp. 74-9.

Kracht, D., Shroff, R., Baig, S., Doyon, A., Jacobi, C., Zeller, R., Querfeld, U., Schaefer, F., Wuhl, E., Schmidt, B. M. and Melk, A. (2011) 'Validating a new oscillometric device for aortic pulse wave velocity measurements in children and adolescents', *Am J Hypertens,* 24(12), pp. 1294-9.

Krueger, D., Vallarta-Ast, N., Checovich, M., Gemar, D. and Binkley, N. (2012) 'BMD measurement and precision: a comparison of GE Lunar Prodigy and iDXA densitometers', *J Clin Densitom,* 15(1), pp. 21-5.

Krueger, T., Westenfeld, R., Ketteler, M., Schurgers, L. J. and Floege, J. (2009) 'Vitamin K deficiency in CKD patients: a modifiable risk factor for vascular calcification?', *Kidney Int,* 76(1), pp. 18-22.

Kröger, H., Kotaniemi, A., Vainio, P. and Alhava, E. (1992) 'Bone densitometry of the spine and femur in children by dual-energy x-ray absorptiometry', *Bone Miner,* 17(1), pp. 75-85.

Kuizon, B. D. and Salusky, I. B. (1999) 'Growth retardation in children with chronic renal failure', *J Bone Miner Res,* 14(10), pp. 1680-90.

Lalayiannis, A. D., Crabtree, N. J., Ferro, C. J., Askiti, V., Mitsioni, A., Biassoni, L., Kaur, A., Sinha, M. D., Wheeler, D. C., Duncan, N. D., Popoola, J., Milford, D. V., Long, J., Leonard, M. B., Fewtrell, M. and Shroff, R. (2020) 'Routine serum biomarkers, but not dual-energy X-ray absorptiometry, correlate with cortical bone mineral density in children and young adults with chronic kidney disease', *Nephrology Dialysis Transplantation*.

Lalayiannis, A. D., Crabtree, N. J., Fewtrell, M., Biassoni, L., Milford, D. V., Ferro, C. J. and Shroff, R. (2019) 'Assessing bone mineralisation in children with chronic kidney disease: what clinical and research tools are available?', *Pediatr Nephrol*.

Lalayiannis, A. D., Ferro, C. J., Wheeler, D. C., Duncan, N. D., Smith, C., Popoola, J., Askiti, V., Mitsioni, A., Kaur, A., Sinha, M. D., McGuirk, S. P., Mortensen, K. H., Milford, D. V. and Shroff, R. (2021a) 'The burden of subclinical cardiovascular disease in children and young adults with CKD and on dialysis', *Clinical Kidney Journal*.

Lalayiannis, A. D., Fewtrell, M., Biassoni, L., Silva, S., Goodman, N., Shroff, R. and Crabtree, N. J. (2021b) 'Studying bone mineral density in young people: The complexity of choosing a pQCT reference database', *Bone,* 143, pp. 115713.

Lang, R. M., Bierig, M., Devereux, R. B., Flachskampf, F. A., Foster, E., Pellikka, P. A., Picard, M. H., Roman, M. J., Seward, J., Shanewise, J. S., Solomon, S. D., Spencer, K. T., Sutton, M. S. and Stewart, W. J. (2005) 'Recommendations for chamber quantification: a report from the American Society of Echocardiography's Guidelines and Standards Committee and the Chamber Quantification Writing Group, developed in conjunction with the European Association of Echocardiography, a branch of the European Society of Cardiology', *J Am Soc Echocardiogr,* 18(12), pp. 1440-63.

Laster, M., Denburg, M., Okuda, Y., Kumar, J., Furth, S., Warady, B., Kalantar-Zadeh, K., Norris, K. and Salusky, I. B. (2021) 'Race and Ethnicity Predict Bone Markers and Fracture in Pediatric Patients With Chronic Kidney Disease', *J Bone Miner Res,* 36(2), pp. 298-304.

Laster, M., Pereira, R. C. and Salusky, I. B. (2019) 'Racial differences in bone histomorphometry in children and young adults treated with dialysis', *Bone,* 127, pp. 114-119.

Laurent, S., Boutouyrie, P., Asmar, R., Gautier, I., Laloux, B., Guize, L., Ducimetiere, P. and Benetos, A. (2001) 'Aortic stiffness is an independent predictor of all-cause and cardiovascular mortality in hypertensive patients', *Hypertension,* 37(5), pp. 1236-41.

Lee, D. C., Gilsanz, V. and Wren, T. A. L. (2007) 'Limitations of Peripheral Quantitative Computed Tomography Metaphyseal Bone Density Measurements', *The Journal of Clinical Endocrinology & Metabolism,* 92(11), pp. 4248-4253.

Leonard, C. M., Roza, M. A., Barr, R. D. and Webber, C. E. (2009) 'Reproducibility of DXA measurements of bone mineral density and body composition in children', *Pediatr Radiol,* 39(2), pp. 148-54.

Leonard, M. B. (2007) 'A structural approach to the assessment of fracture risk in children and adolescents with chronic kidney disease', *Pediatr Nephrol,* 22(11), pp. 1815-24.

Leonard, M. B., Elmi, A., Mostoufi-Moab, S., Shults, J., Burnham, J. M., Thayu, M., Kibe, L., Wetzsteon, R. J. and Zemel, B. S. (2010) 'Effects of Sex, Race, and Puberty on Cortical Bone and the Functional Muscle Bone Unit in Children, Adolescents, and Young Adults', *The Journal of Clinical Endocrinology and Metabolism,* 95(4), pp. 1681-1689.

Levin, A., Bakris, G. L., Molitch, M., Smulders, M., Tian, J., Williams, L. A. and Andress, D. L. (2007) 'Prevalence of abnormal serum vitamin D, PTH, calcium, and phosphorus in patients with chronic kidney disease: results of the study to evaluate early kidney disease', *Kidney Int,* 71(1), pp. 31-8.

Lima, E. M., Goodman, W. G., Kuizon, B. D., Gales, B., Emerick, A., Goldin, J. and Salusky, I. B. (2003) 'Bone density measurements in pediatric patients with renal osteodystrophy', *Pediatr Nephrol,* 18(6), pp. 554-9.

Lin, Y. C., Lyle, R. M., Weaver, C. M., McCabe, L. D., McCabe, G. P., Johnston, C. C. and Teegarden, D. (2003) 'Peak spine and femoral neck bone mass in young women', *Bone,* 32(5), pp. 546-53.

Link, T. M., Saborowski, Kisters, K., Kempkes, M., Kosch, M., Newitt, D., Lu, Y., Waldt, S. and Majumdar, S. (2002) 'Changes in calcaneal trabecular bone structure assessed with high-resolution MR imaging in patients with kidney transplantation', *Osteoporos Int,* 13(2), pp. 119-29.

Litwin, M., Wuhl, E., Jourdan, C., Trelewicz, J., Niemirska, A., Fahr, K., Jobs, K., Grenda, R., Wawer, Z. T., Rajszys, P., Troger, J., Mehls, O. and Schaefer, F. (2005) 'Altered morphologic properties of large arteries in children with chronic renal failure and after renal transplantation', *J Am Soc Nephrol,* 16(5), pp. 1494-500.

London, G. M. (2012) 'Bone-vascular cross-talk', *J Nephrol,* 25(5), pp. 619-25.

London, G. M. (2018) 'Arterial Stiffness in Chronic Kidney Disease and End-Stage Renal Disease', *Blood Purif,* 45(1-3), pp. 154-158.

London, G. M. and Pannier, B. (2010) 'Arterial functions: how to interpret the complex physiology', *Nephrol Dial Transplant,* 25(12), pp. 3815-23.

Lopes, M. B., Karaboyas, A., Bieber, B., Pisoni, R. L., Walpen, S., Fukagawa, M., Christensson, A., Evenepoel, P., Pegoraro, M., Robinson, B. M. and Pecoits-Filho, R. (2020) 'Impact of longer term phosphorus control on cardiovascular mortality in hemodialysis patients using an area under the curve approach: results from the DOPPS', *Nephrology Dialysis Transplantation,* 35(10), pp. 1794-1801.

Lorenz, M. W., Markus, H. S., Bots, M. L., Rosvall, M. and Sitzer, M. (2007) 'Prediction of clinical cardiovascular events with carotid intima-media thickness: a systematic review and meta-analysis', *Circulation,* 115(4), pp. 459-67.

Lurbe, E., Agabiti-Rosei, E., Cruickshank, J. K., Dominiczak, A., Erdine, S., Hirth, A., Invitti, C., Litwin, M., Mancia, G., Pall, D., Rascher, W., Redon, J., Schaefer, F., Seeman, T., Sinha, M., Stabouli, S., Webb, N. J., Wühl, E. and Zanchetti, A. (2016) '2016 European Society of Hypertension guidelines for the management of high blood pressure in children and adolescents', *J Hypertens,* 34(10), pp. 1887-920.

Machuca-Gayet, I., Quinaux, T., Bertholet-Thomas, A., Gaillard, S., Claramunt-Taberner, D., Acquaviva-Bourdain, C. and Bacchetta, J. (2020) 'Bone Disease in Nephropathic Cystinosis: Beyond Renal Osteodystrophy', *Int J Mol Sci,* 21(9).

Malluche, H. H., Blomquist, G., Monier-Faugere, M. C., Cantor, T. L. and Davenport, D. L. (2015) 'High Parathyroid Hormone Level and Osteoporosis Predict Progression of Coronary Artery Calcification in Patients on Dialysis', *J Am Soc Nephrol,* 26(10), pp. 2534-44.

Malluche, H. H., Mawad, H. W. and Monier-Faugere, M. C. (2011) 'Renal osteodystrophy in the first decade of the new millennium: analysis of 630 bone biopsies in black and white patients', *J Bone Miner Res,* 26(6), pp. 1368-76.

Manolagas, S. C. (2000) 'Birth and death of bone cells: basic regulatory mechanisms and implications for the pathogenesis and treatment of osteoporosis', *Endocr Rev,* 21(2), pp. 115-37.

Marques, I. D., Araujo, M. J., Graciolli, F. G., Reis, L. M., Pereira, R. M., Custodio, M. R., Jorgetti, V., Elias, R. M., David-Neto, E. and Moyses, R. M. (2017) 'Biopsy vs. peripheral computed tomography to assess bone disease in CKD patients on dialysis: differences and similarities', *Osteoporos Int,* 28(5), pp. 1675-1683.

Marshall, W. A. and Tanner, J. M. (1969) 'Variations in pattern of pubertal changes in girls', *Arch Dis Child,* 44(235), pp. 291-303.

Marshall, W. A. and Tanner, J. M. (1970) 'Variations in the pattern of pubertal changes in boys', *Arch Dis Child,* 45(239), pp. 13-23.

Mata-Mbemba, D., Rohringer, T., Ibrahim, A., Adams-Webberc, T., Moineddin, R., Doria, A. S. and Vali, R. (2019) 'HR-pQCT imaging in children, adolescents and young adults: Systematic review and subgroup meta-analysis of normative data', *PloS one,* 14(12), pp. e0225663-e0225663.

Mathias, R., Salusky, I., Harman, W., Paredes, A., Emans, J., Segre, G. and Goodman, W. (1993) 'Renal bone disease in pediatric and young adult patients on hemodialysis in a children's hospital', *J Am Soc Nephrol,* 3(12), pp. 1938-46.

Matkovic, V., Goel, P. K., Badenhop-Stevens, N. E., Landoll, J. D., Li, B., Ilich, J. Z., Skugor, M., Nagode, L. A., Mobley, S. L., Ha, E. J., Hangartner, T. N. and Clairmont, A. (2005) 'Calcium supplementation and bone mineral density in females from childhood to young adulthood: a randomized controlled trial', *Am J Clin Nutr,* 81(1), pp. 175-88.

Matkovic, V. and Heaney, R. P. (1992) 'Calcium balance during human growth: evidence for threshold behavior', *Am J Clin Nutr,* 55(5), pp. 992-6.

McDonald, S. P. and Craig, J. C. (2004) 'Long-term survival of children with end-stage renal disease', *N Engl J Med,* 350(26), pp. 2654-62.

McNerny, E. M. B. and Nickolas, T. L. (2017) 'Bone Quality in Chronic Kidney Disease: Definitions and Diagnostics', *Curr Osteoporos Rep,* 15(3), pp. 207-213.

Melk, A., Thurn, D., Doyon, A., Wühl, E., Schaefer, F., Sözeri, B., Bayazit, A. K., Canpolat, N., Duzova, A., Querfeld, U. and Schmidt, B. M. W. (2015) 'Aortic Pulse Wave Velocity in Healthy Children and Adolescents: Reference Values for the Vicorder Device and Modifying Factors', *American Journal of Hypertension,* 28(12), pp. 1480-1488.

Merjanian, R., Budoff, M., Adler, S., Berman, N. and Mehrotra, R. (2003) 'Coronary artery, aortic wall, and valvular calcification in nondialyzed individuals with type 2 diabetes and renal disease', *Kidney International,* 64(1), pp. 263-271.

Messina, C., Lastella, G., Sorce, S., Piodi, L. P., Rodari, G., Giavoli, C., Marchelli, D., Guglielmi, G. and Ulivieri, F. M. (2018) 'Pediatric dual-energy X-ray absorptiometry in clinical practice: What the clinicians need to know', *Eur J Radiol,* 105, pp. 153-161.

Mettler, F. A., Jr., Huda, W., Yoshizumi, T. T. and Mahesh, M. (2008) 'Effective doses in radiology and diagnostic nuclear medicine: a catalog', *Radiology,* 248(1), pp. 254-63.

Mikolajewicz, N., Bishop, N., Burghardt, A. J., Folkestad, L., Hall, A., Kozloff, K. M., Lukey, P. T., Molloy-Bland, M., Morin, S. N., Offiah, A. C., Shapiro, J., van Rietbergen, B., Wager, K., Willie, B. M., Komarova, S. V. and Glorieux, F. H. (2020) 'HR-pQCT Measures of Bone Microarchitecture Predict Fracture: Systematic Review and Meta-Analysis', *Journal of Bone and Mineral Research,* 35(3), pp. 446-459.

Mitchell, J. D., Paisley, R., Moon, P., Novak, E. and Villines, T. C. (2018) 'Coronary Artery Calcium and Long-Term Risk of Death, Myocardial Infarction, and Stroke: The Walter Reed Cohort Study', *JACC Cardiovasc Imaging,* 11(12), pp. 1799-1806.

Mitsnefes, M. M. (2012) 'Cardiovascular disease in children with chronic kidney disease', *Journal of the American Society of Nephrology : JASN,* 23(4), pp. 578-585.

Mitsnefes, M. M., Kimball, T. R., Kartal, J., Witt, S. A., Glascock, B. J., Khoury, P. R. and Daniels, S. R. (2005) 'Cardiac and vascular adaptation in pediatric patients with chronic kidney disease: role of calcium-phosphorus metabolism', *J Am Soc Nephrol,* 16(9), pp. 2796-803.

Mitsnefes, M. M., Kimball, T. R., Witt, S. A., Glascock, B. J., Khoury, P. R. and Daniels, S. R. (2003) 'Left ventricular mass and systolic performance in pediatric patients with chronic renal failure', *Circulation,* 107(6), pp. 864-8.

Mitsnefes, M. M., Laskin, B. L., Dahhou, M., Zhang, X. and Foster, B. J. (2013) 'Mortality risk among children initially treated with dialysis for end-stage kidney disease, 1990-2010', *JAMA,* 309(18), pp. 1921-1929.

Mitsnefes, M. M., Pierce, C., Flynn, J., Samuels, J., Dionne, J., Furth, S., Warady, B. and For the, C. s. g. (2016) 'Can office blood pressure readings predict masked hypertension?', *Pediatric Nephrology,* 31(1), pp. 163-166.

Mittalhenkle, A., Gillen, D. L. and Stehman-Breen, C. O. (2004) 'Increased risk of mortality associated with hip fracture in the dialysis population', *Am J Kidney Dis,* 44(4), pp. 672-9.

Mittra, E., Rubin, C. and Qin, Y. X. (2005) 'Interrelationship of trabecular mechanical and microstructural properties in sheep trabecular bone', *J Biomech,* 38(6), pp. 1229-37.

Modi, Z. J., Lu, Y., Ji, N., Kapke, A., Selewski, D. T., Dietrich, X., Abbott, K., Nallamothu, B. K., Schaubel, D. E., Saran, R. and Gipson, D. S. (2019) 'Risk of Cardiovascular Disease and Mortality in Young Adults With End-stage Renal Disease: An Analysis of the US Renal Data System', *JAMA Cardiol,* 4(4), pp. 353-362.

Moe, S., Drueke, T., Cunningham, J., Goodman, W., Martin, K., Olgaard, K., Ott, S., Sprague, S., Lameire, N. and Eknoyan, G. (2006) 'Definition, evaluation, and classification of renal osteodystrophy: a position statement from Kidney Disease: Improving Global Outcomes (KDIGO)', *Kidney Int,* 69(11), pp. 1945-53.

Moe, S. M. and Chen, N. X. (2004) 'Pathophysiology of vascular calcification in chronic kidney disease', *Circ Res,* 95(6), pp. 560-7.

Moreira, O. C., Oliveira, C. E. P. and De Paz, J. A. (2018) 'Dual energy X-ray absorptiometry (DXA) reliability and intraobserver reproducibility for segmental body composition measuring', *Nutr Hosp,* 35(2), pp. 340-345.

Mostoufi-Moab, S., Kelly, A., Mitchell, J. A., Baker, J., Zemel, B. S., Brodsky, J., Long, J. and Leonard, M. B. (2018) 'Changes in pediatric DXA measures of musculoskeletal outcomes and correlation with

quantitative CT following treatment of acute lymphoblastic leukemia', *Bone,* 112, pp. 128-135.

Moyer-Mileur, L. J., Quick, J. L. and Murray, M. A. (2008) 'Peripheral quantitative computed tomography of the tibia: pediatric reference values', *J Clin Densitom,* 11(2), pp. 283-94.

Mödder, U. I., Hoey, K. A., Amin, S., McCready, L. K., Achenbach, S. J., Riggs, B. L., Melton, L. J., 3rd and Khosla, S. (2011) 'Relation of age, gender, and bone mass to circulating sclerostin levels in women and men', *J Bone Miner Res,* 26(2), pp. 373-9.

Navaneethan, S. D., Schold, J. D., Arrigain, S., Jolly, S. E. and Nally, J. V., Jr. (2015) 'Cause-Specific Deaths in Non-Dialysis-Dependent CKD', *J Am Soc Nephrol,* 26(10), pp. 2512-20.

Naylor, K. L., Garg, A. X., Zou, G., Langsetmo, L., Leslie, W. D., Fraser, L. A., Adachi, J. D., Morin, S., Goltzman, D., Lentle, B., Jackson, S. A., Josse, R. G. and Jamal, S. A. (2015) 'Comparison of fracture risk prediction among individuals with reduced and normal kidney function', *Clin J Am Soc Nephrol,* 10(4), pp. 646-53.

Nelson, A. J., Raggi, P., Wolf, M., Gold, A. M., Chertow, G. M. and Roe, M. T. (2020) 'Targeting Vascular Calcification in Chronic Kidney Disease', *JACC: Basic to Translational Science,* 5(4), pp. 398-412.

Neu, C. M., Manz, F., Rauch, F., Merkel, A. and Schoenau, E. (2001) 'Bone densities and bone size at the distal radius in healthy children and adolescents: a study using peripheral quantitative computed tomography', *Bone,* 28(2), pp. 227-232.

Ng, A. H., Omelon, S., Variola, F., Allo, B., Willett, T. L., Alman, B. A. and Grynpas, M. D. (2016) 'Adynamic Bone Decreases Bone Toughness During Aging by Affecting Mineral and Matrix', *J Bone Miner Res,* 31(2), pp. 369-79.

Nickolas, T. L., Cremers, S., Zhang, A., Thomas, V., Stein, E., Cohen, A., Chauncey, R., Nikkel, L., Yin, M. T., Liu, X. S., Boutroy, S., Staron, R. B., Leonard, M. B., McMahon, D. J., Dworakowski, E. and Shane, E. (2011) 'Discriminants of prevalent fractures in chronic kidney disease', *J Am Soc Nephrol,* 22(8), pp. 1560-72.

Nickolas, T. L., McMahon, D. J. and Shane, E. (2006) 'Relationship between moderate to severe kidney disease and hip fracture in the United States', *J Am Soc Nephrol,* 17(11), pp. 3223-32.

O'Brien, C. E., Com, G., Fowlkes, J., Tang, X. and James, L. P. (2018) 'Peripheral quantitative computed tomography detects differences at the radius in prepubertal children with cystic fibrosis compared to healthy controls', *PLoS One,* 13(1), pp. e0191013.

Oh, J., Wunsch, R., Turzer, M., Bahner, M., Raggi, P., Querfeld, U., Mehls, O. and Schaefer, F. (2002) 'Advanced coronary and carotid arteriopathy in young adults with childhood-onset chronic renal failure', *Circulation,* 106(1), pp. 100-5.

Ohyama, Y., Ambale-Venkatesh, B., Noda, C., Chugh Atul, R., Teixido-Tura, G., Kim, J.-Y., Donekal, S., Yoneyama, K., Gjesdal, O., Redheuil, A., Liu, C.-Y., Nakamura, T., Wu Colin, O., Hundley, W. G., Bluemke David, A. and Lima Joao, A. C. (2016) 'Association of Aortic Stiffness With Left Ventricular Remodeling and Reduced Left Ventricular Function Measured by Magnetic Resonance Imaging', *Circulation: Cardiovascular Imaging,* 9(7), pp. e004426.

Ok, E., Asci, G., Bayraktaroglu, S., Toz, H., Ozkahya, M., Yilmaz, M., Kircelli, F., Sevinc Ok, E., Ceylan, N., Duman, S., Cirit, M., Monier-Faugere, M. C. and Malluche, H. H. (2016) 'Reduction of Dialysate Calcium Level Reduces Progression of Coronary Artery Calcification and Improves Low Bone Turnover in Patients on Hemodialysis', *J Am Soc Nephrol,* 27(8), pp. 2475-86.

Orimo, H. (2010) 'The Mechanism of Mineralization and the Role of Alkaline Phosphatase in Health and Disease', *Journal of Nippon Medical School,* 77(1), pp. 4-12.

Ott, S. M. (2008) 'Histomorphometric measurements of bone turnover, mineralization, and volume', *Clin J Am Soc Nephrol,* 3 Suppl 3, pp. S151-6.

Parfitt, A. M. (1998) 'A structural approach to renal bone disease', *J Bone Miner Res,* 13(8), pp. 1213-20.

Pereira, R. C., Bischoff, D. S., Yamaguchi, D., Salusky, I. B. and Wesseling-Perry, K. (2016) 'Micro-CT in the Assessment of Pediatric Renal Osteodystrophy by Bone Histomorphometry', *Clin J Am Soc Nephrol,* 11(3), pp. 481-7.

Persy, V. and D'Haese, P. (2009) 'Vascular calcification and bone disease: the calcification paradox', *Trends Mol Med,* 15(9), pp. 405-16.

Peters, S. A., den Ruijter, H. M., Bots, M. L. and Moons, K. G. (2012) 'Improvements in risk stratification for the occurrence of

cardiovascular disease by imaging subclinical atherosclerosis: a systematic review', *Heart,* 98(3), pp. 177-84.

Peters, S. A., Grobbee, D. E. and Bots, M. L. (2011) 'Carotid intima-media thickness: a suitable alternative for cardiovascular risk as outcome?', *Eur J Cardiovasc Prev Rehabil,* 18(2), pp. 167-74.

Pham-Short, A., Donaghue, K. C., Ambler, G., Briody, J., Garnett, S., Munns, C. F. and Craig, M. E. (2019) 'Abnormal Cortical and Trabecular Bone in Youth With Type 1 Diabetes and Celiac Disease', *Diabetes Care,* 42(8), pp. 1489-1495.

Pluskiewicz, W., Adamczyk, P., Drozdzowska, B., Szprynger, K., Szczepanska, M., Halaba, Z. and Karasek, D. (2002) 'Skeletal status in children, adolescents and young adults with end-stage renal failure treated with hemo- or peritoneal dialysis', *Osteoporos Int,* 13(5), pp. 353-7.

Pluskiewicz, W., Adamczyk, P., Drozdzowska, B., Szprynger, K., Szczepanska, M., Halaba, Z. and Karasek, D. (2003) 'Skeletal status in children and adolescents with chronic renal failure before onset of dialysis or on dialysis', *Osteoporos Int,* 14(4), pp. 283-8.

Pluskiewicz, W., Adamczyk, P., Drozdzowska, B., Szprynger, K., Szczepanska, M., Halaba, Z. and Karasek, D. (2005) 'Skeletal status in adolescents with end-stage renal failure: a longitudinal study', *Osteoporos Int,* 16(3), pp. 289-95.

Portale, A. A., Wolf, M., Juppner, H., Messinger, S., Kumar, J., Wesseling-Perry, K., Schwartz, G. J., Furth, S. L., Warady, B. A. and Salusky, I. B. (2014) 'Disordered FGF23 and mineral metabolism in children with CKD', *Clin J Am Soc Nephrol,* 9(2), pp. 344-53.

Portale, A. A., Wolf, M. S., Messinger, S., Perwad, F., Juppner, H., Warady, B. A., Furth, S. L. and Salusky, I. B. (2016) 'Fibroblast Growth Factor 23 and Risk of CKD Progression in Children', *Clin J Am Soc Nephrol,* 11(11), pp. 1989-1998.

Preka, E., Ranchin, B., Doyon, A., Vierge, M., Ginhoux, T., Kassai, B. and Bacchetta, J. (2018) 'The interplay between bone and vessels in pediatric CKD: lessons from a single-center study', *Pediatr Nephrol*.

Ramalho, J., Marques, I. D. B., Hans, D., Dempster, D., Zhou, H., Patel, P., Pereira, R. M. R., Jorgetti, V., Moyses, R. M. A. and Nickolas, T. L. (2018) 'The trabecular bone score: Relationships with trabecular and cortical microarchitecture measured by HR-pQCT and

histomorphometry in patients with chronic kidney disease', *Bone,* 116, pp. 215-220.

Raphael, K. L. (2018) 'Metabolic Acidosis and Subclinical Metabolic Acidosis in CKD', *Journal of the American Society of Nephrology : JASN,* 29(2), pp. 376-382.

Rauch, F. and Schoenau, E. (2008) 'Peripheral quantitative computed tomography of the proximal radius in young subjects--new reference data and interpretation of results', *J Musculoskelet Neuronal Interact,* 8(3), pp. 217-26.

Recker, R. R., Davies, K. M., Hinders, S. M., Heaney, R. P., Stegman, M. R. and Kimmel, D. B. (1992) 'Bone gain in young adult women', *Jama,* 268(17), pp. 2403-8.

Rees, L. (2008) 'What parathyroid hormone levels should we aim for in children with stage 5 chronic kidney disease; what is the evidence?', *Pediatric nephrology (Berlin, Germany),* 23(2), pp. 179-184.

Rees, L., Shroff, R., Hutchinson, C., Fernando, O. N. and Trompeter, R. S. (2007) 'Long-term outcome of paediatric renal transplantation: follow-up of 300 children from 1973 to 2000', *Nephron Clin Pract,* 105(2), pp. c68-76.

Reynolds, J. L., Joannides, A. J., Skepper, J. N., McNair, R., Schurgers, L. J., Proudfoot, D., Jahnen-Dechent, W., Weissberg, P. L. and Shanahan, C. M. (2004) 'Human vascular smooth muscle cells undergo vesicle-mediated calcification in response to changes in extracellular calcium and phosphate concentrations: a potential mechanism for accelerated vascular calcification in ESRD', *J Am Soc Nephrol,* 15(11), pp. 2857-67.

Roggen, I., Roelants, M., Sioen, I., Vandewalle, S., De Henauw, S., Goemaere, S., Kaufman, J.-M. and De Schepper, J. (2015a) 'Erratum to: Pediatric Reference Values for Tibial Trabecular Bone Mineral Density and Bone Geometry Parameters Using Peripheral Quantitative Computed Tomography', *Calcified Tissue International,* 97(4), pp. 426-427.

Roggen, I., Roelants, M., Sioen, I., Vandewalle, S., De Henauw, S., Goemaere, S., Kaufman, J. M. and De Schepper, J. (2015b) 'Pediatric reference values for tibial trabecular bone mineral density and bone geometry parameters using peripheral quantitative computed tomography', *Calcif Tissue Int,* 96(6), pp. 527-33.

Roumeliotis, A., Roumeliotis, S., Panagoutsos, S., Theodoridis, M., Argyriou, C., Tavridou, A. and Georgiadis, G. S. (2019) 'Carotid intima-media thickness is an independent predictor of all-cause mortality and cardiovascular morbidity in patients with diabetes mellitus type 2 and chronic kidney disease', *Renal Failure,* 41(1), pp. 131-138.

Russo, D., Palmiero, G., De Blasio, A. P., Balletta, M. M. and Andreucci, V. E. (2004) 'Coronary artery calcification in patients with CRF not undergoing dialysis', *Am J Kidney Dis,* 44(6), pp. 1024-30.

Safar, M. E. (2018) 'Arterial stiffness as a risk factor for clinical hypertension', *Nat Rev Cardiol,* 15(2), pp. 97-105.

Salusky, I. B., Coburn, J. W., Brill, J., Foley, J., Slatopolsky, E., Fine, R. N. and Goodman, W. G. (1988) 'Bone disease in pediatric patients undergoing dialysis with CAPD or CCPD', *Kidney Int,* 33(5), pp. 975-82.

Salusky, I. B., Ramirez, J. A., Oppenheim, W., Gales, B., Segre, G. V. and Goodman, W. G. (1994) 'Biochemical markers of renal osteodystrophy in pediatric patients undergoing CAPD/CCPD', *Kidney Int,* 45(1), pp. 253-8.

Saran, R., Robinson, B., Abbott, K. C., Agodoa, L. Y., Albertus, P., Ayanian, J., Balkrishnan, R., Bragg-Gresham, J., Cao, J., Chen, J. L., Cope, E., Dharmarajan, S., Dietrich, X., Eckard, A., Eggers, P. W., Gaber, C., Gillen, D., Gipson, D., Gu, H., Hailpern, S. M., Hall, Y. N., Han, Y., He, K., Hebert, H., Helmuth, M., Herman, W., Heung, M., Hutton, D., Jacobsen, S. J., Ji, N., Jin, Y., Kalantar-Zadeh, K., Kapke, A., Katz, R., Kovesdy, C. P., Kurtz, V., Lavalee, D., Li, Y., Lu, Y., McCullough, K., Molnar, M. Z., Montez-Rath, M., Morgenstern, H., Mu, Q., Mukhopadhyay, P., Nallamothu, B., Nguyen, D. V., Norris, K. C., O'Hare, A. M., Obi, Y., Pearson, J., Pisoni, R., Plattner, B., Port, F. K., Potukuchi, P., Rao, P., Ratkowiak, K., Ravel, V., Ray, D., Rhee, C. M., Schaubel, D. E., Selewski, D. T., Shaw, S., Shi, J., Shieu, M., Sim, J. J., Song, P., Soohoo, M., Steffick, D., Streja, E., Tamura, M. K., Tentori, F., Tilea, A., Tong, L., Turf, M., Wang, D., Wang, M., Woodside, K., Wyncott, A., Xin, X., Zang, W., Zepel, L., Zhang, S., Zho, H., Hirth, R. A. and Shahinian, V. (2017) 'US Renal Data System 2016 Annual Data Report: Epidemiology of Kidney Disease in the United States', *Am J Kidney Dis,* 69(3 Suppl 1), pp. A7-a8.

Sarkola, T., Manlhiot, C., Slorach, C., Bradley Timothy, J., Hui, W., Mertens, L., Redington, A. and Jaeggi, E. (2012) 'Evolution of the Arterial Structure and Function From Infancy to Adolescence Is related to Anthropometric and Blood Pressure Changes', *Arteriosclerosis, Thrombosis, and Vascular Biology,* 32(10), pp. 2516-2524.

Sarnak, M. J., Levey, A. S., Schoolwerth, A. C., Coresh, J., Culleton, B., Hamm, L. L., McCullough, P. A., Kasiske, B. L., Kelepouris, E., Klag, M. J., Parfrey, P., Pfeffer, M., Raij, L., Spinosa, D. J. and Wilson, P. W. (2003) 'Kidney disease as a risk factor for development of cardiovascular disease: a statement from the American Heart Association Councils on Kidney in Cardiovascular Disease, High Blood Pressure Research, Clinical Cardiology, and Epidemiology and Prevention', *Hypertension,* 42(5), pp. 1050-65.

Schaefer, F., Doyon, A., Azukaitis, K., Bayazit, A., Canpolat, N., Duzova, A., Niemirska, A., Sozeri, B., Thurn, D., Anarat, A., Ranchin, B., Litwin, M., Caliskan, S., Candan, C., Baskin, E., Yilmaz, E., Mir, S., Kirchner, M., Sander, A., Haffner, D., Melk, A., Wuhl, E., Shroff, R. and Querfeld, U. (2017) 'Cardiovascular Phenotypes in Children with CKD: The 4C Study', *Clin J Am Soc Nephrol,* 12(1), pp. 19-28.

Schlieper, G., Aretz, A., Verberckmoes, S. C., Krüger, T., Behets, G. J., Ghadimi, R., Weirich, T. E., Rohrmann, D., Langer, S., Tordoir, J. H., Amann, K., Westenfeld, R., Brandenburg, V. M., D'Haese, P. C., Mayer, J., Ketteler, M., McKee, M. D. and Floege, J. (2010) 'Ultrastructural analysis of vascular calcifications in uremia', *J Am Soc Nephrol,* 21(4), pp. 689-96.

Schlieper, G., Schurgers, L., Brandenburg, V., Reutelingsperger, C. and Floege, J. (2016) 'Vascular calcification in chronic kidney disease: an update', *Nephrology Dialysis Transplantation,* 31(1), pp. 31-39.

Schwartz, G. J., Munoz, A., Schneider, M. F., Mak, R. H., Kaskel, F., Warady, B. A. and Furth, S. L. (2009) 'New equations to estimate GFR in children with CKD', *J Am Soc Nephrol,* 20(3), pp. 629-37.

Seeman, E. (2003) 'The structural and biomechanical basis of the gain and loss of bone strength in women and men', *Endocrinol Metab Clin North Am,* 32(1), pp. 25-38.

Shanahan, C. M. (2013) 'Mechanisms of vascular calcification in CKD-evidence for premature ageing?', *Nat Rev Nephrol,* 9(11), pp. 661-70.

Shanahan, C. M., Cary, N. R., Salisbury, J. R., Proudfoot, D., Weissberg, P. L. and Edmonds, M. E. (1999) 'Medial localization of mineralization-regulating proteins in association with Monckeberg's sclerosis: evidence for smooth muscle cell-mediated vascular calcification', *Circulation,* 100(21), pp. 2168-76.

Sharma, A. K., Masterson, R., Holt, S. G. and Toussaint, N. D. (2016) 'Emerging role of high-resolution imaging in the detection of renal osteodystrophy', *Nephrology (Carlton),* 21(10), pp. 801-11.

Sharma, A. K., Toussaint, N. D., Elder, G. J., Masterson, R., Holt, S. G., Robertson, P. L., Ebeling, P. R., Baldock, P., Miller, R. C. and Rajapakse, C. S. (2018) 'Magnetic resonance imaging based assessment of bone microstructure as a non-invasive alternative to histomorphometry in patients with chronic kidney disease', *Bone,* 114, pp. 14-21.

Sharman, J. E., Davies, J. E., Jenkins, C. and Marwick, T. H. (2009) 'Augmentation Index, Left Ventricular Contractility, and Wave Reflection', *Hypertension,* 54(5), pp. 1099-1105.

Shioi, A., Morioka, T., Shoji, T. and Emoto, M. (2020) 'The Inhibitory Roles of Vitamin K in Progression of Vascular Calcification', *Nutrients,* 12(2), pp. 583.

Shiraishi, A., Takeda, S., Masaki, T., Higuchi, Y., Uchiyama, Y., Kubodera, N., Sato, K., Ikeda, K., Nakamura, T., Matsumoto, T. and Ogata, E. (2000) 'Alfacalcidol Inhibits Bone Resorption and Stimulates Formation in an Ovariectomized Rat Model of Osteoporosis: Distinct Actions from Estrogen', *Journal of Bone and Mineral Research,* 15(4), pp. 770-779.

Shirwany, N. A. and Zou, M.-h. (2010) 'Arterial stiffness: a brief review', *Acta Pharmacologica Sinica,* 31(10), pp. 1267-1276.

Shroff, R., Fewtrell, M., Heuser, A., Kolevica, A., Lalayiannis, A., McAlister, L., Silva, S., Goodman, N., Schmitt, C. P., Biassoni, L., Rahn, A., Fischer, D. C. and Eisenhauer, A. (2020a) 'Naturally Occurring Stable Calcium Isotope Ratios in Body Compartments Provide a Novel Biomarker of Bone Mineral Balance in Children and Young Adults', *J Bone Miner Res*.

Shroff, R., Fewtrell, M., Heuser, A., Kolevica, A., Lalayiannis, A., McAlister, L., Silva, S., Goodman, N., Schmitt, C. P., Biassoni, L., Rahn, A., Fischer, D. C. and Eisenhauer, A. (2021) 'Naturally Occurring Stable Calcium Isotope Ratios in Body Compartments Provide a Novel Biomarker of

Bone Mineral Balance in Children and Young Adults', *J Bone Miner Res,* 36(1), pp. 133-142.

Shroff, R., Heuser, A., Lalayiannis, A., Karabay Bayazit, A., Jankauskiene, A., Bacchetta, J., Askiti, V., Schmitt, C., Mitsioni, A., Crabtree, N., Fewtrell, M., Biassoni, L., Fischer, D.-C. and Eisenhauer, A. (2020b) 'MO055STABLE CALCIUM ISOTOPES: A NOVEL BIOMARKER OF BONE MINERAL CONTENT IN PATIENTS WITH CHRONIC KIDNEY DISEASE', *Nephrology Dialysis Transplantation,* 35(Supplement_3), pp. gfaa140.MO055.

Shroff, R., Lalayiannis, A. D., Fewtrell, M., Schmitt, C. P., Bayazit, A., Askiti, V., Jankauskiene, A., Bacchetta, J., Silva, S., Goodman, N., McAlister, L., Biassoni, L., Crabtree, N., Rahn, A., Fischer, D. C., Heuser, A., Kolevica, A. and Eisenhauer, A. (2022) 'Naturally occurring stable calcium isotope ratios are a novel biomarker of bone calcium balance in chronic kidney disease', *Kidney Int*.

Shroff, R., Long, D. A. and Shanahan, C. (2013) 'Mechanistic insights into vascular calcification in CKD', *J Am Soc Nephrol,* 24(2), pp. 179-89.

Shroff, R., Wan, M., Nagler, E. V., Bakkaloglu, S., Fischer, D. C., Bishop, N., Cozzolino, M., Bacchetta, J., Edefonti, A., Stefanidis, C. J., Vande Walle, J., Haffner, D., Klaus, G. and Schmitt, C. P. (2017) 'Clinical practice recommendations for native vitamin D therapy in children with chronic kidney disease Stages 2-5 and on dialysis', *Nephrol Dial Transplant,* 32(7), pp. 1098-1113.

Shroff, R., Weaver, D. J., Jr. and Mitsnefes, M. M. (2011) 'Cardiovascular complications in children with chronic kidney disease', *Nat Rev Nephrol,* 7(11), pp. 642-9.

Shroff, R. C., Donald, A. E., Hiorns, M. P., Watson, A., Feather, S., Milford, D., Ellins, E. A., Storry, C., Ridout, D., Deanfield, J. and Rees, L. (2007) 'Mineral metabolism and vascular damage in children on dialysis', *J Am Soc Nephrol,* 18(11), pp. 2996-3003.

Shroff, R. C., McNair, R., Figg, N., Skepper, J. N., Schurgers, L., Gupta, A., Hiorns, M., Donald, A. E., Deanfield, J., Rees, L. and Shanahan, C. M. (2008) 'Dialysis accelerates medial vascular calcification in part by triggering smooth muscle cell apoptosis', *Circulation,* 118(17), pp. 1748-57.

Shroff, R. C., McNair, R., Skepper, J. N., Figg, N., Schurgers, L. J., Deanfield, J., Rees, L. and Shanahan, C. M. (2010) 'Chronic mineral

dysregulation promotes vascular smooth muscle cell adaptation and extracellular matrix calcification', *J Am Soc Nephrol,* 21(1), pp. 103-12.

Shuman, W. P., Branch, K. R., May, J. M., Mitsumori, L. M., Lockhart, D. W., Dubinsky, T. J., Warren, B. H. and Caldwell, J. H. (2008) 'Prospective versus retrospective ECG gating for 64-detector CT of the coronary arteries: comparison of image quality and patient radiation dose', *Radiology,* 248(2), pp. 431-7.

Soeiro, E. M. D., Castro, L., Menezes, R., Elias, R. M., Dos Reis, L. M., Jorgetti, V. and Moyses, R. M. A. (2020) 'Association of parathormone and alkaline phosphatase with bone turnover and mineralization in children with CKD on dialysis: effect of age, gender, and race', *Pediatr Nephrol*.

Spiegel, D. M., Raggi, P., Mehta, R., Lindberg, J. S., Chonchol, M., Ehrlich, J., James, G., Chertow, G. M. and Block, G. A. (2004) 'Coronary and aortic calcifications in patients new to dialysis', *Hemodial Int,* 8(3), pp. 265-72.

Sprague, S. M., Bellorin-Font, E., Jorgetti, V., Carvalho, A. B., Malluche, H. H., Ferreira, A., D'Haese, P. C., Drueke, T. B., Du, H., Manley, T., Rojas, E. and Moe, S. M. (2016) 'Diagnostic Accuracy of Bone Turnover Markers and Bone Histology in Patients With CKD Treated by Dialysis', *Am J Kidney Dis,* 67(4), pp. 559-66.

Srivaths, P. R., Silverstein, D. M., Leung, J., Krishnamurthy, R. and Goldstein, S. L. (2010) 'Malnutrition-inflammation-coronary calcification in pediatric patients receiving chronic hemodialysis', *Hemodial Int,* 14(3), pp. 263-9.

Stagi, S., Cavalli, L., Cavalli, T., de Martino, M. and Brandi, M. L. (2016) 'Peripheral quantitative computed tomography (pQCT) for the assessment of bone strength in most of bone affecting conditions in developmental age: a review', *Italian journal of pediatrics,* 42(1), pp. 88-88.

Stagi, S., Cavalli, L., Iurato, C., Seminara, S., Brandi, M. L. and de Martino, M. (2013a) 'Bone health in children and adolescents: the available imaging techniques', *Clin Cases Miner Bone Metab,* 10(3), pp. 166-71.

Stagi, S., Cavalli, L., Iurato, C., Seminara, S., Brandi, M. L. and de Martino, M. (2013b) 'Bone metabolism in children and adolescents: main

characteristics of the determinants of peak bone mass', *Clinical Cases in Mineral and Bone Metabolism,* 10(3), pp. 172-179.

Starke, A., Corsenca, A., Kohler, T., Knubben, J., Kraenzlin, M., Uebelhart, D., Wuthrich, R. P., von Rechenberg, B., Muller, R. and Ambuhl, P. M. (2012) 'Correction of metabolic acidosis with potassium citrate in renal transplant patients and its effect on bone quality', *Clin J Am Soc Nephrol,* 7(9), pp. 1461-72.

Swolin-Eide, D., Hansson, S. and Magnusson, P. (2009) 'Children with chronic kidney disease: a 3-year prospective study of growth, bone mass and bone turnover', *Acta Paediatr,* 98(2), pp. 367-73.

Swolin-Eide, D., Magnusson, P. and Hansson, S. (2007) 'Bone mass, biochemical markers and growth in children with chronic kidney disease: a 1-year prospective study', *Acta Paediatr,* 96(5), pp. 720-5.

Szeto, C. C., Chow, K. M., Woo, K. S., Chook, P., Ching-Ha Kwan, B., Leung, C. B. and Kam-Tao Li, P. (2007) 'Carotid intima media thickness predicts cardiovascular diseases in Chinese predialysis patients with chronic kidney disease', *J Am Soc Nephrol,* 18(6), pp. 1966-72.

Tamminen, I. S., Valta, H., Jalanko, H., Salminen, S., Mäyränpää, M. K., Isaksson, H., Kröger, H. and Mäkitie, O. (2014) 'Pediatric solid organ transplantation and osteoporosis: a descriptive study on bone histomorphometric findings', *Pediatr Nephrol,* 29(8), pp. 1431-40.

Tankó, L. B., Christiansen, C., Cox, D. A., Geiger, M. J., McNabb, M. A. and Cummings, S. R. (2005) 'Relationship between osteoporosis and cardiovascular disease in postmenopausal women', *J Bone Miner Res,* 20(11), pp. 1912-20.

Tawadrous, H., Kamran, H., Salciccioli, L., Schoeneman, M. J. and Lazar, J. (2012) 'Evaluation of arterial structure and function in pediatric patients with end-stage renal disease on dialysis and after renal transplantation', *Pediatr Transplant,* 16(5), pp. 480-5.

Tentori, F., McCullough, K., Kilpatrick, R. D., Bradbury, B. D., Robinson, B. M., Kerr, P. G. and Pisoni, R. L. (2013) 'Response to High rates of death and hospitalization follow bone fracture among hemodialysis patients', *Kidney Int,* 85(1), pp. 166-173.

Tong, A., Manns, B., Wang, A. Y. M., Hemmelgarn, B., Wheeler, D. C., Gill, J., Tugwell, P., Pecoits-Filho, R., Crowe, S., Harris, T., Van Biesen, W., Winkelmayer, W. C., Levin, A., Thompson, A., Perkovic, V., Ju, A., Gutman, T., Bernier-Jean, A., Viecelli, A. K., O'Lone, E., Shen, J.,

Josephson, M. A., Cho, Y., Johnson, D. W., Sautenet, B., Tonelli, M., Craig, J. C. and Investigators, S. I. W. (2018) 'Implementing core outcomes in kidney disease: report of the Standardized Outcomes in Nephrology (SONG) implementation workshop', *Kidney international,* 94(6), pp. 1053-1068.

Torres, P. U., Bover, J., Mazzaferro, S., de Vernejoul, M. C. and Cohen-Solal, M. (2014) 'When, how, and why a bone biopsy should be performed in patients with chronic kidney disease', *Semin Nephrol,* 34(6), pp. 612-25.

Touboul, P. J., Hennerici, M. G., Meairs, S., Adams, H., Amarenco, P., Bornstein, N., Csiba, L., Desvarieux, M., Ebrahim, S., Hernandez Hernandez, R., Jaff, M., Kownator, S., Naqvi, T., Prati, P., Rundek, T., Sitzer, M., Schminke, U., Tardif, J. C., Taylor, A., Vicaut, E. and Woo, K. S. (2012) 'Mannheim carotid intima-media thickness and plaque consensus (2004-2006-2011). An update on behalf of the advisory board of the 3rd, 4th and 5th watching the risk symposia, at the 13th, 15th and 20th European Stroke Conferences, Mannheim, Germany, 2004, Brussels, Belgium, 2006, and Hamburg, Germany, 2011', *Cerebrovasc Dis,* 34(4), pp. 290-6.

Toussaint, N. D., Lau, K. K., Strauss, B. J., Polkinghorne, K. R. and Kerr, P. G. (2008) 'Associations between vascular calcification, arterial stiffness and bone mineral density in chronic kidney disease', *Nephrol Dial Transplant,* 23(2), pp. 586-93.

Townsend, R. R., Anderson, A. H., Chirinos, J. A., Feldman, H. I., Grunwald, J. E., Nessel, L., Roy, J., Weir, M. R., Wright, J. T., Jr., Bansal, N. and Hsu, C. Y. (2018) 'Association of Pulse Wave Velocity With Chronic Kidney Disease Progression and Mortality: Findings From the CRIC Study (Chronic Renal Insufficiency Cohort)', *Hypertension,* 71(6), pp. 1101-1107.

Tsampalieros, A., Griffin, L., Terpstra, A. M., Kalkwarf, H. J., Shults, J., Foster, B. J., Zemel, B. S., Foerster, D. L. and Leonard, M. B. (2014) 'Changes in DXA and quantitative CT measures of musculoskeletal outcomes following pediatric renal transplantation', *Am J Transplant,* 14(1), pp. 124-32.

Tsampalieros, A., Gupta, P., Denburg, M. R., Shults, J., Zemel, B. S., Mostoufi-Moab, S., Wetzsteon, R. J., Herskovitz, R. M., Whitehead, K. M. and Leonard, M. B. (2013a) 'GLUCOCORTICOID EFFECTS ON

CHANGES IN BONE MINERAL DENSITY AND CORTICAL STRUCTURE IN CHILDHOOD NEPHROTIC SYNDROME', *Journal of bone and mineral research : the official journal of the American Society for Bone and Mineral Research,* 28(3), pp. 480-488.

Tsampalieros, A., Kalkwarf, H. J., Wetzsteon, R. J., Shults, J., Zemel, B. S., Foster, B. J., Foerster, D. L. and Leonard, M. B. (2013b) 'Changes in bone structure and the muscle-bone unit in children with chronic kidney disease', *Kidney Int,* 83(3), pp. 495-502.

Turin, T. C., Tonelli, M., Manns, B. J., Ravani, P., Ahmed, S. B. and Hemmelgarn, B. R. (2012) 'Chronic kidney disease and life expectancy', *Nephrology Dialysis Transplantation,* 27(8), pp. 3182-3186.

Valta, H., Mäkitie, O., Rönnholm, K. and Jalanko, H. (2009) 'Bone health in children and adolescents after renal transplantation', *J Bone Miner Res,* 24(10), pp. 1699-708.

van der Meer, I. M., Bots, M. L., Hofman, A., del Sol, A. I., van der Kuip, D. A. and Witteman, J. C. (2004) 'Predictive value of noninvasive measures of atherosclerosis for incident myocardial infarction: the Rotterdam Study', *Circulation,* 109(9), pp. 1089-94.

van der Sluis, I. M., Boot, A. M., Nauta, J., Hop, W. C., de Jong, M. C., Lilien, M. R., Groothoff, J. W., van Wijk, A. E., Pols, H. A., Hokken-Koelega, A. C. and de Muinck Keizer-Schrama, S. M. (2000) 'Bone density and body composition in chronic renal failure: effects of growth hormone treatment', *Pediatr Nephrol,* 15(3-4), pp. 221-8.

Van Dyck, M., Gyssels, A., Proesmans, W., Nijs, J. and Eeckels, R. (2001) 'Growth hormone treatment enhances bone mineralisation in children with chronic renal failure', *Eur J Pediatr,* 160(6), pp. 359-63.

Vasikaran, S., Eastell, R., Bruyere, O., Foldes, A. J., Garnero, P., Griesmacher, A., McClung, M., Morris, H. A., Silverman, S., Trenti, T., Wahl, D. A., Cooper, C. and Kanis, J. A. (2011) 'Markers of bone turnover for the prediction of fracture risk and monitoring of osteoporosis treatment: a need for international reference standards', *Osteoporos Int,* 22(2), pp. 391-420.

Veitch, S. W., Findlay, S. C., Ingle, B. M., Ibbotson, C. J., Barrington, A., Hamer, A. J. and Eastell, R. (2004) 'Accuracy and precision of peripheral quantitative computed tomography measurements at the tibial metaphysis', *J Clin Densitom,* 7(2), pp. 209-17.

Viaene, L., Behets, G. J., Heye, S., Claes, K., Monbaliu, D., Pirenne, J., D'Haese, P. C. and Evenepoel, P. (2016) 'Inflammation and the bone-vascular axis in end-stage renal disease', *Osteoporos Int,* 27(2), pp. 489-97.

Waller, S., Ledermann, S., Trompeter, R., van't Hoff, W., Ridout, D. and Rees, L. (2003) 'Catch-up growth with normal parathyroid hormone levels in chronic renal failure', *Pediatr Nephrol,* 18(12), pp. 1236-41.

Waller, S., Ridout, D. and Rees, L. (2007) 'Bone mineral density in children with chronic renal failure', *Pediatr Nephrol,* 22(1), pp. 121-7.

Waller, S., Shroff, R., Freemont, A. J. and Rees, L. (2008) 'Bone histomorphometry in children prior to commencing renal replacement therapy', *Pediatr Nephrol,* 23(9), pp. 1523-9.

Wan, M., Smith, C., Shah, V., Gullet, A., Wells, D., Rees, L. and Shroff, R. (2013) 'Fibroblast growth factor 23 and soluble klotho in children with chronic kidney disease', *Nephrol Dial Transplant,* 28(1), pp. 153-61.

Ward, K. A., Ashby, R. L., Roberts, S. A., Adams, J. E. and Zulf Mughal, M. (2007) 'UK reference data for the Hologic QDR Discovery dual-energy x ray absorptiometry scanner in healthy children and young adults aged 6-17 years', *Arch Dis Child,* 92(1), pp. 53-9.

Ward, L. M., Ma, J., Rauch, F., Benchimol, E. I., Hay, J., Leonard, M. B., Matzinger, M. A., Shenouda, N., Lentle, B., Cosgrove, H., Scharke, M., Konji, V. N. and Mack, D. R. (2017) 'Musculoskeletal health in newly diagnosed children with Crohn's disease', *Osteoporos Int,* 28(11), pp. 3169-3177.

Wasserman, H., O'Donnell, J. M. and Gordon, C. M. (2017) 'Use of dual energy X-ray absorptiometry in pediatric patients', *Bone,* 104, pp. 84-90.

Weaver, C. M., Gordon, C. M., Janz, K. F., Kalkwarf, H. J., Lappe, J. M., Lewis, R., O'Karma, M., Wallace, T. C. and Zemel, B. S. (2016) 'The National Osteoporosis Foundation's position statement on peak bone mass development and lifestyle factors: a systematic review and implementation recommendations', *Osteoporos Int,* 27(4), pp. 1281-1386.

Weber, L. T. and Mehls, O. (2010) 'Limitations of dual x-ray absorptiometry in children with chronic kidney disease', *Pediatr Nephrol,* 25(1), pp. 3-5.

Wehrli, F. W., Leonard, M. B., Saha, P. K. and Gomberg, B. R. (2004) 'Quantitative high-resolution magnetic resonance imaging reveals structural implications of renal osteodystrophy on trabecular and cortical bone', *J Magn Reson Imaging,* 20(1), pp. 83-9.

Wesseling-Perry, K. (2015) 'Defective skeletal mineralization in pediatric CKD', *Curr Osteoporos Rep,* 13(2), pp. 98-105.

Wesseling-Perry, K., Pereira, R. C., Tseng, C. H., Elashoff, R., Zaritsky, J. J., Yadin, O., Sahney, S., Gales, B., Juppner, H. and Salusky, I. B. (2012) 'Early skeletal and biochemical alterations in pediatric chronic kidney disease', *Clin J Am Soc Nephrol,* 7(1), pp. 146-52.

Wesseling-Perry, K. and Salusky, I. B. (2013) 'Phosphate binders, Vitamin D and Calcimimetics in the Management of Chronic Kidney Disease-Mineral Bone Disorders (CKD-MBD) in Children', *Pediatric nephrology (Berlin, Germany),* 28(4), pp. 617-625.

West, S. L., Lok, C. E., Langsetmo, L., Cheung, A. M., Szabo, E., Pearce, D., Fusaro, M., Wald, R., Weinstein, J. and Jamal, S. A. (2015) 'Bone mineral density predicts fractures in chronic kidney disease', *J Bone Miner Res,* 30(5), pp. 913-9.

Wetzsteon, R. J., Kalkwarf, H. J., Shults, J., Zemel, B. S., Foster, B. J., Griffin, L., Strife, C. F., Foerster, D. L., Jean-Pierre, D. K. and Leonard, M. B. (2011) 'Volumetric Bone Mineral Density and Bone Structure in Childhood Chronic Kidney Disease', *Journal of Bone and Mineral Research,* 26(9), pp. 2235-2244.

Wetzsteon, R. J., Shults, J., Zemel, B. S., Gupta, P. U., Burnham, J. M., Herskovitz, R. M., Howard, K. M. and Leonard, M. B. (2009) 'Divergent Effects of Glucocorticoids on Cortical and Trabecular Compartment BMD in Childhood Nephrotic Syndrome', *Journal of bone and mineral research : the official journal of the American Society for Bone and Mineral Research,* 24(3), pp. 503-513.

Whiting, S. J., Vatanparast, H., Baxter-Jones, A., Faulkner, R. A., Mirwald, R. and Bailey, D. A. (2004) 'Factors that affect bone mineral accrual in the adolescent growth spurt', *J Nutr,* 134(3), pp. 696s-700s.

Whittier, D. E., Boyd, S. K., Burghardt, A. J., Paccou, J., Ghasem-Zadeh, A., Chapurlat, R., Engelke, K. and Bouxsein, M. L. (2020) 'Guidelines for the assessment of bone density and microarchitecture in vivo using high-resolution peripheral quantitative computed tomography', *Osteoporos Int,* 31(9), pp. 1607-1627.

Williams, J. E., Wilson, C. M., Biassoni, L., Suri, R. and Fewtrell, M. S. (2012) 'Dual energy x-ray absorptiometry and quantitative ultrasound are not interchangeable in diagnosing abnormal bones', *Arch Dis Child,* 97(9), pp. 822-4.

Yalcinkaya, F., Ince, E., Tumer, N., Ensari, A. and Ozkaya, N. (2000) 'Spectrum of renal osteodystrophy in children on continuous ambulatory peritoneal dialysis', *Pediatr Int,* 42(1), pp. 53-7.

Yenchek, R. H., Ix, J. H., Shlipak, M. G., Bauer, D. C., Rianon, N. J., Kritchevsky, S. B., Harris, T. B., Newman, A. B., Cauley, J. A. and Fried, L. F. (2012) 'Bone mineral density and fracture risk in older individuals with CKD', *Clin J Am Soc Nephrol,* 7(7), pp. 1130-6.

Yuan, F.-L., Xu, M.-H., Li, X., Xinlong, H., Fang, W. and Dong, J. (2016) 'The Roles of Acidosis in Osteoclast Biology', *Frontiers in physiology,* 7, pp. 222-222.

Zemel, B. S., Kalkwarf, H. J., Gilsanz, V., Lappe, J. M., Oberfield, S., Shepherd, J. A., Frederick, M. M., Huang, X., Lu, M., Mahboubi, S., Hangartner, T. and Winer, K. K. (2011) 'Revised reference curves for bone mineral content and areal bone mineral density according to age and sex for black and non-black children: results of the bone mineral density in childhood study', *J Clin Endocrinol Metab,* 96(10), pp. 3160-9.

Zemel, B. S., Leonard, M. B., Kelly, A., Lappe, J. M., Gilsanz, V., Oberfield, S., Mahboubi, S., Shepherd, J. A., Hangartner, T. N., Frederick, M. M., Winer, K. K. and Kalkwarf, H. J. (2010) 'Height adjustment in assessing dual energy x-ray absorptiometry measurements of bone mass and density in children', *J Clin Endocrinol Metab,* 95(3), pp. 1265-73.

Zierk, J., Arzideh, F., Haeckel, R., Cario, H., Fruhwald, M. C., Gross, H. J., Gscheidmeier, T., Hoffmann, R., Krebs, A., Lichtinghagen, R., Neumann, M., Ruf, H. G., Steigerwald, U., Streichert, T., Rascher, W., Metzler, M. and Rauh, M. (2017) 'Pediatric reference intervals for alkaline phosphatase', *Clin Chem Lab Med,* 55(1), pp. 102-110.

Ziolkowska, H., Brzewski, M. and Roszkowska-Blaim, M. (2008) 'Determinants of the intima-media thickness in children and adolescents with chronic kidney disease', *Pediatr Nephrol,* 23(5), pp. 805-11.

Ziolkowska, H., Paniczyk-Tomaszewska, M., Debinski, A., Polowiec, Z., Sawicki, A. and Sieniawska, M. (2000) 'Bone biopsy results and serum

bone turnover parameters in uremic children', *Acta Paediatr,* 89(6), pp. 666-71.